LIỆT KÊ DANH MỤC CÔNG TRÌNH ĐÃ CÔNG BỐ

A.Các bài báo đăng trên tạp chí ISI – Scopus

1. N. S. Dinh, L. S. B. Dinh, V. A. Truong, "A novel hybrid algorithm: long short-term memory-genetic algorithm for optimizing uncertain revenue of wind farms in electricity markets," *Neural Computing and Applications*, tập 37, trang 24345–24364, 2025. DOI: https://doi.org/10.1007/s00521-025-11582-y

2. V. A. Truong, N. S. Dinh, T. L. Duong, N. T. Le, C. D. Truong và L. T. Nguyen, "Hybrid LSTM-PSO optimization techniques for enhancing wind power bidding efficiency in electricity markets," *Ain Shams Engineering Journal*, tập 16, số 2, p. 103285, 2025. DOI: https://doi.org/10.1016/j.asej.2025.103285

3. V. A. Truong, N. S. Dinh và T. L. Duong, "Profit Maximization of Wind Power Plants in the Electricity Market Based on Linking Models Between Energy Sources," *Arabian Journal for Science and Engineering*, tập 49, số 8, p. 6275–6291, 2024. DOI: https://doi.org/10.1007/s13369-023-08181-1

4. V. A. Truong, T. L. Nguyen và N. S. Dinh, "Controlling Output Power to Enhance the Investment Efficiency of Wind Farms by Maximizing the Capacity of Transmission Transformers and Integrating Energy Storage Systems," *Engineering, Technology & Applied Science Research*, tập 14, số 4, p. 15751–15756, 2024. DOI: https://doi.org/10.48084/etasr.7688

5. N. S. Dinh và T. L. N. Viet Anh Truong, "Optimal Probability Distribution Models for Wind Speed Prediction: Strategies to Advance Wind Energy Development in Vietnam," *International Journal of Electrical and Electronics Engineering*, tập 12, số 1, pp. 17-24, 2025. DOI: https://doi.org/10.14445/23488379/IJEEE-V12I1P103

B.Các bài báo hội thảo khoa học quốc tế đăng tạp chí quốc tế có phản biện

6. N. S. Dinh, T. L. Nguyen và V. A. Truong, "Enhancing Wind Power Profitability Through Integrated Clusters in the Electricity Market," trong *2023 Asia Meeting on Environment and Electrical Engineering (EEE-AM)*, Hanoi, Vietnam, 2023. DOI: https://doi.org/10.1109/EEE-AM58328.2023.10395263

7. T. L. Nguyen, N. S. Dinh, V. A. Truong, T. L. Duong, H. D. Dao và A. T. Do, "Enhancing Total Transfer Capability via Optimal Location of Energy Storage

Systems Using a Hybrid Improved Min-Cut Algorithm and Genetic Algorithm," trong *The International Conference on Engineering Research and Applications, ICERA 2022*. Lecture Notes in Networks and Systems, 2023. DOI: https://doi.org/10.1007/978-3-031-22200-9_57

C.Các bài báo đăng kỷ yếu hội nghị quốc tế có phản biện

8. X. L. Bui, N. S. Dinh và V. A. Truong, "Initiative for Integrating Wind and Thermal Power to Maximize Social Profit," trong *Proceedings of 2024 7th International Conference on Green Technology and Sustainable Development (GTSD)*, Hochiminh, Vietnam, 2024.

D.Các bài báo đăng trên tạp chí khoa học trong nước thuộc danh mục hội đồng chức danh Nhà nước

9. Đ. N. Sang, N. T. Linh và T. V. Anh, "Nâng cao hiệu quả thiết kế đầu tư mở rộng điện gió trong điều kiện cạnh tranh thị trường điện có xét đến tính bất định," *TNU Journal of Science and Technology*, tập 229, số 14, pp. 280 - 288, 2024. DOI: https://doi.org/10.34238/tnu-jst.11135

10. N. S. Dinh, V. A. Truong và T. L. Nguyen, "A robust hybrid algorithm AI and GA for optimizing wind power in electricity market," *Journal of Military Science and Technology*, tập 99, pp. 24-34, 2024. DOI: https://doi.org/10.54939/1859-1043.j.mst.99.2024.24-34

11. Đ. N. Sang, T. V. Anh và N. T. Linh, "Tăng cường hiệu quả đầu tư điện gió trong thị trường điện thông qua kết hợp sự bất định của điện gió với vận hành nhà máy nhiệt điện," *Tạp chí Khoa học và Công nghệ - Đại học Đà Nẵng*, tập 22, số 2, pp. 81-87, 2024. https://jst-ud.vn/jst-ud/article/view/8912

12. T. V. Anh, N. T. Linh và Đ. N. Sang, "Nghiên cứu ứng dụng phương pháp lai trong bài toán lựa chọn hợp lý vị trí và dung lượng hệ thống lưu trữ năng lượng trong hệ thống điện," *Journal of Science & Technology, Trường ĐH Công nghiệp Hà Nội*, tập 59, số 3, pp. 3-10, 2023. DOI: https://doi.org/10.57001/huih5804.2023.100

ORIGINAL ARTICLE

A novel hybrid algorithm: long short-term memory-genetic algorithm for optimizing uncertain revenue of wind farms in electricity markets

Ngoc Sang Dinh[1,2] · Le Song Binh Dinh[3] · Viet Anh Truong[1]

Received: 6 August 2024 / Accepted: 14 August 2025

Abstract
This paper presents a robust hybrid optimization algorithm that combines artificial intelligence with genetic algorithms (GA) to maximize revenue for electricity generation plants, addressing the challenges posed by wind generation uncertainty in liberalized power markets. The novel method leverages the prediction capabilities of the long short-term memory algorithm, a deep learning methodology, to forecast superior genetic traits. These enhanced individuals are then incorporated into the population, accelerating the evolutionary process of the GA and improving its ability to achieve local optimality. The effectiveness of the proposed algorithm is demonstrated through experimental validation of the revenue optimization problem, aiming to increase wind energy utilization by reducing compensation risks related to electricity production fluctuations in the market. The performance of the algorithm in recommending wind power bidding capacity is evaluated using the IEEE 30-bus and 118-bus power system model. Comparative analysis shows that auctioned wind power consumption increased by 12% compared to the traditional GA and by more than 20% compared to the mixed integer linear programming (MILP) method, with a corresponding revenue increase of 7% compared to the MILP scenario. Furthermore, comparison with previous advanced GA research on the optimal power flow problem indicates not only a reduction in the number of generations but also significant savings in computation time; the effectiveness of the approach is confirmed by a more than 22% reduction in the NFFE index (the number of fitness function evaluations).

Keywords Electricity market · Wind farm · Optimal algorithm · Genetic algorithm · Artificial intelligence · Deep learning · Long short term memory

1 Introduction

The integration of wind energy—one of the most prevalent renewable energy sources today—into electricity markets is essential for promoting sustainable development and fostering fair competition [1]. Despite its importance, this process encounters significant challenges due to the inherent volatility of wind power production. Such volatility not only disrupts the operational stability of power systems but also escalates financial risks in the market [2]. First, operational instabilities necessitate the exploration and implementation of optimization-based solutions designed to achieve efficient system performance within the complex, multi-variable framework of power systems. Optimization algorithms have been extensively discussed in the literature as crucial tools for addressing these challenges [3]. Second, from an economic perspective, the unpredictability of wind power generation introduces substantial financial risks, which heighten concerns among financial institutions regarding

https://doi.org/10.1007/s00521-025-11582-y

Published online: 28 August 2025

investments in this energy source. For instance, studies on onshore wind power investments in Canada have illustrated the economic risks posed by such volatility [4]. Furthermore, fluctuations in wind power output often provoke diverse market responses, resulting in financial penalties and operational challenges for wind power producers, as highlighted in recent research [5].

Recent research has increasingly focused on mitigating uncertainties and promoting efficient investment in wind energy participation in electricity markets. A proposed approach to risk mitigation is the combination of contracts for difference with conventional power purchase agreements in the electricity sector [6]. Simultaneously, improving operational efficiency in commercial activities remains a key research focus [7]. From a technical perspective, accurate wind speed forecasting is critical for mitigating risk impacts but is challenged by the complexity of weather patterns and natural conditions, necessitating appropriate compensation mechanisms for electricity buyers [8, 9]. Recent trends highlight the growing adoption of machine learning techniques for wind speed prediction [10], alongside the use of Markov probabilistic models to forecast electricity prices and develop effective bidding strategies in wind power markets [11].

Meta-heuristic (MH) optimization and deep learning (DL) algorithms have become essential tools for enhancing the performance of power systems and renewable energy applications. MH algorithms, such as swarm intelligence and evolutionary approaches, are well known for their reliable and efficient optimization capabilities and extensive applicability [12]. Numerous studies have refined these algorithms to better suit energy-related challenges, as exemplified by the evolutionary-gradient algorithm (EGA) [13] and the enhanced Salp swarm algorithm (ESSA) [14]. In recent years, artificial intelligence (AI)-based algorithms, including machine learning (ML) and DL, have advanced significantly, yielding groundbreaking improvements across various fields, such as increasing the accuracy of wind speed predictions [15]. Beyond the continuous enhancement of individual algorithm families, hybrid approaches combining MH and DL have emerged as a promising research direction [16]. This study [16] also underscores the growing trend of employing MH algorithms to enhance the performance of DL methods, a strategy that has been extensively explored. Notable hybrid techniques include the use of MH algorithms for optimizing weights in DL architectures [17], the application of GA to improve soil moisture prediction accuracy using LSTM networks [18], and the Enhanced Sine Cosine Algorithm (SCA) for hyperparameter tuning in LSTM and gated recurrent unit (GRU) networks for energy forecasting [19]. Conversely, the reverse approach—leveraging DL techniques to enhance the optimization performance of MH algorithms—remains underdeveloped, presenting a significant opportunity for future research.

The gap in integrating DL methods within the framework of MH algorithms to improve the efficiency and convergence rate of wide-scale optimization, as discussed in this paper, is explored. The solution leverages the accurate predictions from LSTM networks within the evolutionary process of GA to optimize and improve wind energy investment efficiency in the electricity market. This algorithm utilizes the evolutionary principle that future generations inherit superior traits while employing LSTM, a DL technique, to predict the improved components of future generations' chromosomes within the GA framework. By integrating these predicted superior individuals into the evolutionary process, the algorithm enhances optimization efficiency and achieves better results compared to traditional methods. The performance of the algorithm is validated through experiments on the IEEE 30-bus and 118-bus electricity system. The results highlight the potential of this algorithm in improving prediction accuracy and optimization in wind integration compared to traditional GA methods and other upgraded GA variants studied in [20]. Additionally, the algorithm demonstrates advantages over MILP methods applied in mathematical modeling, as referenced in [7]. The main contributions of this paper are summarized as follows:

1) We propose a powerful optimization algorithm, the LSTM-GA hybrid algorithm. The strength of this methodology lies in accelerating convergence in optimization tasks, a common limitation of MH algorithms due to substantial computational load and the numerous iterations required to reach the target. To address this, a stage of chromosome prediction is integrated within the evolutionary cycle. By leveraging the predictive power of LSTM, past individuals are linked to create superior chromosomes that are closer to the

target. These evolved individuals, akin to conditioned mutations in evolutionary algorithms, facilitate a more efficient convergence process. Furthermore, LSTM-based predictions enable overcoming local barriers and progressing toward global solutions, especially when the initial LSTM training data is expanded.

2) The effectiveness of this new hybrid algorithm is demonstrated through experimental validation by optimizing the auction electricity output of wind farms in competitive electricity markets. The results of the bidding optimization showcase significant benefits with a model integrating three distinct energy investors-wind farms, thermal power plants, and energy storage systems (ESS). The experimental findings also align with multi-factor and multi-objective problems involving various stochastic factors, such as wind speed fluctuations and combined financial investment goals in wind, thermal, and energy storage operations within competitive electricity market management.

The GA- and LSTM-based approach tested in this paper represents just one of the many experimental choices, with the theoretical foundation suggesting further exploration into integrating other metaheuristic and deep learning algorithms, such as PSO, or other algorithms like swarm intelligence methods and deep learning techniques.

2 Mathematical model

The problem at hand is determining the optimal bidding capacity for wind energy in the day-ahead power market to maximize benefits for wind farm operators. In this context, we introduce the concept of power deviation in bidding, which is the difference between the bid power value of wind farms in the electricity market and the predicted power value with the highest probability, known as WPD. Current research often focuses on accurately predicting wind speed when WPD equals zero. However, maximizing the benefits in this scenario is uncertain because unstable factors in wind power output can lead to substantial penalties, potentially discouraging investment in the wind power sector.

2.1 The objective function

The objective function is the revenue as described by [21], including the revenue from wind, ESS, and thermal sources.

$$\{F = R_w + R_E + R_T\} \tag{1}$$

This revenue includes two components: direct and uncertain revenue. Direct revenue comes from electricity sales based on the previous auction schedule, while uncertain revenue relates to income from excess electricity sales or costs incurred for compensating shortfalls when wind power production deviates from forecasts.

$$R_E = \eta_E(\lambda_C - \lambda_B)P_E \tag{2}$$

The term R_w^d denotes the guaranteed revenue derived from the committed wind power production P_{ws} in energy market. Conversely, R_w^u refers to the variable income component, which depends on the stochastic nature of wind speed, ΔP_w. This component is modeled as the discrepancy observed in the real-time output of wind energy compared to expected values, P_{wav}, and schedule. R_E represents the income generated from ESS, which is a function of storage efficiency η_E, the discharged power P_E, and the price margin between the selling price of stored electricity λ_C and the charging cost λ_B. For thermal power plants, R_T represents the revenue of the thermal power plant, comprising both direct electricity sales revenue R_T^d and uncertain revenue R_T^u. A potential power

shortage influences uncertain revenue due to insufficient wind power output or a decrease in power production from wind power.

2.1.1 The direct revenue

This revenue is the first component in wind and thermal revenues [21],

$$R_w = R_w^d(P_{\mathrm{ws}}) + R_w^u(\Delta P_w) \tag{3}$$

$$R_T = R_T^d(P_{Ts}) + R_T^u(\Delta P_T) \tag{4}$$

Accordingly, it is defined as the following expression,

$$R_w^d = \lambda_w x P_{\mathrm{ws}} \tag{5}$$

$$R_T^d = \lambda_T x P_{Ts} \tag{6}$$

The bidding prices for wind (λ_w) and thermal plants (λ_T) correspond to the bid quantities of wind power (P_{ws}) and thermal power (P_{Ts}) in the respective electricity markets. For investors to benefit, it is crucial to accurately predict both the selling prices of electricity and the bid power production, as detailed in [11]. Typically, wind power pricing is estimated using the average rate of the market's leading energy contributor as a reference point. The European electricity market serves as an example, where the wind power price is typically determined based on the average selling price of gas, as it is the predominant energy source in this market [22].

2.1.2 The uncertain income components

Uncertain revenue arises when there is a deviation in wind power production from the plan. First, if there is excess electricity, it will be sold at the price, which is usually much lower than the auction price due to its unexpected nature. Next, if there is a shortage of electricity, a thermal power plant will sell reserve power output to make up for this shortfall in wind power. If the thermal power plant cannot fully compensate, the ESS will cover the remaining deficit. Finally, if the ESS is still insufficient to compensate for the shortfall, the wind power owner must pay a contract penalty. The uncertain revenue and cost components in (3) and (4) are determined by the following expressions [23],

$$R_w^u = \begin{cases} R_{Rw}(\Delta P_w(WPD)), if \Delta P_w > 0 \\ -C_{Pw}(\Delta P_w(WPD)), if \Delta P_w < 0 \end{cases} \tag{7}$$

$$R_T^u = \begin{cases} R_{PT}(\Delta P_T(WPD)), if \Delta P_T > 0 \\ -R_{RT}(\Delta P_T(WPD)), if \Delta P_T < 0 \end{cases} \tag{8}$$

The bidding error probability f_w in this problem is chosen to follow a Weibull distribution, commonly used in wind speed forecasting, which can be referenced [24]. Meanwhile, the purchase price of electricity from thermal power plants, ESS, and penalty prices depend on commitments but are typically higher than the auction price. The revenue and cost components are as follows,

$$R_{Rw} = k_R \lambda_w \tau_{\text{out}} = k_R \lambda_w \sum_{(P_{\text{ws}}+\tau_{\text{in}})}^{P_{\text{wr}}} (p_w - P_{\text{ws}}) f_w(p_w) dp_w \tag{9}$$

$$C_{\text{Pw}} = C_{\text{PT}} + C_{\text{PE}} + C_{P0} \tag{10}$$

$$C_{\text{PT}} = k_{P1} \lambda_w \tau_{\text{out}} = \begin{cases} k_{P1} \lambda_w \sum_{(P_{\text{ws}}-\tau_{\text{in}}-\Delta P_T)}^{(P_{\text{ws}}-\tau_{\text{in}})} (P_{\text{ws}} - p_w) f_w(p_w) dp_w, if |\tau_{\text{out}}| < \Delta P_T \\ k_{P1} \lambda_w \Delta P_T, if |\tau_{\text{out}}| \geq \Delta P_T \end{cases} \tag{11}$$

$$C_{\text{PE}} = k_{P2} \lambda_w (\tau_{\text{out}} - \Delta P_T) = \begin{cases} k_{P2} \lambda_w \sum_{(P_{ws}-\tau_{in}-\Delta P_T-P_E)}^{(P_{ws}-\tau_{in}-\Delta P_T)} (P_{ws} - p_w) f_w(p_w) \mathrm{d}p_w, if \Delta P_T < |\tau_{out}| < (\Delta P_T + P_E) \\ k_{P2} \lambda_w P_E, if |\tau_{\text{out}}| \geq (\Delta P_T + P_E) \end{cases} \tag{12}$$

$$C_{P0} = k_{P0} \lambda_w (\tau_{\text{out}} - \Delta P_T - P_E) = k_{P0} \lambda_w \sum_{0}^{(P_{ws}-\tau_{in}-\Delta P_T-P_E)} (P_{ws} - p_w) f_w(p_w) \mathrm{d}p_w \tag{13}$$

The coefficients, k_R and k_{Pi}, correspond to the reduction in the price of surplus power sales and the increase in compensation price.

2.1.3 Fitness function

The objective of maximizing benefits can be attained by optimizing the profit function specified in Eq. (1).

$$max\{F\} \tag{14}$$

2.2 The constraints

2.2.1 Flow power system constraints

The operational constraints of the power transmission system are considered to consist of basic conditions related to the objective function as follows: conditions for optimizing societal benefits, conditions for maintaining the stability of transmission power, limits on bus voltage operation, and limits on transmission line capacity [25].

$$min\left\{\sum C_{\text{gen,i}}\right\} \tag{15}$$

$$P_{Gi} - P_{Di} - \sum_{j \in \text{bus}} V_i V_j \left(G_{ij} \cos\delta_{ij} + B_{ij} \sin\delta_{ij}\right) = 0 \tag{16}$$

$$Q_{Gi} - Q_{Di} - \sum_{j \in \text{bus}} V_i V_j \left(G_{ij} \sin\delta_{ij} + B_{ij} \cos\delta_{ij}\right) = 0 \tag{17}$$

$$V_{i \in \text{bus}}^{\min} \leq V_{i \in \text{bus}} \leq V_{i \in \text{bus}}^{\max} \tag{18}$$

$$S_{i \in \text{branch}} \leq S_{i \in \text{branch}}^{\max} \tag{19}$$

C_{gen} represents the cost of electrical sources; $P_{Gi}, Q_{Gi}, P_{Di}, Q_{Di}$ refers to the active and reactive power associated with generators and loads at the buses, and G_{ij}, B_{ij} signify the branch admittance; $S_i, S_i^{\max}$ indicate the apparent power of the operation and the rated capacity of branches; V_i represents the operating voltage of buses; the voltage phase difference between buses is denoted by δ_{ij}; and $V_i^{\min}, V_i^{\max}$ are the limited minimum and maximum of voltages.

2.2.2 Wind turbine condition constraints

In the condition of wind turbine operation, the wind speed at which the turbine can operate is limited. When the wind speed is too low, there is insufficient energy for the turbine blades to function. Conversely, in high wind conditions, such as during a storm, the turbine must be protected by folding the blades and ceasing operation. Additionally, the electrical power output of the wind turbine also adheres to the probability distribution of wind speed, specifically the Weibull distribution.

$$v_{in} \leq v \leq v_{\text{out}} \tag{20}$$

2.2.3 ESS operation condition constraints

The ESS system exists only when there is a benefit in constructing the system, including a wind plant. The stored energy with battery types, such as lithium batteries, is selected with cost and revenue as the following expressions [26],

$$C_{\text{ESS}} \leq R_{\text{ESS}} \tag{21}$$

$$\text{Chi phi } C_{\text{ESS}} = C_{\text{Inv}} + N_e C_O (1-\alpha) P_{\text{ESS}} \tag{22}$$

$$\text{Doanh thu } R_{\text{ESS}} = N_e \left(k_{P2} \lambda_w - \lambda_{\text{buy}}\right)(1-\alpha) P_{\text{ESS}} \tag{23}$$

ESS investment and operating costs are denoted as C_{Inv} and $C_O.N_e$

Defined by the deep discharge coefficient α, N_e indicates the total number of equivalent deep discharges throughout the ESS's operational life, with P_{ESS} representing its nominal capacity.

2.2.4 Regulatory and operational constraints in power market activities

The market mechanism, as day-ahead, is structured around the alignment of electricity supply and demand, considering both quantity and pricing criteria. Bidding data represent the proposed generation volumes and corresponding prices from electricity producers, alongside purchase bids from consumers or distribution entities. The matching conditions are expressed through Eqs. (24) và (25), as follows [27],

$$\min \left\{ \sum_{i}^{\text{Gen}} P_i^{\text{gen}} x \lambda_i \right\} \tag{24}$$

$$\sum_{i}^{\text{Gen}} P_i^{\text{gen}} = \sum_{j}^{\text{Load}} P_j^{\text{load}} \tag{25}$$

P_i^{gen} and λ_i are the power output and bidding price of power plant in the electricity market. Power output and offering prices are often based on electricity production costs for thermal power plants. This cost function is calculated according to expressions (26) to (28), as follows [21],

$$C_{Ti}(P_{Ti}) = a_i + b_i P_{Ti} + c_i P_{Ti}^2 \tag{26}$$

$$\lambda_{Ti} = \frac{\partial C_{Ti}}{\partial P_{Ti}} = b_i + c_i P_{Ti} \tag{27}$$

$$\lambda_w = k_w max\{\lambda_{Ti}\} \tag{28}$$

In the envisaged thermal power price, denoted as λ_{Ti}, the coefficients a_i, b_i, and c_i represent the cost factors associated with various types of turbines, contingent upon the primary kind of fuel used and turbine technology. $k_w \leq 1$ is the wind power price ratio compared to thermal power. When $k_w = 1$, the wind power price corresponds to source g, the thermal power source with the highest successful bid.

$$\lambda_w = \lambda_{Tg} = b_g + c_g P_{Tg} \tag{29}$$

Then, the wind power price adjustment coefficients in expressions (9) and (11)–(13) are calculated,

$$k_R = \frac{\lambda_{Rw}}{\lambda_w} = \frac{b_g + c_g\left(P_{Tg} - \Delta P_w\right)}{b_g + c_g P_{Tg}} = \left(1 - \frac{c_g \Delta P_w}{\lambda_w}\right) \tag{30}$$

$$k_{P1} = \frac{\lambda_{Tg}}{\lambda_w} = 1 \tag{31}$$

$$k_{P2} = \frac{\lambda_{Ew}}{\lambda_w} = \frac{1}{\lambda_w}\left[\frac{C_{\text{Inv}}}{N_e(1-\alpha)P_{\text{ESS}}} + C_O + \lambda_{\text{buy}}\right] = \frac{1}{\lambda_w}\left(UIC_{\text{ESS}} + C_O + \lambda_{\text{buy}}\right) \tag{32}$$

$$k_{P0} = \frac{\lambda_{Pw}}{\lambda_w} = \frac{b_g + c_g\left[P_{Tg} + \Delta P_w - \Delta P_T - (1-\alpha)P_{ESS}\right]}{b_g + c_g P_{Tg}} = \left(1 + \frac{c_g\left[\Delta P_w - \Delta P_T - (1-\alpha)P_{ESS}\right]}{\lambda_w}\right) \tag{33}$$

3 Optimization methods

The continued prominence of the MH algorithm in optimization problems is attributed to its effectiveness in managing the intricacies of nonlinear target functions, which many other algorithms struggle with [28]. This reference also emphasizes that algorithms in the evolutionary techniques group, along with their advancements, frequently lead in both theoretical research and practical applications, with GA serving as a notable example developed in this paper due to its widespread applicability in the energy sector. Regarding the LSTM algorithm, a boosted RNN, it is one of the most widely used deep learning tools for time series prediction [29]. LSTM has the capability to maintain long-term information and continuously update parameters, enabling effective handling of complex data sequences. By leveraging these strengths and its ability to operate under limited data conditions,

integrating gene prediction using LSTM after learning from previous evolutionary processes into subsequent hybridization with GA further optimizes the management of complex data.

3.1 GA algorithm

The primary genetic algorithm relies on evolution over multiple generations, wherein each generation consists of one or several populations undergoing some main activities: selection, crossover, and mutation [30]. Each individual in the population is characterized by a chromosome containing a gene sequence. The information in each gene represents the value of a variable initialized at the start and changing across generations. Consequently, each chromosome constitutes a complete set of variables within the objective function. Therefore, the objective function value calculated for each individual is assessed to determine its survival within the population, and the ultimate best deal will be the solution to the problem at hand.

The implementation steps of the GA algorithm are as follows:

(i) Step 1: Randomize the initial population with a predetermined number of individuals.
(ii) Step 2: Evaluate the objective function for all individuals in the population. Order and select the best individuals for comparison with the best individual of the previous generation and record the superior individuals.
(iii) Step 3: Select individuals adapted to survive while eliminating the remaining individuals. This selection can follow specific rules, such as Tournament Selection, Rank Selection, or other selection rules.
(iv) Step 4: Perform crossover between parents to generate offspring. Crossover techniques may include single-point and double-point, Uniform Crossover, or other crossover methods.
(v) Step 5: Mutate the genes of some individuals at a specific rate. This operation aims to accelerate convergence or escape from loops that may lead to local optima. Various mutation techniques exist, such as Power Mutation, Uniform Mutation, and others.

After each computing step 2 to 4, a new generation is created in the population. This process is repeated continuously until the problem is solved.

3.2 LSTM techniques

LSTM, introduced by Hochreiter and Schmidhuber [31], is a neural network architecture rooted in the deep learning theory of RNNs to address their limitations. It comprises interconnected and recurrent network units called cells strategically designed to retain gradient values over short and long intervals. Using memory cells to store information, LSTM demonstrates enhanced capabilities in discovering and utilizing long-range contextual dependencies, as depicted in Fig. 1a.

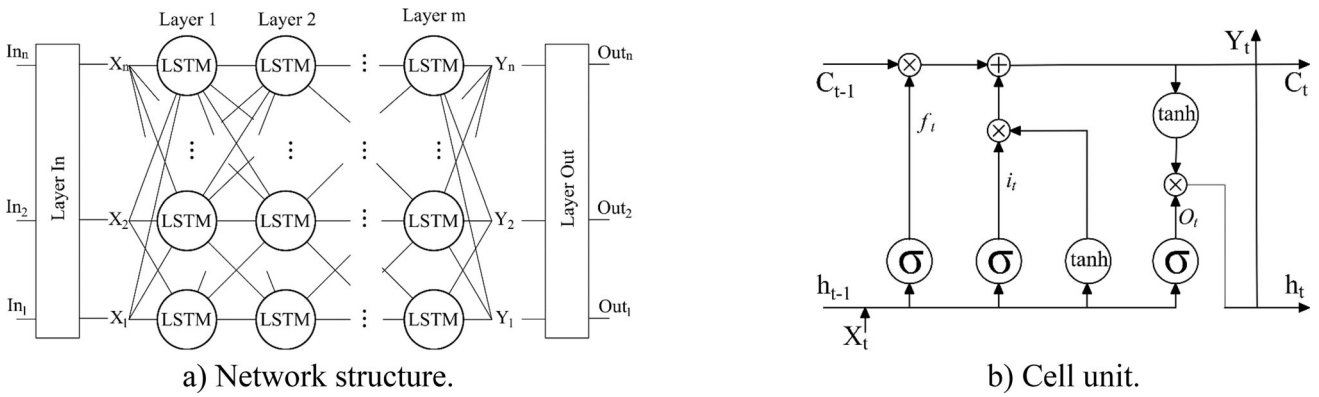

Fig. 1 Design of LSTM

$$f_t = \sigma\left(W_f X_t + W_{Hf} h_{t-1} + b_f\right) \tag{34}$$

$$i_t = \sigma(W_i X_t + W_{Hi} h_{t-1} + b_i) \tag{35}$$

$$O_t = \sigma(W_o X_t + W_{Ho} h_{t-1} + b_o) \tag{36}$$

$$C_t = C_{t-1} \otimes f_t + i_t \otimes \tanh(W_c X_t + W_{Hc} h_{t-1} + b_c) \tag{37}$$

$$h_t = O_t \otimes \tanh(C_{t-1}) \tag{38}$$

Equations (34) to (38) define the mathematical formulation that captures the input–output behavior of each memory cell within the LSTM architecture, in [32]. These memory cells are organized into multiple hidden layers, which form the core of the LSTM units forming the hidden layer between input and output. As shown in Fig. 1(b), the overall network comprises at least three main components: an input layer, a sequence of LSTM layers, and a final output layer responsible for producing the data output.

At each time step t, the updated memory state and the corresponding hidden unit are computed as shown in Eqs. (37) and (38). The forget gate, input gate, and output gate—essential components in regulating the flow of information—are mathematically formulated in Eqs. (34) through (36). Nonlinear transformations are performed using the sigmoid (σ) and hyperbolic tangent (tanh) functions. Interactions between the input, memory, and output units within hidden layers are captured via element-wise multiplication, denoted by the symbol $\otimes$. The hidden state from the previous time step, h_{t-1}, contributes to the current computations through element-wise addition with the learned weight parameters. These parameters are encoded as matrix weights $W(f, i, O, C)$ and biases $b(f, i, O, C)$, which vary across different gates. After processing these elements, the resulting internal state is stored in C_t, representing the current cell memory. During the training process with historical data, the weight matrix and bias variables gradually adapt to the predicted data. The more accurate and complete the training data, the more these matrices tend toward stable convergence.

3.3 Hybrid LSTM-GA algorithm

The hybrid algorithm is built on the basis of the evolutionary process, as shown in Fig. 2a. The key difference is the integration of an additional phase in which a number of modern individuals appear in the population of each generation. These modern individuals have superior genetic sets predicted based on the LSTM algorithm, leveraging deep learning from the evolutionary process of past genetic sets. These individuals then continue to

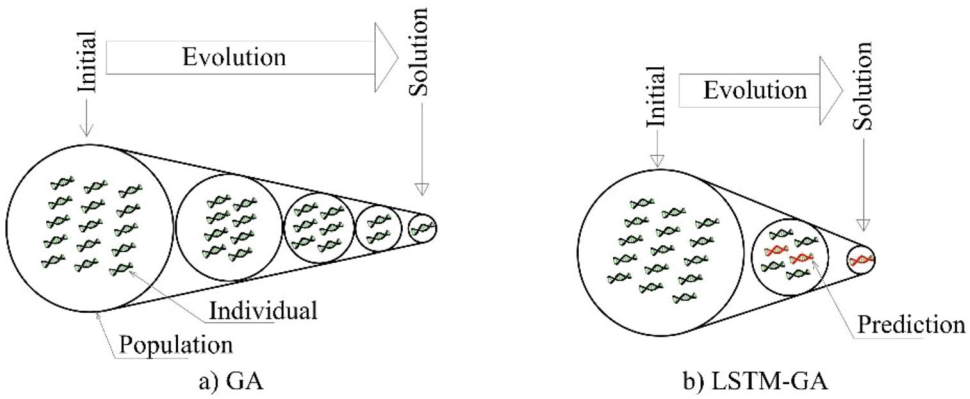

Fig. 2 Evolutionary progression

evolve according to the GA algorithm, which shortens the convergence cycle, as illustrated in Fig. 2b. The algorithm process is further detailed in Fig. 3, with the following steps:

(i) Step 1:

Initialize power system parameters. Generators, loads, buses, and branches parameters.

Initialize wind speed PDF data basing on the Weibull distribution. Construction of wind power probability distribution.

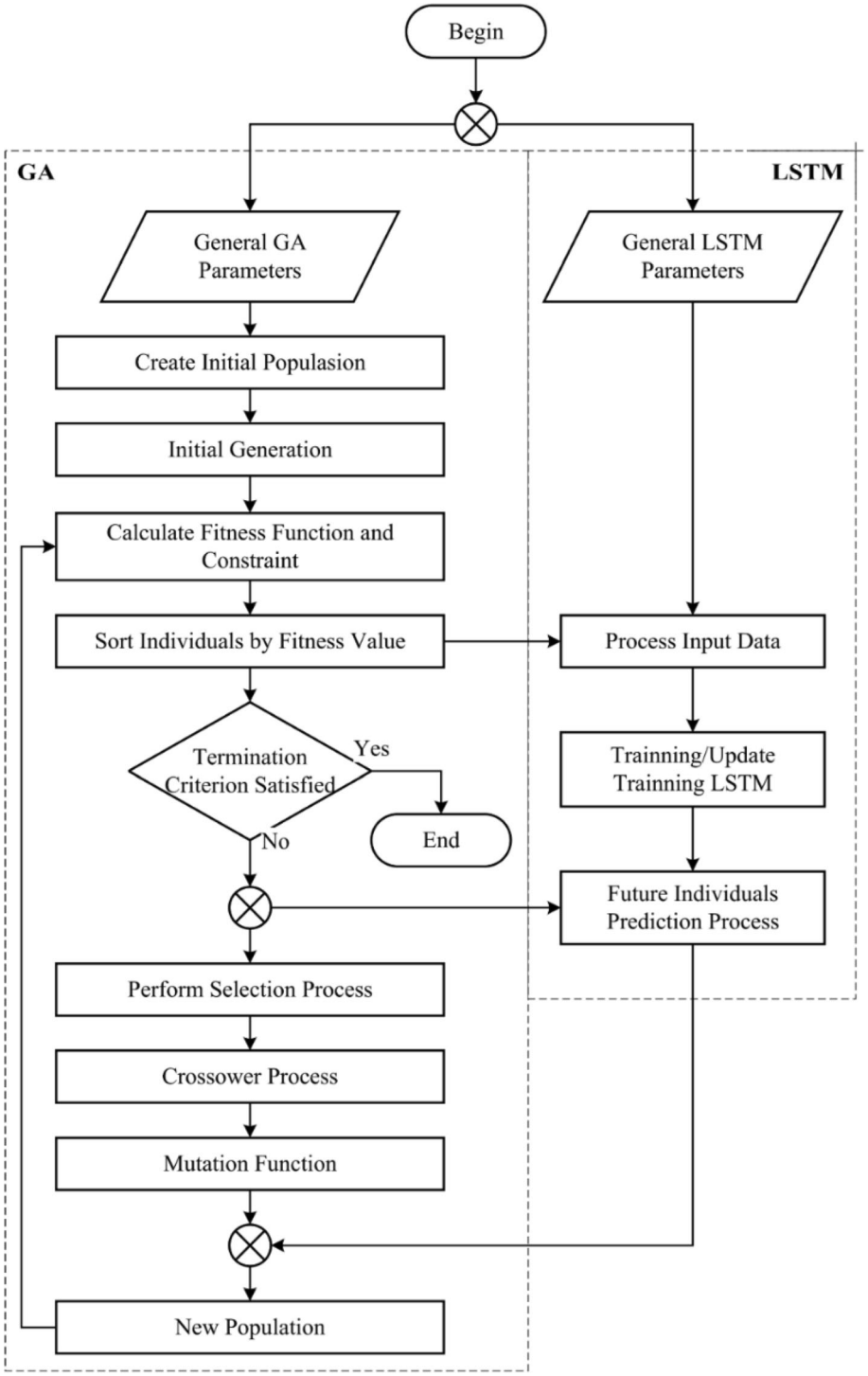

Fig. 3 Flowchart of LSTM-GA Algorithm

Configure GA parameters. Choose methods and ratios for selection, crossover, mutation, and prediction processes.

Initiating the LSTM parameters involves choosing the depth of intermediate LSTM layers, the architecture of the layer neuron, and the corresponding parameters.

(ii) Step 2: The predefined quantity is used to randomly initialize the population.
(iii) Step 3: Perform an OPF assessment on the power system, incorporating system limits, then calculate the adjustment factors for the wind power selling price. Finally, evaluate the objective function for each individual within the population.
(iv) Step 4: Implement hybrid model. With GA, the selection, crossover, and mutation processes are executed. LSTM processes individual datasets to fit the LSTM input layer architecture. Training for the initialization and update training will be gradually updated with subsequent iterations. Predict future individuals.
(v) Step 5: Construct a population for the new generation consisting of selected individuals, offspring from crossover, and mutated individuals, considering predicted individuals.
(vi) Step 6: Continue iterating through steps (iii) to (v) until the problem's termination condition is satisfied.

The proposed method's algorithmic procedure is depicted in the flowchart shown in Fig. 3. The diagram features two vertical processes: the left side outlines the fundamental steps of the traditional Genetic Algorithm (GA), while the right side depicts the operational sequence of the LSTM model. A distinctive feature of the proposed algorithm is the integration of these two processes, which are interwoven during critical stages, as shown in the figure. Initially, both processes operate independently. The input data for the LSTM is pre-processed using the genetic structures of individuals from the GA population. While the GA evolution process remains separate from LSTM's prediction phase, the predicted advanced gene structures generated by the LSTM are reintegrated into the population, enhancing subsequent evolutionary iterations of the GA. These advanced gene structures accelerate the evolutionary process toward the objective. Meanwhile, the evolved gene pool undergoes continuous learning by the LSTM, which updates its network weights for the next prediction phase. This iterative cycle of prediction and evolution continues until the algorithm achieves its objective or meets predefined termination criteria. This synergistic integration of GA and LSTM not only enhances the algorithm's efficiency but also leverages the strengths of both methods, enabling rapid convergence to optimal solutions.

4 Test and discuss

4.1 Data of test

The experimentation is carried out using the IEEE 30-bus power system as a reference model [33]. The system consists of a total of six power sources, including both thermal and wind energy plants, connected through thirty nodes and forty-one branches, as detailed in the case_ieee30.m file from the MATPOWER reference [34]. Specifically, four thermal power plants are positioned at nodes 1, 2, 8, and 13. Additionally, two wind farms are incorporated at nodes 5 and 11. Each wind turbine within these farms has a rated power capacity of 3 MW, and operates within the following wind speed parameters: v_{in} = 3m/s (cut-in speed), v_r = 16m/s (rated speed), and v_{out} = 25m/s (cut-out speed). The wind farm at bus 5 hosts 25 turbines, while the one at bus 11 contains 20 turbines. The wind farm at bus five was chosen for comparative evaluation in the test problem, and the data was examined in Vietnam, as shown in Table 1. The wind power source at bus 11 assumes Weibull data, as outlined in the reference [21].

The GA design is based on the methodology described in [30]. The evolutionary process modifies genes to achieve the desired objective. Through successive generations, the population in each generation undergoes three fundamental evolutionary operations: selection, crossover, mutation, and prediction. The input parameters are

Table 1 Specification of wind plants

Wind power generation plants				
Wind farm #	No. of turbines	Rate power, P_{wr}(MW)	Weibull PDF parameter	Weibull mean,M_{wbl}
11	20	60	c = 10, k = 2	v = 8.862m/s

[a]Corresponds to the compensation coefficient of 1.6

provided in Table 2. The structure of the chromosome is illustrated in Fig. 4. In this design, gene 1 represents the WPD. Gene 2 corresponds to the peak power generation eligible for reimbursement in wind plants, representing the upper limit of energy production eligible for financial compensation. Gene 3 refers to the capacity bidding value of thermal generators that are associated with wind farms, indicating the amount of power these plants are willing to offer in coordination with the wind farm's operation. Gene 4 quantifies the penalty rate increase, which is applied in relation to the spot market electricity selling price, highlighting the extent to which penalties escalate when the market price fluctuates.

The design of the LSTM model is based on the framework provided in [29]. It incorporates several essential components, starting with input layers that process the data, followed by the LSTM hidden layers that capture the temporal dependencies. To prevent overfitting, a dropout layer is included, enhancing the model's generalizability. The architecture also features a fully connected layer, which generates the output response, and a regression layer that produces the final prediction. The parameters used in the model are detailed in Table 3. The model utilizes five input features, comprising the four variables in the chromosome and the fitness value of the corresponding individual.

The integration of LSTM into GA is updated according to the flowchart illustrated in Fig. 3.

4.2 Result of test

Assuming 15 identical test runs for each algorithm to observe the convergence process and compare the optimal results of the original GA and LSTM-GA.

4.2.1 Convergence process

The two radar charts in Fig. 5 illustrate the convergence process of experiments conducted on two algorithms: the original GA in (a) and the LSTM-GA hybrid in (b). The innermost circle represents the solution to the problem, with each dot signifying an optimization point in the iterative process. As iterations progress, the dots become increasingly darker red, with the darkest red indicating the final iteration, corresponding to the solution. Overall, the optimal values exhibit a clear tendency to converge toward the center of the circle across iterations. However, the hybrid algorithm in (b) demonstrates a significantly more concentrated trend toward the center compared to the more dispersed distribution observed with the original algorithm in (a). This suggests a faster convergence

Table 2 Input parameters of GA

Parameters	Original GA	Hybrid GA
Population	50	50
Crossover rate	0.8	0.8
Mutation rate	0.1	0.1
Prediction rate	0	0.05
Maximum iterations	20	20
Evolutionary Activity	3 actions (selection, crossover, mutation)	4 actions (selection, crossover, mutation, forecast)

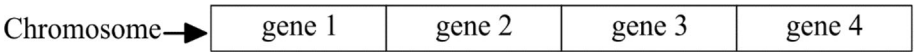

Fig. 4 Structure of a chromosome

Table 3 Input and train parameters of LSTM

Initial architecture		Training	
Parameters	Value	Parameters	Value
Input layers	01	Maximum epochs	100
LSTM layers	120	Gradient threshold	1
Output layers	02	Initial learn rate	0.001
Dropout rate	0.2	Learn rate drop period	20
Features	5	Minimum batch size	20

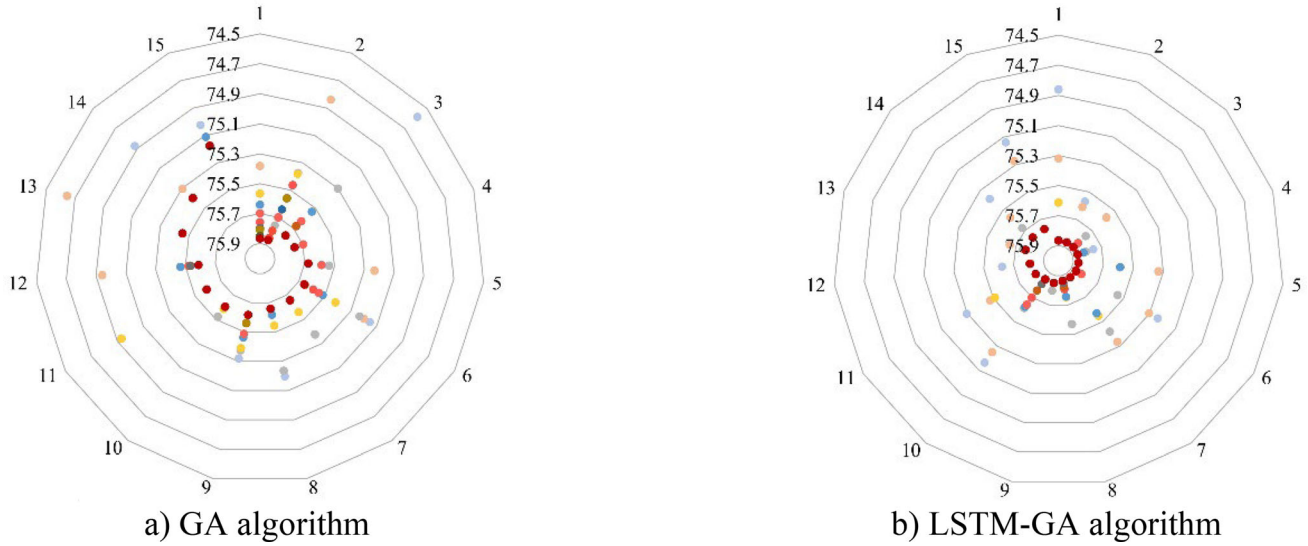

Fig. 5 Convergence process of the algorithms

rate for the hybrid algorithm, evident from the dense spiral pattern of darker dots near the central circle in (b). Furthermore, in (a), the points are scattered in the outer circles during the initial iterations and then gradually progress evenly toward the center. In contrast, in (b), the points are similarly dispersed during the early iterations but subsequently exhibit sudden leaps and rapid spirals toward the center. Thus, during the initial generations of the evolutionary process, both algorithms exhibit similar behaviors, with the LSTM component having limited influence. However, as the generations advance, the LSTM component significantly accelerates the hybrid algorithm, enabling it to overcome obstacles and efficiently reach the solution.

Figure 6 provides a clearer depiction of the experimental results, illustrating the solution trajectory across multiple trials and comparing two algorithms, GA and LSTM-GA. Each dot represents the solution value at a particular iteration within a single trial. Evidently, the dispersion of dots in (a) is broader than in (b), indicating that the new algorithm demonstrates stronger convergence capabilities. By the final iteration, the dots in (a) remain dispersed, whereas those in (b) are nearly concentrated into a single point. This suggests that the original algorithm's solutions may exhibit greater error, whereas the hybrid algorithm achieves higher precision. Furthermore, during the initial phase (iterations 1 through approximately 10), the graph in (b) exhibits a steeper and smoother slope, particularly after iterations 4–5. In contrast, the graph in (a) shows occasional plateaus or abrupt jumps in solution values. This demonstrates that the hybrid algorithm maintains consistent progress across

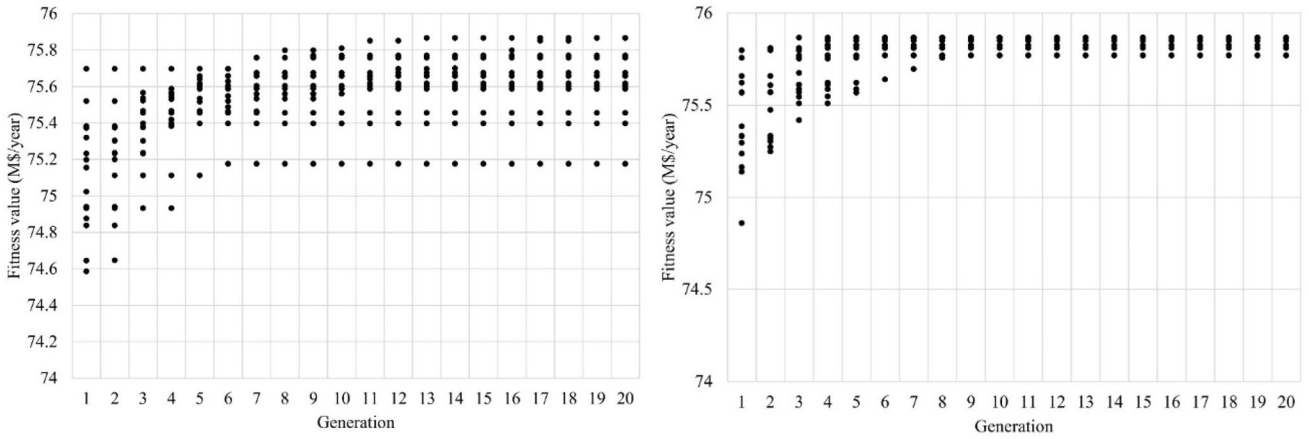

Fig. 6 Test runs of the algorithms

iterations, while the original algorithm may become locally stagnant, showing no improvement over several generations before a sudden leap.

To conclude, the early stage of optimization techniques, iterations 1 through approximately 6, are nearly identical. This indicates that integrating LSTM does not influence performance during this phase, as clearly illustrated in Fig. 7, which compares a typical test run of both algorithms. However, the hybrid method achieves the target faster after about five subsequent iterations, stabilizing around iteration 9, as opposed to extending to iteration 14 in the original algorithm (see the GA convergence points in the figure). More specifically, the steep gradient in the hybrid algorithm's graph between iterations 4 and 8, as shown in the figure, demonstrates the optimal exploitation of LSTM for predicting superior genomes during this phase. Therefore, it is recommended to continuously update and train the LSTM model during the initial stages without deploying predictions until after iteration 4 in the test problem presented in this paper. This approach reduces the time required for prediction execution and accelerates the hybrid algorithm's performance. Further investigation into this critical timing is essential to establish principles for optimizing hybrid algorithms, which is a crucial direction for future research following this study.

4.2.2 Optimize wind power auction performance

Following the model that links wind plants, thermal power, and ESS in the test, the benefits of the joint venture group are guaranteed to be optimal, as shown in Table 4, as a result of the LSTM-GA algorithm. The detailed average results are $WPD_{bus5} = -16.7\%$, $WPD_{bus11} = -16.4\%$, $P_{ESS5} = 9$ MW, and $P_{ESS11} = 10$ MW. In this table, the recommended reduced wind power auction capacity bias is approximately 15–18% of predicted wind

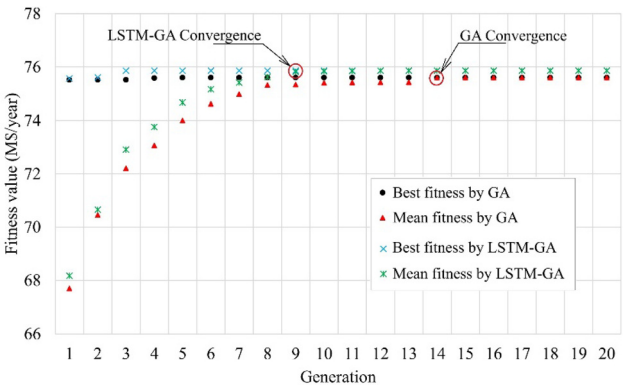

Fig. 7 Comparison of GA and LSTM-GA implementations

Table 4 Optimization of wind revenue by LSTM-GA

Executions	WPD (%)		ESS power (MW)			Revenue (M$/year)
	bus 5	bus 11	bus 5	bus 11	Sum	
1	− 15.9	− 16.4	11	8	19	75.9
2	− 17.2	− 16.5	20	12	32	75.8
3	− 18.2	− 15.9	6	15	21	75.8
4	− 15.8	− 16.0	6	9	15	75.9
5	− 15.7	− 16.8	5	9	14	75.9
6	− 17.3	− 17.1	6	14	20	75.8
7	− 18.4	− 15.8	18	7	25	75.8
8	− 15.8	− 16.1	5	10	15	75.9
9	− 15.7	− 16.1	3	15	18	75.9
10	− 15.9	− 16.0	6	12	18	75.9
11	− 18.3	− 16.2	10	4	14	75.8
12	− 18.3	− 16.2	10	4	14	75.9
13	− 16.4	− 16.4	14	14	28	75.9
14	− 16.1	− 16.4	5	12	17	75.9
15	− 16	− 17.5	11	11	22	75.9
Mean	− 16.7	− 16.4	9	10	19	

generation at bus 5 and about 16–17% at bus 11, based on wind data from [21]. At that time, the optimal proposed storage capacity is about 19 MW to achieve the maximum revenue target.

Compared to the optimal results from the GA algorithm and previous research by [7], Table 5 shows a decrease in wind power bidding across all proposed scenarios, with WPD being negative. However, the reduction gradually lessens from scenarios 1 to 3, and the LSTM-GA scenario exhibits the lowest stability in WPD values, ranging from − 15 to − 18%. This result suggests that recommendation wind power bidding is 20% higher than in scenario 1 and about 12% higher than in scenario 2. This approach helps improve investment efficiency and supports the sustainable development of wind energy.

In the context of an electricity market operating under particular electricity price indices and penalty schemes, the uncertainties associated with the specified Weibull parameters are accounted for by the findings from the experiments, which are informed by the input data outlined in Sect. 4.1. In regions with varying wind speeds, which lead to different uncertainty profiles, the wind speed probability distribution function will adjust the computational results according to the formulas (7) to (13) from Sect. 2.1.2. In the same vein, the volatility in the market, driven by fluctuations in price indices, will influence the outcomes as defined by Eqs. (24) to (33) in Sect. 2.2.4. The exploration of these factors could be considered for future investigations beyond the current study.

Table 5 Compare optimal wind power bidding in the scenarios

Scenarios	Optimal methods	WPD (%)		ESS power (MW)	Wind power output (MW)	Revenue (M$/year)
		Wind bus 5	Wind bus 11			
1	MILP in [7][a]	-30%	-30%	10	95	71
2	GA	(− 15%) ÷ (− 28%)	(− 16%) ÷ (− 28%)	18	97 ÷ 114	75.9
3	LSTM-GA	(− 15%) ÷ (− 18%)	(− 16%) ÷ (− 17%)	19	111 ÷ 114	75.9

4.2.3 Testing on IEEE 118-bus system

The 118-bus benchmark system comprises 54 generators, 2 reactors, 12 capacitors, 9 transformers, and 186 transmission branches, from the case118.m file in the MATPOWER library [34]. Two wind power plants, each with a maximum capacity of 400 MW, are assumed to be installed at buses 59 and 116, consistent with [35]. The specifications of the wind power sources and associated energy storage systems are provided in the previous section. In the electricity market, the penalty rate for wind power shortage is set at 1.6. The structures and parameters for both the GA and LSTM-GA algorithms follow the descriptions provided earlier. The experimental results for these approaches appear in Fig. 8.

Running 100 generations for each algorithm yields example results showing stable convergence around the objective of M$460–470. These outcomes correspond to the following optimal proposals: WPD in the range of 17–19%, wind power output between 650 and 660 MW, and ESS maximum power of 75–88 MW. As Fig. 8 shows, the algorithm incorporating LSTM clearly converges faster, stabilizing around generation 20, while the original GA takes up to generation 50 to reach similar stability. This indicates that as system complexity increases, the effectiveness of integrating LSTM-based predictive elements into the GA search process becomes more evident.

4.2.4 Testing the OPF problem on the IEEE 30-bus system

The proposed algorithm addresses the OPF problem on the IEEE 30-bus system from [36]. The results show comparisons with four models to improve the GA algorithm as presented in [20], including: [A] penalties in the GA; [B] GA with adjusting population size; [C] GA with multiple points; and [D] GA with specific initial constraints.

As shown in Table 6, there is a marked reduction in the iteration count we compare to similar studies on the population size per generation. Although the optimal cost results do not differ significantly from those in previous studies, the efficiency gains are evident. Notably, the NFFE index is substantially lower, showing a 22% reduction compared to the most recent study [37]. This indicates that the proposed algorithm achieves faster performance due to reduced computational processing demands.

Furthermore, Fig. 9 provides additional insights into the algorithm's performance. It illustrates that the benefits of the integration become evident only after the loop has passed 10 generations. This delay suggests an initial period where the algorithm calibrates and stabilizes before realizing its full potential. The most pronounced effectiveness is observed between generations 10 and 40, where the algorithm demonstrates optimal performance improvements. This period of heightened efficiency suggests that the integration strategy is particularly effective during these generations, resulting in faster convergence and improved optimization outcomes.

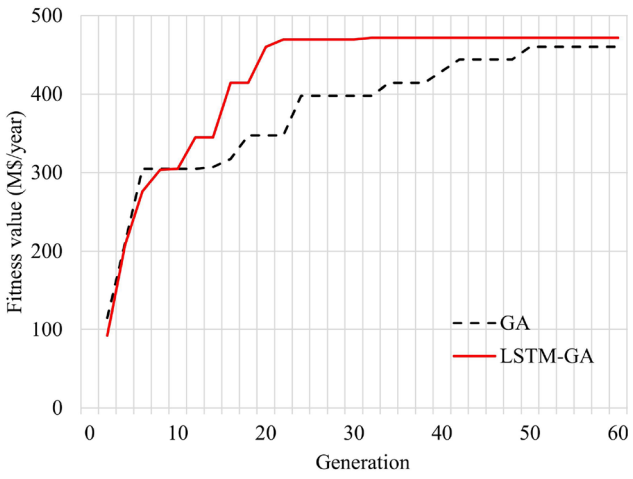

Fig. 8 Convergence on 118-bus System

Table 6 Assessment of different methodological approaches

Ref	[A]	[B]	[C]	[D]	LSTM-GA
Populations	80	400	50	200	50
Generations	200	50	200	500	156
NFFE	16,000	~ 17,000	10,000	12,000	~ 7800
Cost ($)	802.06	799.84	801.49	801.05	800.74

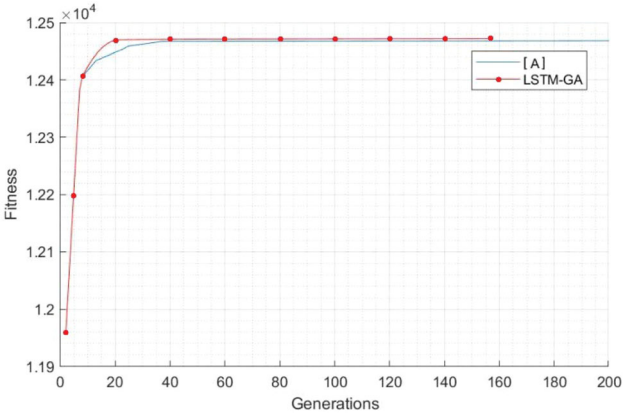

Fig. 9 Comparison of [36] and proposed algorithm

5 Conclusion

The novelty of the proposed hybrid algorithm in this study lies in its enhancement of GA's optimization performance by leveraging the predictive capabilities of LSTM—distinct from prior research, which primarily focuses on using GA to optimize the weights and architectures of LSTM or other neural networks for improved prediction tasks.

Specifically, the proposed method integrates GA and LSTM in a manner that demonstrates strong potential in both theoretical and practical domains. From a theoretical standpoint, the LSTM-predicted superior genetic sets contribute to faster and more diverse evolutionary processes within the GA framework. Experimentally, the hybrid algorithm achieves a notable reduction in convergence time, shortening the process by approximately five generations in the IEEE 30-bus system, and up to 25 in the 118-bus system. Additionally, the experimental results show that the algorithm has a greater ability to escape local optima, as LSTM predictions can explore solution spaces beyond the boundaries of local peaks.

Moreover, this approach opens promising avenues for future research, particularly in the integration of deep learning techniques with meta-heuristic optimization algorithms. It may inspire the development of novel hybrid frameworks that were beyond the scope of this study and could be extended to a wide range of application domains beyond power system optimization. Notably, the advantages of the proposed method become increasingly evident in large-scale systems with high dimensionality and complex dynamics, especially in environments characterized by the inherent variability and unpredictability of renewable energy sources.

Importantly, the proposed technique also addresses a critical challenge in assessing revenue efficiency in dynamic electricity markets, particularly those with high penetration of wind power. The inherent uncertainty of wind generation introduces real-time fluctuations and operational instability, affecting electricity prices and the profitability of market participants. The interactive and competitive nature of bidding behavior further complicates the optimization landscape, presenting a high-dimensional problem with numerous local optima. Experimental results have demonstrated that the proposed hybrid algorithm not only achieves faster convergence but also yields superior solutions compared to conventional methods, such as MILP, standard GA, and recently developed GA-based variants in OPF. This performance advantage is particularly evident in scenarios with high

renewable integration, where uncertainty and complexity pose significant challenges for traditional optimization techniques.

By applying the LSTM-GA algorithm to both the IEEE 30-bus and 118-bus test systems, this study confirms its effectiveness in improving operational efficiency in systems integrating wind power, thermal generation, and energy storage. Furthermore, the results highlight the algorithm's broader applicability to a range of complex power system optimization problems, including optimal power flow, generation expansion planning, and transmission system expansion in large-scale networks.

Author contribution Anh Viet Truong provided ideas and checked them. Sang Ngoc Dinh wrote the introduction, discussion, and conclusion. Binh Le Song Dinh wrote the codes. All authors reviewed the manuscript.

Funding No financial support was received to develop this manuscript.

Data availability Data sharing is not applicable to this article as no new data were created or analyzed in this study.

Declarations

Conflict of interests The authors declare no competing interests.

Ethical approval Not applicable.

Consent to participate The authors are committed to actively contributing to the article.

Consent for publication The authors commit to publishing the article upon acceptance.

References

1. Birkeland D, AlSkaif T (2024) Research areas and methods of interest in European intraday electricity market research—a systematic literature review. Sustain Energy, Grids Netw 38:101368
2. Haugen M, Farahmand H, Jaehnert S, Fleten S-E (2023) Representation of uncertainty in market models for operational planning and forecasting in renewable power systems: a review. Energy Syst 6:1–36
3. Ribeiro MHDM, Silva RGD, Moreno SR, Canton C, Larcher JHK, Stefenon SF, Mariani VC, Coelho LDS (2024) Variational mode decomposition and bagging extreme learning machine with multi-objective optimization for wind power forecasting. Appl Intell 54:3119–3134
4. Mohamed E, Seresht NG, Jafari P, AbouRizk S (2024) Risk assessment for onshore wind projects in Canada. Renew Sustain Energy Rev 191:114145
5. Hu X, Jaraitė J, Kažukauskas A (2021) The effects of wind power on electricity markets: a case study of the Swedish intraday market. Energy Econ 96:105159
6. Schlecht I, Maurer C, Hirth L (2024) Financial contracts for differences: the problems with conventional CfDs in electricity markets and how forward contracts can help solve them. Energy Policy 186:113981
7. Truong VA, Dinh NS, Duong TL (2024) Profit maximization of wind power plants in the electricity market based on linking models between energy sources. Arabian J Sci Eng 49:6275–6291
8. Kumar K, Prabhakar P, Verma A, Saroha S, Singh K (2024) Advancements in wind power forecasting: a comprehensive review of artificial intelligence-based approaches. Multimed Tools Appl 1573–7721:2024
9. Ghimire S, Deo RC, Casillas-Pérez D, Salcedo-Sanz S (2024) Two-step deep learning framework with error compensation technique for short-term, half-hourly electricity price forecasting. Appl Energy 353:122059
10. Yang Y, Lou H, Wu J, Zhang S, Gao S (2024) A survey on wind power forecasting with machine learning approaches. Neural Comput Appl 36:12753–12773
11. Cao D, Hu W, Xu X, Dragičević T, Huang Q, Liu Z, Chen Z, Blabjerg F (2020) Bidding strategy for trading wind energy and purchasing reserve of wind power producer—a DRL based approach. Electr Power Energy Syst 117:105648
12. Velasco L, Guerrero H, Hospitaler A (2024) A literature review and critical analysis of metaheuristics recently developed. Arch Comput Methods Eng 31:125–146
13. Hosseini E, Reinhardt L, Rawat DB (2022) Optimizing gradient methods for IoT applications. IEEE Internet Things J 9(15):13694–13704

14. Qais M, Hasanien H, Alghuwainem S (2019) Enhanced salp swarm algorithm: application to variable speed wind generators. Eng Appl Artif Intell 80:82–96
15. Bhagat SK, Tiyasha T, Shather AH, Jamei M, Kumar A, Al-Khafaji Z, Goliatt L, Shafik SS, Alawi OA, Yaseen ZM (2024) Wind speed prediction and insight for generalized predictive modeling framework: a comparative study for different artificial intelligence models. Neural Comput Appl 36:14119–14150
16. Hosseini E, Al-Ghaili AM, Kadir DH, Gunasekaran SS, Ahmed AN, Jamil N, Deveci M, Razali RA (2024) Meta-heuristics and deep learning for energy applications: review and open research challenges (2018–2023). Energy Strategy Rev 53:101409
17. Sagu A, Gill NS, Gulia P, Singh PK, Hong W-C (2023) Design of metaheuristic optimization algorithms for deep learning model for secure IoT environment. Sustainability 15(3):2204
18. Kara A, Pekel E, Ozcetin E, Yıldız GB (2024) Genetic algorithm optimized a deep learning method with attention mechanism for soil moisture prediction. Neural Comput Appl 36:1761–1772
19. Bacanin N, Jovanovic L, Zivkovic M, Kandasamy V, Antonijevic M, Deveci M, Strumberger I (2023) Multivariate energy forecasting via metaheuristic tuned long-short term memory and gated recurrent unit neural networks. Inf Sci 642:119122
20. Georgios P, Pandelis B (2023) Review and comparison of genetic algorithm and particle swarm optimization in the optimal power flow problem. Energies 16(3):1152
21. Biswas PP, Suganthan PN, Amaratunga GAJ (2017) Optimal power flow solutions incorporating stochastic wind and solar power. Energy Convers Manage 148:1194–1207
22. "Energy prices and Costs in Europe: report from the commission to the european parliament, the council, the european economic and social committee and the committee of the regions. European Commssion, Brussels, 2020
23. Wang Z, Wang W, Liu C, Wang Z, Hou Y (2018) Probabilistic forecast for multiple wind farms based on regular vine copulas. IEEE Trans Power Syst 33(1):578–589
24. Wais P (2017) A review of Weibull functions in wind sector. Renew Sustain Energy Rev 70:1099–1107
25. Abedi A, Hesamzadeh MR, Romerio F (2022) Adaptive robust vulnerability analysis of power systems under uncertainty: a multilevel OPF-based optimization approach. Int J Electr Power Energy Syst 134:107432
26. Cao M, Xu Q, Qin X, Cai J (2020) Battery energy storage sizing based on a model predictive control strategy with operational constraints to smooth the wind power. Int J Electr Power Energy Syst 115:1–10
27. Bertrand G, Papavasiliou A (2018) An analysis of threshold policies for trading in continuous intraday electricity markets, In: 2018 15th international conference on the European energy market (EEM), Lodz, Poland
28. Salgotra R, Sharma P, Raju S, Gandomi AH (2024) A contemporary systematic review on meta-heuristic optimization algorithms with their MATLAB and Python code reference. Arch Comput Methods Eng 31:1749–1822
29. Al-Selwi SM, Hassan MF, Abdulkadir SJ, Muneer A, Sumiea EH, Alqushaibi A, Ragab MG (2024) RNN-LSTM: from applications to modeling techniques and beyond—systematic review. J King Saud Univ-Comput Inf Sci 36(5):102068
30. Mirjalili S (2019) Genetic Algorithm. In: Mirjalili S (ed) Evolutionary Algorithms and Neural Networks, vol 780. Springer Cham, UK p, pp 43–55
31. Hochreiter S, Schmidhuber J (1997) Long short-term memory. Neural Comput 9(8):1735–1780
32. Shahid F, Zameer A, Muneeb M (2021) A novel genetic LSTM model for wind power forecast. Energy 223:120069
33. Alsac O, Stott B (1974) Optimal load flow with steady-state security. IEEE Trans Power Appar Syst PAS-93(3):745–751
34. Zimmerman RD, Murillo-Sánchez CE, Thomas ARJ (2011) MATPOWER: steady-state operations, planning, and analysis tools for power systems research and education. IEEE Trans Power Syst 26(1):12–19
35. Moradi-Sepahvand M, Amraee T (2023) Secure expansion of energy storage and transmission lines considering bundling option under renewable penetration. Appl Energy 347:121414
36. Bakirtzis A, Biskas P, Zoumas C, Petridis V (2002) Optimal power flow by enhanced genetic algorithm. IEEE Trans Power Syst 17(2):29–236
37. Lai L, Ma J, Yokoyama R, Zhao M (1997) Improved genetic algorithms for optimal power flow under both normal and contingent operation states. Int J Electr Power Energy Syst 19(5):287–292

https://doi.org/10.1007/s00521-025-11582-y

Authors and Affiliations

Ngoc Sang Dinh[1,2] · Le Song Binh Dinh[3] · Viet Anh Truong[1]

✉ Ngoc Sang Dinh
sangdn.ncs@hcmute.edu.vn

[1] Hochiminh City University of Technology and Education (HCMUTE), Ho Chi Minh City, Vietnam

[2] University of Architecture Hochiminh City (UAH), Ho Chi Minh City, Vietnam

[3] Industrial University of Hochiminh City (IUH), Ho Chi Minh City, Vietnam

Ain Shams Engineering Journal 16 (2025) 103285

Contents lists available at ScienceDirect

Ain Shams Engineering Journal

journal homepage: www.sciencedirect.com

Hybrid LSTM-PSO optimization techniques for enhancing wind power bidding efficiency in electricity markets

Viet Anh Truong [a], Ngoc Sang Dinh [a,c,*], Thanh Long Duong [b], Ngoc Thien Le [c], Cong Dinh Truong [c], Linh Tung Nguyen [d]

[a] Hochiminh City University of Technology and Education, Ho Chi Minh City 71300, Viet Nam
[b] Industrial University of Hochiminh City, Ho Chi Minh City 71400, Viet Nam
[c] University of Architecture Hochiminh City, Ho Chi Minh City 72400, Viet Nam
[d] Electric Power University, Ha Noi City 11900, Viet Nam

ARTICLE INFO

Keywords:
Optimal algorithm
Long short-term memory
Particle swarm optimization
Wind farm
Electricity market

ABSTRACT

Past research has predominantly focused on utilizing meta-heuristic algorithms to optimize neural network structures, while the exploration of deep learning in optimization has remained relatively limited. The proposed hybrid approach seeks to enhance wind power bidding strategies, improving profitability by predicting optimal output power for day-ahead electricity markets. This method integrates Long Short-Term Memory (LSTM) with Particle Swarm Optimization (PSO), leveraging LSTM's ability to predict the active movement tendencies of particles for more efficient and faster optimization. Experiments conducted on the IEEE 30-bus power system show that the LSTM-PSO hybrid outperforms mathematical models and standalone PSO algorithms. It also delivers an optimal wind power bidding strategy, yielding peak annual revenue, while recommending a 16 % reduction in bidding output power variance in models that integrate wind power with thermal power and energy storage systems (ESS). Ultimately, this approach fosters confidence in wind energy investment, contributing to sustainable development.

1. Introduction

1.1. General

The wind power industry is regarded as one of the most rapidly growing renewable energy sources in the early 2020s [1]. While its appeal lies in its critical role in sustainable development, it also faces several potential challenges, including adverse impacts on operational techniques [2], financial investment risks [3], and market volatility in electricity trading [4], primarily due to its inherent uncertainty. To address these challenges, numerous studies have proposed effective solutions. For instance, accurate wind speed forecasting, as demonstrated in [5], enables proactive control of electricity output during operations. Policies that combine Contracts for Differences (CfDs) with conventional Power Purchase Agreements (PPAs) have proven effective in mitigating financial risks in electricity markets [6]. Moreover, increasing financial penalties for wind power fluctuations has been shown to minimize the negative impacts on market participants [7]. Another promising approach involves integrating wind power operations with thermal power plants and energy storage systems to enhance investment efficiency [8]. Most of these studies aim to optimize specific objectives, particularly in the renewable energy sector, as emphasized in [9].

Based on their broad applicability, diversity, and adaptability to complex multi-objective problems, MH algorithms—particularly swarm intelligence techniques such as PSO—are widely recognized for their robust optimization capabilities [10]. Notably, numerous studies have enhanced these algorithms for applications in the energy sector, such as the development of a multi-objective optimization algorithm (M−MOPSO) to optimize hybrid solar–wind–battery systems [11], or the improvement of the Salp Swarm Algorithm (SSA) for controlling the maximum power point of wind turbines [12]. However, in complex problems that account for the stochastic uncertainty of renewable energy, challenges remain regarding the speed and global convergence probability of MH methods, especially in large and high-dimensional search spaces. To address these challenges, researchers often employ staged process partitioning methods [13] or integrate multiple algorithms to leverage their respective strengths [14].

* Corresponding author.
E-mail address: sangdn.ncs@hcmute.edu.vn (N.S. Dinh).

https://doi.org/10.1016/j.asej.2025.103285
Received 12 October 2024; Received in revised form 14 December 2024; Accepted 21 January 2025

Moreover, the rapid development of Artificial Intelligence (AI), particularly DL techniques, has demonstrated significant potential in addressing complex problems [15]. Among the prominent DL architectures recently highlighted are Recurrent Neural Networks (RNN), Generative Adversarial Networks (GAN), and Long Short-Term Memory (LSTM) networks [16]. RNNs primarily focus on short-term sequence predictions with a relatively simple transition function. In contrast, GANs excel in generating synthetic data during the learning process, which enhances training quality and brings results closer to the target. LSTMs, an advanced variant of RNNs, are specifically designed to improve the analysis and processing of sequential data, particularly for retaining long-term dependencies. Each DL architecture has its specific domain of application. RNNs and LSTMs perform effectively in tasks with clear temporal sequences, with LSTMs standing out for their ability to handle tightly coupled dependencies within sequential data [17]. Additionally, LSTMs demonstrate capabilities in multi-agent navigation, obstacle avoidance, and maintaining robust performance across sequences of varying lengths [18].

1.2. Mutation and Contribution

The development of MH algorithms and DL has advanced significantly and continues to progress to meet the growing demands of technological advancements. In addition to independent improvements, the integration of these algorithms to enhance performance has emerged as a natural trend. Recent studies have increasingly focused on developing hybrid techniques that combine DL with MH. The use of MH to optimize the architecture and prediction processes of DL models has become particularly prevalent. For instance, the Whale Optimization Algorithm (WOA) has been applied to fine-tune the hyperparameters of an LSTM network for thermal load forecasting [19]. A PSO-LSTM hybrid model proposed in [20] has demonstrated superior performance in soil moisture prediction. Additionally, the method introduced in [21] combines LSTM and GAN to forecast solar power generation based on cloud patterns, while the PSO-LSTM hybrid technique has been successfully employed for electricity price prediction [22]. However, most current studies focus on leveraging MH to optimize the architecture and parameters of DL models for improved prediction quality. Conversely, the potential of DL to enhance the capabilities of MH algorithms in solving optimization problems appears to have received insufficient attention.

Based on the identified research gap, this paper proposes a method that integrates DL with MH algorithms to enhance the speed and efficiency of global optimization processes. The proposed approach employs the LSTM model, a type of neural network known for its accurate predictive capabilities, to assist the PSO algorithm in optimizing wind power investments in electricity markets. The PSO algorithm operates based on the principle of swarm intelligence, where particles move within the search space by leveraging their own experiences as well as the collective experience of the swarm. The proposed method takes advantage of the LSTM model to predict the future positions and velocities of particles. These predicted particles are then perturbed and integrated into the current swarm, fostering effective interactions among particles and enabling the PSO algorithm to achieve optimal solutions more rapidly and efficiently. The effectiveness of the proposed method is validated on the IEEE 30-bus standard power system. Experimental results demonstrate that the method not only improves prediction accuracy but also optimizes wind power integration more effectively compared to the traditional PSO algorithm and other enhanced PSO variants discussed in [23]. Furthermore, the method shows significant superiority over the integer linear programming-based mathematical optimization approach applied in a previous study [8].

The main contributions of this paper are summarized as follows:

- This paper proposes a robust hybrid algorithm named LSTM-PSO, which combines the AI capabilities of LSTM with the optimal motion characteristics of PSO. The key highlight of this method lies in its ability to accelerate convergence and overcome local optima in optimization problems, addressing one of the common limitations of most MH algorithms. To achieve this, LSTM is utilized to predict the superior characteristics of future particles by learning the evolutionary patterns from historical particle behavior data. The predicted particles are then refined through perturbation and integrated into the PSO movement process. The exceptional attributes of these predicted particles serve as a strong driving force, propelling the swarm rapidly toward the global objective. Moreover, the predicted particle coordinates have the potential to bypass local constraints, enabling the swarm to overcome barriers and enhance global convergence efficiency effectively.
- Applying the hybrid algorithm to determine the optimal wind farm output power for bidding in the electricity market. This research identifies a combination model of wind power, thermal power, and energy storage systems (WTEM), as examined in [24], to maximize benefits based on the bidding power output calculated by the hybrid algorithm. Furthermore, the evaluation results are compared against the optimal power flow (OPF) problem as discussed in the studies referenced in [23].

2. Method

MH algorithms remain popular in optimization due to their ability to handle complex nonlinear objective functions, which often pose significant challenges for traditional algorithms. Research [25] has demonstrated the superior performance of swarm intelligence algorithms, particularly PSO, in both theoretical studies and practical applications, especially in the energy sector. In addition, LSTM has proven to be highly effective in time series forecasting [17]. Its ability to retain long-term dependencies, continuously update parameters, and handle complex sequential data enables LSTM to learn efficiently even with limited training data [26]. Building on these strengths, LSTM is integrated into PSO to predict the coordinates and velocities of particles in future iterations. After learning from prior movement patterns, LSTM provides positional and velocity information to guide subsequent movements in PSO. This integration results in the proposed LSTM-PSO hybrid algorithm presented in this study.

This investigation focuses on optimizing wind power output bidding in the electricity market. Traditionally, wind power owners base their bids on predicted future output, aiming for the highest probability [27]. However, due to the unpredictable nature of electricity price fluctuations, wind farm revenues may significantly decrease if compensation accounts for uncertain output changes. Consequently, the optimal bidding power output of wind farms is no longer a value predicted with the highest probability [24]. Thus, this study proposes exploring algorithms to determine the optimal bidding capacity for wind power in the WTEM model. Introducing the concept of power deviation (WPD), which measures the difference between bid values and predicted wind power output, offers a more nuanced approach. Current prediction methods often set WPD to zero, potentially neglecting scenarios where output uncertainty incurs penalties, undermining investor confidence in wind power.

2.1. Mathematical model

(i) Fitness Function

The social benefits in the WTEM model can be assessed through the income generated as the objective of the problem [24]. Due to the uncertainty of wind power in the group, the revenue includes two components: direct revenue and uncertain income, as follows [24]:

$$\text{Maximize } \{R_\Sigma = R_w + I_W\} \tag{1}$$

The first component of expression (1) is direct revenue, R_w in (2). Within it, there is direct wind revenue, R_w^d, corresponding to the

auctioned wind power output, P_{ws}, and direct thermal revenue, R_T^d, corresponding to the auctioned thermal power output, P_{Ts}. Direct revenue in the day-ahead electricity market is based on the unit price, λ_w, λ_T, and the bidding power quantities, P_{ws}, P_{Ts}, of wind and thermal plants respectively.

$$R_w = R_w^d(P_{ws}) + R_T^d(P_{Ts}) \tag{2}$$

$$C_{PT} = k_{P1}\lambda_w\tau_{out} = \begin{cases} k_{P1}\lambda_w \sum_{(P_{ws}-\tau_{in}-\Delta P_T)}^{(P_{ws}-\tau_{in})} (P_{ws}-p_w) f_w(p_w)dp_w, if|\tau_{out}| < \Delta P_T \\ k_{P1}\lambda_w \Delta P_T, if|\tau_{out}| \geq \Delta P_T \end{cases} \tag{13}$$

$$C_{PE} = k_{P2}\lambda_w(\tau_{out} - \Delta P_T) = \begin{cases} k_{P2}\lambda_w \sum_{(P_{ws}-\tau_{in}-\Delta P_T-P_E)}^{(P_{ws}-\tau_{in}-\Delta P_T)} (P_{ws}-p_w) f_w(p_w)dp_w, if \Delta P_T < |\tau_{out}| < (\Delta P_T + P_E) \\ k_{P2}\lambda_w P_E, if|\tau_{out}| \geq (\Delta P_T + P_E) \end{cases} \tag{14}$$

$$R_w^d = \lambda_w x P_{ws} \tag{3}$$

$$R_T^d = \lambda_T x P_{Ts} \tag{4}$$

Both the electricity selling price and the power output in the bidding process must be accurately predicted in order to benefit the investor, as outlined in documents [27,28]. The selling price of wind electricity is often forecasted based on the price index of the dominant energy source in the electricity market. An example of a dominant thermal power source in the market is referenced in [29].

The second component of equation (1) is the uncertain income, I_w, determined by equation (5). It depends on the predicted probability of wind power output, contingent on the discrepancy between the actual power output sold in real-time, P_{wav}, and the bid power output, P_{ws}, denoted as ΔP_w. This uncertain income may be positive when surplus wind power output is sold and generates revenue, R_w^u, or it may be negative in the event of power output shortage. In such cases, there is a need to incur a cost to purchase energy immediately from thermal plants, C_T, or from ESS, C_E, or to be penalized according to contracts, C_P.

$$I_w = R_w^u(\Delta P_w) - (C_E + C_T + C_P) \tag{5}$$

$$C_E = \eta_E(\lambda_C - \lambda_B)P_E \tag{6}$$

$$C_T = R_T^d(P_{Ts}) + R_T^u(\Delta P_T) \tag{7}$$

$$C_P = \lambda_P \Delta P_P \tag{8}$$

$$\Delta P_w = P_{wav} - P_{ws} \tag{9}$$

The cost component of ESS is determined based on the efficiency, η_E, the stored power capacity, P_E, and the price differential for stored energy, λ_C, with the electricity purchase price, λ_B. The cost component of a thermal plant corresponds to the direct electricity sales revenue, R_T^d, and the uncertain revenue, R_T^u. The final cost component is the contract penalty, calculated based on the penalty price, λ_P, and the penalized power output, ΔP_P. The wind power output may exceed or fall short at the time of electricity sale in the market.

In case considering the probability distribution of predicted power output, the components of uncertain revenue and costs are described by the Weibull probability distribution and are determined by the following expressions, which are modified from [30],

$$R_w^u = \begin{cases} R_{Rw}(\tau_{out}), if \tau_{out} > 0 \\ -C_{Pw}(\tau_{out}), if \tau_{out} < 0 \end{cases} \tag{10}$$

$$R_{Rw} = k_R\lambda_w\tau_{out} = k_R\lambda_w \sum_{(P_{ws}+\tau_{in})}^{P_{wr}} (p_w - P_{ws}) f_w(p_w)dp_w \tag{11}$$

$$C_{Pw} = C_{PT} + C_{PE} + C_{P0} \tag{12}$$

$$C_{P0} = k_{P0}\lambda_w(\tau_{out} - \Delta P_T - P_E) = k_{P0}\lambda_w \sum_{0}^{(P_{ws}-\tau_{in}-\Delta P_T-P_E)} (P_{ws}-p_w) f_w(p_w)dp_w \tag{15}$$

$$R_T^u = \begin{cases} R_{PT}(\Delta P_T), if \Delta P_T > 0 \\ -R_{RT}(\Delta P_T), if \Delta P_T < 0 \end{cases} \tag{16}$$

Where, τ_{out} presents the amount of output power exceeding the agreed-upon range corresponding to the bid price for the electricity market. When $\tau_{out} > 0$ indicates surplus wind power output; the excess is sold to any buyer in need in the market at a negotiated price. Due to uncertainty, surplus electricity prices are typically very low, even with the possibility of no buyers. Conversely, when there is a deficit, $\tau_{out} < 0$, wind farm operators are obligated to purchase electricity from backup sources in the market to compensate for customers — failure to purchase results in contract penalties at an extremely high price. Pursell electricity from backup sources in this scenario is sudden, leading to significantly higher purchasing prices compared to selling in the market.

The uncertain factors related to wind revenue are described in equation (10). Surplus electricity sales revenue and compensation costs for shortfall electricity are expressed through equations (11) and (12), respectively. In these equations, there are two scaling coefficients, k_R and k_{Pi}, representing the surplus electricity sales price reduction and compensation electricity price increase. These coefficients are random and depend on the supply and demand of the electricity market at the spot delivery time. The value of k_R ranges from 0 to 1, and k_{Pi} ranges from 1 to 2.5, potentially higher. The uncertain costs include payments to thermal plants (C_{PT}), ESS (C_{PE}), and customers penalized for power output shortfall (C_{P0}), corresponding to the reserve power output of thermal plants (ΔP_T) and ESS (P_E). Meanwhile, the uncertain revenue of thermal plants is determined through equation (7). The wind power output probability distribution function, f_w, is established based on the wind speed probability distribution outlined in [24,31]. This probability distribution function utilizes a two-parameter Weibull distribution c and k according to the references [32].

(ii) Constraints

The operational constraints of the power transmission system include optimal operating conditions, nodal voltage limits, and power transmission capacity of the transmission lines [33],

$$P_{Gi} - P_{Di} - \sum_{j\in bus} V_i V_j \left(G_{ij}cos\delta_{ij} + B_{ij}sin\delta_{ij}\right) = 0 \tag{17}$$

$$Q_{Gi} - Q_{Di} - \sum_{j\in bus} V_i V_j \left(G_{ij}sin\delta_{ij} + B_{ij}cos\delta_{ij}\right) = 0 \tag{18}$$

$$V_{i\in bus}^{min} \leq V_{i\in bus} \leq V_{i\in bus}^{max} \tag{19}$$

$$S_{i\in branch} \leq S_{i\in branch}^{max} \tag{20}$$

where P_{Gi}, Q_{Gi}, P_{Di} and Q_{Di} represent the active and reactive power of generation sources and loads at bus i; G_{ij}, B_{ij} perform the admittance of the branch connecting buses i-j; S_i, S_i^{max} denote the operated and rated

apparent capacity of the branch; V_i is the operating voltage of the bus; δ_{ij} is the phase angle difference of voltage between the buses and V_i^{min}, V_i^{max} are the minimum and maximum allowable voltage for bus i.

Next are the operational constraints of wind turbines, ref. [34], The speed is limited to the operating range specified by the manufacturer. The lower bound ensures energy conditions for blade operation to commence, while the upper bound ensures no mechanical damage to the equipment,

$$v_{in} \le v \le v_{out} \tag{21}$$

For ESS operational conditions, the system only exists to ensure benefits. Operating costs and revenues refer to [35] and are represented,

$$C_{ESS} \le R_{ESS} \tag{22}$$

$$\text{Cost} \quad C_{ESS} = C_{Inv} + N_e C_O (1-\alpha) P_{ESS} \tag{23}$$

$$\text{Revenue} \quad R_{ESS} = N_e \left(k_{P2}\lambda_w - \lambda_{buy}\right)(1-\alpha) P_{ESS} \tag{24}$$

The investment and operation costs of ESS are denoted as C_{Inv} and C_O. N_e represents the equivalent number of deep discharges over the lifetime of ESS, corresponding to the deep discharge coefficient α and the rated capacity of ESS, P_{ESS}.

Finally, the principle of electricity market operation, the day-ahead electricity market model, is an example based on matching orders between supply and demand in terms of quantity and price. Bid and ask electricity price data correspond to the buying and selling prices offered for the next day by electricity buyers, such as electricity consumers or distribution companies. Electricity sellers mainly consist of various types of power sources concentrated at the electricity market management center. The adjustment of electricity prices in situations of excess or insufficient electricity generation can be determined as follows, see reference [36].

$$k_R = \frac{\lambda_{Rw}}{\lambda_w} = \frac{b_g + c_g\left(P_{Tg} - \Delta P_w\right)}{b_g + c_g P_{Tg}} = \left(1 - \frac{c_g \Delta P_w}{\lambda_w}\right) = 1 - \beta \tag{25}$$

$$k_{P1} = \frac{\lambda_{Tg}}{\lambda_w} = 1 \tag{26}$$

$$k_{P2} = \frac{\lambda_{Ew}}{\lambda_w} = \frac{1}{\lambda_w}\left[\frac{C_{Inv}}{N_e(1-\alpha)P_{ESS}} + C_O + \lambda_{buy}\right] = \frac{1}{\lambda_w}\left(UIC_{ESS} + C_O + \lambda_{buy}\right) \tag{27}$$

$$k_{P0} = \frac{\lambda_{Pw}}{\lambda_w} = \frac{b_g + c_g\left[P_{Tg} + \Delta P_w - \Delta P_T - (1-\alpha)P_{ESS}\right]}{b_g + c_g P_{Tg}} = \left(1 + \frac{c_g\left[\Delta P_w - \Delta P_T - (1-\alpha)P_{ESS}\right]}{\lambda_w}\right) = 1 + \gamma \tag{28}$$

Where,

$$\beta = \frac{c_g \Delta P_w}{\lambda_w} = B(\Delta P_w) \tag{29}$$

$$\gamma = \frac{c_g\left[\Delta P_w - \Delta P_T - (1-\alpha)P_{ESS}\right]}{\lambda_w} = Y(\Delta P_w) \tag{30}$$

The coefficients b and c represent the non-fee component of the thermal power coefficient; β and γ are random variables. The expressions constructed are based on the assumption of maximizing the linked benefits of wind and thermal plants associated with competitive electricity market constraints, and the profit of the ESS ensures enough of its investment and operational costs. The symbol UIC_{ESS} represents the unit investment cost of the ESS.

2.2. Optimization approach

(i) PSO Algorithm

The PSO algorithm describes the movement dynamics of a swarm as it seeks a target [37]. This intelligent movement process operates based on principles of competition, interaction, and randomness. The swarm's activities maintain relationships among individuals and between individuals and the leader. The velocity and position of the individuals, which simulate movement in a multi-dimensional space, represent the outcomes of each iteration, as cited in [38], and are expressed through the following fundamental equations:

$$\vec{V}_{t+1}^{i} = \vec{V}_t^{i} + \varphi_1 R_{1t}^{i}\left(\vec{p}_t^{i} - \vec{x}_t^{i}\right) + \varphi_2 R_{2t}^{i}\left(\vec{g}_t - \vec{x}_t^{i}\right) \tag{31}$$

$$\vec{x}_{t+1}^{i} = \vec{x}_t^{i} + \vec{V}_{t+1}^{i} \tag{32}$$

Where φ1 and φ2 are the self-velocity and social interaction weights; R_1 and R_2 are uniformly distributed random vectors; $\vec{p}_t^{i}$ and $\vec{g}_t$ are the position vectors relative to the best individual in the same iteration and the best in previous iterations; and $\vec{x}$ is the coordinates of individual position.

(ii) LSTM Algorithm

In 1997, Hochreiter and Schmidhuber proposed the LSTM algorithm [39]. The architecture of an LSTM algorithm consists of at least three network layers: one input layer, one output layer for data, and a set of LSTM layers situated between the input and output layers. The LSTM layer comprises multiple hidden layers connected by Cells, structured as illustrated in Fig. 1, and the mathematical model representing the input–output relationships of each Cell is expressed in equations (33) to (37) in ref [40].

$$f_t = \sigma\left(W_f X_t + W_{Hf} h_{t-1} + b_f\right) \tag{33}$$

$$i_t = \sigma(W_i X_t + W_{Hi} h_{t-1} + b_i) \tag{34}$$

$$O_t = \sigma(W_o X_t + W_{Ho} h_{t-1} + b_o) \tag{35}$$

$$C_t = C_{t-1} \otimes f_t + i_t \otimes tanh(W_c X_t + W_{Hc} h_{t-1} + b_c) \tag{36}$$

$$h_t = O_t \otimes tanh(C_{t-1}) \tag{37}$$

In the weight matrix, the bias variables are represented as $W(f, i, O, C)$ and $b(f, i, O, C)$ respectively. Here, h_{t-1} denotes the previously hidden unit is an element-wise weighted summation and C_t becomes the current Cell after processing. The transformation functions are represented by tanh and σ. Equations (33) to (35) represent forget, input, and output values, respectively. Equations (36) and (37) show the current memory cell and hidden unit at time step t.

(iii) Proposed Hybrid LSTM-PSO Algorithm

The proposed method in this paper aims to enhance the intrinsic quality of the PSO algorithm. Deep learning techniques are employed to

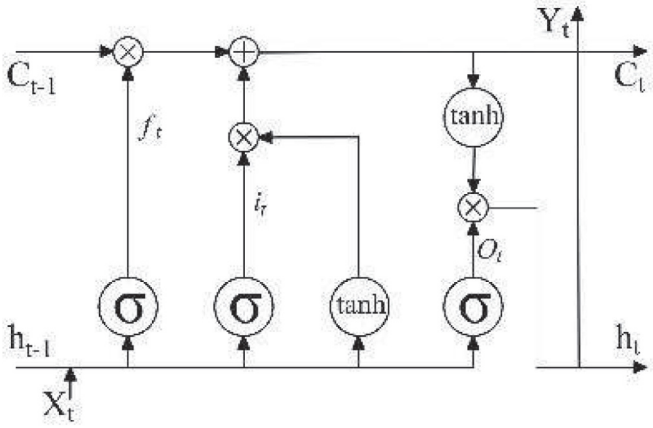

Fig. 1. Structure of a Cell unit of the LSTM algorithm.

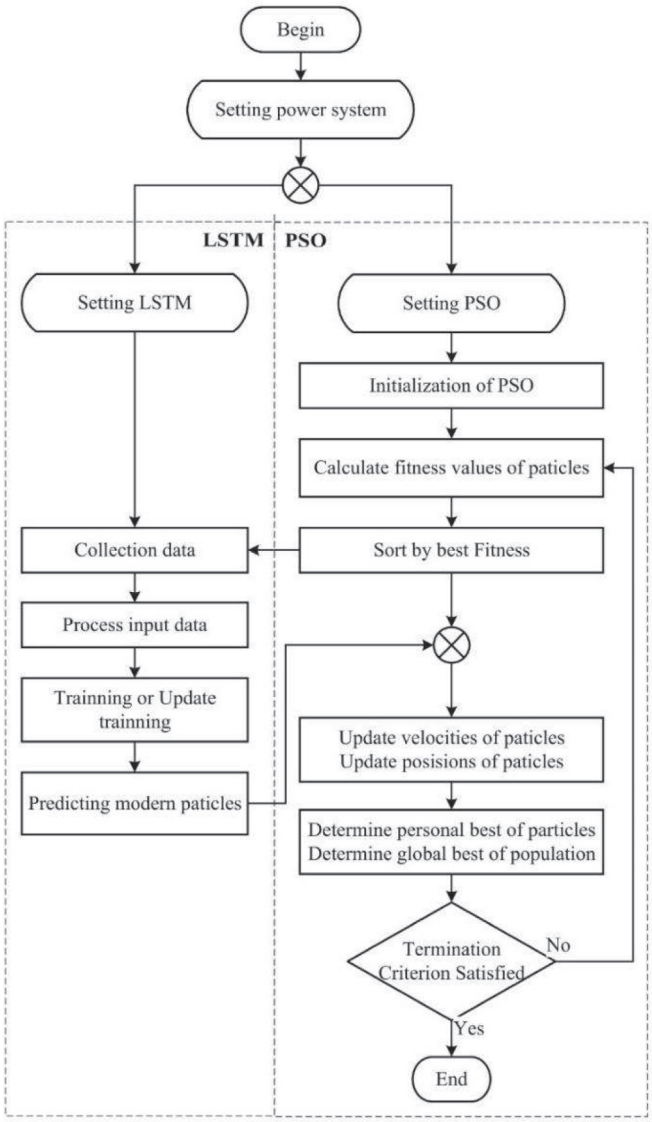

Fig. 2. Flowchart LSTM-PSO Algorithm.

refine collective knowledge during individual movement. The LSTM architecture predicts more advanced individuals during the perturbation phase. These modern individuals not only contain valuable knowledge but also significantly influence the better optimization of coordinates and velocities of neighboring individuals. This process accelerates the optimization problem and enables the overcoming of local optima that traditional PSOs may encounter. The algorithmic process is illustrated in Fig. 2, delineated by the following steps:

Step 1: Set up the operational parameters of the power system, such as power sources, electrical loads, buses, and branches. Initialize wind turbine operation data, including wind power output probability distribution according to the Weibull probability distribution model of wind speed.

Initialize PSO properties. Choose the method and parameters in the expression of PSO coordinate and velocity movement. The expected movement space in four dimensions: x_1 is the difference in wind power output between the bid and the forecast; x_2 is the maximum power output that can be compensated for wind farms; x_3 is the bid power output value of thermal plants linked to wind farms and x_4 is the level of penalty rate increase compared to the spot electricity selling price in the electricity market.

Initialize LSTM properties. Choose the structure of input and output layers, the number of intermediate LSTM hidden layers, and related parameters.

Step 2: Initialize the initial population randomly according to a predetermined selection size.

Step 3: Perform OPF on the power system with constraints, determine the wind electricity selling price and the electricity price adjustment factors, and compute the objective function for individuals in the population.

Step 4: Training LSTM – First, data preprocessing based on the set of coordinates, velocities, and fitness values of previous individuals. The process includes, but is not limited to, data cleaning, normalization, augmentation, transformation, and fusion. Next, the training process is continuously updated, and although it operates independently, the data is dynamically updated and processed in response to any changes within the PSO cycle.

Step 5: Execute LSTM to predict modern individuals—each movement iteration performs prediction once. The prediction output consists of a certain number of future individuals, generated according to a predefined proportion specified by the algorithm. These future individuals are perturbed or integrated into the existing population to participate in the movement process alongside the entire swarm of PSO particles.

Step 6: Perform the PSO cycle operations, perturb the previously predicted particles, update the positions and velocities of the particles, evaluate their fitness, and update the pbest and gbest values.

Step 7: Repeat steps until the termination condition of the problem is met.

3. Experiments and results

3.1. Experimental data

(i) IEEE 30-bus System

The operational parameters of the IEEE 30-bus power system are utilized for experimentation [41], structured according to [42], comprising six sources, thirty nodes, and forty-one branches. Among the power sources are four thermal power sources located at buses 1, 2, 8, and 13, as shown in Table 1. Additionally, two sources are wind power sources at buses 5 and 11, as outlined in Table 2.

The rated power of each wind turbine is 3 MW, with operating parameters v_{in} = 3 m/s; v_r=16 m/s and v_{out} = 25 m/s. Thus, there are 25 turbines on bus 5 and 20 turbines on bus 11. The wind power sources for buses 5 and 11 assume Weibull data from reference [34], as provided in Table 2. Predicted wind speeds for each year are assumed to be consistent and divided into two seasons, peak and off-peak, with 24-hour electricity output per day as given in reference [27]. Predicted power output values, probability of exceeding predictions, and probability of falling below predictions are provided in Fig. 3.

(ii) Implementation of Data PSO Algorithm and LSTM Architecture

Selecting data settings for the PSO algorithm includes the following parameters: The swarm size in PSO is chosen to be 100 particles. InertiaRange – Limits the inertia constant within the range of (0.1–1.1). InitialSwarmSpan – Limits the initial position of individuals to be initialized at 2000. MaxStallIterations – Limits the maximum number of iterations a particle can move without improvement to 25 times. MinNeighborsFraction – The minimum ratio of neighbors affecting an individual is 0.25. SelfAdjustmentWeight and SocialAdjustmentWeight –

Table 1
Parameter of thermal generators.

Bus	Rated Power	a	b	c
1	200	0	20	0.038431975
2	80	0	20	0.25
8	35	0	40	0.01
13	40	0	40	0.01

Table 2
Parameter of wind power.

Bus		5	11
Wind power generation plants	No. of turbines	25	20
	Rate power, P_{wr}(MW)	75	60
	Weibull PDF parameter	c = 9, k = 2	c = 10, k = 2
	Weibull mean,M_{wbl}	v = 7.976 m/s	v = 8.862 m/s

The ratio of self-adjusting speed weight and community interaction weight is 1.49.

For the LSTM deep learning architecture, the configuration parameters include an input layer with five features (04 variables representing the dimensions considered by PSO and 01 fitness of the corresponding individual), 50 LSTM hide layers with 0.01 of recurrent weights L2 factor, a dropout layer with rate 0.2 to overfitting, a fully connected layer with one response output, and finally, a regression layer to output the prediction results.

3.2. Result

The optimization problem is solved by three different methods as follows.

(i) AC mixed-integer linear programming approach (ACDD)

The electricity revenue of all power plants in the IEEE 30-bus system according to objective function (1) is illustrated in Fig. 4. This is a result of an approximate calculation based on the optimal power distribution AC with discretized data, utilizing the optimal power flow distribution tool RunOPF available in Matpower 8.0b1 on Matlab software. The power deviation bidding results, WPD calculated as the percentage ratio between the wind power output bidding decision in the day-ahead electricity market and the predicted peak power output, are shown in Fig. 4. The graph depicts continuous revenue fluctuations based on the variation of WPD from each wind farm. The peak revenue is achieved within the range of WPD, approximately between −10 % and −30 %, and minimizes within the range of + 10 % to + 30 %. An important feature to emphasize is that the revenue peak consistently shifts towards the negative side of the WPD deviation. Detailed results in Table 5.

(ii) Pure Algorithm PSO

The problem is executed 15 times with a maximum of 25 individual movements per execution, and the fitness results of the problem are provided in Fig. 5. The figure illustrates that the PSO algorithm typically converges to a local optimum after around 15 to 20 iterations. However, an inherent drawback of this algorithm is its susceptibility to getting trapped in local optima. Fig. 5 shows the solution of PSO executions exhibiting dispersion due to the potential entrapment in local optima, as mentioned, resulting in disparate experimental outcomes among executions.

(iii) Proposed Hybrid Algorithm LSTM-PSO

Fifteen independent experimental runs of the LSTM-PSO algorithm

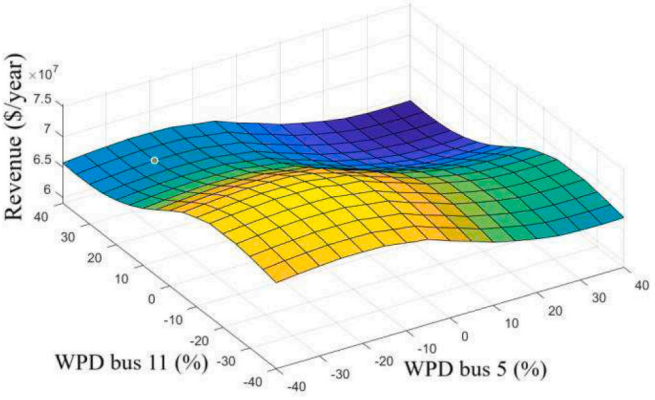

Fig. 4. Distribution of revenue within wind farms, in case P_{ESS} = 10.

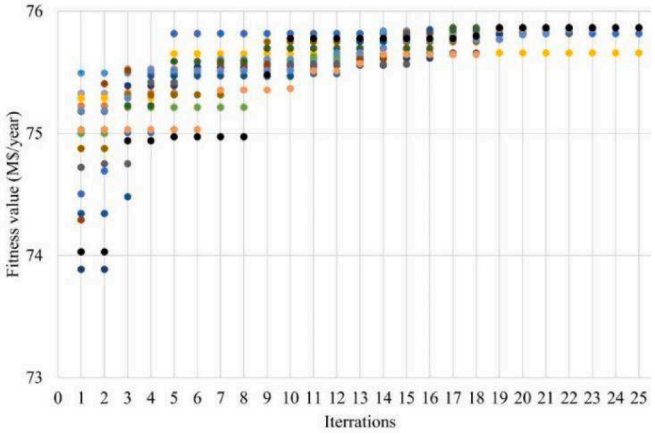

Fig. 5. Fitness results of 15 executions of pure PSO.

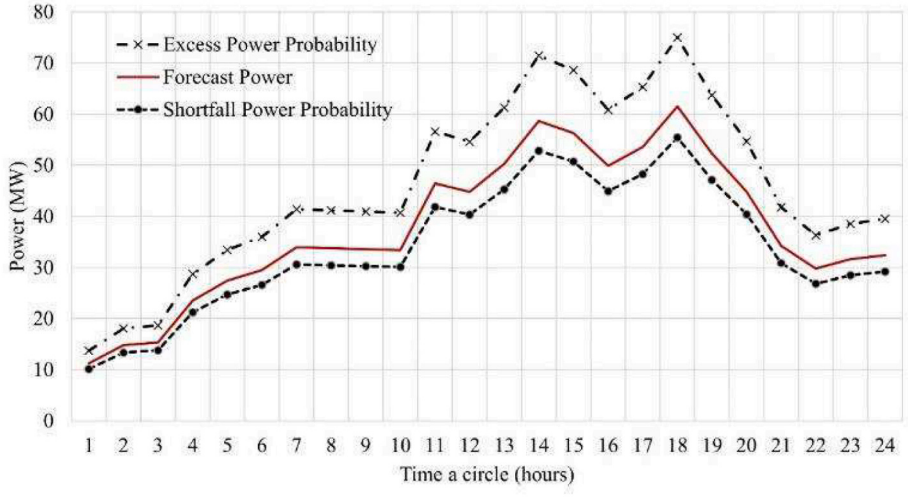

Fig. 3. Range of wind power output chart in peak season.

Table 3
LSTM-PSO variable results.

Executions	Fitness (M $/year)	WPD (%)		ESS Power (MW)		
		Wind bus 5	Wind bus 11	Wind bus 5	Wind bus 11	Sum
1	75.9	−16.3	−15.8	8	0	8
2	75.9	−16.4	−16.4	9	10	19
3	75.9	***−15.6***	−16.4	15	6	21
4	75.9	***−15.6***	−16.2	11	15	26
5	75.9	−16.0	−16.4	3	5	8
6	75.9	***−16.5***	−15.7	11	5	16
7	75.7	−16.1	−15.9	5	8	13
8	75.9	−16.4	−16.4	20	3	23
9	75.9	−16.3	−15.8	9	11	20
10	75.9	−16.4	−16.0	5	6	11
11	75.9	−16.0	***−16.5***	6	11	17
12	75.9	−16.1	−16.0	12	4	16
13	75.9	−16.4	−15.9	7	7	14
14	75.9	−15.8	−16.0	3	4	7
15	75.9	***−15.6***	***−15.6***	17	3	20
Mean		***−16.1***	***−16.1***	***9***	***7***	***16***

with the selected input data were conducted, and the results of these executions are presented in Table 3. The convergence process is also visualized using scatter plots in Fig. 6 Overall, the fitness value converges to M75.9 $/year; the WPD of the two wind farms fluctuates within the range of −15.6 % to −16.5 %; and the total ESS power shows variability but averages approximately 16 MW. More detailed results are provided in Table 5.

Fig. 5 and Fig. 6 demonstrate that the simulation results of PSO and LSTM-PSO exhibit similar trends, particularly in the early stages before 5–7th iteration. The most significant difference is that the hybrid algorithm (LSTM-PSO) displays a more focused convergence pattern, especially from iteration 16 onwards, whereas the results of PSO remain dispersed across executions until iteration 25th.

4. Discussion

4.1. Hybrid algorithm LSTM-PSO

Fig. 7 illustrates the target deviation during the convergence process of the compared algorithms. The solid region represents the LSTM-PSO algorithm, while the hatched region with stripes corresponds to the PSO algorithm. Key highlights, deemed critical for the analysis, have been selectively extracted and detailed in Table 4. Overall, the hatched region exhibits a larger area, overlapping and extending beyond the solid region. The boundary of the hatched region demonstrates pronounced fluctuations, while the boundary of the solid region appears smoother,

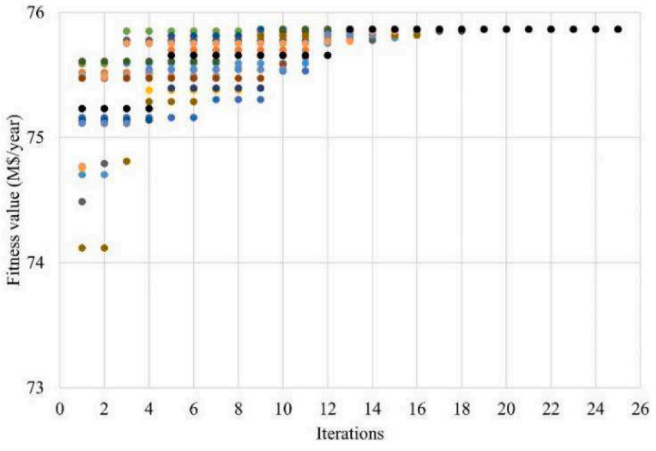

Fig. 6. Performance fitness of 15 executions of LSTM-PSO.

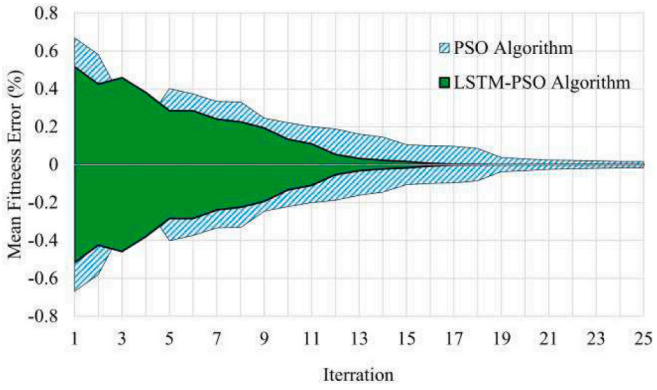

Fig. 7. Comparing PSO and LSTM-PSO process errors.

Table 4
Highlight key notes.

Key compare	PSO	LSTM-PSO
Convergence process	fluctuation	**smooth**
+ *Early phase (1–5)*	*Nearly LSTM-PSO*	*Nearly PSO*
+ *Second phase (6–16)*	*The graph curves gently and extends over a longer range.*	*The graph converges directly in a straight path.*
+ *End phase (17–25)*	*continues to extend gradually, causing the convergence point to be farther away.*	*already approached its previous convergence point.*
Convergence iterations	Nearly 25	**16–17**
Convergence probability	disperse at 25th iteration	**Focus in a point**

indicating greater stability. This observation underscores the convergence characteristics of the LSTM-PSO algorithm, which stabilizes and converges to a single point as early as the 16th iteration. In contrast, the PSO algorithm remains dispersed, with its convergence process extending to around the 25th iteration. These distinctions clearly highlight the superior stability and efficiency of the LSTM-PSO algorithm in achieving optimized convergence.

In terms of the convergence process, three distinct phases can be identified:

- First phase: During the initial five iterations, the particle movements in both methods are almost identical. The rate of fitness improvement for individual particles gradually decreases, and the achieved fitness boundaries remain nearly unchanged in both approaches. This suggests that the impact of the LSTM in the hybrid algorithm is relatively ineffective during this stage. This is understandable, as the

Table 5
Compare results with studies.

Approaches		AC [24][1]	ACDD	PSO	LSTM-PSO
WPD (%)	Bus 5	−30 %	−20 %	−16 %±0.5 %	(−15.6 %)÷(−16.5 %)
	Bus 11	−30 %	−20 %	***(−16 %)÷ (−26 %)***	***(−15.6 %)÷ (−16.5 %)***
Max power of Wind farms (MW)		95	108	98 ÷ 114	***113 ÷ 114***
ESS power (MW)		10	10	18	16
Peak revenue		71	75	***75.9***	***75.9***
+ M$/year		94 %	98.8 %	100 %	100 %
+ %					

[1] Corresponds to the compensation coefficient of 1.6.

time and data available for LSTM training are still limited and dispersed, leading to predictions that do not yet provide significant improvements.

- Second phase: Over the next ten iterations, the pace of achieving the objective increases significantly in the hybrid algorithm. Most particles converge and stabilize at extreme points during this period. As a result, the hybrid algorithm shortens the optimization process, achieving the desired outcomes around iterations 15–17, which is five to seven iterations faster than the pure PSO algorithm.
- Final phase: From the 15th iteration onward, the results of the hybrid method become highly concentrated. Although the independent runs are conducted separately, the extreme values are nearly indistinguishable. In contrast, for the pure PSO algorithm (hatch plot), the extreme values still exhibit slight dispersion at the same stage, indicating inconsistency in results across different runs.

Thus, experiments demonstrate that the new algorithm effectively addresses most of the limitations of the original PSO. First, with individuals predicted by LSTM, they can achieve better velocities and coordinates, which are integrated into the swarm community. This creates strong motivation, enabling the swarm to move faster towards the destination, reducing the number of iterations by approximately 5–7 in the experiment. Additionally, individuals generated by LSTM can surpass local boundaries where the swarm may be confined within a restricted region. This facilitates overcoming obstacles and progressing towards the global optimum.

Considering the actual execution time of algorithms on a machine with an Intel Core i7-8550U CPU, GeForce MX150 GPU, and 20 GB of RAM, the average completion time for a single optimization cycle is between 1–2 min for the example discussed in this paper. In the PSO cycle, the most time-consuming step is running OPF; in LSTM, the longest time is spent during the training phase. Since these cycles are multithreaded and executed in parallel, they do not significantly impact each other's execution time. In the short time of this example, distinguishing speed over time is challenging. However, the extended duration of LSTM primarily arises from the training phase, which only occurs at the initial stage. Therefore, for large problems, the convergence time of the algorithm will be noticeably faster due to a reduction in the number of iterations.

4.2. Optimal wind power output and ESS in electricity market

Although the approaches and methods vary, their objectives all focus on optimizing the efficiency of wind power utilization in the electricity market and maximizing the investment benefits for wind power industry development. Evaluating these methods is based on three main factors. Firstly, the optimal output power value of wind farms is measured by the deviation index WPD and variance from forecasts. Secondly, investment in ESS power capacity in joint ventures to optimize the efficiency of the entire integration system. Finally, the ability to utilize the highest wind power output in the electricity market to consider the potential for full wind power exploitation and related social benefits.

The proposed optimization model in the paper aims to improve the efficiency of wind farm investments by addressing competitive disadvantages and compensating for uncertainty in its output when participating in the electricity market, as mentioned in [15]. The study results indicate that integrating wind farms with thermal power sources minimizes the risk of profit loss due to electricity output shortages in competitive environments. The study also proposes a reasonable power output bidding method, suggesting adjusting the bidding output capacity range for wind power rather than bidding solely based on the highest predicted output power, as done previously. Additionally, it means integrating storage capacity into proportion to stabilize uncertainty in wind power output. Substantial revenue improvements are achieved when bidding in the suggested direction, as indicated by the optimized results from the mentioned hybrid algorithm. These results are compared among three optimization methods, as shown in Table 5.

Table 5 presents the results of two groups of approaches: AC, according to [24], and ACDD, which are the mixed-integer linear programming approaches, and the *meta*-heuristic and the hybridization. The results indicate an essential recommendation in wind power output bidding, suggesting that the bid power output for wind farms should be slightly lower than the predicted power output. This is illustrated by the negative WPD deviation achieved in all approaches, which means the best bidding value for wind power is achieved when the bidding output capacity is lower than the highest predicted probability. Specifically, the hybrid algorithm method yields the highest revenue at $75.9/year, with the WPD exhibiting relative deviations ranging from −15.6 % to −16.7 %, depending on the Weibull statistics of each wind farm.

With the proposed approach, the maximum bid power output for wind farms can reach up to 114 MW. This exceeds the testing results of other methods and is 1.2 times higher than the method referenced in [15], which only achieved 95 MW and nearly double that of the standalone wind power model also mentioned in that document, which reached 65 MW. These results indicate that integrating wind power sources into the power system can significantly enhance wind energy utilization efficiency. This minimizes the risk of wind power uncertainty in the system and leads to higher bid-winning wind power output.

Furthermore, results from the optimization methods also indicate that investing in ESS can improve wind energy exploitation efficiency. With an objective function including the cost and profit of the ESS, the highest benefit is consistently achieved in locations with ESS, as shown in Table 5. The LSTM-PSO algorithm demonstrates an average ESS power capacity of around 16 MW. This indicates that utilizing ESS sources has helped mitigate the risk of wind power shortage during electricity market operations.

The experimental results based on the input data presented in Section 4.1 reflect uncertainty modeled through Weibull parameters within the context of an electricity market operating based on electricity purchase price indices and regulatory penalties. For places with differing wind speed conditions, variations in uncertainty levels will lead to changes in calculation outcomes, as defined through expressions (11) to (15) in Section 2.1.2. Similarly, if the electricity market experiences volatility, electricity price indices will directly impact the problem through expressions (25) to (30) in Section 2.2.4. A more detailed study of these factors can be conducted in subsequent research to provide a deeper understanding of the relationship between uncertainty factors and the operational efficiency of the electricity market.

4.3. Testing the OPF problem

Another way to evaluate the effectiveness of the new algorithm is to test the optimal power flow (OPF) problem using the IEEE 30-bus system and compare the results with those from the studies reviewed in [23]. Five such comparisons are presented in Table 6.

Table 6 demonstrates a reduction in the number of iterations required compared to similar studies. Although the optimal cost results show minimal differences from prior research—800.9 $/year compared to the minimum of 800.4 $/year in case [46]—the improvement in computational efficiency is clearly evident. Notably, the Number of Fitness Function Evaluations (NFFE), recorded at 3000 evaluations, is

Table 6
Comparison of the implementation of methods.

Ref.	Populations	Generations	NFFE	Cost ($)
[43]	500	50	25,000	800.41
[44]	500	50	25,000	802.04
[45]	150	***20***	***3,000***	800.74
[46]	200	50	10,000	***800.40***
[47]	200	20	4,000	801.84
LSTM-PSO	***100***	30	***3,000***	800.90

comparable to that in scenario [45] and significantly lower than in most other scenarios, which range from 4000 to 25,000 evaluations.

5. Conclusion

This study demonstrates the potential of integrating PSO with LSTM networks to address complex optimization problems, particularly in the context of wind power integration within electricity markets. The proposed hybrid algorithm achieves several notable advancements:

First, improved convergence speed. The hybrid algorithm demonstrates a significantly faster convergence rate compared to the pure PSO algorithm, particularly after the initial ten iterations, where the LSTM network starts to contribute meaningfully. The hybrid algorithm achieves convergence and stability within 15 iterations, whereas the pure PSO continues to show dispersion at this stage.

Second, enhanced self-adaptation and refinement. The LSTM network within the hybrid algorithm enables a process of internal self-improvement, allowing the algorithm to learn from previous iterations and adjust its search strategy. This leads to more refined individual solutions and faster convergence towards the global optimum.

Third, effective handling of uncertainty. In wind power integration, the hybrid LSTM-PSO algorithm effectively manages the uncertainty associated with wind power output. It determines the optimal bid power output for wind farms by considering factors such as WPD deviation and potential profit loss. Additionally, integrating an ESS into the optimization process further mitigates the risks of wind power variability.

Fourth, improved wind power utilization. The hybrid algorithm consistently achieves a higher maximum bid power output for wind farms compared to other methods, demonstrating its effectiveness in maximizing wind power utilization within the electricity market while accounting for the inherent uncertainty of wind energy.

Finally, reduced computational burden. When applied to OPF problems, the LSTM-PSO algorithm requires fewer iterations to reach optimal solutions, as indicated by a lower NFFE indicator. This demonstrates its computational efficiency in solving complex power system optimization problems.

These results not only validate the effectiveness of the PSO-LSTM hybrid approach but also highlight its potential for broader applications. Future research could extend this work by exploring alternative metaheuristic algorithms, such as Genetic Algorithms or Differential Evolution, combined with advanced deep learning models like Transformers or Convolutional Neural Networks. Such integrations could further enhance algorithmic efficiency and enable the development of hybrid solutions tailored to practical challenges in renewable energy, finance, and data science.

However, alongside the achievements, there remain certain limitations that warrant further investigation. First, the optimization performance may extend beyond the LSTM-PSO hybrid algorithms. It would be worthwhile to explore other deep learning and metaheuristic algorithms to assess optimization effectiveness. Second, the training data for LSTM in the initial iterations is relatively small, which can easily lead to overfitting, potentially resulting in inaccurate predictions during this phase. To address this issue, regularization techniques need to be employed within the algorithm to enhance performance. Nevertheless, this could be improved by utilizing pre-trained architectures, or larger datasets in large-scale optimization problems.

Ethics approval

Not applicable.

Consent to Participate

The authors are committed to actively contributing to the article.

Consent for Publication

The authors commit to publishing the article upon acceptance.

Funding

No financial support was received to develop this manuscript.

CRediT authorship contribution statement

Viet Anh Truong: Methodology, Conceptualization. **Ngoc Sang Dinh:** Writing – original draft, Methodology. **Thanh Long Duong:** Resources. **Ngoc Thien Le:** Software, Resources. **Cong Dinh Truong:** Data curation. **Linh Tung Nguyen:** Formal analysis.

Declaration of competing interest

The authors declare that they have no known competing financial interests or personal relationships that could have appeared to influence the work reported in this paper.

Acknowledgments

Authors extend sincere gratitude to Hochiminh City University of Technology and Education, Vietnam, with special thanks to Laboratory C201.

References

[1] Priddle R. World Energy Transitions Outlook 2023. France: International Energy Agency (IEA); 2023.
[2] Haugen M, Farahmand H, Jaehnert S, Fleten S-E. Representation of uncertainty in market models for operational planning and forecasting in renewable power systems: a review. Energy Systems 2023.
[3] Mohamed E, Seresht NG, Jafari P, AbouRizk S. Risk assessment for onshore wind projects in Canada. *Renew Sustain Energy Rev* 2024;191:114145.
[4] Cong R, Fujiyama A, Matsumoto T. An optimal scheme assists the municipalities in Fukuoka, Japan in achieving their goal of 100% renewable energy supply and future decarbonization. *Energy Nexus* 2024;13:100277.
[5] Mohammed A-A-Q, Ahmed AE, Ahmad OA, Mohamed AE. Wind power forecasting using optimized LSTM by attraction–repulsion optimization algorithm. *Ain Shams Eng J* 2024:103150.
[6] Schlecht I, Maurer C, Hirth L. Financial contracts for differences: The problems with conventional CfDs in electricity markets and how forward contracts can help solve them. *Energy Policy* 2024;186:113981.
[7] Hu X, Jaraitė J, Kažukauskas A. The effects of wind power on electricity markets: A case study of the Swedish intraday market. *Energy Econ* 2021;96:105159.
[8] Truong AV, Nguyen LT, Dinh SN. Controlling output power to enhance the investment efficiency of wind farms by maximizing the capacity of transmission transformers and integrating energy storage systems. *Eng, Technol Appl Sci Res* 2024;14(4):15751–6.
[9] Ribeiro MHDM, Silva RGd, Moreno SR, Canton C, Larcher JHK, Stefenon SF, et al. Variational mode decomposition and bagging extreme learning machine with multi-objective optimization for wind power forecasting. *Appl Intell* 2024;54:3119–34.
[10] Velasco L, Guerrero H, Hospitaler A. A literature review and critical analysis of metaheuristics recently developed. *Arch Comput Meth Eng* 2024;31:125–46.
[11] Nkalo UK, Inya OO, Obi PI, Bola AU, Ewean DI. A modified multi-objective particle swarm optimization (M-MOPSO) for optimal sizing of a solar–wind–battery hybrid renewable energy system. *Sol Compass* 2024;12:100082.
[12] Qais M, Hasanien H, Alghuwainem S. Enhanced salp swarm algorithm: Application to variable speed wind generators. *Eng Appl Artif Intel* 2019;80:82–96.
[13] Kaur S, Kumar Y, Koul A, Kamboj SK. A Systematic Review on Metaheuristic Optimization Techniques for Feature Selections in Disease Diagnosis: Open Issues and Challenges. *Arch Comput Meth Eng* 2023;30:1863–95.
[14] Camacho-Vallejo J-F, Corpus C, Villegas JG. Metaheuristics for bilevel optimization: A comprehensive review. *Comput Oper Res* 2024;161:106410.
[15] Kaveh M, Mesgari MS. Application of Meta-heuristic algorithms for training neural networks and deep learning architectures: a comprehensive review. *Neural Process Lett* 2022;55:4519–622.
[16] Shrouti D, Bayas A, Joshi N, Misal M, Mahajan S, Gite S. Story Generation Using GAN, RNN and LSTM. Adv. Comput. 2024;2053:193–204.
[17] Al-Selwi SM, Hassan MF, Abdulkadir SJ, Muneer A, Sumiea EH, Alqushaibi A, et al. RNN-LSTM: From applications to modeling techniques and beyond—Systematic review. *J. King Saud Univ. – Comput. Informat. Sci.* 2024;36(5):102068.
[18] Zhao E, Zhou N, Liu C, Su H, Liu Y, Cong J. Time-aware MADDPG with LSTM for multi-agent obstacle avoidance: a comparative study. *Complex Intell Syst* 2024;10:4141–55.
[19] Cui X, Zhu J, Jia L, Wang J, Wu Y. A novel heat load prediction model of district heating system based on hybrid whale optimization algorithm (WOA) and CNN-LSTM with attention mechanism. *Energy* 2024;312:133536.
[20] Wu Z, Cui N, Zhang W, Liu C, Jin X, Gong D, et al. Estimating soil moisture content in citrus orchards using multi-temporal sentinel-1A data-based LSTM and PSO-LSTM models. *J Hydrol* 2024;637:131336.
[21] Son Y, Zhang X, Yoon Y, Cho J, Choi S. LSTM–GAN based cloud movement prediction in satellite images for PV forecast. *J Ambient Intell Hum Comput* 2023;14:12373–86.

[22] Gundu V, Simon SP. PSO–LSTM for short term forecast of heterogeneous time series electricity price signals. *J Ambient Intell Hum Comput* 2021;12:2375–85.
[23] Georgios P, Pandelis B. Review and Comparison of Genetic Algorithm and Particle Swarm Optimization in the Optimal Power Flow Problem. *Energies* 2023;16(3):1152.
[24] Truong VA, Dinh NS, Duong TL. Profit maximization of wind power plants in the electricity market based on linking models between energy sources. *Arab J Sci Eng* 2023;48(8).
[25] Salgotra R, Sharma P, Raju S, Gandomi AH. A contemporary systematic review on meta-heuristic optimization algorithms with their MATLAB and python code reference. *Arch Comput Meth Eng* 2024;31:1749–822.
[26] Topaloglu I. Deep learning based a new approach for power quality disturbances classification in power transmission system. *J Electr Eng Technol* 2023;18:77–88.
[27] Cao D, Hu W, Xu X, Dragičević T, Huang Q, Liu Z, et al. Bidding strategy for trading wind energy and purchasing reserve of wind power producer – A DRL based approach. *Electr Power Energy Syst* 2020;117:105648.
[28] Shinde P, Amelin M. A literature review of intraday electricity markets and prices. *IEEE Milan PowerTech* 2019:18938508.
[29] Energy Prices and Costs in Europe: Report from the commission to the european parliament, the council, the european economic and social committee and the committee of the regions European Commssion, Brussels, 2020.
[30] Wang Z, Wang W, Liu C, Wang Z, Hou Y. Probabilistic forecast for multiple wind farms based on regular vine copulas. *IEEE Trans Power Syst* 2018;33(1):578–89.
[31] Wais P. A review of Weibull functions in wind sector. *Renew Sustain Energy Rev* 2017;70:1099–107.
[32] Mdee OJ. Performance evaluation of Weibull analytical methods using several empirical methods for predicting wind speed distribution. *Energy Source* 2020:1–24.
[33] Abedi A, Hesamzadeh MR, Romerio F. Adaptive robust vulnerability analysis of power systems under uncertainty: A multilevel OPF-based optimization approach. *Int J Electr Power Energy Syst* 2022;134:107432.
[34] Biswas PP, Suganthan PN, Amaratunga GAJ. Optimal power flow solutions incorporating stochastic wind and solar power. *Energ Conver Manage* 2017;148:1194–207.
[35] Cao M, Xu Q, Qin X, Cai J. Battery energy storage sizing based on a model predictive control strategy with operational constraints to smooth the wind power. *Int J Electr Power Energy Syst* 2020;115:1–10.
[36] Bertrand G, Papavasiliou A. An Analysis of Threshold Policies for Trading in Continuous Intraday Electricity Markets. *15th International Conference on the European Energy Market (EEM)*. 2018.
[37] Kennedy J, Eberhart R. Particle Swarm Optimization. Proceedings of ICNN'95 - International Conference on Neural Networks. WA, Australia: Perth; 1995.
[38] Bonyadi MR, Michalewicz Z. Particle Swarm Optimization for Single Objective Continuous Space Problems: A Review. *Evol Comput* 2017;25(1):1–54.
[39] Hochreiter S, Schmidhuber J. Long Short-Term Memory. *Neural Comput* 1997;9(8):1735–80.
[40] Shahid F, Zameer A, Muneeb M. A novel genetic LSTM model for wind power forecast. *Energy* 2021;223:120069.
[41] "MATPOWER Test Cases," 24 January 2018. [Online]. Available: https://matpower.org/docs/ref/matpower5.0/case_ieee30.html. [Accessed 25 July 2023].
[42] Alsac O, Stott B. Optimal load flow with steady-state security, IEEE Trans Power Apparatus Syst, Vols. PAS-93, no. 3, pp. 745-751, 1974.
[43] Abido MA. Optimal power Flow using particle swarm optimization. *Int J Electr Power Energy Syst* 2002;24(7):563–71.
[44] He S, Wen J, Prempain E, Wu Q, Fitch J, Mann S. An improved particle swarm optimization for optimal power flow. International Conference on Power System Technology, Singapore. 2004.
[45] Swarup K. Swarm intelligence approach to the solution of optimal power flow. *J Indian Institute Sci* 2006;86:439–55.
[46] Naderi E, Pourakbari-Kasmaei M, Abdi H. An efficient particle swarm optimization algorithm to solve optimal power flow problem integrated with FACTS devices. *Appl Soft Comput* 2019;80:243–62.
[47] Umapathy P, Venkataseshaiah C, Arumugam M. Particle Swarm Optimization with Various Inertia Weight Variants for Optimal Power Flow Solution. *Discrete Dynamics in Nature and Society*. 2010.

Viet Anh Truong was born in 1971. He received the B.Eng., M. Eng., and Ph.D. degrees in electrical engineering from the Ho Chi Minh City University of Technology (HCMUT), Vietnam National University (VNUHCM), Ho Chi Minh City, Vietnam in 1994, 1999, and 2004, respectively. He is currently working with the Faculty of Electrical and Electronics Engineering and the Power System and Renewable Energy Laboratory (C201), Ho Chi Minh City University of Technology and Education, Ho Chi Minh City. His current research areas include Power system analysis, renewable energy, reconfiguration distribution network with various objectives. He has published more than 80 articles in national and international journals, workshops, and conferences.

Ngoc Sang Dinh was born in 1972. He received a B.Eng. degree in Power System Engineering in 1994 and an M.Eng. degree in Electrical Engineering in 2004 from Ho Chi Minh City University of Technology, Ho Chi Minh City, Vietnam. He currently works with the Department of Urban Engineering, University of Architecture Hochiminh City (UAH), Ho Chi Minh City, Vietnam. His research interests are power system plans, renewable energy power generation, artificial intelligence-based algorithms, and their application in optimization problems.

Thanh Long Duong received the B.Eng. and M.Eng. degrees in electrical engineering from the University of Technical Education Ho Chi Minh City, Vietnam, in 2003 and 2005, respectively, and the Ph.D. degree in electrical engineering from Hunan University, China, 2014. He currently works with the Faculty of Electrical Engineering Technology, Industrial University of Ho Chi Minh City, Ho Chi Minh City, Vietnam. His research interests include power system operation, power system optimization, FACTS, renewable energy, optimization algorithm, and power markets.

Ngoc Thien Le was born in Phu Yen, Vietnam in 1983. He received the B.E. degree in electrical engineering from HCMC University of Technology and Education, Vietnam, in 2006, and the M.E. degree in telecommunication from Ho Chi Minh City University of Technology, Vietnam, in 2008. He got the Ph.D. degree at the Department of Electrical Engineering, Chulalongkorn University, Thailand in 2016. His research interests include data analysis for smart grid and smart grid communication, Apply AI and DL models for healthcare.

Cong Dinh Truong was born in 1972. He received a B.Eng. degree in Power System Engineering in 1996 and an M.Eng. degree in Electrical Engineering in 2006 from Ho Chi Minh City University of Technology, Ho Chi Minh City, Vietnam. He currently works with the Department of Urban Engineering, University of Architecture Hochiminh City (UAH), Ho Chi Minh City, Vietnam. His research interests are power system plans, renewable energy power generation.

Linh Tung Nguyen, He was born in 1982 and graduated with a bachelor's and master's degree in electrical and electronic engineering from Hanoi University of Science and Technology (2005, 2010). He defended his PhD thesis in 2018 at the Vietnam Academy of Science and Technology with the thesis "Building artificial intelligence algorithms for the problem of reconfiguration network distribution". He currently works at the Department of Control and Automation, Electric Power University (EPU), Hanoi, Vietnam. His current research areas include electrical systems, smart electrical systems, renewable energy, smart factories, reconfiguration distribution network with various objectives, artificial intelligence applications, big data for energy-related problems, digital transformation in energy sector. He has published more than 30 articles in national and international journals, workshops, and conferences.

Arabian Journal for Science and Engineering
https://doi.org/10.1007/s13369-023-08181-1

RESEARCH ARTICLE-ELECTRICAL ENGINEERING

Profit Maximization of Wind Power Plants in the Electricity Market Based on Linking Models Between Energy Sources

Viet Anh Truong[1] · **Ngoc Sang Dinh**[1,2] · **Thanh Long Duong**[3]

Received: 27 December 2022 / Accepted: 26 July 2023

Abstract
A major barrier to wind sources when participating in an electricity market is inaccurate forecasting of wind power. The wind power uncertainty affects the plant's scheduled generation power, bidding price, and profitability. The profits of wind farms may be increased by determining the suitability of power output and bidding strategy in the electricity market, which is one of the challenges for wind plant producers because it is difficult to predict wind power accurately. To solve this problem, wind farm owners need to have plans to reserve power or link with other wind plants to be able to fully meet the contracted power. This paper proposed models linking wind farms or wind farms and other energy sources such as thermal power and energy storage systems. The simulation results on the IEEE 30-bus system show that the profits of a wind plant are increased when there is a backup power agreement from the thermal power plant or energy storage systems. It also demonstrates that the profitability of a wind power plant can be enhanced up to 132% by implementing a backup power agreement with a thermal power plant or energy storage systems. Furthermore, the wind output power increases significantly, reaching 95 MW in the integration models compared to the original model of 55 MW, thereby generating substantial social welfare.

Keywords Wind power · Electricity market · Energy storage systems · Uncertain · Bidding strategy · Generation expansion plan

Abbreviations

ESS	Energy storage system
EWF	ESS with wind farms model
ISO	Independent system operator of the electricity market
IWF	Independent wind farm model
LWF	Linking wind farms model
MPG	Manageable power generations
PDF	Probability distribution function
PPA	Power purchase agreement
TWF	Thermal plants with wind farms model
UPG	Uncertain power generations
WBF	Wind benefit function
WPP	Wind power plant
Penalty	In this context, it refers to the consequence of a violation under contract, which may involve compensation specified in PPA or remediation measures, such as purchasing products on the spot market to compensate the contracting party

List of Symbols

λ_e	Buying prices from integrated ESS
λ_p	Penalty prices
λ_T	Buying prices from integrated thermal plants
λ_{TG}	Thermal power prices in market
λ_w	Wind power prices
ΔP_w	Penalty power ($P_p - P_{Tp} - P_e$)
a_i, b_i, c_i	Operating cost ratios of thermal generation i
C_e	Costs, wind has to pay to purchase electricity from integrated ESSs
C_{e0}	Fixed ESS costs

✉ Thanh Long Duong
duongthanhlong@iuh.edu.vn

[1] Faculty of Electrical and Electronics Engineering, Hochiminh City University of Technology and Education (HCMUTE), Ho Chi Minh City, Vietnam

[2] Department of Urban Engineering, University of Architecture Hochiminh City (UAH), Ho Chi Minh City, Vietnam

[3] Faculty of Electrical Engineering Technology, Industrial University of Hochiminh City (IUH), Ho Chi Minh City, Vietnam

Published online: 16 August 2023

C_{Pw}	Compensation or penalty cost
C_T	Operating costs of the thermal generation
C_{Tp}	Costs, wind has to pay to purchase electricity from thermal plants
$f(v)$	Probability density function
$f_{\Sigma w}$	Probability density function of integrated wind farms
k, c	Weibull parameters
k_P	Penalty price ratio $(1 - 2.4)$
k_R	Reserve price ratio (0–1)
N_{TG}	Number of thermal plants
N_w	Number of integrated winds
P_w	Wind power probability
$P_{\Sigma w}$	Summary output power of integrated winds
P_e	Power, wind buys from integrated ESSs $(0 - P_{er})$
P_{er}	Maximum ESS output power
P_p	Shortfall wind power, deviation from schedule $\begin{cases} 0, & P_{wav} \geq P_{ws} \\ P_{ws} - P_{wav}, & P_{wav} < P_{ws} \end{cases}$
P_{Tav}	Actual output power of thermal plants $(0 - P_{Tr})$
P_{Tp}	Power, wind buys from integrated thermal plants $(0 - P_{TR})$
P_{Tr}	Rated power of thermal plants
P_{TR}	Limited power buying from integrated thermal plants $(P_{Tr} - P_{Ts})$
P_{Ts}	Schedule output power of thermal plants in market $(0 - P_{Tr})$
P_w	Variable output wind power $(0 - P_{wr})$
P_w^{Optimal}	Optimal wind power, when wind revenue reaches maximum
P_{wav}	Actual output wind power $(0 - P_{wr})$
P_{wr}	Rated wind power
P_{ws}	Scheduled wind power $(0 - P_{wr})$
P_{wu}	Uncertain wind power $(P_{wav} - P_{ws})$
R_w	Wind revenue
R_w^{Peak}	Maximum wind revenue
R_{ws}	Direct wind revenue, following scheduled power
R_{wu}	Uncertain wind revenue, following uncertain power
R_{Rw}	Reserve wind revenue following power over-schedule
v	Wind speed
v_{in}, v_{out}	Cut-in and cut-out wind speeds (3 m/s, 25 m/s)
v_r	Rated wind speed (16 m/s)

1 Introduction

In recent years, wind power has emerged as a rapidly growing renewable energy source globally [1]. Reports indicate that global wind energy exploitation has been increasing by over 50 GW annually since 2014, reaching 591 GW in 2018, with a 9.6% growth compared to last year [2]. Furthermore, the global total energy demand increased by approximately 160% from 1990 to 2017, representing a 1.6-fold increase over a 27-year period, according to the report in [3]. The importance of energy for economic and social development became evident during the energy crisis in Europe in 2022 when restrictions on natural gas supply from key countries caused sharp price fluctuations, impacting essential commodity costs worldwide and highlighting the risks associated with fossil fuel dependence. Consequently, governments worldwide have been focusing on developing renewable energy sources to reduce reliance on fossil fuels, in which wind energy is playing a significant role [1]. This energy source is the most convenient and efficient alternative, which has rapidly developed in the past decades in most developing countries [3]. Additionally, the increasing share of wind power has potential environmental benefits [4, 5].

Another way, the incentives for renewable energy sources in general, and specifically for wind energy, have exhibited a gradual decline in recent times, resulting in an upward trajectory of wind power prices, while investments have experienced a slight deceleration [6]. This consequence can be attributed to the need for wind power investors to exercise greater prudence during the bidding process for energy sales in the electricity market, necessitating comprehensive information following regulatory requirements, including the power output and bidding prices. However, formulating accurate production plans by forecasting the future presents an exceedingly complex undertaking fraught with inherent risks. The intrinsic uncertainty associated with the electricity production output from a wind power plant at any given moment constitutes a significant obstacle to equitable and competitive participation in the electricity market.

In examples of recent studies on wind power impacts on electricity markets, researchers have highlighted the increasing integration of renewable energy sources, including wind energy, in the power system, which introduces uncertainty into the electricity market [7]. Consequently, there is a pressing need for effective solutions to lessen the severity. In this context, the paper [8] proposes a novel optimization approach in hybrid power systems encompassing renewable energy and energy storage, aiming to enhance overall investment efficiency. In contrast, others argue that electricity market transactions benefit the system by lowering prices and balancing market volumes through system flexibility [9].

Therefore, developing and integrating wind power into the electricity market are inevitable. However, its downside is associated with the inherent uncertainty that significantly impacts the electricity system's operational conditions and power supply and introduces market disturbances. Firstly, the utilization of combined wind power, as discussed in the

literature [10], demonstrates that its actual power output may deviate from the expected plans, leading to suboptimal operation of power plants and inefficient power flow. Furthermore, the electricity market becomes more complex when the predicted electricity supply is subject to changes during trading periods, resulting in unpredictable fluctuations in electricity prices [11]. The transactions in the intraday markets serve as examples and are subject to evaluation in the report. [12]. Consequently, there is a pressing need to explore and implement solutions to investigate and mitigate these challenges to maximize the benefits of wind power integration [13].

Additionally, developing accurate forecasting strategies for wind power is paramount to mitigate the impact of weather-related uncertainties on wind power generation. Incorporating the wind probability distribution function (PDF), such as Weibull PDF, is a commonly employed method that can enhance the reliability of WPP owners by offering a more comprehensive assessment of revenue uncertainties associated with wind power in the market. By adopting advanced management techniques and optimizing bidding decisions, wind plant owners can improve their financial performance and maximize societal welfare.

In summary, the participation of wind power in the competitive electricity market significantly impacts both technics and economics, particularly the income of wind power investors. To evaluate the extent of the influence of wind power uncertainty on bidding behavior and its benefits in the electricity market, this study investigates the variability of wind power revenue considering random factors such as wind speed probability, penalty values for contractual breaches resulting from power output shortages, and the conduct of generation owners when interconnected with wind power, as in [3]. Building upon this analysis, the paper proposes methodologies for integrating wind power with thermal plants and energy storage systems to enhance investment efficiency. To provide a more comprehensive analysis, the report examines the revenue fluctuations in wind power to ascertain the optimal offer power and maximize the associated benefits. These income changes are influenced by two key factors: (i) the probability distribution of wind speed at the specific wind turbine location and (ii) the apparent variations in a ratio, which are penalty values for contractual breaches resulting from wind power output shortages.

Simulation experiments are conducted using the IEEE 30-bus system to evaluate four models. The results demonstrate the remarkable effectiveness of these models in mitigating financial losses for wind power investments in the face of uncertainties. Based on these findings, the study also recommends potential strategies for wind power owners to adopt in the competitive electricity market.

The main contribution of the paper is outlined as follows:

(i) This study proposes three linking models of wind power with other energy sources, particularly thermal plants, and ESSs, in a competitive electricity market for enhancing profits of wind power plants.
(ii) The wind optimal power output decisions in electricity markets are also covered in this study.
(iii) The IEEE 30-bus system with an integrated wind farm and ESS is investigated in this study.

2 Mathematical Model

Classification of electricity sources based on their operational supply perspective involves two primary energy sources: high active energy (MPG) and dependent energy (known as uncertain energy, denoted as UPG). The MPG, such as thermal or hydroelectric power plants, can regulate their energy output and supply electricity as needed. In contrast, UPG, including wind and solar power, relies on unpredictable natural conditions, and their electricity production is uncertain and uncontrollable. Integrating UPG, particularly wind power, into the power system presents optimal operation, stability and security challenges. The intermittent nature of wind power can lead to unexpected imbalances in energy supply and demand, causing risks of energy surplus or shortfall during operation, and can disorder everyday electricity market transactions.

This study examines the modeling of three distinct energy sources involved in the electricity market: wind power, thermal power and energy storage systems.

2.1 Wind Model in the Electricity Market

Within the market framework, the revenue generated by a wind power source can be classified into two components: direct income stemming from predetermined energy quantities and uncertain payment [10]. According to projections, an energy production plan and the bidding price for wind power can yield direct revenue for owners. Conversely, deviations between the supplied actual electricity and the predetermined schedule can result in either additional revenue or losses, constituting uncertain revenue. For instance, when the energy output exceeds the forecasted amount at a given point in time, surplus energy income is paid by a reserve price, which often falls significantly below the direct electricity selling price. Conversely, owners must procure energy from alternative sources to compensate for the shortfall or face penalties if the energy output falls short of the initially planned bid, and these costs are collectively known as penalty costs. The penalty fees are typically considerably higher than the direct electricity selling price.

The following expression is used to model wind farm revenue:

$$R_w(P_w) = \sum R_{w,i} = \sum \left[R_{ws,i}\left(P_{ws,i}\right) + R_{wu,i}\left(\Delta P_{w,i}\right) \right] \tag{1}$$

where P_w is the total wind power sold in the electricity market; $R_{w,i}$, $R_{ws,i}$, $R_{wu,i}$ are sum, direct and uncertain revenue of the i-th wind farm; and $P_{ws,i}$ và $\Delta P_{w,i} = P_{wav,i} - P_{ws,i}$ are planned power and actual power difference $P_{wav,i}$ be compared with the plan of$i$-th wind power.

2.2 Direct Revenue

Direct revenue of the$i$-th wind farm is determined corresponding to the offered price and wind power provided in the electricity market, determined by the formula (2).

$$R_{ws,i}(P_{ws,i}) = \lambda_{w,i} P_{ws,i} \tag{2}$$

In expression (2), the revenue is proportional to two variables. The first variable is the wind power output sold according to the bidding plan based on the production forecast at the given time, P_{ws}. A higher planned power value leads to higher revenue and vice versa. However, setting a higher one carries increased risks for wind owners due to the associated uncertainty. The bidding method depends on the electricity market in which it participates.

The second proportional value, $\lambda_{w,i}$, represents the direct unit price associated with the$i$-th wind producer. This coefficient is predicted and bid on by the wind plant owner [2]. It may be the price that ensures sufficient income to cover the investment and operation costs of the wind power plant. However, in a market pricing mechanism, this number can be influenced by the average electricity prices of the dominant power sources in the electricity market, which are determined by the supply and demand dynamics. For instance, in the EU electricity market, the pricing calculation for wind power can be based on the price of gas-fired power as it is a significant dominant energy source [6].

Assuming that the dominant power source in the electricity market determines the production and operation costs of the thermal plants, the selling price of thermal power in the electricity market depends primarily on secondary fuel costs. This cost can be calculated using the following expression:

$$C_T(P_{TG}) = \sum_{i=1}^{N_{TG}} \left(a_i + b_i P_{TG,i} + c_i P_{TG,i}^2 \right) \tag{3}$$

$$\lambda_{TG,i} = b_i + c_i P_{TG,i} \tag{4}$$

Here, a_i, b_i and c_i represent the cost coefficients of the$i$-th thermal generation that generates the generating power $P_{TG,i}$. The total number of thermal generations is N_{TG}. $\lambda_{TG,i}$ denotes the unit price of this generation.

2.3 Final Evaluation of Uncertainties in Wind Power

The second component of Eq. (1) represents the volatile income, which consists of two parts:

Firstly, it includes the revenue from selling surplus energy (reserve revenue, R_{Rw}). When WPP exceeds the previously anticipated levels, the excess energy can be sold at a relatively lower price than the average market price, and there may be instances where no buyers are available [2].

Secondly, it involves the financial liability incurred to address energy shortages (referred to as penalty costs, C_{Pw}). When electricity production falls short of the predicted supply in the electricity market, wind power owners must purchase additional electricity in the electricity market to compensate for the energy deficit caused by their shortfall. Alternatively, they may face penalties as outlined in the power purchase agreement (PPA) with the market operator (ISO) or the buyers. In such cases, the price of the purchased electricity or the penalty price (collectively called penalty price) is often significantly higher than the direct selling price of wind power [2].

In Eq. (5), the uncertain income of the i-th wind power source is represented as follows:

$$R_{wu,i}\left(\Delta P_{w,i}\right) = \begin{cases} R_{Rw,i}\left(\Delta P_{w,i}\right), & \text{if} P_{\text{wav},i} \geq P_{ws,i} \\ C_{Pw,i}\left(\Delta P_{w,i}\right), & \text{if} P_{\text{wav},i} \leq P_{ws,i} \end{cases} \tag{5}$$

Reserve income is defined as,

$$\begin{aligned} & R_{Rw,i}\left(\Delta P_{w,i}\right) \\ & = k_{R,i}\lambda_{w,i}\left(P_{\text{wav},i} - P_{ws,i}\right) \\ & = k_{R,i}\lambda_{w,i} \int_{P_{ws,i}}^{P_{wr,i}} \left(p_{w,i} - P_{ws,i}\right) f_w\left(p_{w,i}\right) dp_{w,i} \end{aligned} \tag{6}$$

And the penalty is,

$$\begin{aligned} & C_{Pw,i}\left(\Delta P_{w,i}\right) \\ & = k_{P,i}\lambda_{w,i}\left(P_{\text{wav},i} - P_{ws,i}\right) \\ & = k_{P,i}\lambda_{w,i} \int_{0}^{P_{ws,i}} \left(p_{w,i} - P_{ws,i}\right) f_w\left(p_{w,i}\right) dp_{w,i} \end{aligned} \tag{7}$$

$P_{\text{wav},i}$ và $P_{wr,i}$ denote the actual available and rated output power from the same plant. $f_w\left(p_{w,i}\right)$ is the wind power probability density function for the i-th wind power plant. $k_{R,i}$ represents the reserve revenue ratio on the i-th wind power plant. The parameter $k_{P,i}$ denotes the penalty ratio when wind power output experiences a shortfall. This ratio

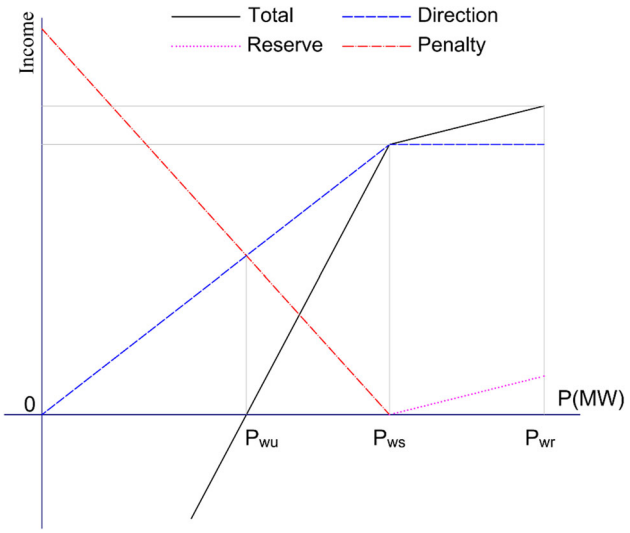

Fig. 1 Revenue components of an uncertain wind farm

is subject to random fluctuations corresponding to temporal supply–demand dynamics within electricity markets or negotiations between buyers and sellers. Contractual penalties may significantly exceed the typical transaction value, reaching multiples ranging from several to tens of times. Consequently, market participants often seek to offset their deficiencies by procuring electricity from alternative sources. The price of such purchased electricity is also influenced by the supply–demand dynamics within the electricity market, typically surpassing the average market selling price by a ratio of several times. Within this study, an investigation will be conducted into penalty coefficients ranging from 1.0 to over 2.4.

Visualize the curves of the total, direct revenue, reserve income, and penalty expenses, as shown in Fig. 1. This figure shows wind revenue in direct and uncertain (reserve/penalty) cases is linear, wherein cash flow scarcely increases in the case of wind power (P_w) which is more significant than the schedule (P_{ws}), but it dramatically decreases when P_w is lower than P_{ws}. In particular, wind farm owners would not get any income but have to pay when Pw is lower than P_{wu}, a case the penalty is over the direct.

2.3.1 Stochastic Wind and Uncertainty Models

The wind speed distribution at the turbine site decides the wind energy uncertainty. Consequently, finding the exact probability distribution for each wind speed is of the utmost importance in wind energy assessment. Although many different wind speed distribution models have been applied in previous studies, the two-parameter Weibull function is accepted as the most popular technique [14]. It has been widely used by researchers involved in wind speed and wind energy analysis for many years. In this case, the frequency of the wind speed model is written by the following,

$$f(v) = \left(\frac{k}{c}\right)\left(\frac{v}{c}\right)^{k-1} e^{-\left(\frac{v}{c}\right)^k} \tag{8}$$

where v is the wind speed; c and k are Weibull PDF parameters. Dimensionless factor k determines the shape of the curve and is called a shape factor. Parameter c, in m/s, is the scale parameter. The distributions take different forms with different values of k and c.

Figure 2 shows a probability distribution of wind speed at two places with parameters, $c = 9$; $k = 2$ and $c = 10$; $k = 2$. It can be seen that the wind speed distribution follows the Weibull probability density function [15] and [16].

Turbine power output is the result of the wind kinetic according to Weibull probability distribution on its blades, and it is described as follows [10],

$$P_w(v) = \begin{cases} 0, & v < v_{in} \text{ and } v > v_{\text{out}} \\ P_{wr}\left(\frac{v - v_{\text{in}}}{v_r - v_{\text{in}}}\right), & v_{\text{in}} \le v \le v_r \\ P_{wr}, & v_r < v \le v_{\text{out}} \end{cases} \tag{9}$$

where v_{in}, v_r and v_{out} represent the cut-in, rated and cut-out wind speeds of the turbine. P_{wr} is the rated output power of the wind turbine.

Figure 3 shows two identical wind turbines in two locations: Gen 1 with $c = 9$ m/s; $k = 2$ and Gen 2 with $c = 10$ m/s; $k = 2$. Wind turbine parameters are P_{wr}= 3 MW; v_{in} = 3 m/s; v_r= 16 m/s; and v_{out}= 25 m/s.

Accordingly, there are two regions in Fig. 3 where the probability of sudden increase is at zero and rated power. When the wind speed is lower than v_{in} or greater than v_{out}, the wind turbine will not operate, so the power is zero. Besides, when the wind speed is in the range v_r to v_{out}, the wind turbine power reaches the highest corresponding to the rated power.

2.3.2 Objective Function

The energy investment goal gets the highest benefit. More clearly, an uncertain wind farm in the electricity market needs to bid the sold electricity price and power output to maximize revenue. To achieve that, investors need to sell the most direct energy, while the penalty is minimal. The objective function of the problem, in this case, is the maximum wind farm revenue according to exp. (1), and more detail is exp. (2), and (5).

$$\text{maximize } \{F = R_w(P_w)\} \tag{10}$$

In case the wind power owner has integration into the MPG, such as ESS, or contracts with them to minimize the

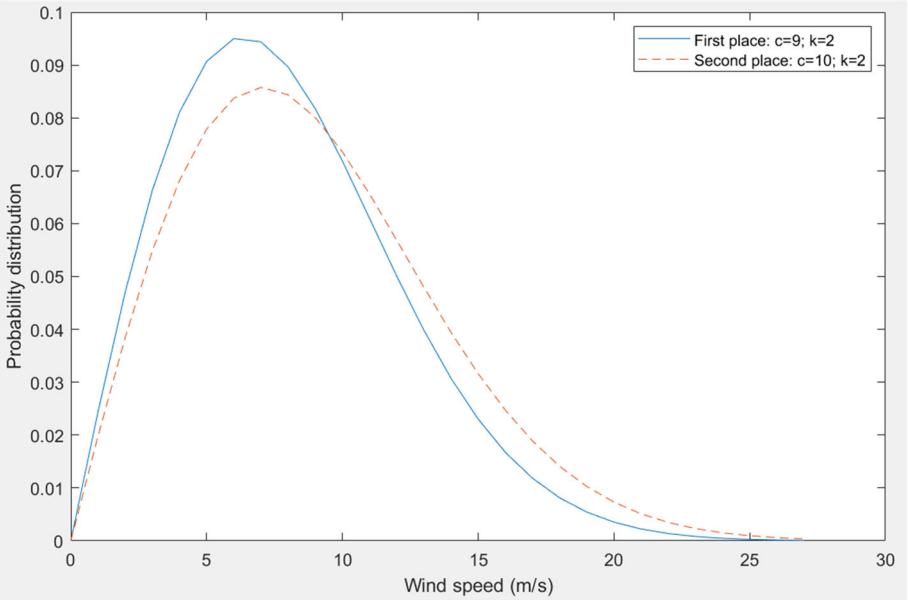

Fig. 2 Weibull probability distribution on wind speed at $c = 9$; $k = 2$ and $c = 10$; $k = 2$

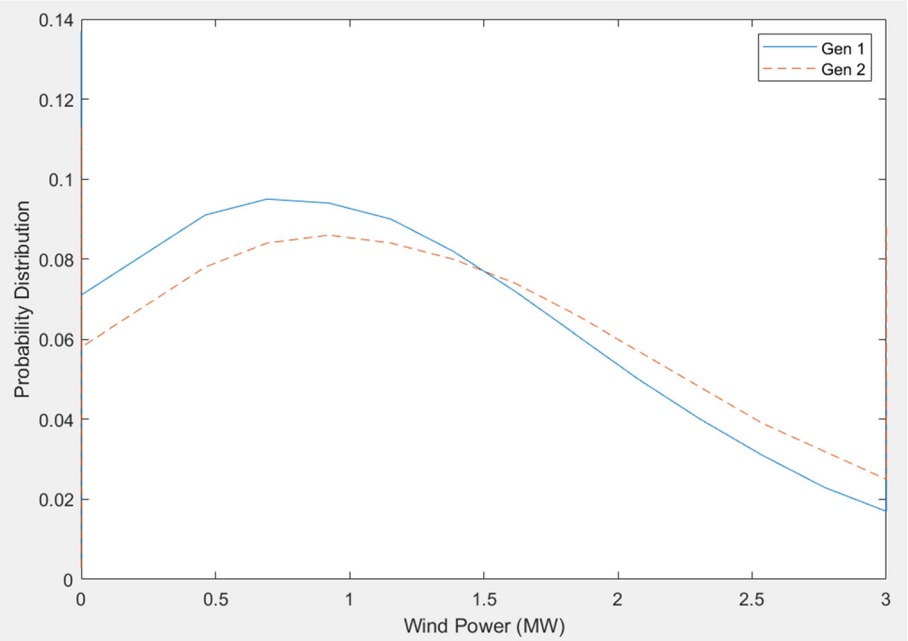

Fig. 3 Wind power probability distribution

cost of penalties due to uncertainty, the objective function will be,

$$\text{maximize } \left\{F = R_w(P_w) - C_{Pw}\left(P_p\right)\right\} \tag{11}$$

Here, C_{Pw} denotes the payment for an amount of transaction power P_p.

3 Proposed Linking Model

Different operational frameworks can exist in electricity markets, including competitive bidding behavior among plant employers, resembling a natural law. Wind owners' bidding behavior operates independently from others, and individual profit objectives typically drive their deci-

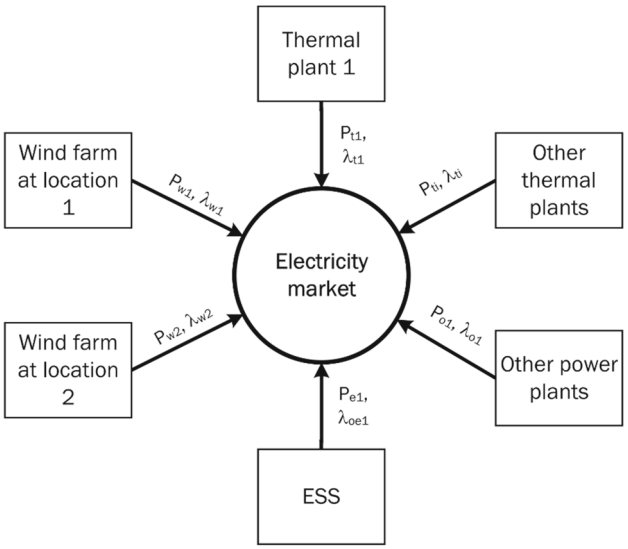

Fig. 4 IWF model

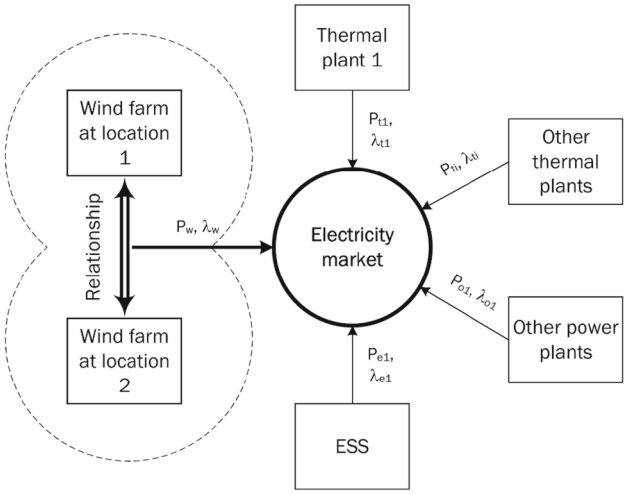

Fig. 5 LWF model

sions. This operative model is called the independent wind farm (IWF). The outcomes of this model are determined according to a defined objective function (10) and are entirely random in the electricity market, as demonstrated by [2].

Figure 4 illustrates the architecture of a conventional electricity market under the IWF model. It consists of wind farms in different geographical locations, thermal power plants, and other plants. Each established plant submits multi-parameters, which include two critical pieces of information: the electricity selling price, λi, and the power production plan for the corresponding Pi.

To examine and assess the impact of wind power uncertainty on the electricity market, this study proposes several integrated models beyond the fundamental IWF model:

(i) The Linking Wind Farms model (LWF) establishes integrations among wind farms situated in different geographical locations. A notable feature is that these distinct wind farms possess varying wind probability density functions, allowing them to compensate for power deficits as required mutually.
(ii) Thermal Plants with Wind Farms model (TWF): This model integrates thermal power plants with wind farms. It capitalizes on the advantageous characteristic of thermal power plants as an MPG plant, capable of proactively compensating for wind power shortages through standby power.
(iii) Energy Storage Systems with Wind Farms model (EWF): This model incorporates energy storage systems (ESS) with wind farms, which could be an expanded investment framework to enhance the efficiency of wind farms. This model uses ESS to store surplus wind power and compensate for any energy shortfall when deemed necessary. Furthermore, ESS can sell electricity during high market prices, augmenting investment effectiveness.

4 LWF Model

The LWF model, depicted in Fig. 5, involves a coordinated blending of multiple wind farms during the bidding process to mitigate uncertainty-related risks. By integrating wind farms, they can compensate for each other's electricity production shortfall when needed, thus reducing the risk and cost of addressing power deficits for both farms.

To model the uncertainty of WPP, a probability density function (PDF) is established for an equivalent virtual WPP using expressions (12) and (13).

$$f_{\Sigma w}(P_{\Sigma w}) = \prod_{i=1}^{N_w} f_{w,i}\left(P_{w,i}\right) \tag{12}$$

$$P_{\Sigma w} = \sum_{i=1}^{N_w} P_{w,i} \tag{13}$$

where $f_{\Sigma w}$ is a probability distribution combination from the wind farms $f_{w,i}$, and $P_{\Sigma w}$ are the wind power total, respectively.

The revenue of WPP is also calculated based on the mathematical model from exp. (10), like the IWF model, but PDF is the virtual wind plant.

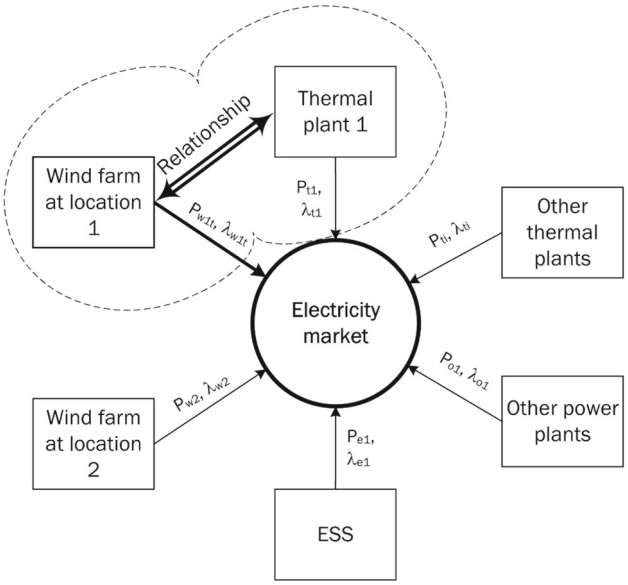

Fig. 6 TWF model

5 TWF Model

This model is shown in Fig. 6,

The objective function is determined as stated in Eq. (11), similar to previous models. However, a portion of the penalty cost is substituted with the thermal operation cost, compensating for the energy deficit resulting from the uncertainty of WPP. The calculation of this thermal cost, $C_{Tp}(P_{Tp})$, follows Eq. (3), or (14), in case the transaction contract value. It is notably lower than the penalty cost computed in IWF, particularly in the case of gas-fired thermal power plants. This disparity arises because the maximum electricity price in the market consistently exceeds the thermal generation cost.

$$C_{Tp}(P_{Tp}) = \lambda_T P_{Tp}; \quad P_p \in (0 \div P_{TR}) \tag{14}$$

The unit price λ_T is agreed upon in the contract, usually higher than the mean market price, because if it is lower, it has already been purchased by other market customers. Furthermore, wind power is only traded when this price is lower than the penalty coefficient because wind farms will only benefit from the amount paid to thermal power plants less than the penalty amount.

Nevertheless, it is essential to note that the electricity supplied by the thermal plant to compensate for the shortfall in WPP is constrained by its reserve power, P_{TR}, as indicated by the expression provided in Eq. (15).

$$P_{TR} = P_{Tr} - P_{Ts} \tag{15}$$

Here, P_{Tr} và P_{Ts} represents the rate and schedule power, according to the respective selling schedule of the thermal plants.

The uncertainty component in (11) is transformed from (5), and the result is shown as follows,

$$R_{wu}(P_{\mathrm{p}}) = \begin{cases} R_w(P_{\mathrm{p}}), & \text{if } P_p \geq 0 \\ C_{Tp}(P_{Tp}), & \text{if } P_{TR} \geq -P_p > 0 \\ C_{Pw}(P_p), & \text{if } -P_p > P_{TR} \end{cases} \tag{16}$$

$$P_p = P_{Tav} - P_{Ts}$$

When $-P_p > P_{TR}$,

$$C_{Pw}(P_{\mathrm{p}}) = C_{Pw}(\Delta P_{\mathrm{p}}) + C_p(P_{\mathrm{TR}})$$

$$\Delta P_p = P_p - P_{TR}$$

Here, P_p is the deviation of actual wind power from the schedule in the market; R_w, C_{Tp} and C_{Pw} are wind reserve revenue, agreement purchase and penalty cost; and P_{Tav} and P_{Ts} are actual and scheduled powers in the electricity market of thermal plants.

6 EWF Model

So far, the ESS investment capital still seems to be substantially high to bring profits to investors, so it is usually only built for particular needed purposes without other alternatives [17–19]. However, another vital active power source usually made synchronously with renewable projects is energy storage systems (ESS), which solve the complicated problems in power system operation with renewable [17]. One of their principal effects is used as a source of energy to compensate for the shortfall. ESS is a type of power that can supply electricity when needed and store energy when it is over-demand [18, 19]. Therefore, this idea is moderately suitable for wind energy sources when excess energy can be stored in the ESS and dispensed to the grid when there is a shortage, leading to minimizing penalty losses in the electricity market. Additionally, inside a linking of wind and ESS generations, ESS power will compensate for the shortfall of wind power when required and considerably reduces the risk of a wind penalty. As a result, wind farms would have effective combinations of thermal and ESS generations, as shown in Fig. 7.

An ESS's profit comes from the difference between the selling and purchasing price. Therefore, during periods of reduced load leading to low electricity prices, ESS won the bid for storage. After that, the sale occurs when the electricity price rises due to an overload or a penalty for lack of power output from UPGs. The ESS profit can represent as follows,

$$C_e(P_{\mathrm{e}}) = \lambda_e . P_e + C_{e0,i} \tag{17}$$

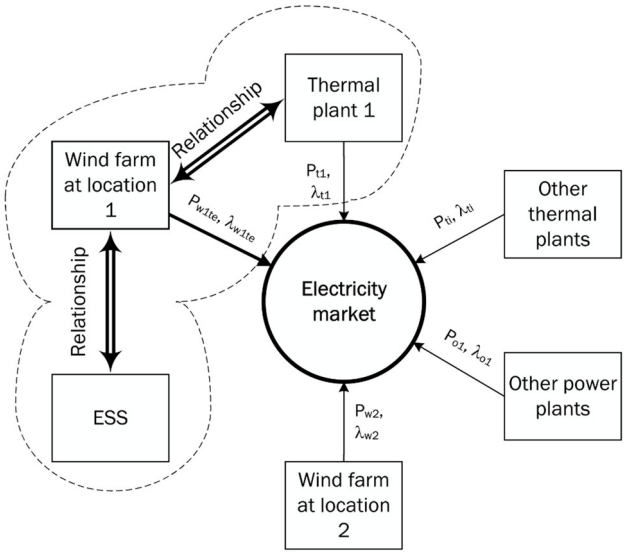

Fig. 7 EWF model

in which λ_e is the ESS energy unit price corresponding to the power P_e, and $C_{e0,i}$, which is the necessary cost for maintaining the operation of the ESS.

Like the TWF model, wind farm revenue is in (11). But exp. (16), the wind uncertainty fun is changed on C_p, as:

$$C_p(P_{\mathrm{p}}) = C_{Tp}(P_{Tp}) + C_e(P_{\mathrm{e}}) \tag{18}$$

$$0 \le P_{Tp} \le P_{TR} \text{ and } 0 \le P_e \le P_E$$

The recharge result of (16),

$$C_{wu}(P_{\mathrm{p}}) = \begin{cases} R_w(P_{\mathrm{p}}), & \text{if } P_{\mathrm{p}} \ge 0 \\ C_{Tp}(P_{Tp}), & \text{if } P_{TR} \ge -P_{\mathrm{p}} > 0 \\ C_{Tp}(P_{\mathrm{TR}}) + C_e(P_{\mathrm{e}}), & \text{if } P_E + P_{TR} \ge -P_{\mathrm{p}} > P_{TR} \\ C_{Pw}(P_{\mathrm{p}}), & \text{if } -P_{\mathrm{p}} > P_E + P_{TR} \end{cases} \tag{19}$$

An additional spent component must be paid for the ESS cost as indicated in Eq. (19). Therefore, two payments are incurred when the wind power output falls below the scheduled level. First, the thermal generators are given priority for operation. Second, the ESS is utilized to supplement the excess power of the remaining compensation. Lastly, in cases where WPP remains insufficient, it is necessary to compensate by purchasing electricity from the market or facing penalties.

The flowchart for determining profit maximization of wind power plants in the electricity market based on linking models between energy sources is presented in Fig. 8

7 Simulation Results

The IEEE 30-bus system is used to test models and evaluate the method's effectiveness [20]. This system is detailed in thirty buses, 41 branches and six generations [21]. The power grid parameters are taken according to the given standard data. Four thermal plants at buses 1, 2, 8 and 13 are in Table 1. Two generations of buses 5 and 11 are replaced by wind farms. There are 25 wind turbines at bus 5 and 20 at 11 with a rated power of 3MW per turbine. Weibull's PDF parameters, in this case, are the same as the following shape (k) and scale (c) parameters are provided in Table 2, and the Weibull PDF on wind speed and power of each wind turbine is shown in Figs. 2 and 3, respectively.

7.1 IWF Model

Figure 9 depicts the bidding prices of two wind farms in the market based on the mean costs of thermal generations. From that, it could be seen that wind prices slightly decrease when power grows from zero to maximum. This change is due to a decrease in thermal power, leading to the market price being deducted from the company value (3).

However, the revenue of Bus-5 wind generators is calculated by exp. (10) varies depending on the power region, as shown in Fig. 10. The cash flow increases almost linearly as power is less than 25MW and nearly linearly decreases when its power is more than 40MW and reaches peaks in the range of 30–40 MW linking on the penalty scale. The linear changes due to Weibull PDF in the respective interval are shallow, so the increase in revenue only depends on direct income. In contrast, their decrease depends mainly on the penalty. Significantly, the maximum cash flow area roughly tends to the peak of Weibull PDF, as shown in the exact figure.

Figure 10 also shows that the revenue growth region is less dependent on the penalty ratio, but the downward slope is dramatically dependent on the penalty level. For example, in the case of wind power of 70 MW, the revenue is nearly \$80/h with a penalty ratio of k_P= 1.0 but negative nearly \$80/h when k_P= 2.4. Additionally, the position of the cash flow peak also changes with the penalty coefficient. When it is smallest, i.e., k_P= 1.0, revenue is highest at 45 MW wind power. Meanwhile, the maximum is down when the penalty increases and reaches the lowest when k_P= 2.4, corresponding to wind power reduced to 30 MW.

7.2 LWF Model

In the integration of bus 5 and 11, as the LWF model, the mixed PDF is calculated based on Eqs. (12) and (13). The resulting PDF distribution shifts toward higher power values, as depicted in Fig. 11. Furthermore, the aggregate revenue corresponding to this distribution is illustrated in Fig. 12.

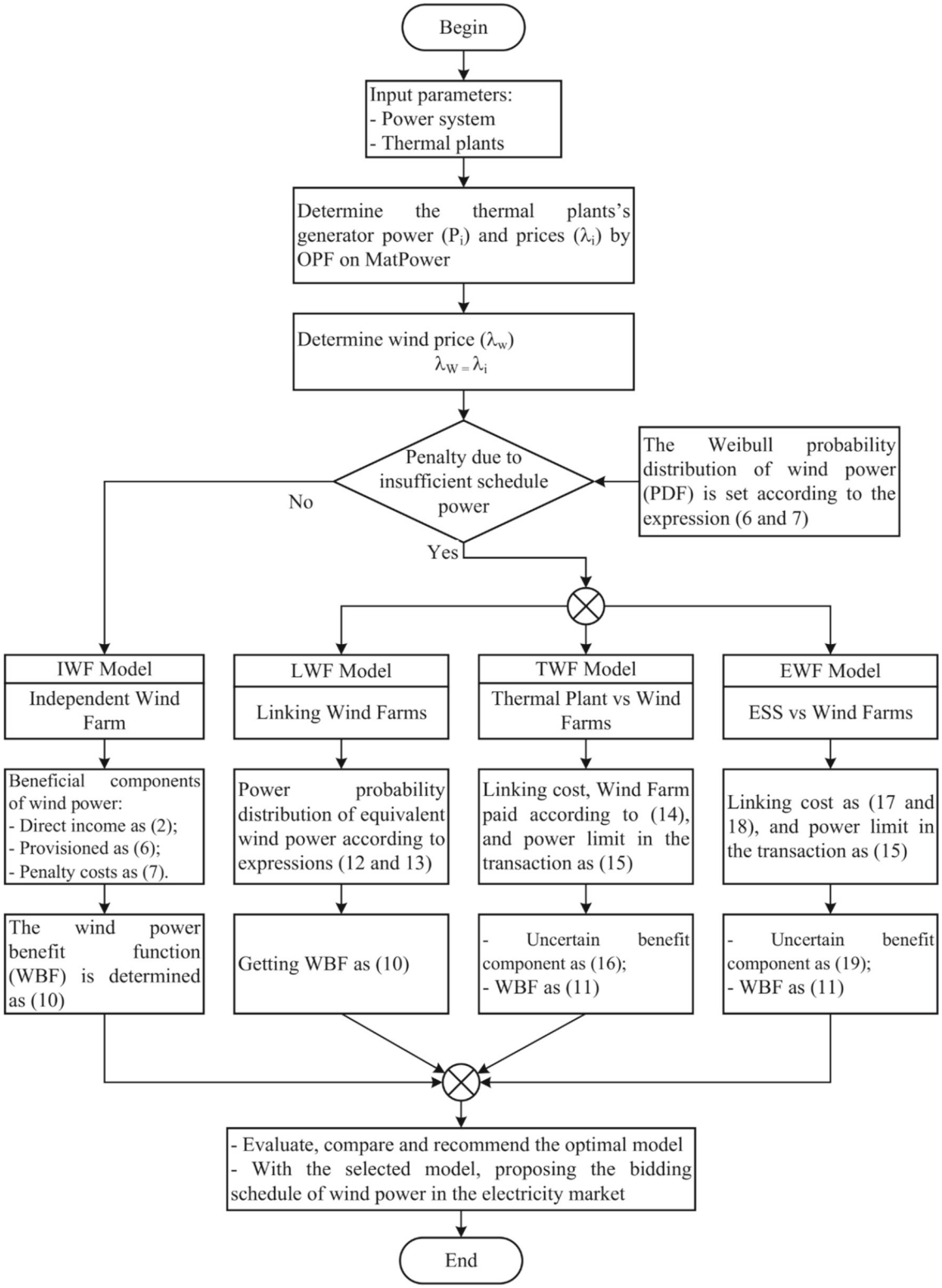

Fig. 8 Flowchart to determine profit maximization of wind power plants in the electricity market based on linking models between energy sources

Table 1 Parameter of thermal generators

Generator	Bus	a	b	c
TG1	1	0	2	0.00375
TG2	2	0	1.75	0.0175
TG3	8	0	3.25	0.00834

Table 2 Parameter of wind power

Wind power generation plants				
Wind farm #	No. of turbines	Rate power, P_{wr}(MW)	Weibull PDF parameter	Weibull mean, M_{wbl}
5	25	75	$c = 9,\ k = 2$	$v = 7.976$m/s
11	20	60	$c = 10\ \ k = 2$	$v = 8.862$m/s

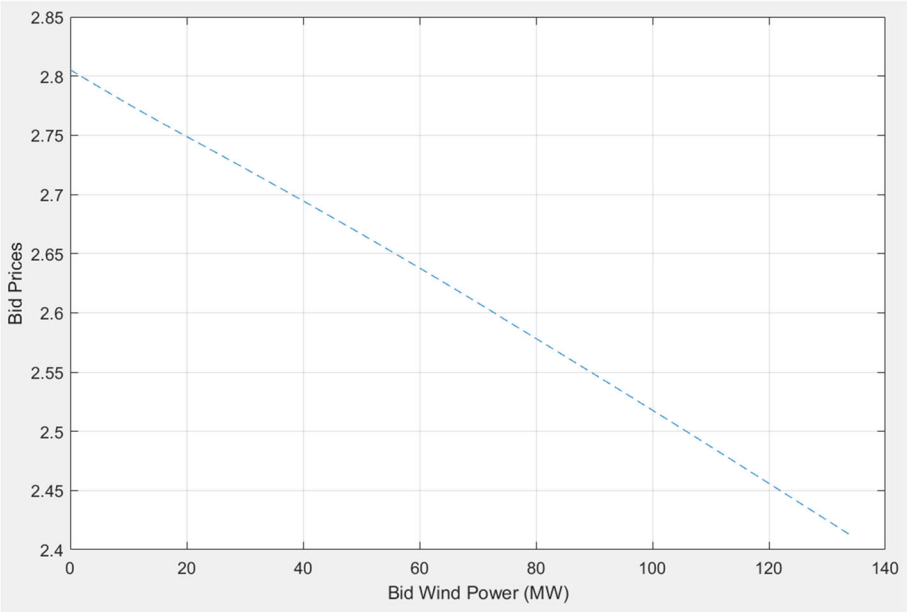

Fig. 9 Wind bidding price

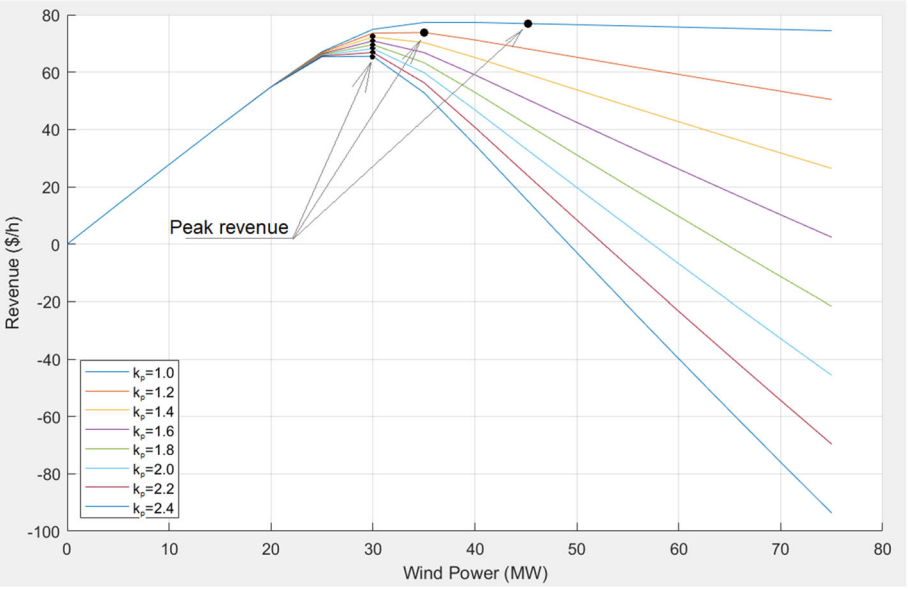

Fig. 10 Revenue of Bus-5 wind power

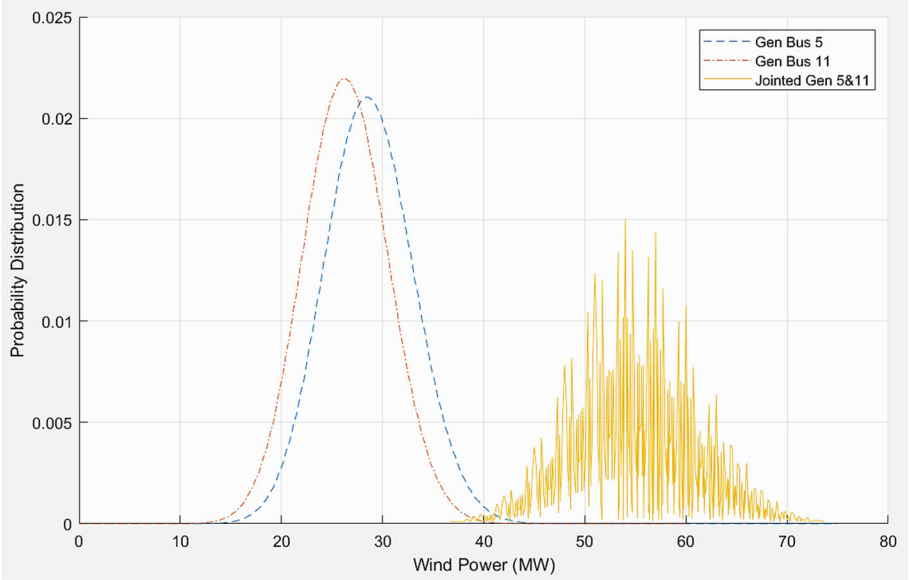

Fig. 11 Wind power probability distribution of each farm and joint bus 5 and 11

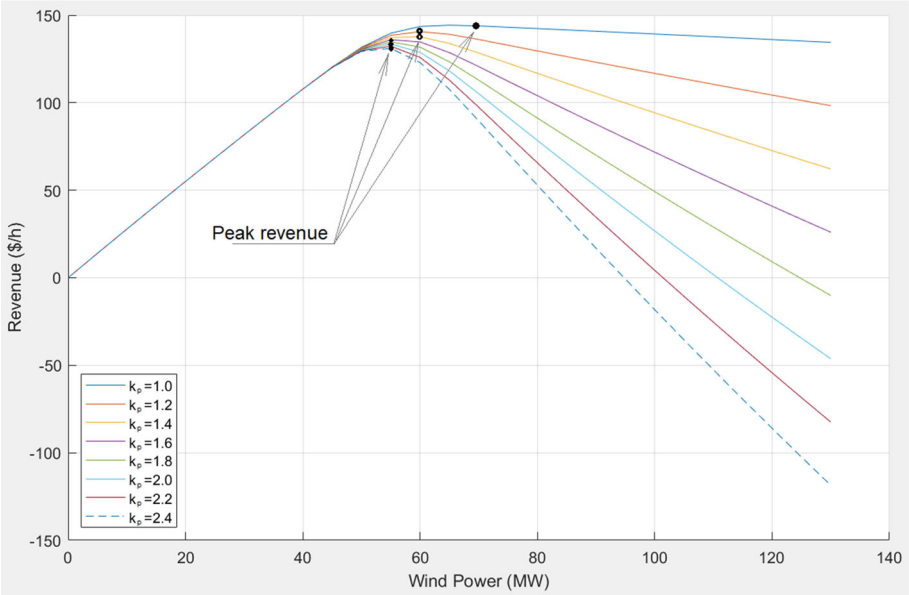

Fig. 12 WPP's revenue LWF model

Table 3 Comparison IWF vs. LWF

k_P	IWF				LWF			
	λ_{TG}	λ_p	P_w^{Optimal}	R_w^{Peak}	λ_{TG}	λ_p	P_w^{Optimal}	R_w^{Peak}
1.0	2.693	2.693	80	148.3	2.623	2.623	65	144.3
1.2	2.714	3.2568	65	142.2	2.638	3.1656	60	140.6
1.4	2.722	3.8108	60	138.4	2.638	3.6932	60	137.6
1.6	2.722	4.3552	60	134.8	2.652	4.2432	55	136.0
1.8	2.728	4.9104	55	132.7	2.652	4.7736	55	134.8
2.0	2.728	5.456	55	130.8	2.652	5.304	55	133.5
2.2	2.728	6.0016	55	128.9	2.652	5.8344	55	132.3
2.4	2.728	6.5472	55	126.9	2.652	6.3648	55	131.0

While the shape of the curves in Fig. 12 resembles the IWF case, adjustments are made in the extreme regions to align with the Weibull PDF. Once again, the revenue peaks at the around location, with an optimal total wind power range of approximately 55–65 MW. Notably, when the penalty ratio surpasses 1.5, the optimal power value remains constant, set explicitly at 55MW, as indicated in Table 3. This persistence can be attributed to wind power owners' inclination to identify the most favorable probability for tendering electricity output, thereby mitigating potential losses arising from penalties imposed due to power shortfall.

The cash flow comparison of the base model and the LWF model is presented in Table 3 and Fig. 13. It can be observed that the no-joint venture scenario yields higher profitability when the penalty coefficient is below 1.5. Conversely, the linking approach demonstrates significantly more significant benefits when this ratio exceeds 1.5. Notably, there is minimal variation in the optimal power levels between the two models. This low change can be attributed to reaching a probability balance, wherein the optimal power levels closely align between the two models. However, the integrated wind cases exhibit higher revenue, which can be attributed to the increased certainty facilitated by the exchange of electricity production from linking farms. Consequently, the comparison results suggest that wind power sources should consider joint ventures only when incurs substantial penalties ($k\_Pk > 1.5$) in the electricity market under these circumstances.

7.3 TWF Model

Suppose a commercial relationship is established between the Bus-1 thermal generators and wind power plants. This thermal has a rated power of 200MW, and the transaction commitment price is a 10% profit. Figure 14 shows the WPP's revenue after linking with the Bus-1 thermal generation.

From Fig. 14, the shape of the curves also changes bumpier along the growth path. However, each case has only one maximum value, and the downward slope remains consistent.

In models where the penalty price surpasses the cost of operating thermal power plants under commitment, the cash flow peak experiences a significant elevation. For example, when k_P>1.1, the maximum revenue has been raised from less than 150S/h, in Fig. 14, to over \$180/h. Nonetheless, like the previous models, a higher penalty factor also lowers the revenue peak.

Furthermore, the optimal bidding power is also increased from around 60MA, in the LWF model, to nearly 90MW, seeing in the above figure. The certainty of wind compensation by the thermal plant leads to wind owners' trust, and a higher bidding power offer is the cause of this increase.

7.4 EWF Model

Let's consider a hypothetical ESS system with a maximum power of 10MW, and the buying pricing factor is determined to be 1.5 times the market average price. The curves are split into three patterns in this model in Fig. 15. The first occurs when the penalty cost is lower than the cost of commitments to thermal and ESS generations. Typically, k_P=1.0 in this figure; this curve remains unchanged from the LWF model. The second type has a curve like the TWF model. The penalty cost is over the commitment to pay for the thermal plant. Therefore, it leads to participation in the excess energy of that thermal, like k_P=1.2–1.4. However, that penalty fee is still lower than the ESS cost, so it has no effect. The last is the case with the contribution of thermal and ESS generations when k_P>1.5.

With the above results, a higher penalty rate is more conducive to the cooperation of generations. When the penalty factor is lower than 1.1, generation cooperation does not seem feasible because the penalty value is too low, discouraging the participation of thermal generations and ESS because of the higher cost. On the other hand, thermal power agreements come into effect when the penalty factor is between 1.2 and 1.4, while ESS does not. Income increases proportionally with the participation of these thermal power plants. After all, the best wind benefits are obtained when the ESS plant participates with its vital penalty coefficient higher than 1.5.

The results in Fig. 15 also show that WPP's revenue is higher with the contribution of thermal power and ESS. It could reach close to 200\$/hr for k_P=1.6, while this value is just over 170\$/hr with the same penalty factor in the TWF model, in Fig. 14, and just over 135\$/hr in the IWF and LWF models, in Figs. 10 and 12.

Table 4 gives a more transparent comparison with the TWF model. The maximum revenue and optimal bidding power are usually higher than the TWF in the cases of ESS participating, k_P>1.5, while it is the same in other cases. The highest increase in the value corresponds to k_P=1.6 which is \$196.3/h compared to \$175/h in TWF. The bidding optimal wind power also increased to 95MW compared to only 80MW in the TWF, and around 55-60MW in the previous models, as in Table 3.

8 Comparison and Evaluation

Comparing the simulated outcomes of the four depicted models in Fig. 16, it is evident that the optimal revenue of the WPP exhibits a progressive increase across the successive models. The integration of power sources fosters augmented benefits for WPP, particularly exemplified by the fourth model, which involves the amalgamation of WPP with both thermal

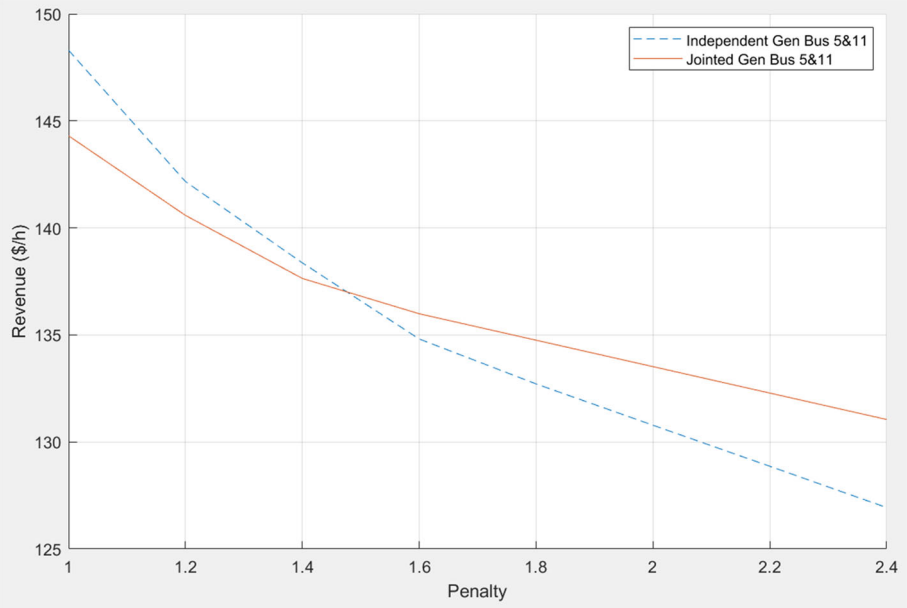

Fig. 13 Comparison in optimal revenue IWF vs. LWF

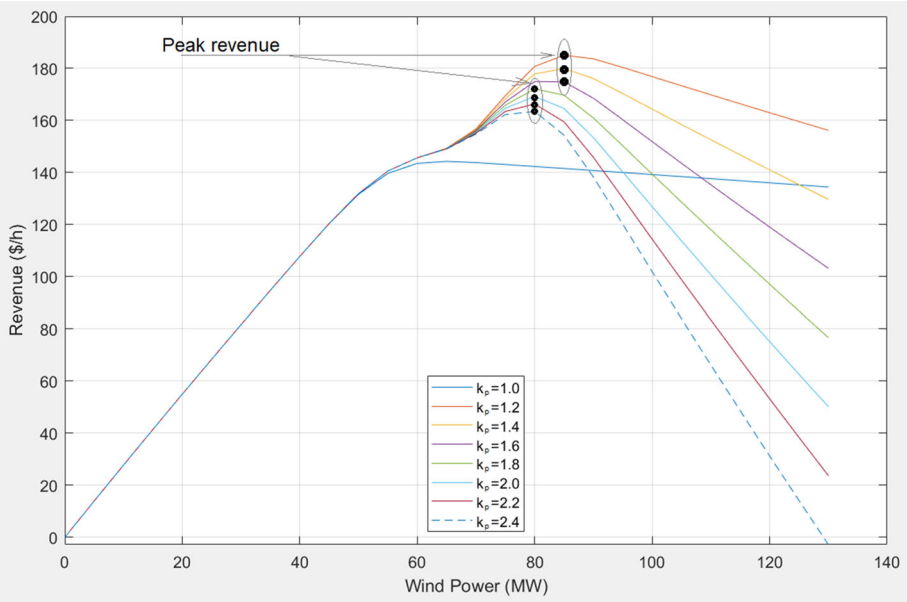

Fig. 14 WPP's revenue TWF model

plants and ESS. This integration engenders notable mitigation of uncertainties associated with wind farms through integrative relationships, thereby empowering wind farms to actively augment their bid-based energy supply within electricity markets. The results indicate that the generated revenue can potentially exceed the baseline model by up to 132%, reaching 196.3$/h, in contrast to the baseline revenue of 148.3$/h.

When scrutinizing the impact of the penalty ratio on the bidding behavior of wind farms within each model, it becomes apparent that a higher penalty ratio engenders a propensity for decreased WPP revenue due to an amplified risk of damages, as elucidated in Fig. 16. Nonetheless, the collaborative endeavor among power plants diminishes the peril of compensation by facilitating proactive interplay between them. Furthermore, an optimal penalty ratio seems to exist wherein revenue attainment reaches its zenith, approximating a value of 1.6.

Noteworthy, not all forms of integration yield favorable outcomes for WPP. For instance, when the penalty ratio descends below 1.4, the revenue generated by the LWF model modality proves less effective, as the IWF model appears to yield higher profits. Conversely, excessive reliance on integration may incite an overabundance of electricity supply within the market, leading to scheduling overlaps and

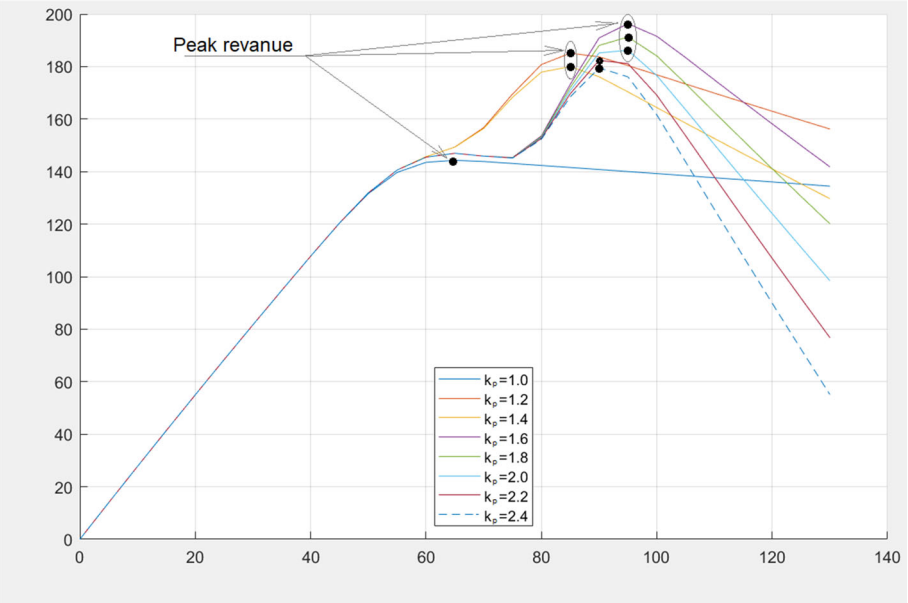

Fig. 15 WPP's revenue EWF model

Table 4 Comparison of TWF vs. EWF

k_P	TWF				EWF			
	λ_{TG}	λ_p	P_w^{Optimal}	R_w^{Peak}	λ_{TG}	λ_p	P_w^{Optimal}	R_w^{Peak}
1.0	2.623	2.623	65	144.3	2.623	2.623	65	144.3
1.2	2.563	3.0756	85	185.1	2.563	3.0756	85	185.1
1.4	2.563	3.5882	85	180.0	2.563	3.5882	85	180.0
1.6	2.578	4.1248	80	175.0	2.533	4.0528	95	196.3
1.8	2.578	4.6404	80	172.1	2.533	4.5594	95	191.2
2.0	2.578	5.156	80	169.2	2.533	5.066	95	186.2
2.2	2.578	5.6716	80	166.4	2.548	5.6056	90	182.3
2.4	2.578	6.1872	80	163.5	2.548	6.1152	90	179.5

imperiling the stability of the power system, thereby causing financial losses for wind power stakeholders.

Moreover, in models characterized by higher penalty prices, the susceptibility to compensation emerges as a substantial factor influencing the benefits derived from wind power. Hence, meticulous consideration should be accorded to determining bidding prices and the quantity of electricity production in wind farm operations. The strategic integration among diverse power sources mitigates the risk of penalty for power deficiencies, yielding more conspicuous benefits for both wind plant owners and societal welfare by optimizing the utilization of renewable energy sources.

Conversely, the expected behavior of conventional wind farms exhibits a bias toward individual gains, prompting wind farms to allocate more significant investments in ESS infrastructure. As portrayed in Fig. 16, including ESS within the integration framework amplifies the bidding wind power. For instance, in the EWF model, wind farms can attain a power of up to 95MW, in contrast to a mere 55MW within the IWF model.

As renewable energy sources increase in operational power, they confer considerable societal benefits by diminishing reliance on dwindling fossil fuel reserves. In the EWF model, the augmentation of wind power supply within the electricity market manifests significant social effects. The penetration of wind energy within the power system in this model can surge to nearly 173% in the simulated instances, resulting in a substantial curtailment of fossil fuel exploitation and promoting the realization of a more sustainable global milieu.

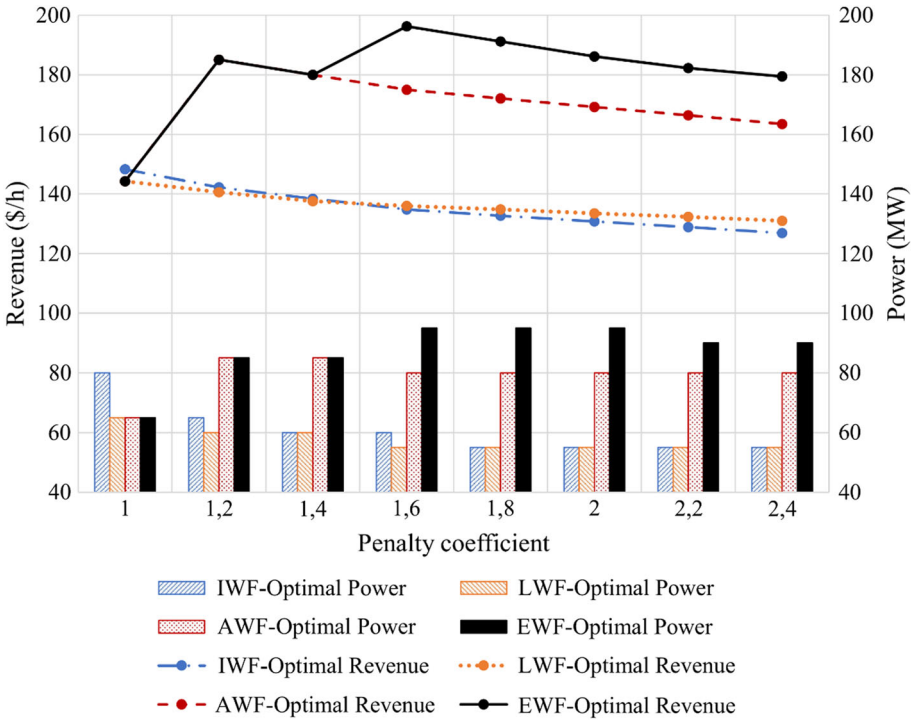

Fig. 16 Comparison in optimal revenue and power of models

9 Conclusion

Accurately forecasting the power output of wind farms is a critical challenge for WPPs when participating in electricity supply bidding within the electricity market. Recent reductions in policies promoting wind power development have further intensified the difficulties wind farm owners face, leading to possible losses in investment in WPP projects. In tandem with increased research and technological advancements, adopting a power multi-plant management strategy represents a pivotal driver for advancing renewable energy sources, particularly in wind farms. And in the long-term perspective, when wind power attains equal competitiveness with other energy sources in the electricity market, this study seems to contribute significantly to this promising domain's advancement.

This study introduces integrated power plant management models, combining wind farms with thermal plants and energy storage systems, offering enhanced effectiveness for both wind power owners and more comprehensive societal welfare within electricity markets. Experimental results on the widely recognized on IEEE 30-bus power system corroborate the outcomes. Firstly, the revenue generated by wind farms experiences a notable increase when integrated with thermal plants and energy storage systems, up to 132%. Secondly, the proposed models demonstrate a significant enhancement in the power production of wind farms, resulting in a considerable increase in sellable wind power output from 55MW up to 95MW. This improvement contributes to promoting environmentally renewable energy consumption practices, thereby advancing the pursuit of sustainable energy solutions.

To provide further insight, the model entailing the ownership of all three types of power plants (wind, thermal and ESS) demonstrates the highest profitability for wind farms, particularly when the penalty ratio exceeds 1.5, where surpassing neighboring models by at least 10% as illustrated in Fig. 15. Additionally, the models involving the joint ownership of wind and thermal power plants exhibit a 25% higher profitability than the remaining models. Conversely, strategies integrating multiple wind farms display relatively modest increases in profitability, amounting to only a few percentage points. These findings underscore the notion that a diversified portfolio of power sources enhances the certainty of wind energy and yields more incredible benefits within the competitive electricity market.

Acknowledgements This work was supported by the Ho Chi Minh City University of Technology and Education, Vietnam, under Project T2022-69.

References

1. Hammons, T.J.: Integrating renewable energy sources into European grids. Electr. Power Energy Syst. **30**(8), 462–475 (2008)
2. Cao, D.; Hu, W.; Xu, X.; Dragičević, T.; Huang, Q.; Liu, Z.; Chen, Z.; Blabjerg, F.: Bidding strategy for trading wind energy and purchasing reserve of wind power producer – A DRL based approach. Electr. Power Energy Syst. **117**, 105648 (2020)

3. Mohamed, B.A.B.: Principle parameters and environmental impacts that affect the performance of wind turbine: an overview. Arab. J. Sci. Eng. **47**, 7891–7909 (2022)
4. Wang, N.; Li, J.; Hu, W.; Zhang, B.; Huang, Q.; Chen, Z.: Optimal reactive power dispatch of a full-scale converter based wind farm considering loss minimization. Renew. Energy **139**, 292–301 (2019)
5. Li, J.; Wang, N.; Zhou, D.; Hu, W.; Huang, Q.; Chen, Z.; Blaabjerg, F.: Optimal reactive power dispatch of permanent magnet synchronous generator-based wind farm considering levelised production cost minimisation. Renew. Energy **145**, 1–12 (2020)
6. "Energy Prices and Costs in Europe: Report from the commission to the european parliament, the council, the european economic and social committee and the committee of the regions," European Commssion, Brussels, 2020.
7. Shinde, P.; Amelin, M.: A literature review of intraday electricity markets and prices. IEEE Milan PowerTech, p. 18938508, (2019).
8. Hamanah, W.; Abido, M.; Alhems, V.: Optimum sizing of hybrid PV, wind, battery and diesel system using lightning search algorithm. Arab. J. Sci. Eng. **45**, 1871–1883 (2020)
9. Dobschinski, J.; Pascalis, E.D.; Wessel, A.; Bremen, L. v.; Lange, B.; Rohrig, K.; Drenan, Y.-M. S..; Fraunhofer, I.; ForWind, O.; Germany, E.: The potential of advanced shortest-term forecasts and dynamic prediction intervals for reducing the wind power induced reserve requirements. In: Scientific Proceedings of the European Wind Power Conference, p. 177–182 (2010).
10. Biswas, P.P.; Suganthan, P.N.; Amaratunga, G.A.J.: Optimal power flow solutions incorporating stochastic wind and solar power. Energy Convers. Manage. **148**, 1194–1207 (2017)
11. Pape, C.: The impact of intraday markets on the market value of flexibility—decomposing effects on profile and the imbalance costs. Energy Economics **76**, 186–201 (2018)
12. Neuhoff, K.; Ritter, N.; Salah-Abou-El-Enien, A.; Vassilopoulos, P.: Intraday Markets for Power: Discretizing the Continuous Trading. University of Cambridge, Energy Policy Research Group (2016)
13. Dai, T.; Qiao, W.: Trading wind power in a competitive electricity market using stochastic programing and game theory. IEEE Trans. Sustain. Energy **4**(3), 805–815 (2013)
14. Wais, P.: A review of Weibull functions in wind sector. Renew. Sustain. Energy Rev. **70**, 1099–1107 (2017)
15. Roy, R.; Jadhav, H.T.: Optimal power flow solution of power system incorporating stochastic wind power using Gbest guided artificial bee colony algorithm. Electr. Power Energy Syst. **64**, 562–578 (2015)
16. Panda, A.; Tripathy, M.: Security constrained optimal power flow solution of wind-thermal generation system using modified bacteria foraging algorithm. Energy **93**(1), 816–827 (2015)
17. Alismail, F.S.: Chance constraints optimal planning strategy of energy storage systems and Tie-Lines under wind power uncertainties to improve the reliability. Arab. J. Sci. Eng. **46**, 9935–9944 (2021)
18. Hadjipaschalis, L.; Poullikkas, A.; Efthimiou, V.: Overview of current and future energy storage technologies for electric power applications. Renew. Sustain. Energy Rev. **13**(6–7), 1513–1522 (2009)
19. Dunn, H. K.; Tarascon, J.-M.: Electrical energy storage for the grid: A battery of choices. Science,**334**, 928–935 (2011).
20. Alsac, O.; Stott, B.: Optimal load flow with steady-state security. IEEE Trans. Power Apparatus Syst. PAS-93(3), 745–751 (1974).
21. Ferrero, R.; Shahidehpour, S.; Ramesh, V.: Transaction analysis in deregulated power systems using game theory. IEEE Trans. Power Syst. **12**(3), 1340–1347 (1997)

Controlling Output Power to Enhance the Investment Efficiency of Wind Farms by Maximizing the Capacity of Transmission Transformers and Integrating Energy Storage Systems

Truong Viet Anh
Hochiminh City University of Technology and Education, Ho Chi Minh City, Vietnam
anhtv@hcmute.edu.vn

Nguyen Tung Linh
Faculty of Control and Automation, Electric Power University, Ha Noi City, Vietnam
linhnt@epu.edu.vn

Dinh Ngoc Sang
University of Architecture Hochiminh City, Ho Chi Minh City, Vietnam | Hochiminh City University of Technology and Education, Ho Chi Minh City, Vietnam
sang.dinhngoc@uah.edu.vn (corresponding author)

Received: 1 May 2024 | Revised: 29 May 2024 and 4 June 2024 | Accepted: 6 June 2024

 DOI: https://doi.org/10.48084/etasr.7688

ABSTRACT

This study addresses inherent challenges stemming from uncertainty associated with the integration of wind energy into the electricity market. A novel approach is proposed to leverage the capabilities of dynamic transformers to optimize the utilization of uncertain wind power output, thereby enhancing financial investment efficiency for wind power stakeholders. The flexible combination of wind turbines (WTB), transmission transformers (TTS), and Energy Storage Systems (ESS) can actively reserve or provision electricity. Electricity generation control is based on optimal analysis results using linear integer programming algorithms that consider temperature fluctuations, lifespan of transformers, and electricity market prices. Maximizing the dynamic transformer's efficiency as proposed and optimizing revenue and costs from the fluctuating wind power output significantly improves financial performance metrics when investing in wind farm projects. Financial figures highlighted in the paper emphasize notable benefits, particularly for wind farm expansion projects. The potential return on investment ratio is expected to increase up to 5.64 times compared to conventional wind farm investment scenarios, with an improvement to increase from 4.4% to 24.8%.

Keywords-wind power optimization; electricity market; energy storage systems; dynamic transformer

I. INTRODUCTION

The report in [1] provides valuable insights into the inevitable transition process towards renewable energy as a crucial energy source in the future. Wind energy stands out as a leading candidate, with a significantly remarkable growth rate in many countries worldwide [2]. It is anticipated that increased wind power capacity will reach approximately 1,400 GW during the period 2020 – 2025 [3]. Vietnam's power development plan for the period 2021-2030 emphasizes strategic priority on wind energy development to achieve net-zero emissions by 2050 [4]. Specifically, by 2030, the capacity is expected to exceed 28 GW and strive to reach over 100 GW by 2050 [5]. However, wind energy faces significant challenges when entering the competitive environment of the electricity market, primarily due to its inherent uncertainty [6]. Research provides diverse coordinated models of various types of power plants to minimize risks due to wind power production instability [7, 8]. In addition to turbines, which constitute the primary components of a wind farm, transformers, and transmission lines are critical elements significantly influencing land clearance compensation. The

capacity of transmission transformers is typically designed to accommodate the peak power production capability of wind energy, resulting in low operational capacity utilization for the majority of the time. Moreover, the variability of wind power output can lead to power shortages or curtailment when the output exceeds the transmission capacity limits of the transformers [9]. Recent research efforts have concentrated on optimizing the efficiency of transmission transformers within wind farm investments to enhance overall effectiveness. Notable examples include studies on optimal wind power models integrated with thermal transmission capabilities and transformer cooling systems [10, 11]. Investigations have also expanded to wind turbines based on the operational models of distributed transformers [12]. Furthermore, the advancement of Energy Storage Systems (ESS) is of considerable interest in the optimization of Renewable Energy Sources (RES) [13]. However, there is a scientific gap in the optimization of wind farm expansion combined with ESS when expanding transformers and transmission lines is not feasible and the comparison of this strategy with investing in new wind farms. Based on the reasons above, this study introduces two main proposes: (i) a method for controlling the output power supply of wind energy to optimize energy utilization efficiency by coordination between the maximizing transformer transmission capacity and energy storage and (ii) the incorporation of wind speed uncertainty into the problem of controlling wind output power. To substantiate these proposals, a mathematical model is constructed and experiments are conducted on a combined model of three components: Wind turbine - Transmission transformer - ESS (WTE). The optimization is based on the economic investment efficiency index, Net Present Value (NPV) and Return on Investment (RoI) [10, 14] and follows this sequence:

- Revisiting the scenario of transmission transformer design, focusing on temperature variations and ensuring longevity according to design and production standards of past transformer investments.
- The scenario of integrating the ESS with the operational conditions of the transformer to store and control the output power of the wind farm for optimal efficiency was simulated.
- The probabilistic distribution model of wind energy uncertainty was also integrated to assess investment efficiency.
- All experiments demonstrated the effectiveness of the proposed investment combination according to the tested investment efficiency calculation method.

The main contributions of the current article are:

- A method for enhancing wind power investment efficiency by integrating transmission transformers into an investment set is proposed. First, the transmission capacity of transformers is maximized in order to enhance the role of the ESS in controlling wind power output for the electricity market and second, a probabilistic model of stochastic wind power variation that provides a more comprehensive and accurate approach for the optimization of the operation of the ESS and transmission transformers is developed.
- The experimental results on the IEEE 30-bus power system show that the NPV can potentially increase more than 6.75 times in the proposed model, reaching €17.28 million, compared to €2.56 million in the traditional design model, indicating a significant risk reduction and increased investor confidence in wind power, which is particularly advantageous for expanding existing wind farms.

Maximizing the power capacity of the transmission transformer combined with energy storage, along with an assessment of the wind speed probability, has enhanced the investment efficiency in wind power for the proposed case compared to traditional optimal design methods and brought about the following benefits:

- The expansion of existing wind farms without the need to upgrade transmission transformers or the associated transmission lines. This mitigates challenges related to land acquisition and inherent difficulties associated with investment in transmission systems.
- Encourages investors to be more interested in the wind energy sector despite its uncertainties.

II. MATHEMATICAL MODEL

In this article, three main investment components (WTB, TTS, and ESS) are considered mathematically.

A. Fitness Function

NPV and RoI criteria are aimed as [10, 14]:

$$\max NPV = \sum_{i=1}^{n} \frac{CashFlow_i}{(1+IRR)^i} - InitialInvestment \quad (1)$$

or:

$$max\ ROI = \frac{NPV}{InitialInvestment} \quad (2)$$

In this study, a value of 20 years is assumed to represent the typical lifespan of a wind farm [11]. The discount or interest rate is denoted by IRR and expressed as a percentage. Further elucidation of the initial investment and cash flow is delineated below [10]:

$$InitialInvestment = C_{II} = C_{tw} + C_{tr} + C_{ESS} \quad (3)$$

$$CashFlow_i = Benefits_i - Cost_i + Certificate_i \quad (4)$$

$$Cost_i = C_{tur,i}^{O\&M} + C_{tr,i}^{O\&M} + C_{ESS,i}^{O\&M} \quad (5)$$

The cash flow in period i is denoted by $CashFlow_i$, $Cost_i$ represents all the costs in the i period, C_{tw}, C_{tr}, and C_{ESS} represent the input parameters reflecting the investment costs associated with WTB, TTS, and ESS, respectively, $C_{tur}^{O\&M}$, $C_{tr}^{O\&M}$, and $C_{ESS}^{O\&M}$ are the operation and maintenance costs, P_t^{wav} represents the operational power of the wind farm. The revenue generated from green energy certification is represented by $Certificate_i$. An example is the value of 0.305 €/MWh for 2019 in Sweden [8].

B. Wind Power Model in the Electricity Market

$$Benefits = \sum_{t=1}^{T} R_{ws}(P_t^{ws}) + \sum_{t=1}^{T} R_{wu}(\Delta P_t^{w}) \quad (6)$$

with:

$$\Delta P_t^w = P_t^{wav} - P_t^{ws}$$

where R_{ws}represents the direct revenue obtained from selling electricity based on the bidding contracts within the electricity market. Bidding output power is P_t^{ws}, while R_{wu} denotes the uncertain income and includes revenue reserves and compensatory costs related to power shortages [7].

$$R_{ws} = \sum_{t=1}^{T} \lambda_{w,t}.P_t^{ws} \quad (7)$$

$$R_{wu} = \begin{cases} \sum_{t=1}^{T} R_{Rw}(\Delta P_t^w), & \text{if } \Delta P_t^w \geq 0 \\ \sum_{t=1}^{T} C_{Pw}(\Delta P_t^w), & \text{if } \Delta P_t^w < 0 \end{cases} \quad (8)$$

where $\lambda_{w,t}$ represents the wind direct price [15], R_{Rw}, C_{Pw} are the revenues from selling reserved energy and the compensatory cost [16]:

$$R_{Rw}(\Delta P_t^w) = k_R.\lambda_{w,t}.\int_{P_t^{ws}}^{P^{wr}} (p_t^w - P_t^{ws}).f_w(p_t^w).dp_t^w \quad (9)$$

$$C_{Pw}(\Delta P_t^w) = k_P.\lambda_{w,i}.\int_{0}^{P_t^{ws}} (p_t^w - P_t^{ws}).f_w(p_t^w).dp_t^w \quad (10)$$

where k_R , k_P are the reserve and compensation price coefficients, $f_w(p_{w,i})$ is the wind power probability density function [16, 17].

C. Modeling of TTS

The cost of the transformer is described by [18, 19]:

$$C_{tr} = RI_{tr}.P_{tr}^r \quad (11)$$

where RI_{tr} represents the TTS's financial investment rate, the illustrative example of Sweden is documented in [10], P_{tr}^r signifies the rated power, here selected according to IEC [19], including three components:

$$I_t^2.S_{size} \geq P_t^{wav} \text{ or } S_{size} \geq \frac{P_t^{wav}}{I_t^2} \quad (12)$$

The TTS's rated apparent power S_{size} must not exceed the wind farm power limit:

$$\theta_t^{hst} \leq \theta_t^{hst,max} \quad (13)$$

$$\theta_t^{top} \leq \theta_t^{top,max} \quad (14)$$

The variable θ_t^{hst} represents the hot spot temperature on the coil while θ_t^{top} denotes the top oil temperature. The last constraint of the transformer is the lifespan LOL, given V as the annual aging rate of the transformer:

$$\text{LOL} = \sum_t^T V_t \quad (15)$$

$$\text{LOL} \leq \frac{Transformer's\ Lifetime}{Wind\ Farm's\ Lifetime}.8760 \quad (16)$$

D. ESS Model

The proposition of employing lithium-ion battery technology for testing, investment cost, and operation and maintenance (O&M) is analyzed in [20, 21].

$$C_{ESS} = RI_{ESS}.E_{ESS} \quad (17)$$

$$Revenue_{ESS} = \sum_{t=1}^{T}(\lambda_{R,t}.E_{R,t}) - \sum_{t=1}^{T}(\lambda_{D,t}.E_{D,t})$$

$$Cost_{ESS} = C_{ESS}^{O\&M} \quad (18)$$

Two pivotal modes are balanced:

- Direct Energy: surplus and deficit energy levels. The charge and discharge energy are given by:

$$E_R^D = \int_{t_1}^{t_2}\left(P_{forecast}(t) - P_{max}^{Tra}\right)dt \quad (19)$$

$$E_D^D = \int_0^{t_1}\left(P_{max}^{Tra} - P_{forecast}(t)\right)dt + \int_{t_2}^{24}\left(P_{max}^{Tra} - P_{forecast}(t)\right)dt \quad (20)$$

where $P_{forecast}(t)$ represents the forecasted wind power, P_{max}^{Tra} is the maximum transmission power of the transformer, E_R^D and E_D^D are dependent on the forecasted wind energy and the maximum transmission power of the transformer.

- Uncertain Energy: the probability of wind power output surpassing the forecast.

$$E_R^U = \int_{t_1}^{t_2}\left(\int_{P_{max}^{Tra}}^{P^{wr}}(p_t^w - P_{max}^{Tra}).f_w(p_t^w).dp_t^w\right)dt + + \int_{t_o}^{t_1}\left(\int_{P_{forecast}}^{P^{wr}}(p_t^w - P_{forecast}).f_w(p_t^w).dp_t^w\right)dt \quad (21)$$

$$E_D^U = \int_{t_o}^{t_1}\left(\int_{P_{forecast}}^{P^{wr}}(p_t^w - P_{forecast}).f_w(p_t^w).dp_t^w\right)dt \quad (22)$$

where $t_o - t_1$ and $t_1 - t_2$ are the maximum predicted wind power output, which is less and more significant than the transformer's limit capacity. The result of storage energy capacity is:

$$E_R = E_R^D + E_R^U \quad (23)$$

$$E_D = E_D^D + E_D^U \quad (24)$$

E. Optimization Problem

The study evaluates the approach's effectiveness by optimizing three distinct scenarios: Scenario 1 – Conventional wind power plant investment (TS): This scenario represents the traditional approach of investing in wind power plants. Scenario 2 – Optimized wind power plant investment with capacity expansion considerations (OWS): This scenario incorporates the proposed methodology to enhance the efficiency of wind power plant investments, specifically emphasizing the benefits of expanding wind power capacity. Scenario 3 –ESS power integration within the system is explored in this scenario (EWS).

III. EXPERIMENTAL PART

A. Power System Data

The IEEE 30-bus system was utilized as a testbed. The system comprises 30 buses, 41 branches, and six generations [22, 23]. Four thermal plants are situated on buses 1, 2, 8, and 13, and two wind farms on buses 5 and 11, their specific characteristics can be found in [16].

B. TS Scenario

1) Wind Farm Data

The wind initial investment cost is approximately 750,000 €/MW, and O&M expenses are at 1.5% over 20 years [7].

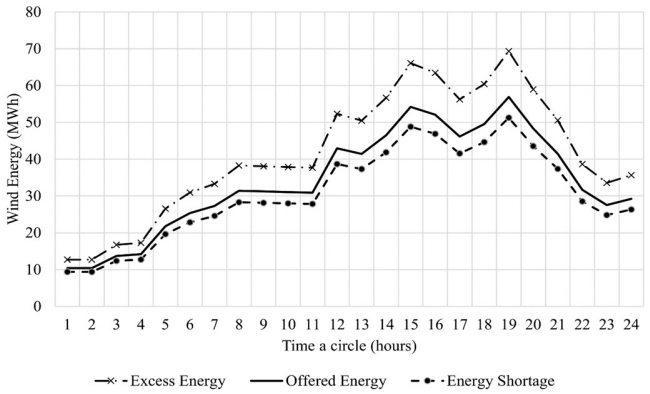

Fig. 1. Daily wind power output in peak season on Bus 5.

Wind power output forecasts are divided into two seasons: the peak season and the low season [24]. Weibull PDF is used to get wind power probability in [7]. Figure 1 illustrates the highest probability of electricity generation during the peak season for the wind farm at bus 5, presented as the solid line in the central graph. The observed trend closely follows the predicted wind output power—notably, the highest probability of electricity generation at 7:00 PM amounts to nearly 57 MWh. The higher or lower electricity generation probability exhibits fluctuations around the predicted values. The deviation levels are approximately 10% for power shortage probabilities and over 20% for probabilities of power exceeding the forecast.

2) Transformer Data

Transformer's initial investment is assumed to be 30,000 €/MVA, and the estimated O&M cost for it is 3% [10]. The parameters and specifications for the forced oil circulation were taken from [19]. Figure 2 illustrates the results of the temperature profile of the transformer oil and the maximum temperature of the winding coil for a day, considering the peak-season operation transformer power. The top oil and winding coil temperatures increase with the power and reach a maximum value of 140 °C at the peak power location at 7 pm. Based on the calculated results under the transformer operating conditions, the transformer's most minor feasible operational power is determined to be 57 MVA. However, the selected rated power will be 63 MVA.

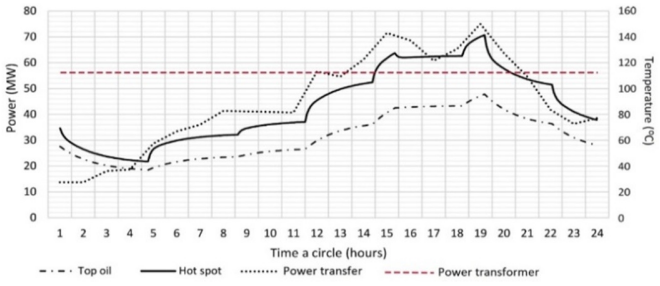

Fig. 2. Daily temperature profile of the power transformer.

3) NPV

The optimal power distribution using the Matpower 7.0 tool is utilized for the IEEE 30-Bus system. The cost varies within the range of 26-31.7 €/MW. Combining this with the daily wind power output chart, the estimated average selling price of wind power at bus 5 is 30.34 €/MWh during off-peak hours and 27.71 €/MWh during peak hours. The NPV and cash flow with compensation factor can be seen in Table I.

TABLE I. CASH FLOW

Year	0	1	2	…	20
Cash flow (k€)	-58,140	4,271	4,271	4,271	4,271
NPV (k€)	2,562				

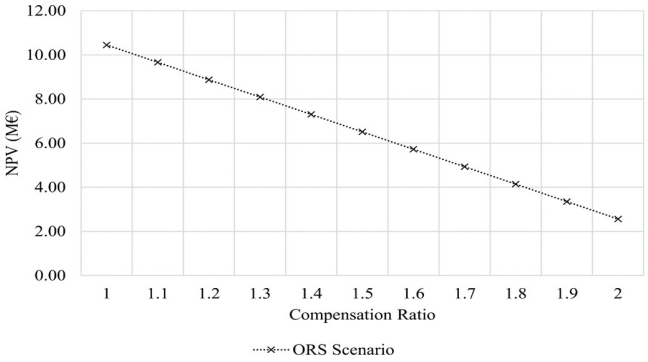

Fig. 3. NPV dependent on k_p.

Figure 3 exhibits the notable impact of the compensation factor k_p in the electricity market arising from the uncertainties associated with wind power on the effectiveness of project investment. As k_p increases, NPV diminishes, and this decline in NPV appears to follow a nearly linear trend. Furthermore, when k_p doubles the electricity selling price in the electricity market, the NPV experiences a reduction exceeding 75% of the initial projected benefit. Consequently, any alterations in electricity pricing policies that affect the ratio of price differentials for electricity suppliers significantly influence the revenue of power plant owners.

C. OWS Scenario

Two essential steps are undertaken: (i) Ascertaining the maximum wind power output at bus 5 based on the operating temperature conditions of the transmission transformer, and (ii) Computing the NPV of the scenario.

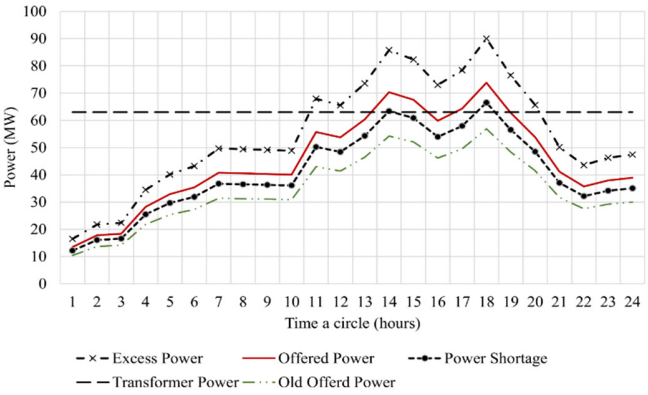

Fig. 4. Types of wind output power in peak season at bus 5.

This study uses the mathematical method from [19]. The results reveal the maximum achievable wind power output at bus 5 is P_{max} = 90 MW, as illustrated in Figure 4. The peak power has risen from 75 MW to 90 MW, leading to a substantial increment in the highest bidding power, signifying a remarkable growth of almost 30%. However, there are two specific time intervals during the day wherein wind power surpasses the rated power of the transformer. This excess reserve energy cannot be marketed to the electricity grid, causing a daily reduction in electricity output by 7.17 MWh.

D. EWS Scenario

An integration of ESS will be needed to harness surplus wind energy in the OWS scenario. Charge and dischage enegy can be seen in Figure 5 Based on the calculated results, an ESS with an energy of 140 MWh can be chosen. The NPV is computed using (1). The remarkable result of this scenario reveals an NPV value of approximately 17.28 M€, serving as a noteworthy finding.

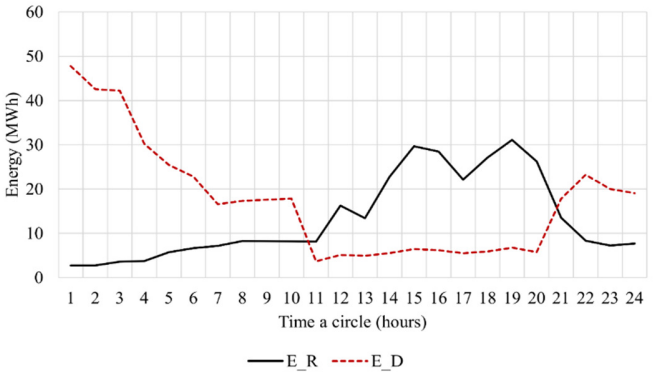

Fig. 5. Recharge and discharge energy.

IV. DISCUSSION

A. NPV

Figure 6 illustrates the NPV results of a wind power plant experiment conducted on the IEEE 30-bus power system across three scenarios: traditional, wind rate power expansion, and integrated scenarios incorporating ESS. All scenarios yield positive NPV values, indicating financial viability. The wind rate power expansion scenario with ESS integration shows the highest revenue potential. The NPV of this scenario remains largely unaffected by changes in the wind price compensation ratio. In terms of investor benefits, the wind rate power expansion scenario surpasses the traditional scenario, highlighting increased revenue from expanded wind rate power. The integrated ESS scenario experiences a significant NPV surge, with 65.1% showing no compensation requirement and a notable 573% increase with a compensation price set at 2. Contract compensations are generally undesirable in competitive electricity markets but unavoidable due to unpredictable factors like wind power. Compensation prices significantly influence NPV in scenarios 1 and 2 but remain stable at around 17.28 M€ in scenario 3, thanks to ESS intervention mitigating potential penalties or need for expensive electricity purchases.

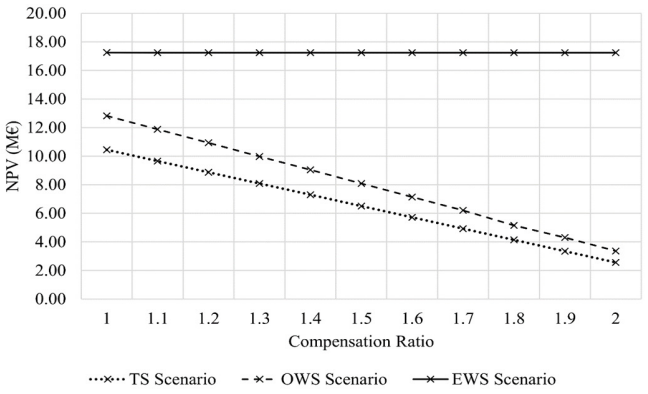

Fig. 6. Comparision of wind NPV in the three considered scenarios.

B. Investment Efficiency

TABLE II. FINANCIAL METRIC COMPARISON

Scenario	TS	OWS	EWS
Wind output power (MW)	75	90	90
Consider uncertainty	Yes	Yes	Yes
NPV (M€)	2.56	3.36	17.28
NPV/WP (k€/MW)	34.1	37.3	192
RoI (%)	4.4	4.8	24.8
Need extensive transmission system.	Yes	No	No

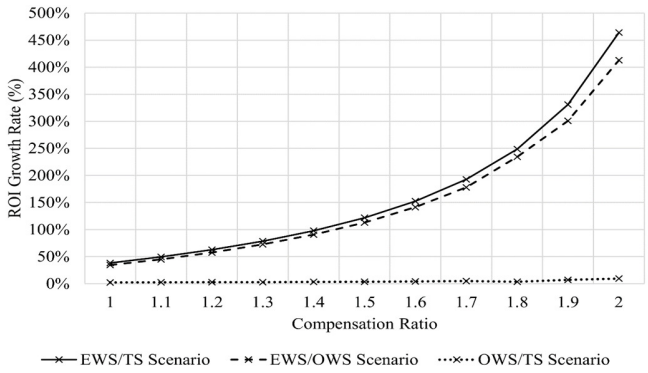

Fig. 7. Comparision of wind RoI in the three considered scenarios.

Figure 6 illustrates a clear trend where the RoI in the EWS scenario sharply increases with higher compensation rates for wind power output deficits. Specifically, when the compensation factor hits 2.0, RoI spikes by over 4.5 times. This notable ratio signifies an investment efficiency rarely achieved in traditional financial projects. Table II presents a comparative analysis of financial metrics and investment conditions across the three considered scenarios. Scenario 3 demonstrates the highest economic indicators, with RoI exceeding 29%, a significant improvement over the other scenarios. Investing in wind rate power expansion with integrated ESS, as seen in the EWS scenario, proves to be a favorable and recommended strategy for financial investors, offering benefits to both investors and society. However, this investment scenario warrants scrutiny of specific uncertainties, including the wind power output probability and TTS limitations, to mitigate potential instances necessitating additional transmission investments and resulting in extra capital costs.

V. CONCLUSION

The proposed model optimizes the expansion of wind farms integrated with ESS without the need to upgrade transmission transformers, thereby enhancing the investment efficiency of wind farms. This outcome not only benefits existing wind farms by encouraging expansion but also applies to optimization problems for new wind farm investments in the WTE group. Moreover, the proposed model offers tangible value compared to traditional wind farm investments by mitigating losses caused by wind power's inherent uncertainty. This reduction in uncertainty positively impacts project profitability, presenting a significant advantage in optimizing power transmission transformer operations.

The model also presents an optimal method integrating project investment evaluation based on two financial indices. Evaluation of two financial metrics across these scenarios consistently yielded positive outcomes, showing increasing economic benefits. Notably, the return on investment increased significantly from 4.4% to 24.8% from the first to the third scenario, indicating improved capital investment efficiency for the WTE mixture. The investment solution in the third scenario offers a unique benefit by eliminating the need to expand the electricity transmission system to connect wind farms to the power system. This reduces financial and workforce costs associated with assessing transmission line environments, land clearance, and compensation for new substations and transmission lines, which is not recommended.

ACKNOWLEDGEMENT

This work was supported by Ho Chi Minh City University of Technology and Education, Vietnam, under Project T2024-153.

REFERENCES

[1] *Renewables 2021 - Global status report*. Paris, France: International Energy Agency, 2021.

[2] M. B. A. Bashir, "Principle Parameters and Environmental Impacts that Affect the Performance of Wind Turbine: An Overview," *Arabian Journal for Science and Engineering*, vol. 47, no. 7, pp. 7891–7909, Jul. 2022, https://doi.org/10.1007/s13369-021-06357-1.

[3] "Global Wind Report 2021," *Global Wind Energy Council*, Mar. 24, 2021. https://gwec.net/global-wind-report-2021/.

[4] Vietnam National Electricity Planning for the period 2021 to 2030, vision 2023. Hanoi, Vietnam: Institute of Energy, 2023.

[5] Prime Minister, Approving the Plan to implement the National Power Development Master Plan for the 2021-2030 period, with a vision toward 2050, vol. 262/QD-TTg. 2024.

[6] N. T. Linh and P. V. Long, "A Novel Solution Method for the Distribution Network Reconfiguration Problem based on an Objective Function and considering the Cost of Electricity Transmission," *Engineering, Technology & Applied Science Research*, vol. 13, no. 6, pp. 12366–12372, Dec. 2023, https://doi.org/10.48084/etasr.6568.

[7] V. A. Truong, N. S. Dinh, and T. L. Duong, "Profit Maximization of Wind Power Plants in the Electricity Market Based on Linking Models Between Energy Sources," *Arabian Journal for Science and Engineering*, vol. 49, no. 5, pp. 6275–6291, May 2024, https://doi.org/10.1007/s13369-023-08181-1.

[8] T. Cai, M. Dong, K. Chen, and T. Gong, "Methods of participating power spot market bidding and settlement for renewable energy systems," *Energy Reports*, vol. 8, pp. 7764–7772, Nov. 2022, https://doi.org/10.1016/j.egyr.2022.05.291.

[9] T. Dridi, H. Jouini, A. Mami, A. E. Mhamedi, and E. M. Dafaoui, "Application of the Levenberg-Marquardt Algorithm in Solving the Economic Emission Dispatch Problem Integrating Renewable Energy," *Engineering, Technology & Applied Science Research*, vol. 12, no. 4, pp. 8850–8855, Aug. 2022, https://doi.org/10.48084/etasr.5002.

[10] A. Molina Gomez, K. Morozovska, T. Laneryd, and P. Hilber, "Optimal sizing of the wind farm and wind farm transformer using MILP and dynamic transformer rating," *International Journal of Electrical Power & Energy Systems*, vol. 136, Mar. 2022, Art. no. 107645, https://doi.org/10.1016/j.ijepes.2021.107645.

[11] M. Fantauzzi, D. Lauria, F. Mottola, and D. Proto, "Estimating Wind Farm Transformers Rating through Lifetime Characterization Based on Stochastic Modeling of Wind Power," *Energies*, vol. 14, no. 5, Jan. 2021, Art. no. 1498, https://doi.org/10.3390/en14051498.

[12] O. D. Ariza Rocha, K. Morozovska, T. Laneryd, O. Ivarsson, C. Ahlrot, and P. Hilber, "Dynamic rating assists cost-effective expansion of wind farms by utilizing the hidden capacity of transformers," *International Journal of Electrical Power & Energy Systems*, vol. 123, Dec. 2020, Art. no. 106188, https://doi.org/10.1016/j.ijepes.2020.106188.

[13] T. Zuo *et al.*, "A Review of Optimization Technologies for Large-Scale Wind Farm Planning With Practical and Prospective Concerns," *IEEE Transactions on Industrial Informatics*, vol. 19, no. 7, pp. 7862–7875, Jul. 2023, https://doi.org/10.1109/TII.2022.3217282.

[14] R. Li *et al.*, "Techno-economic analysis of a wind-photovoltaic-electrolysis-battery hybrid energy system for power and hydrogen generation," *Energy Conversion and Management*, vol. 281, Apr. 2023, Art. no. 116854, https://doi.org/10.1016/j.enconman.2023.116854.

[15] P. Shinde and M. Amelin, "A Literature Review of Intraday Electricity Markets and Prices," in *IEEE Milan PowerTech*, Milan, Italy, Jun. 2019, pp. 1–6, https://doi.org/10.1109/PTC.2019.8810752.

[16] P. P. Biswas, P. N. Suganthan, and G. A. J. Amaratunga, "Optimal power flow solutions incorporating stochastic wind and solar power," *Energy Conversion and Management*, vol. 148, pp. 1194–1207, Sep. 2017, https://doi.org/10.1016/j.enconman.2017.06.071.

[17] J. V. Seguro and T. W. Lambert, "Modern estimation of the parameters of the Weibull wind speed distribution for wind energy analysis," *Journal of Wind Engineering and Industrial Aerodynamics*, vol. 85, no. 1, pp. 75–84, Mar. 2000, https://doi.org/10.1016/S0167-6105(99)00122-1.

[18] N. Viafora, K. Morozovska, S. H. H. Kazmi, T. Laneryd, P. Hilber, and J. Holbøll, "Day-ahead dispatch optimization with dynamic thermal rating of transformers and overhead lines," *Electric Power Systems Research*, vol. 171, pp. 194–208, Jun. 2019, https://doi.org/10.1016/j.epsr.2019.02.026.

[19] IEC, *Power transformers–Part 7: Loading guide for oil-immersed power transformers*, First edition. Geneva, Switzerland: International Electrotechnical Commission, 2005.

[20] M. M. Rahman, A. O. Oni, E. Gemechu, and A. Kumar, "Assessment of energy storage technologies: A review," *Energy Conversion and Management*, vol. 223, Nov. 2020, Art. no. 113295, https://doi.org/10.1016/j.enconman.2020.113295.

[21] K. Mongird *et al.*, "Energy Storage Technology and Cost Characterization Report," Pacific Northwest National Laboratory, Richland, WA, USA, Technical Report PNNL-28866, Jul. 2019, https://doi.org/10.2172/1573487.

[22] O. Alsac and B. Stott, "Optimal Load Flow with Steady-State Security," *IEEE Transactions on Power Apparatus and Systems*, vol. PAS-93, no. 3, pp. 745–751, May 1974, https://doi.org/10.1109/TPAS.1974.293972.

[23] R. W. Ferrero, S. M. Shahidehpour, and V. C. Ramesh, "Transaction analysis in deregulated power systems using game theory," *IEEE Transactions on Power Systems*, vol. 12, no. 3, pp. 1340–1347, Aug. 1997, https://doi.org/10.1109/59.630479.

[24] D. Cao *et al.*, "Bidding strategy for trading wind energy and purchasing reserve of wind power producer – A DRL based approach," *International Journal of Electrical Power & Energy Systems*, vol. 117, May 2020, Art. no. 105648, https://doi.org/10.1016/j.ijepes.2019.105648.

SSRG International Journal of Electrical and Electronics Engineering
ISSN: 2348-8379/ https://doi.org/10.14445/23488379/IJEEE-V12I1P103

Volume 12 Issue 1, 17-24, January 2025

Original Article

Optimal Probability Distribution Models for Wind Speed Prediction: Strategies to Advance Wind Energy Development in Vietnam

Sang Ngoc Dinh[1,2], Anh Viet Truong[1], Linh Tung Nguyen[3,*]

[1]*Faculty of Electrical and Electronics Engineering, Hochiminh University of Technology and Education, Hochiminh City, Vietnam.*
[2]*Department of Urban Infrastructure Engineering, University of Architecture Hochiminh City, Hochiminh City, Vietnam.*
[3]*Faculty of Control and Automation, Electric Power University, Hanoi City, Vietnam.*

**Corresponding Author : linhnt@epu.edu.vn*

Received: 02 November 2024 Revised: 04 December 2024 Accepted: 05 January 2025 Published: 25 January 2025

Abstract - *This paper aims to provide data and propose viable strategies for effectively harnessing wind energy by introducing probabilistic models for wind speed prediction. The objective is to improve the accuracy of wind speed forecasts, thereby mitigating risks for stakeholders and building investor confidence in the development of wind energy. This aligns with the Vietnamese government's strategy to reduce greenhouse gas emissions, aiming to achieve 23,896 MW of wind power capacity by 2030, including 75% onshore and 25% offshore wind power. Wind speed data measured in a locality in Vietnam from 2017 to 2022 were evaluated using fitting methods and goodness of fit methods to determine the most appropriate probability distribution model. Findings indicate that the Gamma model best fits this locality under short-term, medium-term, and long-term forecasting scenarios. However, it is suggested that the Normal distribution model should be slightly prioritized in medium-term and long-term scenarios, whereas the Generalized Extreme Value model is found to be the least suitable.*

Keywords - *Wind energy, Wind speed forecast, Probability distribution, Energy development strategy, Renewable.*

1. Introduction

1.1. Literature Review

The increasing global focus on renewable energy sources like wind power is driven by the need to reduce greenhouse gas emissions and achieve sustainable development [1]. While wind power presents a promising solution, the inherent uncertainty in energy production due to fluctuating wind speeds poses significant challenges for stakeholders in the energy market [2]. This uncertainty can impact technical and economic aspects, including potential compensation to electricity buyers during energy shortages [3]. Previous studies have significantly focused on employing probability distribution models to reduce uncertainties in wind speed forecasting and optimize wind energy utilization. For instance, the Weibull distribution has been widely applied to assess wind energy uncertainties in the integration of wind and thermal energy systems, as well as to analyze wind speed patterns in Bangladesh [4]. Additionally, the Generalized Extreme Value (Ev) model has been utilized to calibrate aggregated wind speed forecasts in weather prediction [5]. Global wind energy development strategies, such as the European Union's clean energy transition [6] and South Asia's renewable energy development plan [7], have highlighted the critical role of selecting appropriate distribution models in managing wind energy uncertainties.

1.2. Motivations and Contributions

In Vietnam, which has pledged to achieve net-zero emissions by 2050 [8], and in neighboring regions, research on wind speed probability distribution models tailored to the local context remains scarce. While some survey data are available from areas with substantial wind potential, a comprehensive assessment of the suitability of these distribution models for the region's unique climatic conditions and wind characteristics is still lacking. This gap has led to an insufficient scientific foundation to guide investors and policymakers in advancing sustainable wind energy development.

1.3. Key Contributions of the Study Include

1.3.1. Identifying Optimal Probability Distribution Models

This study employs rigorous evaluation techniques such as Maximum Likelihood Estimation (ML), R-Square (R^2), Root Mean Square Error (RMSE), Chi-Square (X^2), and Kolmogorov–Smirnov (KS) tests [9], to determine the most suitable probability distribution models for measured wind speed data in Vietnam.

1.3.2. Supporting Wind Energy Development Strategies

The study provides detailed data and analyses to support policy formulation and the implementation of wind energy development strategies in Vietnam up to 2030, with a long-term vision extending to 2050. Additionally, it contributes to promoting investments in wind energy that are aligned with global sustainable development goals.

1.3.3. Enhancing Forecast Accuracy

The research proposes solutions to improve the accuracy of wind speed forecasts, minimize uncertainties in energy production, and optimize the economic efficiency of wind energy projects in Vietnam. These findings are valuable for Vietnam and have broad applicability to similar geographical regions in Southeast Asia that face comparable challenges in wind power development. The study contributes to reducing wind speed forecasting errors in the region by leveraging the wind speed data provided in this research.

2. Methodology of Wind Speed Probability Distribution Assessment

The paper focuses on evaluating and selecting appropriate probability distribution models for the surveyed area to improve wind speed forecasting accuracy and assess uncertainty levels, as discussed in [10]. Based on the forecasting time horizon, predictions can be categorized into four types: very short-term, short-term, medium-term, and long-term [11]. Regarding probability distribution models, the literature in [12] describes their wide range of applications across various fields, with commonly used models including Gamma (Gm) and Ev. Notably, [13] emphasizes that the Weibull (Wb) model is one of the most widely used models in the energy sector. Therefore, this study proposes to evaluate the Wb, Gm, and Ev distribution models in addition to the Normal (Nm) distribution model.

2.1. Probability Distribution Models

2.1.1. Weibull Distribution

The Probability Distribution Function (PDF) of the Wb model is described by the following expression [14]:

$$f(x) = \begin{cases} \frac{c}{\sigma}\left(\frac{x}{\sigma}\right)^{(c-1)} e^{-\left(\frac{x}{\sigma}\right)^c} & x \geq 0 \\ 0, & x < 0, \end{cases} \quad (1)$$

Here, the indices σ và c describe the scale and shape of the distribution. The cumulative probability distribution is transformed into [13]:

$$F(x) = 1 - e^{-\left(\frac{x}{\sigma}\right)^c}, x \geq 0 \quad (2)$$

2.1.2. Gamma Distribution

$$f(x) = \begin{cases} \frac{1}{\sigma^c \Gamma(c)} x^{(c-1)} e^{-\left(\frac{x}{\sigma}\right)} & x \geq 0 \\ 0, & x < 0, \end{cases} \quad (3)$$

$$F(x) = \frac{1}{\sigma^c \Gamma(c)} \gamma\left(c, \frac{x}{\sigma}\right), x \geq 0 \quad (4)$$

The Gm distribution has recently merged in predicting wind speeds in various regions, such as India [15], showing a close relationship with normal and exponential distributions. The probability and cumulative distribution functions are described as follows [13]. The coefficients σ and c also have the same meaning as Wbl. Particularly Γ is called the gamma function and is calculated by (c-1)! [16].

2.1.3. Generalized Extreme Value Distribution

The Ev model is a continuous probability distribution comprising three extreme components: Frechet and Weibull. The probability distribution and cumulative distribution are described as follows [14, 13]:

$$f(x) = \begin{cases} \frac{1}{\sigma}\left[1 + c\left(\frac{x-\mu}{\sigma}\right)\right]^{-\left(1+\frac{1}{c}\right)} e^{-\left[1+c\left(\frac{x-\mu}{\sigma}\right)\right]^{-\left(\frac{1}{c}\right)}} & 1 + c\left(\frac{x-\mu}{\sigma}\right) \geq 0 \\ 0, & 1 + c\left(\frac{x-\mu}{\sigma}\right) < 0, \end{cases} \quad (5)$$

$$F(x) = e^{-\left[1+c\left(\frac{x-\mu}{\sigma}\right)\right]^{-\left(\frac{1}{c}\right)}}, 1 + c\left(\frac{x-\mu}{\sigma}\right) \geq 0 \quad (6)$$

The coefficients c, σ, μ are sharp, scale and local, respectively.

2.1.4. Normal Distribution

Nm is commonly used in many different fields for standard probability statistics. The PDF is represented as follows [17]:

$$f(x) = \frac{1}{\sigma\sqrt{2\pi}} e^{-\left(\frac{(x-\mu)^2}{2\sigma^2}\right)} \quad (7)$$

The coefficient μ represents the average value, while σ describes the normal distribution coefficient.

2.2. Fitting Methods and Goodness of Fit

Determining the most appropriate parameters of the probability distribution model is the initial step. Once the parameters are clearly defined, goodness of fit methods are applied to evaluate and select the most suitable probability distribution model for the dataset [14, 18].

2.2.1. Maximum Likelihood Fitting

ML is one of the widely used methods for fitting and estimating the parameters of wind speed distribution models [19]. First, the likelihood function or the logarithmic likelihood function is constructed, and then the parameter values are searched for to maximize this function. Iterative methods such as Newton's are employed to estimate the maximum likelihood efficiently in an asymptotic sense and to achieve minimal variance [20]. Additionally, some studies have applied an improved ML method, known as the alternative maximum likelihood method, for modeling wind speed distribution. This method is based on the idea of linearizing the nonlinear terms

using a Taylor series and deriving parameter estimators in a non-iterative manner. Ultimately, the results of ML fitting establish the best parameters for the evaluated probability distribution model.

2.2.2. R-Square Evaluation

The R-squared represents the square of the correlation between the observed values and the predicted values. It is also referred to as the square of the multiple correlation coefficient and the multiple coefficient of determination. This metric measures the degree of success in explaining the variability of the measured data. It is commonly used to assess how well a nonlinear function fits a given statistical data set. The higher the value, the better the fit. The R-squared value is calculated as follows [20]:

$$R^2 = 1 - \frac{\sum_{i=1}^{n}(y_i - x_i)^2}{\sum_{i=1}^{n}(y_i - \bar{y})^2} \quad (8)$$

Here, y and x are the corresponding statistical and functional values, $\bar{y}$ is the average functional value.

2.2.3. Root Mean Square Error

The RMSE quantifies the discrepancy between observed probabilities and those estimated by the probability function, indicating the model's goodness of fit. A lower RMSE value signifies a better fit. Due to its sensitivity to outliers, RMSE is often used in conjunction with the square index. The calculated value is [20],

$$RMSE = \left[\frac{1}{n}\sum_{i=1}^{n}\left(F_i - \hat{F}_i\right)^2\right]^{\frac{1}{2}} \quad (9)$$

F and $\hat{F}$ represent probability functions and observed values.

2.2.4. Chi-Square Evaluation

The chi-square statistic, based on the frequency of occurrences, is commonly used to assess the accuracy of probability distribution functions. Therefore, this statistic indicates whether the chosen distribution function is valid when evaluated against a critical value. The statistic is calculated as follows [14]:

$$X^2 = \sum_{i=1}^{N}\frac{(O_i - E_i)^2}{E_i} \quad (10)$$

In this context, Oi represents the number of observations estimated using each distribution's estimated probability density function. Ei denotes the expected number of observations, calculated through a frequency histogram based on the measured data.

2.2.5. Kolmogorov–Smirnov Evaluation

The Kolmogorov-Smirnov statistic assesses the maximum difference between the cumulative distribution function of a model and the empirical distribution function. When the measured value increases or decreases too abruptly in comparison to the distribution function, it indicates that the chosen distribution may be inappropriate. The statistic is calculated using the following expression [14]:

$$KS = max(|F_1(x) - F_2(x)|) \quad (11)$$

Where F1(x) is the cumulative probability measured compared with the theoretical probability, F2(x).

3. Data

3.1. Wind Power Development Strategy of Vietnam by 2030

3.1.1. Review of Wind Power Development Strategy

Table 1. Wind power planning data by 2030 [21]

Regions	Planning by 2030 (MW)		
	Total	Onshore	Offshore
Northern	8,264	5,764	2,500
Middle	4,791	4,291	500
Southern	10,841	7,841	3,000
Total	23,896	17,896	6,000

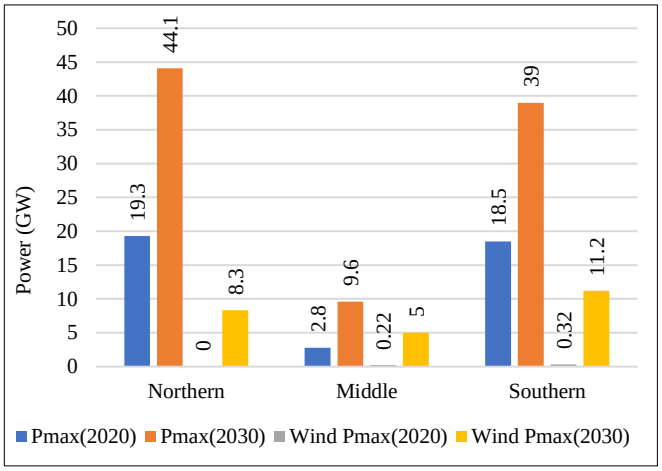

Fig. 1 Electricity load and wind power by 2030 [8, 22]

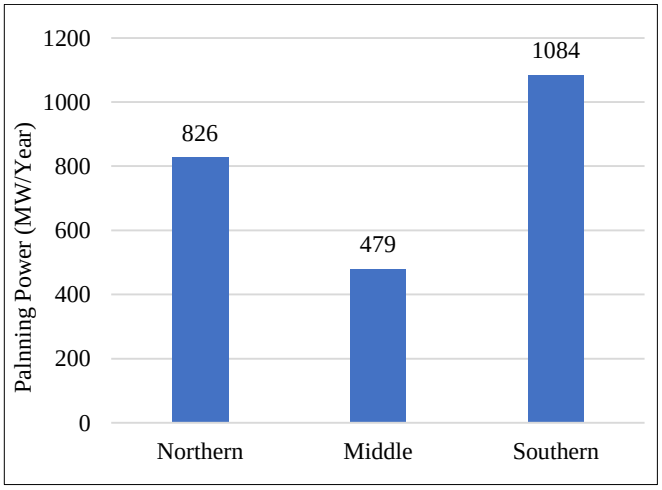

Fig. 2 Annual average increase in wind power [21]

Table 2. Installed wind power capacity of countries

Countries		Potential (MW)	Year	Installed Capacity (MW)
Afghanistan	[7]	66.726	2019	0
Bangladesh		20.000	2019	3
Bhutan		63.895	2019	1
India		102.778	2020	32878
Maldives		288	2019	1
Nepal		3.000	2019	0
Pakistan		346.000	2020	792
Sri Lanka		24.000	2019	146
Vietnam		821.173	2022	3986

According to the forecast in [8], electricity demand is expected to reach a peak load of over 92,000 MW by 2030, while total power capacity expansion is projected to be around 138,000 MW. Wind power is expanding rapidly, with a planned increase of nearly 24,000 MW, as outlined in Table 1, reflecting an annual growth rate of approximately 28%. The southern region is leading this growth, with an annual increase of 21%, while the middle region shows the slowest growth at 9%, as indicated in Figure 1. The northern region is growing at about 16% annually, with average annual capacity increases of 826 MW in the north, 479 MW in the middle region, and 1,084 MW in the south, as shown in Figure 2. By 2030, wind power capacity is projected to exceed 10,000 MW, largely based on detailed plans for onshore wind projects. Currently, 58% of the remaining capacity is in the planning phase and open to investors. This capacity is evenly divided between onshore and offshore wind power, with approximately 7,800 MW allocated to onshore and 6,000 MW to offshore. According to the wind power development plan in [21], wind energy is expected to make up more than 13% of Vietnam's total energy capacity by 2030, with an estimated 28,000 MW. However, this only taps into about 13% of the country's full wind energy potential. As reported in [8], Vietnam has over 200,000 MW of onshore wind capacity and around 600,000 MW offshore.

3.1.2. Comparison of Asian Countries

According to reference [21], Vietnam is among the countries with a robust wind energy investment and development strategy, driven by strong initial government support policies and a substantial, favorable wind energy resource base, as shown in Table 2.

3.2. Wind Speed Data

The wind speed data was collected from a midland region in the south-central coast of Vietnam, an area with a significant future wind energy development strategy [8]. Wind speeds were measured at a height of 10 meters above ground level. The data was recorded at 10-minute intervals, encompassing maximum speed, minimum speed, average speed, and standard deviation. The dataset utilized for the research spans six years, from 2017 to 2022. Three simulations of the dataset were conducted: (i) short-term, the data was divided into hourly sample subsets for each day; (ii) medium-term, the data was segmented into daily sample subsets for each month; and (iii) long-term, the data was organized into monthly sample subsets for each year. Figure 3 illustrates the measured data over a span of six years. While not immediately evident, it is observed that the pattern remains largely consistent across four seasons within each year: (1) Season 1: from December of the preceding year to February. (2) Season 2: from March to May. (3) Season 3: from June to August. (4) Season 4: from September to November. Seasons 1 and 3 exhibit higher wind speeds than Seasons 2 and 4.

4. Experimental Results and Discussion

4.1. Comparison of Models

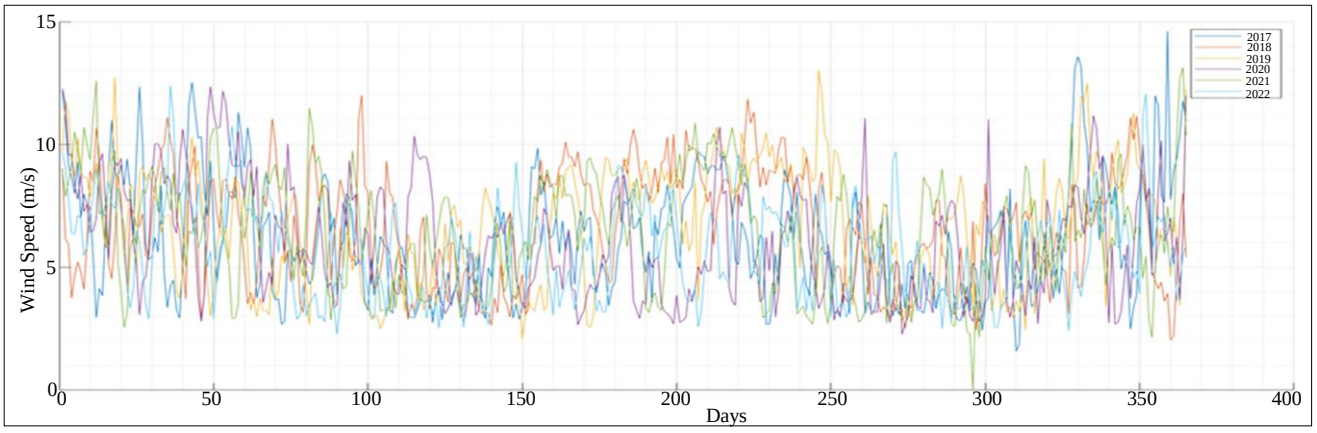

Fig. 3 Wind velocity data measured

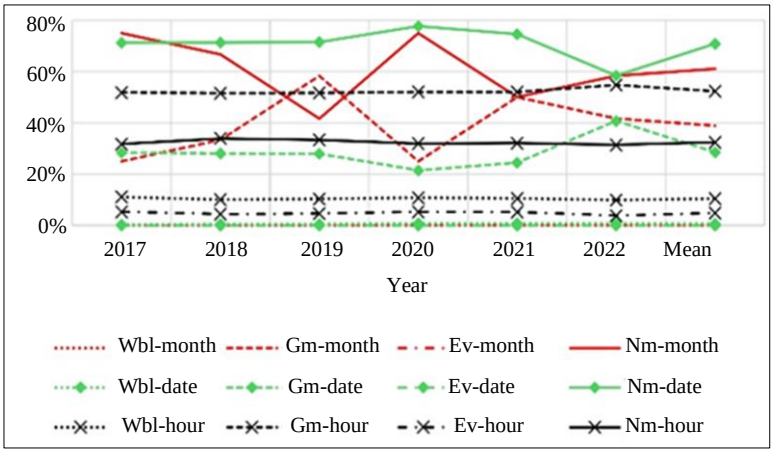

Fig. 4 Dominance ratio of distribution models

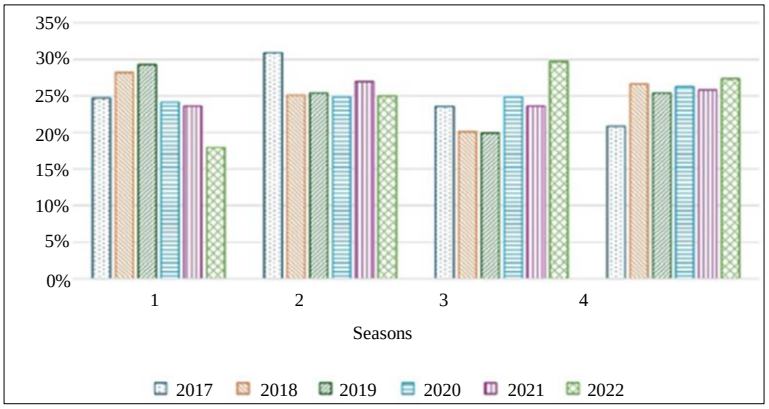

Fig. 5 Dominant dates of Nm distribution

The survey results of four distribution types with three illustrated cases are presented in Figure 4. The curves depict a relatively stable trend in the selection count over the years. However, the case for months exhibits variability, particularly between the Nm and Ev distributions. The highest selection rate occurs with the Nm distribution in the daily case, averaging around 70%. Conversely, the lowest is observed with the Wb distribution in both monthly and daily cases. Upon closer examination of each case, Gm holds the highest selection proportion for short-term hourly predictions, followed by Nm, Wb, and Ev, which is the least preferred. For medium and long-term cases, the Nm distribution predominates, especially in the medium-term, followed by Gm. Wb and Ev's distributions are scarcely chosen in these scenarios. Hence, for short-term predictions, the Gm distribution appears most suitable, although other distributions should also be considered, albeit with lesser suitability. Conversely, for medium and long-term predictions, the Nm distribution seems more appropriate. Wb and Ev distributions are discouraged for use in these contexts.

4.2. Medium-Term Case

Figure 5 presents the results of the proportion of Nm selection distribution across seasons over the years. Cases suggest a seemingly equivalent outcome across all four seasons. However, some anomalous fluctuations are believed to be weather-related. For instance, in the second season of 2017, the prevalence of storms compared to other years led to a notably higher proportion of Nm selection distribution [23, 24]. Conversely, in the first season of 2022, the presence of tropical low-pressure systems and weaker cold air mass compared to previous years resulted in a significantly lower proportion [25]. Thus, a medium-term case based on Nm distribution is recommended but remains contingent upon weather conditions.

4.3. Short-Term Case

Figures 6 and 7 further confirm the superiority of the Gm distribution in the hourly and annual analysis. While alternative distributions are viable, Gm and Nm stand out as the more dominant, with significantly higher selection probabilities of 0.55 and 0.31, respectively. In contrast, Wb shows a lower probability of 0.10, and Ev has the lowest at just 0.04. Between the hours of 12:00 to 15:00, there appears to be a balance between these two distribution models. Perhaps the high and stable wind velocities mitigate the influence of distribution types. The Wb distribution warrants consideration due to its stability, whereas Ev exhibits a lower preference ratio. A comparison across months in 2022 in Figure 8 illustrates relatively stable preference ratios for the models. However, the

Nm distribution experienced a sharp decline in February, attributed to abrupt decreases in tropical pressure rates and cold air in that month of 2022. In the case of seasons, the Gm distribution seems less volatile, while the others fluctuate across Seasons 2 and 3, as depicted in Figure 9, corresponding to seasons characterized by high wind speed fluctuations due to weather fluctuations.

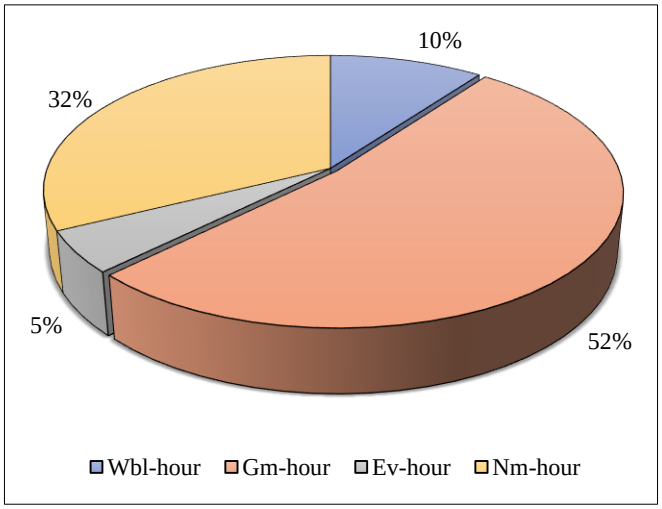

Fig. 6 Mean dominant in six years

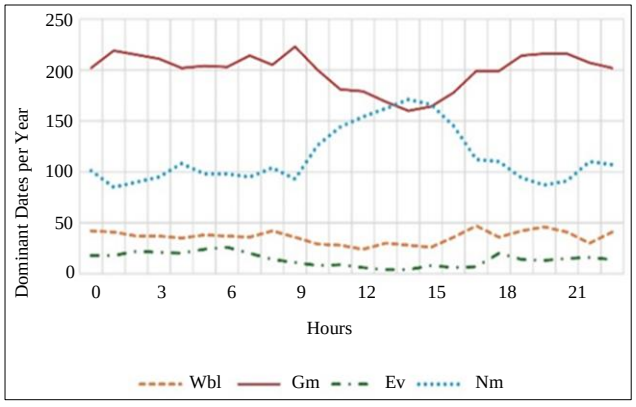

Fig. 7 Dominant dates in short-term simulation by 2022

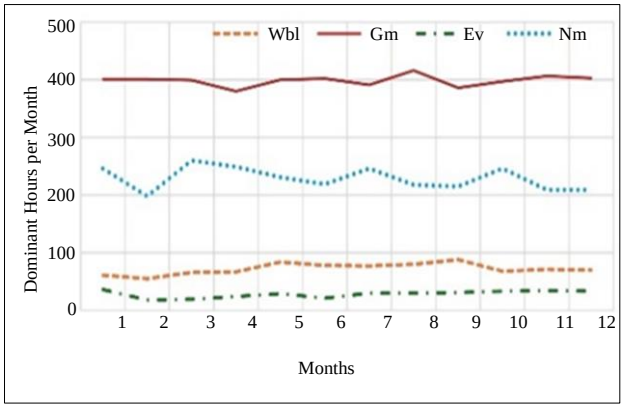

Fig. 8 Dominant in months by 2022

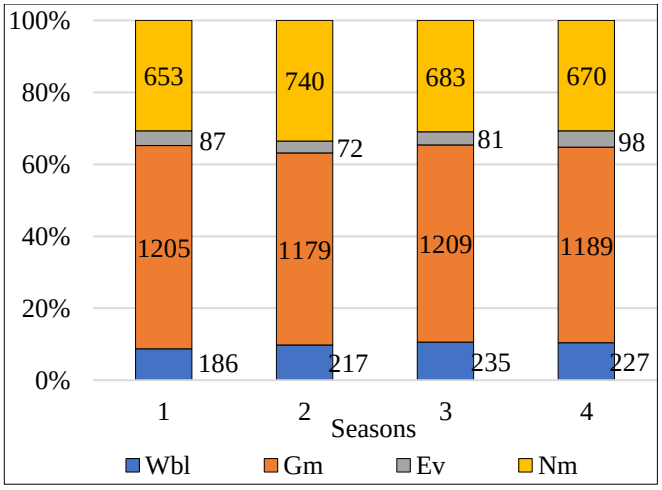

Fig. 9 Dominant in seasons by 2022

4.4. Comparison of Countries

Table 1. Survey of wind speed probability distribution models of countries

Countries	Ref.	Year of Survey	Proposed Model
Turkey	[12]	2013	Extreme Value
Trinidad and Tobago	[14]	2000-2015	Rayleigh
Iran	[13]	2008-2010	Gamma
Vietnam	This article	2017-2022	Gamma

Although various studies have applied the Weibull probability distribution to assess error deviations in wind speed predictions for optimization problems in wind energy, survey data from several countries suggest that other distribution models may provide greater accuracy, as summarized in Table 3. For instance, Turkey recommends the Extreme Value model, Trinidad and Tobago proposes the Rayleigh model, Iran suggests the Gamma model, and, in line with Iran's findings, Vietnam is also recommended to use the Gamma model, as supported by the results of this study.

5. Conclusion

The findings of this research, based on the analysis and evaluation of wind speed data, are designed to enhance the strategy for wind energy development in alignment with Vietnam's power planning objectives. The study demonstrates that the Gm probability distribution is the most effective for predicting hourly short-term wind power generation. In some cases, the Nm distribution may serve as a viable alternative or complement to Gm. Importantly, these results diverge from those presented in reference [12], where the Ev distribution provided superior overall model performance. The Wb distribution, often utilized in some prior scientific studies, should also be considered but appears to be less suitable, a sentiment aligned with the assertion in reference [14]. For medium-term, daily-based forecasting, it is advisable to

prioritize the selection of the Nm distribution for evaluation over others. Conversely, a combination of both Nm and Gm distributions is recommended for long-term projections based on experimental findings. On the horizon axis, the process of selecting distributions appears to be less contingent upon seasons or months within the year. However, when examined by hourly intervals, the time frame between 12:00 and 15:00 shows minimal differentiation between the distributions Gm and Nm. Beyond this timeframe, the evaluation outcomes favor the proposed Gm distribution model. Despite the clear achievements highlighted by the research results, certain limitations remain, particularly regarding unusual weather patterns. The evaluation identified several unexpected storms, such as those in the second season of 2017 and the early season of 2022, in Figure 5, which could disrupt predictions. Correspondingly, for such anomalies, the Nm probability distribution is suitable across various localities, aligning with findings from previous studies.

Conflicts of Interest

The authors affirm the absence of relevant financial or non-financial conflicts of interest. Data Availability Statement: The data supporting the findings of this study are available from the corresponding author upon reasonable request.

References

[1] Irena, Future of Wind Deployment, Investment, Technology, Grid Integration and Socio-Economic Aspects (A Global Energy Transformation Paper), International Renewable Energy Agency, 2019. [Online]. Available: https://www.irena.org/publications/2019/Oct/Future-of-wind

[2] Lunjie Wang et al., "Analysis of Low-Carbon Comprehensive Energy System Scheduling Considering Multiple Uncertainties," *Clean Technologies and Environmental Policy*, vol. 26, pp. 2919-2935, 2024. [CrossRef] [Google Scholar] [Publisher Link]

[3] Bo Li, and Mohammad Ghiasi, "A New Strategy for Economic Virtual Power Plant Utilization in Electricity Market Considering Energy Storage Effects and Ancillary Services," *Journal of Electrical Engineering and Technology*, vol. 16, pp. 2863-2874, 2021. [CrossRef] [Google Scholar] [Publisher Link]

[4] Saima Jahan, Nurulkamal Masseran and W.Z. Wan Zin, "Wind Speed Analysis using Weibull and Lower Upper Truncated Weibull Distribution in Bangladesh," *Energy Reports*, vol. 11, pp. 5456-5465, 2024. [CrossRef] [Google Scholar] [Publisher Link]

[5] Sándor Baran, Patrícia Szokol and Marianna Szabó, "Truncated Generalized Extreme Value Distribution-Based Ensemble Model Output Statistics Model for Calibration of Wind Speed Ensemble Forecasts," *Environmetrics*, vol. 32, no. 6, pp. 1-24, 2021. [CrossRef] [Google Scholar] [Publisher Link]

[6] Patricia Márquez-Sobrino et al., "Twenty Years of Energy Policy in Europe: Achievement of Targets and Lessons for the Future," *Clean Technologies and Environmental Policy*, vol. 25, pp. 2511-2527, 2023. [CrossRef] [Google Scholar] [Publisher Link]

[7] Madhushree Mitra, Nayan Ranjan Singha, and Pijush Kanti Chattopadhyay, "Review on Renewable Energy Potential and Capacities of South Asian Countries Influencing Sustainable Environment: A Comparative Assessment," *Sustainable Energy Technologies and Assessments*, vol. 57, 2023. [CrossRef] [Google Scholar] [Publisher Link]

[8] Vietnam's National Electricity Development Plan for the Period 2021-2030, Vision to 2050, Vietnam Briefing, 2023. [Online]. Available: https://www.vietnam-briefing.com/news/vietnams-national-electricity-development-plan-2021-2030-roadmap-approved.html/

[9] Bulent Yaniktepe et al., "Comparison of Eight Methods of Weibull Distribution for Determining The Best-Fit Distribution Parameters with Wind Data Measured from the Met-Mast," *Environmental Science and Pollution Research*, vol. 30, pp. 9576-9590, 2023. [CrossRef] [Google Scholar] [Publisher Link]

[10] Suraj Kumar Bhagat et al., "Wind Speed Prediction and Insight for Generalized Predictive Modeling Framework: A Comparative Study for Different Artificial Intelligence Models," *Neural Computing and Applications*, vol. 36, pp. 14119-14150, 2024. [CrossRef] [Google Scholar] [Publisher Link]

[11] Yun Wang et al., "A Review of Wind Speed and Wind Power Forecasting with Deep Neural Networks," *Applied Energy*, vol. 304, 2021. [CrossRef] [Google Scholar] [Publisher Link]

[12] Fatma Gül Akgül, and Birdal Şenoğlu, "Comparison of Wind Speed Distributions: A Case Study for Aegean Coast of Turkey," *Energy Sources, Part A: Recovery, Utilization, and Environmental Effects*, vol. 45, no. 1, pp. 2453-2470, 2019. [CrossRef] [Google Scholar] [Publisher Link]

[13] Mohammed Wadı, "Five Different Distributions and Metaheuristics to Model Wind Speed Distribution," *Journal of Thermal Engineering*, vol. 7, no. 14, pp. 1898-1920, 2021. [CrossRef] [Google Scholar] [Publisher Link]

[14] Isa Dookie et al., "Evaluating Wind Speed Probability Distribution Models with A Novel Goodness of Ft Metric: A Trinidad and Tobago Case Study," *International Journal of Energy and Environmental Engineering*, vol. 9, pp. 323-339, 2018. [CrossRef] [Google Scholar] [Publisher Link]

[15] Gaurav Kumar Gugliani et al., "Comparison of Probability Distributions Used for Harnessing The Wind Energy Potential: A Case Study From India," *Stochastic Environmental Research and Risk Assessment*, vol. 38, pp. 2213-2230, 2024. [CrossRef] [Google Scholar] [Publisher Link]

[16] Robert V. Hogg, Joseph W. McKean and Allen T. Craig, *Introduction to Mathematical Statistics*, 8th ed., United States of America: Pearson Education, 2019. [Google Scholar] [Publisher Link]

[17] T.B.M.J. Ouarda et al., "Probability Distributions of Wind Speed in the UAE," *Energy Conversion and Management*, vol. 93, pp. 414-434, 2015. [CrossRef] [Google Scholar] [Publisher Link]

[18] Qiwei Li, Jianzhou Wang, and Haipeng Zhang, "Comparison of the Goodness-of-Fit of Intelligent-Optimized Wind Speed Distributions and Calculation in High-Altitude Wind-Energy Potential Assessment," *Energy Conversion and Management*, vol. 247, 2021. [CrossRef] [Google Scholar] [Publisher Link]

[19] Yu-Le Wu et al., "Maximum-Likelihood Model Fitting for Quantitative Analysis of SMLM Data," *Nature Methods*, vol. 20, pp. 139-148, 2023. [CrossRef] [Google Scholar] [Publisher Link]

[20] Huanyu Shi et al., "Wind Speed Distributions Used in Wind Energy Assessment: A Review," *Frontiers in Energy Research*, vol. 9, 2021. [CrossRef] [Google Scholar] [Publisher Link]

[21] The Prime Minister, The Socialist Republic of Vietnam, Approving the Plan to implement the National Power Development Master Plan for the 2021-2030 period, with a vision toward 2050, Hanoi, 2024. [Online]. Available: https://english.luatvietnam.vn/cong-nghiep/decision-262-qd-ttg-2024-plan-to-implement-the-national-power-development-master-plan-for-2021-2030-309182-d1.html

[22] Decision 500/QD-TTg: Approving the Vietnam's National Electricity Development Plan for the Period 2021-2030, Vision to 2050, Vietnam, 2023. [Online]. Available: https://climate-laws.org/document/decision-no-500qd-ttg-on-approving-the-national-electricity-development-plan-for-2021-2030-vision-to-2050-7019

[23] Disaster Resilience for Sustainable Development: Asia-Pacifc Disaster Report 2017, United Nations Publications, Bangkok, Thailand, 2018. [Online]. Available: https://issuu.com/pannature/docs/asia-pacificdisasterreport2017full

[24] Dirk Schwede, and Yuanchen Wang, "Reference Weather Datasets for Building Simulation In Vietnam Considering Thermal and Hygrothermal Characteristics," *Building and Environment*, vol. 220, 2022. [CrossRef] [Google Scholar] [Publisher Link]

[25] Viet Nam Monsoon Storms and Floods 2022 Final Report, Vietnam, 2023. [Online]. Available: https://adore.ifrc.org/Download.aspx?FileId=711358

Enhancing Wind Power Profitability through Integrated Clusters in the Electricity Market

Ngoc Sang Dinh
University of Architecture Hochiminh City;
Hochiminh City University of Technology and Education
Hochiminh City, Vietnam
sang.dinhngoc@uah.edu.vn

Tung Linh Nguyen
Faculty of Control and Automation
Electric Power University (EPU)
Hanoi City, Vietnam
linhnt@epu.edu.vn

Viet Anh Truong
Faculty of Electrical and Electronics Engineering
Hochiminh City University of Technology and Education
Hochiminh City, Vietnam
anhtv@hcmute.edu.vn

***Abstract*—In the context of wind power sources participating in the electricity market, they frequently encounter significant challenges arising from their inherent uncertainties. Compared to the initial projections, deviations in their power output could potentially lead to decreased revenue for investors. This necessitates compensation or penalties due to shortfalls in wind power output. This study thoroughly investigates and assesses proposed integration scenarios to mitigate the risk of such penalties or compensation requirements. These scenarios involve the integration of multiple wind turbines and wind farms, aiming to enable mutual offsetting of electricity output power in cases of emergency power shortages. Through simulation-based experiments on the IEEE 30-bus system, the findings of this study unequivocally demonstrate that the financial viability of wind power plants within integrated clusters exceeds that of their standalone economic operations.**

Keywords—Wind Farm, Electricity Market, Uncertain, Generation Expansion Plan

I. INTRODUCTION

Renewable energy has recently been rapidly emerging and developing globally, particularly in medium and large-scale wind farms [1]. The approximate growth rate of around 10% during 2017-2018 represents an unprecedented and unpredictable pace of expansion [2]. The 2022 energy crisis in Europe underscored the vital role of energy in economic and social development, as the economies of developed nations faced severe repercussions due to volatile energy conditions. The rise in prices of essential commodities highlighted the risks associated with dependency on fossil fuels. Consequently, Nations globally have concentrated on advancing renewable energy sources to diminish dependence on fossil fuels, with wind energy assuming a pivotal role [3]. Furthermore, the increasing proportion of wind energy holds promising environmental benefits [4, 5].

Incentives for renewable energy have been limited in many regions lately, despite their previous efforts to promote sustainable energy sources. Wind power investment nowadays has the potential to yield favorable financial returns for investors while also engaging in business transactions of buying and selling their products on equal terms with traditional energy sources. Participating in competitive electricity markets has become a new trend in the European electricity market [6].

However, the primary drawback of wind power, when integrated into the real-time dynamics of the electricity market, is its inherent uncertainty. This uncertainty poses a significant barrier to wind energy's equal and unrestricted participation in competitive electricity markets. Several research endeavors have delved into examining the influence of wind power on the electricity grid and the consequences stemming from its inherent uncertainty [7]. Several proposed methods aim to reduce costs related to energy imbalances through market participation [8]. Conversely, some contend that transactions in the electricity market contribute to system improvement by reducing prices and aligning market volume through the system's inherent flexibility [9].

In conclusion, uncertainty's ramifications on the economic and technical aspects of the power system are intricate and challenging to determine with certainty [10, 11, 12]. Integrating uncertain wind power sources into the competitive electricity market presents significant hurdles and is subject to various unpredictable factors. Unlike investments in conventional power sources, where the benefits are readily apparent for investors and society, wind power demands substantial financial resources with uncertain economic efficiency for investors and ambiguous impacts on energy management agencies and the community.

This study delves into the assessment of wind power's impact on investment financials, aiming to develop financial operating methods that mitigate the influence of uncertainty. Specifically, while individual wind turbines may be affected by varying weather conditions, the collective operation of multiple turbines can reduce the extent of such impacts. While a single wind farm may not benefit its owner considerably, the synergy of numerous wind farms can generate more substantial advantages. Moreover, utilizing the Weibull probability density function (PDF) in evaluating and analyzing wind speed enables a more precise estimation of wind power generation for the electricity market. This improvement in wind power prediction reduces uncertainty for investors, thus mitigating unforeseen consequences.

Three wind power scenarios were simulated using the IEEE 30-BUS system to demonstrate the effectiveness of these analyses. The results indicate a significant reduction in the impact of uncertainty on investors when integrated into a more diverse financial community. Wind energy revenue also increases with their integration into the electricity market, highlighting the more significant influence when the market's compensation level is higher.

The main contributions of this paper are as follows:

- Investigation and assessment of the degree of uncertainty's impact on different financial strategies of wind power.
- Conducting a comparative financial analysis of autonomous and integrated wind power scenarios and

2023 Asia Meeting on Environment and Electrical Engineering (EEE-AM) | 979-8-3503-8106-1/23/$31.00 ©2023 IEEE | DOI: 10.1109/EEE-AM58328.2023.10395263

proposing customized strategies for wind plant integration in the electricity market.

- Providing practical test cases of wind power operation scenarios on the standard IEEE 30-BUS power system, detailed in this study.

II. Mathematical Model

A. Wind Power Model

Wind farms have two revenue components: direct revenue and uncertain revenue [10]. The direct revenue is generated by selling electricity according to the scheduled direct bidding on the electricity market, selling the amount of wind power predicted in advance. On the other hand, the uncertain revenue includes two components: revenue from selling excess energy beyond the initial prediction and compensation (or penalty) costs incurred due to energy shortfall compared to the initial forecast.

$$R_w(P_w) = \sum R_{w,i} = \sum\left[R_{ws,i}\left(P_{ws,i}\right) + R_{wu,i}\left(\Delta P_{w,i}\right)\right] \quad (1)$$

$$\Delta P_{w,i} = P_{wav,i} - P_{ws,i}$$

In this context, P_w represents the aggregate wind power distributed in the electricity market, while $R_{ws,i}$, $R_{wu,i}$, and $R_{w,i}$ denote the direct, uncertain, and cumulative revenue, respectively. Additionally, $P_{ws,i}$ correspond to the projected power and $\Delta P_{w,i}$ is the deviation between the bidding and actual power.

1) Direct revenue

The wind farm indexed as i generates revenue directly based on the forecasted wind energy output and its contribution to the electricity market, as determined by the formula (1), where g_i represents the coefficient associated with direct costs.

$$R_{ws,i}\left(P_{ws,i}\right) = g_i P_{ws,i} \quad (2)$$

The coefficient g_i for electricity selling prices and the proposed electricity production plan P_{ws} in the electricity market are two influential factors directly contributing to revenue. Rational electricity production results from wind energy predictions based on wind speed, while the coefficient g_i is proportional to the average selling price in the market. Accordingly, this electricity selling price coefficient is often influenced by large-capacity power sources, which are the sources that can provide stable electricity to the power system. For example, within the European Union energy market, wind power pricing is incorporated into the thermal electricity price coefficient, underscoring the substantial contribution of wind energy.

$$C_{T0}(P_{TG}) = \sum_{i=1}^{N_{TG}}\left(a_i + b_i P_{TG,i} + c_i P_{TG,i}^2\right) \quad (3)$$

$$\lambda_{TG,i} = b_i + c_i P_{TG,i} \quad (4)$$

$$g = \overline{\lambda_{TG}} = \frac{\sum_{i=1}^{N_{TG}} \lambda_{TG,i}}{P_{TG}} \quad (5)$$

The cost coefficients of thermal plants, a_i, b_i, and c_i, for producing the output power $P_{TG,i}$. Besize, $\lambda_{TG,i}$ signifies the thermal unit price, while $\overline{\lambda_{TG}}$ represents the mean price.

2) Uncertain cost

The second element in equation (1)denotes unpredictable revenue, encompassing a blend of revenue and cost components. The revenue is generated through the sale of reserve energy; on the other hand, the cost component involves expenses incurred by compensation, and equation (6) expresses the uncertain revenue.

$$R_{wu,i}\left(\Delta P_{w,i}\right) = \begin{cases} R_{Rw,i}\left(\Delta P_{w,i}\right), & if\ P_{wav,i} \geq P_{ws,i} \\ C_{Pw,i}\left(\Delta P_{w,i}\right), & if\ P_{wav,i} \leq P_{ws,i} \end{cases} \quad (6)$$

Here, $R_{Rw,i}$ and $C_{Pw,i}$ present the revenue from selling reserve power and the compensation cost under the plan of bidding power. Reserve income is defined as,

$$R_{Rw,i}\left(\Delta P_{w,i}\right) = k_{R,i} g_i \left(P_{wav,i} - P_{ws,i}\right)$$

$$= k_{R,i} g_i \int_{P_{ws,i}}^{P_{wr,i}} \left(p_{w,i} - P_{ws,i}\right) f_w\left(p_{w,i}\right) dp_{w,i} \quad (7)$$

And the compensation is,

$$C_{Pw,i}\left(\Delta P_{w,i}\right) = k_{P,i} g_i \left(P_{wav,i} - P_{ws,i}\right)$$

$$= k_{P,i} g_i \int_{0}^{P_{ws,i}} \left(p_{w,i} - P_{ws,i}\right) f_w\left(p_{w,i}\right) dp_{w,i} \quad (8)$$

$k_{R,i}$ và $k_{P,i}$ present the reserve and compensation/penalty coefficient on the wind power plant. $f_w\left(p_{w,i}\right)$ is the wind power PDF for the wind power plant. $P_{wav,i}$ và $P_{wr,i}$ are the actual available and rated output power from the same plant.

B. Weibull Model

The two-parameter Weibull distribution is widely employed in numerous studies related to wind power production. According to Document [13], this model is commonly utilized to represent the probability distribution of wind speed, and it is expressed as follows:

$$f(v) = \left(\frac{k}{c}\right)\left(\frac{v}{c}\right)^{k-1} e^{-\left(\frac{v}{c}\right)^k} \quad (9)$$

$$P_w = \begin{cases} 0.0, & v > v_o\ and\ v < v_u \\ P_{wr}\left(\frac{v - v_u}{v_r - v_u}\right), & v_r \geq v \geq v_u \\ P_{wr}, & v_o \geq v > v_r \end{cases} \quad (10)$$

The curve's shape in equation (9) is determined by the dimensionless factor *k*, known as the shape factor, with parameter *c* representing the scale in m/s. Variations in the values of *k* and *c* yield different forms of distributions. The wind speed, denoted by *v*, is governed by the Weibull PDF parameters *c* and *k*. The wind output power is derived from [10], with the rated power, P_{wr}, and the wind speed of rated, cut-in, and cut-out are respective, v_r, v_u, and v_o.

Fig. 1 illustrates two wind turbines in different locations and with identical specifications in TABLE II. This figure shows two distinct regions of a sudden increase in probability, specifically in the low wind speed boundaries. The turbine remains inactive below the threshold wind speed (v_{in}), resulting in zero electricity output for wind speeds ranging from zero to v_{in}. On the other hand, when the wind speed exceeds v_{out}, the turbine's power output cannot exceed

its allowable power, leading to the cumulative probability of wind speeds greater than v_{out} resulting in the corresponding rated power output of the turbine.

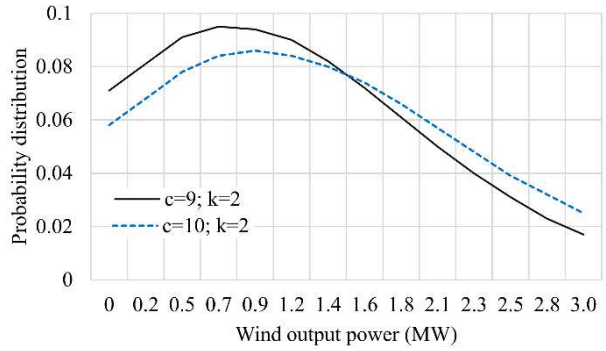

Fig. 1. Wind power probability distribution

C. Objective Function

The primary objective outlined at the outset of this research is to focus on the financial efficiency of wind energy investments. The income from wind power comprises two essential components: direct revenue and the sale of excess energy. Conversely, compensatory measures encompass the costs associated with inaccurate forecasting in the electricity market. These essential expressions have been explicitly presented in equation (1) and further elaborated upon in equations (2)-(4),

$$maximize\ \{F = R_w(P_w)\} \tag{11}$$

Calculating and analyzing the results in the steps is shown in the flowchart at Fig. 2.

III. Developing Experimental Scenarios

This study examines three proposed scenarios as follows: (i) Single turbine scenario (STS): A standalone wind turbine is independently invested in and participates in electricity sales. This approach is impractical due to its inefficiency; (ii) Multiple-turbine wind farm scenario (MTS): This traditional scenario involves numerous wind turbines comprising government support and investments; (iii) Integrated multiple wind farm scenario (MWS): There are instances of commercial integration that can yield mutual benefits for all parties involved.

A. STS scenario

A fundamental electricity market with various energy sources, including wind power. In this case, the wind power source consists of only one turbine invested at a suitable location. Let's assume the wind turbine has specific technical parameters and is installed at a place with Weibull data, as mentioned in Gen 1. The Weibull PDF of the turbine is illustrated in Fig. 1; the revenue is determined by equation (1).

B. MTS scenario

In this scenario, the electricity market still considers the wind power source as a participant in selling electricity, similar to the STS scenario. However, the wind power source itself consists of multiple wind turbines. Each turbine has similar power generation characteristics since they are located close to each other. Thus, the composite probability distribution of the set of turbines is determined as follows,

$$PDF_{\mathrm{F}}(P_t) = \prod_{i=1}^{N_T} PDF_{T,i}(P_{t,i}) \tag{12}$$

$$P_F = \sum_{i=1}^{N_T} P_{t,i} \tag{13}$$

In which, PDF_{F} and P_F represent the probability distribution and output power of the combination of wind farm turbines. PDF_T and P_{t} denote the total wind power. The variable i ranges from 0 to the maximum number of turbines in the farm, N_T, representing the index of each turbine. The composite PDF is established based on the variation of the index i for each turbine independently. The computation method for wind farm revenue follows a similar approach to the previous model, with the distinction that it involves aggregating probability density functions from turbines within the same cluster.

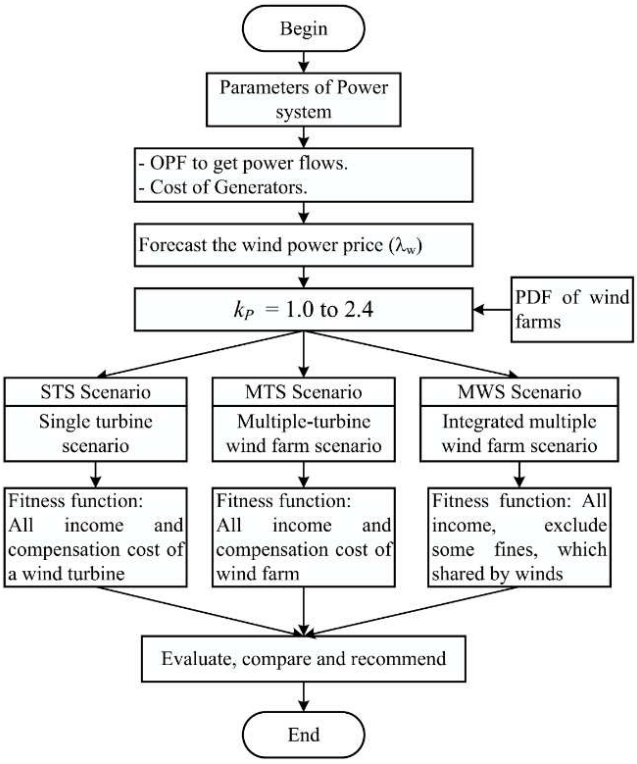

Fig. 2. Flowchart Model

C. MWS scenario

The wind farms may belong to the same or different owners, following a certain principle in electricity business transactions, integration is necessary to ensure mitigated consequences of uncertainties and to bring optimal benefits to all market participants.

Unlike the MTS scenario, each wind farm has a distinct characteristic PDF as it is constructed in different locations. And creating a virtual wind farm, the combined PDF method is similar (12) and (13).

IV. IV. Simulation Results

The proposed scenarios have been assessed using the IEEE 30 bus RTS system. This system consists of thirty buses, forty-one branches, and six sources, and its grid parameters have been sourced from references [14, 15]. Four thermal power plants are situated at buses 1, 2, 8, and 13, as detailed in TABLE I; and tow wind farms at buses 5 and 11. There are 25 turbines on bus 5, with a combined power of

75MW, and 20 turbines on bus 11, with a total power of 60MW. The wind speed predictions for these farms are obtained using the Weibull two-parameter distribution in TABLE II.

TABLE I. PARAMETER OF THERMAL GENERATORS

Generator		Gen 1	Gen 2	Gen 3
Bus		1	2	8
Cost ratios	*a*	0	0	0
	b	2	1.75	3.25
	c	0.00375	0.0175	0.00834

TABLE II. PARAMETER OF WIND POWER

Bus		5	11
Wind power generation plants	*No. of turbines*	25	20
	Rate power, P_{wr}(MW)	75	60
	Weibull PDF parameter	c=9, k=2	c=10, k=2
	Weibull mean, M_{wbl}	v=7.976m/s	v=8.862m/s
Turbine	P_{wr}= 3MW, v_u=3m/s; v_r=16m/s and v_o=25m/s		

The selling price of wind power is determined at approximately 2.42-2.8 $/MWh, derived from calculating the average electricity generation cost of thermal power sources under the assumption that thermal energy predominates in the electricity market. For the excess selling price of electricity, it is assumed not to be considered. In contrast, the compensatory electricity price is determined based on the multiplier *k* with the dimensions 1.0-2.4.

A. STS Scenario

A 3MW wind turbine is installed at bus 5 of the system. The PDF distribution according to Gen 1 in Fig. 1 is applied. The highest probability is determined at 7m/s, as shown in (10), corresponding to a turbine power output of approximately 0.7MW, as illustrated in Fig. 3. Turbine revenue results are given in TABLE III.

TABLE III. TURBINE REVENUE

k	1.0	1.2	1.4	1.6	1.8	2.0	2.2	2.4
Revenue	2.6	2.1	1.5	0.9	0.4	-0.2	-0.7	-1.3

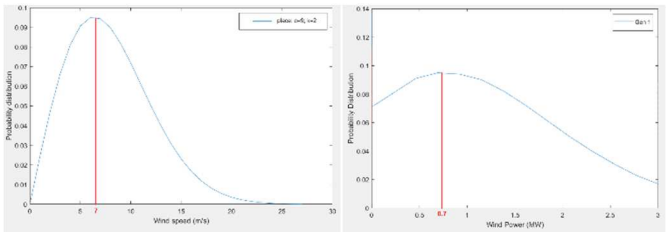

Fig. 3. PDF of turbine

With the results mentioned above, the wind turbine revenue decreases consistently as the compensation ratio increases, can be understood because as the compensation ratio rises, even though the probability of electricity shortfall remains constant, the cost of compensation increases, leading to a general decrease in wind power owner's revenue. The revenue will become negative at a certain compensation ratio, implying that wind power owners no longer benefit and no longer desire to invest in wind power projects, which will become more evident in the wind farm scenario.

B. MTS Scenario

This scenario considers a complete wind farm at bus 5 of the IEEE 30-bus power system. PDF was assembled from 25 turbines on the farm, resulting in Fig. 4, with a peak slightly shifted towards the lower power output, around 30-32MW.

The revenue of wind generators at Bus-5, presented in Fig. 5, exhibits variation across different power regions. The cash flow demonstrates an almost linear increase when the power output is below 25MW, while it experiences a nearly linear decline for power outputs exceeding 40MW. Notably, the revenue peaks within the range of 30 to 40MW, closely associated with the compensation scale. The compensation factor influences these changes in revenue.

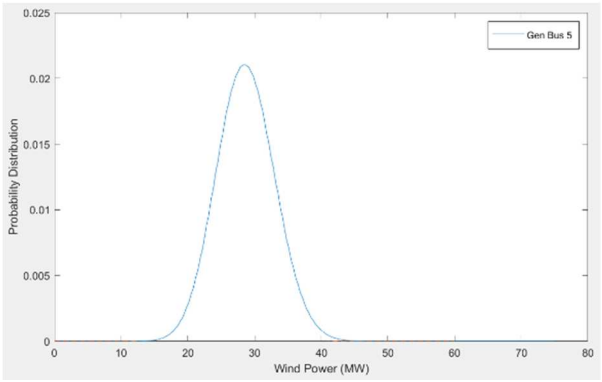

Fig. 4. PDF of the wind farm on bus 5

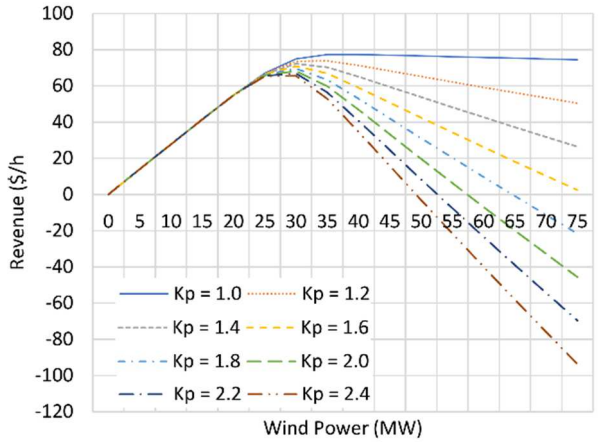

Fig. 5. Revenue of wind farm at bus 5

C. MWS Scenario

In this research, we investigate the integration of two distinct wind farms situated on buses 5 and 11. The main focus is to explore the potential benefits of allowing these wind power plants to exchange their generated electricity in the electricity market, aiming to mitigate the adverse effects of wind power fluctuations. The PDF of the virtual wind power source, resulting from the combination of these two wind farms, is represented by a specific curve, Fig. 6. The PDF obtained from the integrated model demonstrates characteristics of a similar shape, featuring a slightly lower peak and smoother slopes compared to previous scenarios.

To assess the economic implications of this integration, we analyze the revenue outcomes for the wind farm located at bus 5 compared to a scenario where integration with other wind farms is not considered, as depicted in Fig. 7.

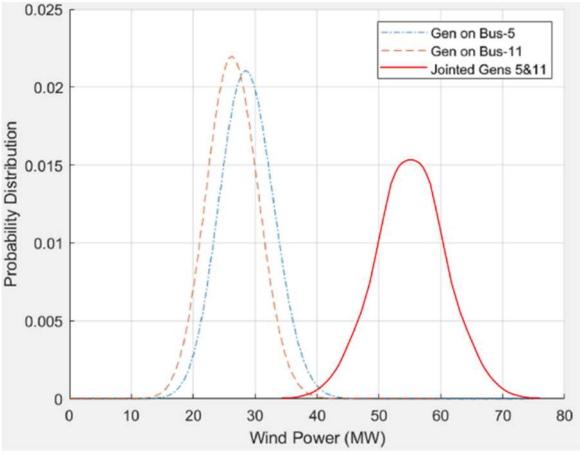

Fig. 6. PDF of wind farm at bus 5 and bus 11

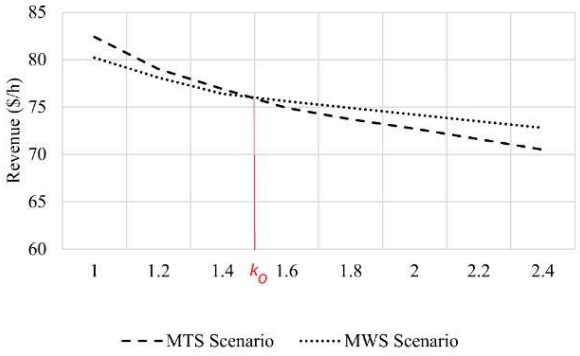

Fig. 7. Comparision of revenue MTS and MWS scenario

V. DISCUSS

The bidding behavior of wind farms changes when they are integrated. In a conventional setup, each wind farm bids the electricity output based on its wind speed forecasts, aiming to maximize its benefits. However, due to uncertainty, they tend to select cautious bidding plans with lower electricity output than the forecast to avoid compensation situations. This trend shows that the offered output power decreases as the compensation level increases. On the other hand, relaxing constraints reduces the risk of penalties for scenarios with integration between different wind power sources, making wind power owners more comfortable bidding higher electricity output in the market. As illustrated in Fig. 8, an increase in compensation levels leads to a declining trend in bidding output power. However, the trend stabilizes, yielding higher values compared to previous scenarios. This suggests a positive shift in the behavior of wind power owners, as they offer increased electricity output.

The research highlights the significance of integrating wind power farms and the potential for collaboration among them within the competitive electricity market and provides valuable insights for policymakers and investors, enabling effective planning and investment in wind energy projects. Consequently, this contributes to leveraging renewable energy sources to promote sustainable development.

The study emphasizes the significance of integrating wind power sources and highlights the potential for cooperation among wind farms in the competitive electricity market. This research provides valuable insights for policymakers and investors to plan and invest in wind energy projects effectively, thereby harnessing renewable energy sources to promote sustainable development.

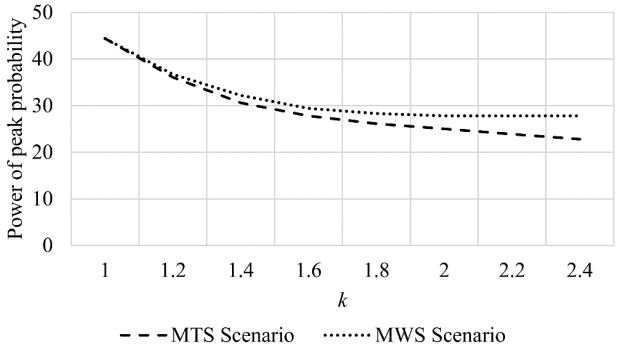

Fig. 8. Comparison of revenue MTS and MWS scenario

VI. CONCLUSION

In conclusion, this paper has introduced a method based on mathematical uncertainty in wind energy to analyze and evaluate the advantages for wind farm investors operating in an uncertain, competitive electricity market. Through tests involving three wind power revenue determination scenarios, the study has demonstrated that collaborative integration of wind turbines and wind farms can substantially enhance efficiency and benefits for wind plant investors. The integration scale is directly proportional to the magnitude of the benefits obtained from these partnerships.

Integrating the wind farm at bus 11 with the wind farm at bus 5 in the IEEE 30-Bus system yielded an approximate 4-5% increase in revenue. Although this increment may seem modest in isolation, its significance becomes apparent when viewed within the broader context of the entire investment cycle, spanning 20-25 years. This outcome holds promise for heightened wind power benefits accruing to investors.

To summarize, this study presents a valuable method for optimizing wind power investment amidst energy market uncertainty, emphasizing the importance of strategic cooperation and appropriate compensation policies to maximize efficiency and benefits from wind farm owners. These findings provide valuable insights for wind energy investors, policymakers, and stakeholders to make informed decisions and foster the development of sustainable and efficient wind power projects.

REFERENCES

[1] "Renewables 2021 - Global status report," International Energy Agency (IEA), Paris, France, 2021.

[2] D. Cao, W. Hu, X. Xu, T. Dragičević, Q. Huang, Z. Liu, Z. Chen and F. Blabjerg, "Bidding strategy for trading wind energy and purchasing reserve of wind power producer – A DRL based approach," *Electrical Power & Energy Systems,* vol. 117, p. 105648, 2020.

[3] T. J. Hammons, "Integrating renewable energy sources into European grids," *Electrical Power & Energy Systems,* vol. 30, no. 8, pp. 462-475, 2008.

[4] N. Wang, J. Li, W. Hu, B. Zhang, Q. Huang and Z. Chen, "Optimal reactive power dispatch of a full-scale converter based wind farm

considering loss minimization," *Renewable Energy,* vol. 139, pp. 292-301, 2019.

[5] J. Li, N. Wang, D. Zhou, W. Hu, Q. Huang, Z. Chen and F. Blaabjerg, "Optimal reactive power dispatch of permanent magnet synchronous generator-based wind farm considering levelised production cost minimisation," *Renewable Energy,* vol. 145, pp. 1-12, 2020.

[6] "Energy Prices and Costs in Europe: Report from the commission to the european parliament, the council, the european economic and social committee and the committee of the regions," European Commssion, Brussels, 2020.

[7] P. Shinde and M. Amelin, "A Literature Review of Intraday Electricity Markets and Prices," *IEEE Milan PowerTech,* p. 18938508, 2019.

[8] H. Holttinen, "Handling of wind power forecast errors in the Nordic power market," *International Conference on Probabilistic Methods Applied to Power Systems,* p. 9475028, 2006.

[9] J. Dobschinski, E. D. Pascalis, A. Wessel, L. v. Bremen, B. Lange, K. Rohrig, Y.-M. S. Drenan, I. Fraunhofer, O. ForWind and a. E. Germany, "The potential of advanced shortest-term forecasts and dynamic prediction intervals for reducing the wind power induced reserve requirements," *Scientific Proceedings of the European Wind Power Conference,* p. 177–182, 2010.

[10] P. P. Biswas, P. N. Suganthan and G. A. J. Amaratunga, "Optimal power flow solutions incorporating stochastic wind and solar power," *Energy Conversion and Management,* vol. 148, pp. 1194-1207, 2017.

[11] K. Abaci and V. Yamacli, "Differential search algorithm for solving multi-objective optimal power flow problem," *International Journal of Electrical Power & Energy Systems,* vol. 79, pp. 1-10, 2016.

[12] N. Daryani, M. T. Hagh and S. Teimourzadeh, "Adaptive group search optimization algorithm for multi-objective optimal power flow problem," *Applied Soft Computing,* vol. 38, pp. 1012-1024, 2016.

[13] P. Wais, "A review of Weibull functions in wind sector," *Renewable and Sustainable Energy Reviews,* vol. 70, pp. 1099-1107, 2017.

[14] O. Alsac and B. Stott, "Optimal Load Flow with Steady-State Security," *IEEE Transactions on Power Apparatus and Systems,* Vols. PAS-93, no. 3, pp. 745-751, 1974.

[15] R. Ferrero, S. Shahidehpour and V. Ramesh, "Transaction analysis in deregulated power systems using game theory," *IEEE Transactions on Power Systems,* vol. 12, no. 3, pp. 1340-1347, 1997.

Enhancing Total Transfer Capability via Optimal Location of Energy Storage Systems Using a Hybrid Improved Min-Cut Algorithm and Genetic Algorithm

Tung Linh Nguyen[1], Ngoc Sang Dinh[2], Viet Anh Truong[3], Thanh Long Duong[4], Dao Huy Du[5(✉)], and Do Anh Tuan[6]

[1] Hochiminh City, Vietnam
linhnt@epu.edu.vn
[2] Hochiminh University of Architecture, Hochiminh City, Vietnam
[3] Hochiminh University of Technology and Education, Hochiminh City, Vietnam
[4] Industrial University of Hochiminh City, Hochiminh City, Vietnam
[5] Thai Nguyen University of Technology, Thai Nguyen Province, Vietnam
daohuydu@tnut.edu.vn
[6] Chau Industrial Techonology Joint Stock Company, Ha Noi, Vietnam

Abstract. This paper proposes a new optimal approach to determine the location and size of the Energy Storage System (ESS) in transmission expansion planning (TEP). The proposed method combines two steps in sequence: the improved Min-Cut algorithm (IMCA) and the Genetic Algorithm (GA) algorithm to reduce the search space and time for finding the optimal solution satisfying many constraints. This algorithm reduces the computational volume significantly compared to previous algorithms and thereby shortens the calculation time leading to investors making timely and competitive ESS system investment decisions. The research results are applied in determining the position of the ESS in the IEEE 24-bus system, which shows the possibility of a solution to the TEP problem.

Keywords: TEP · Energy storage systems · Min-cut algorithm · Genetic algorithm

1 Introduction

In the problem of electricity system development planning, there are many problems with planning for transmission expansion to achieve one or more specific goals. Among them, efficiency optimization is considered one of the essential planning stages. Therefore, critical planning solutions such as Transmission Line Expansion Planning (TEP), Generation Expansion Planning (GEP) has been studied extensively in [1, 2].

TEP is still a vital solution for solving planning problems in the long run. Still, it is not always a perfect solution to solve overload and congestion to achieve stability and reliability [3]. The common disadvantage of TEP solutions is that they are expensive

D. C. Nguyen et al. (Eds.): ICERA 2022, LNNS 602, pp. 512–524, 2023.
https://doi.org/10.1007/978-3-031-22200-9_57

or have limitations on the number of additional towlines, constraints on the number of lines per pole, or the cost of building a new towline. In this case, more powerful and economical methods are often used to improve the system, such as restructuring the power grid for the existing power source [4], controlling the power flow using FACTS [5], or solutions to build new renewable energy sources [6, 7]. However, these methods have pros and cons to varying degrees, and they are not perfectly interchangeable.

In recent years, the development of renewable energy sources is gradually replacing fossil energies. The energy from solar and wind has developed rapidly in many countries worldwide [6, 7].

The characteristic of these energy sources is that they cannot be controlled according to the operator commands but depend on natural conditions at each time. Therefore, when the electricity demand is lower than generating capacity, the energy transmitted to the grid affects the security of the power system. In contrast, when electricity demand is high at a time when the renewable energy plant is not generating electricity. For controlling these power sources, one of the solutions is to use ESS in the power system. The ESS will store the excess energy on the grid and transmit it back to the grid at the request of the dispatcher to satisfy goals [1, 8].

Types of ESS sources are pretty flexible in construction but could redistribute the power flow on the system to reduce the load on the part of the power transmission system at the required location. However, like the fundamental problem of power system planning, the issues of concern are determining the location and capacity of the necessary ESSs to be installed on the power system, also known as the optimal problem when TEP incorporates an energy storage system (ESSTEP).

The organization of the paper consists of six parts as follows. Part 1 introduces. Part 2 introduces the theory of methods to solve the TEP problem and proposes a new model to solve the ESSTEP programming problem. Part 3 Details IMCA algorithm and its application in the search space reduction method in an optimization problem. Part 4 mathematical optimization model to solve the ESSTEP programming problem. Part 5 experiments on IEEE-RTS 24-bus system and gives discussion results. Section 6 offers some concluding remarks.

2 ESSTEP Problem

In TEP planning, the optimization problem is one of the most important to be solved to meet the operator's goals. In studies on TEP, the many different models and algorithms to solve optimization problems have been mentioned as AC and DC mathematical models, meta-heuristic algorithms PSO, GA [2].

In the long-term options, the solution to expand the transmission line is one of the more suitable options. However, this solution's investment loss is relatively significant compared with other aggressive solutions, such as using FACTs or ESS in the short term [3, 5].

Active power sources such as ESS can also provide electricity when the power system is congested at peak load and ensure stable operation of the power system without expanding the transmission power system. Moreover, ESS also enhances the system's transmission capacity by injecting more power into the grid to reduce congestion and pressure on existing power sources, ensuring the security of the power system [3, 4].

In the recent commercial market with different energy storage technologies, the battery is still the most popular storage device today [4]. In addition, to solve the problem of short-term capacity shortage, there are other types of technologies such as flywheels, supercapacitors. Energy storage by Hydrogen, compressed air are technologies with larger capacity, and higher energy storage capacity, so it is more flexible in the power system. Specific application conditions corresponding to each type of technology are classified as shown in Fig. 1.

As stated in the introduction, when planning TEP, it is also necessary to consider the issue of incorporating ESSTEP. The weaknesses in the ESS are also the weaknesses of ESSTEP. Therefore, recent studies have developed large-capacity, high-performance ESS tools in response speed and efficiency to solve the TEP problem [5]. Various methods and models have been proposed in the literature in this field to solve the difficulties mentioned above of the TEP planning problem. The models and techniques can be organized as follows:

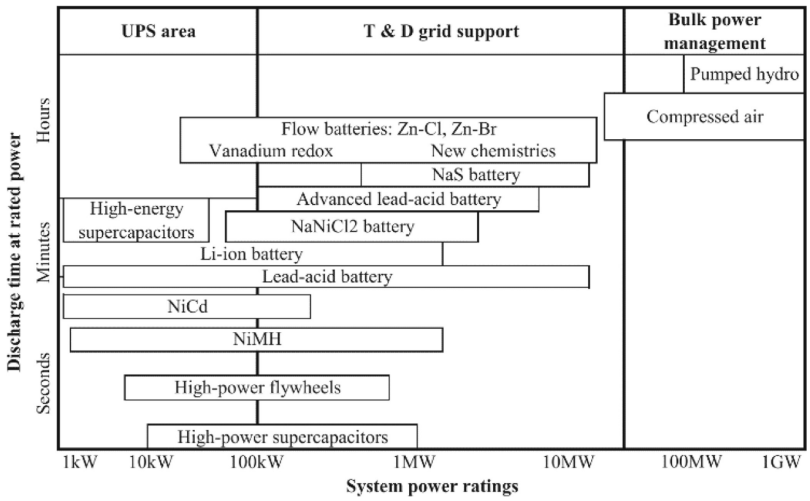

Fig. 1. Classification of ESSs [6]

Classical Optimization Algorithm: A commonly used analytic technique, and the results are often optimal global solutions to the universal version of the initial integer problem, where the initial data are integers, which are replaced by continuous variables. The computational loads in these algorithms are often huge. Thus there are many obstacles to solving extensive programming problems for medium and large power systems, like most real power systems. In addition, this method can interfere with the convergence problem in some cases, as in [6, 7].

Application of the minimum cross-sectional algorithm (MCA): different from other algorithms, this algorithm always gives precise results, and the computational volume is relatively low, so some studies use it to find the position of the minimum cross-section. Optimal placement of FACTS installations [5, 8], solving bottlenecks in the power

system [8], as well as studies on stability and reliability in transmission expansion planning [9, 10].

Meta-heuristics Algorithms: These algorithms are inspired by optimizations in natural laws. They are extended to specific search procedures and can be used in almost any case, and this is a particularly suitable solution for complex problems with many uncertain constraints. Algorithms are often used to determine optimal or non-optimal results of general issues, even for correspondingly large systems involving enormous computational efforts [11].

Despite many advantages, the convergence probability and large computational volume of meta-heuristic algorithms are concerns of researchers, and this is an opportunity to propose applying a hybrid method to overcome this problem. The defects in solving optimization problems in TEP are presented in this paper; this hybridization leads to a two-stage matching algorithm. First, improve the MCA algorithm to fit the objective of the optimization problem, which is known as "limited search space. "The later stage, called "Optimization of the Solution," uses a genetic algorithm (GA) to find the optimal global result in the reduced space of the previous stage. This process is perfectly designed to overcome the disadvantage of the meta-heuristic algorithm as mentioned above.

3 MCA Algorithm

3.1 Basic MCA Algorithm

In the 1950s, the problem of finding congestion of an undirected graph was proposed by Ford and Fulkerson by determining the smallest slice of that undirected graph. This solution is the premise for the MCA algorithm. Mechtild Stoer and Frank Wagner developed this algorithm to apply it to computer programs in 1997 and called it the Min-Cut algorithm [12]. This model is also used to determine the optimal location of TCSC to solve the problem of congestion in the power system [5]. The basic MCA algorithm flowchart is shown in Fig. 2.

Subject to:
a matrix (n x n) of magnitude total [A] (this case power per capacity of lines).
n is the number of nodes.
$\sum sj = \sum a_{sj}$, $\sum jt = \sum a_{jt}$ - magnitude total with generators, loads of i cut and j branch.
S(i), T(i) - i cut with generators, loads.
u, v - buses.
{s}, {t} - set of nodes generators, loads.
MC(i) - mincut step i.
MF - maxflow.

3.2 Improved MCA Algorithm

The traditional MCA algorithm mentioned above is limited because it does not include the distributed power flow on the transmission line, which leads to inadequate implementation of problem-solving objectives, such as when choosing a branch. In the minimum

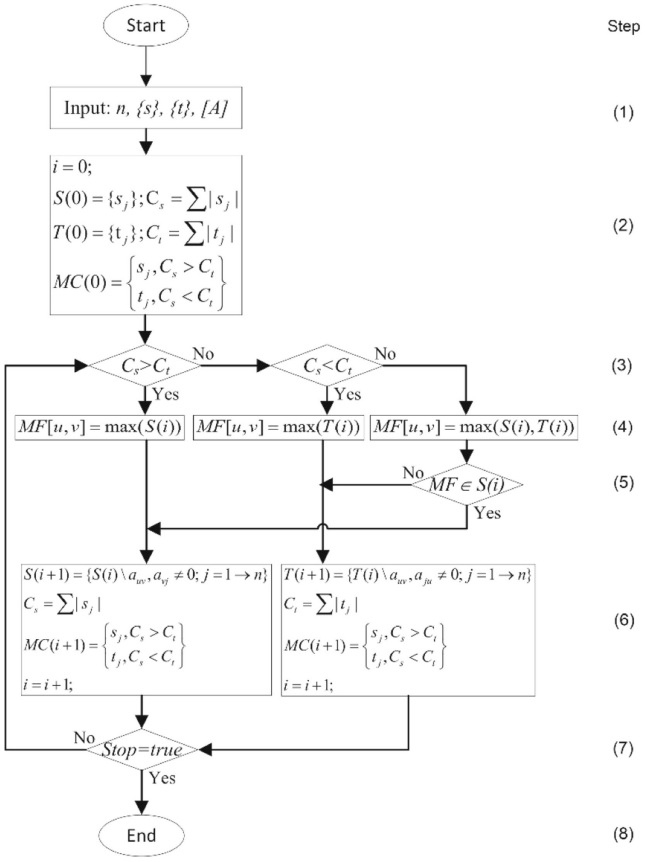

Fig. 2. Base MCA algorithm [5]

cut to solve congestion problems, transmission lines with large power distribution can be ignored while these are critical locations that need to overcome congestion. Adding branches with more significant power distribution to min-cut is an improvement of the MCA algorithm to overcome the shortcomings of traditional MCA, which is proposed in this paper.

The power flow distribution is the first step added to the Fig. 2 flowchart to check for congested branches in the power system. When any branch is overloaded (congestion) due to a high-power flow, it should be taken to update to the min-cut set during algorithm execution.

Steps 6 and 2 of the added flowchart

$$s_j(new) = s_j + K_j$$

$$t_j(new) = t_j + K_j$$

$$\left[P_{flow}\right] = runopf\,(sys)$$

Importance,

$$K_j = \gamma\left(1 - \frac{P_{flow(j)}}{P_{rate(j)}}\right)$$

γ is an essential factor in this improvement. The value of γ is chosen according to the contribution of power flow per branch. With the updates mentioned above compared to the basic MCA algorithm, each branch is checked for power flow. The result is the minimum possible cross-sectional set, including the units in the congested area in the power system.

4 ESSTEP Mathematical Model

4.1 Function Fitness

Several recent studies on power system expansion planning have considered the installation of ESS. However, it is not yet widespread in the commercial market because the investment capital of ESS is still relatively high in the market [13]. Therefore, the problem of optimizing the location and capacity of ESSs in the TEP planning to achieve a reasonable cost when investing in a new ESS and the cost of operating efficient power sources is expressed by the following objective function:

$$\text{minimize } C^T = \sum_i C_i^T + \sum_j C_j^{ESS}. \tag{1}$$

Subject to,

- C_i^T – generation cost of i source and calculated by:

$$C_i^T = \sum_{i \in G} c_i(t).A_i(t) \tag{2}$$

- C_j^{ESS} – investment cost of j ESS and calculated by:

$$C_j^{ESS} = \sum_{i \in G_{ess}} P_i^{ess}.c_{ess} + C_0 \tag{3}$$

With constrantion as.

- $P_{Gi} - P_{Di} - \sum_{j \in bus} V_i V_j (G_{ij} \cos \delta_{ij} + B_{ij} \sin \delta_{ij}) = 0$.(4)
- $Q_{Gi} - Q_{Di} - \sum_{j \in bus} V_i V_j (G_{ij} \sin \delta_{ij} + B_{ij} \cos \delta_{ij}) = 0$. (5)
- $V_{i \in bus}^{\min} \leq V_{i \in bus} \leq V_{i \in bus}^{\max}$.(6)
- $S_{i \in branch} \leq S_{i \in branch}^{\max}$.(7)
- Location of ESSs $\in$ mincut(8)

With,
c_{ess} – ESSs Fun investment.
C_0 – an rate of ESSs cost.

t – An evaluation cycle (years).
$c_i(t)$ – i generation cost in t cycle.
$A_i(t)$ – i generation energy in t cycle.
P_i^{ess} – i ESS capacity.
$P_{Gi}, Q_{Gi}, P_{Di}, Q_{Di}$ – Power of generator and load.
$S_{i\in branch}^{\max}$ – Capacity of i branch.
δ_{ij} – Voltage angle.
$V_{i\in bus}^{\min}, V_{i\in bus}^{\max}$ – Min and max voltage.

4.2 IMCA—GA Two Steps Algorithm

The optimization problem (1) with many solved methods has been studied previously using heuristic, meta-heuristic algorithms, or mathematics [2]. The advantages and disadvantages of each method are not the same, but all the problems scientists and planners are most interested in are related to finding the global extreme of the fastest problem, especially for large power systems.

Among the more recently used algorithms, GA is a standard method used in TEP programming to solve the dark problem. However, its characteristic is that computation is too large in some systems like most other meta-heuristic methods, and sometimes problem results can be trapped in local extremes.

Therefore, this paper proposes a two-stage combination between IMCA, an improved MCA algorithm, and a GA algorithm to enhance the problem of computational volume and local extremes of the GA algorithm, as mentioned.

The diagram in Fig. 3 depicts the hybrid problem as mentioned above in a five-step sequence:

(1) Current capacity trend distribution of the operating power system.
(2) Use the IMCA algorithm in this paper to find the minimum cross-section set.
(3) Determine the minimum cross-sectional search space defined in step 2.
(4) Solve the optimization problem (1) by GA algorithm with the limit in space in step 3.
(5) Finally, the position and capacity of the ESSs.

5 24-Bus IEEE Test

They are using a standard IEEE RTS 24-bus power system to check the feasibility of the proposed method in this paper. This system consists of 36 branches and 10 power sources, and the data of this power system can be found in documents [14, 15], summarized in Fig. 4.

According to the survey time, it is assumed that the power load capacity and power source increase equally at all nodes. When the ratio increased to 160% of the standard capacity (4,560MW and 5,448MW respectively according to Tables 1 and 2), the system started to become congested at branches 6–10 and 7–8.

The power flow in step 1 (according to 4.2) is calculated using Matpower 6.0 software according to the system data in this case and using the IMCA algorithm to determine

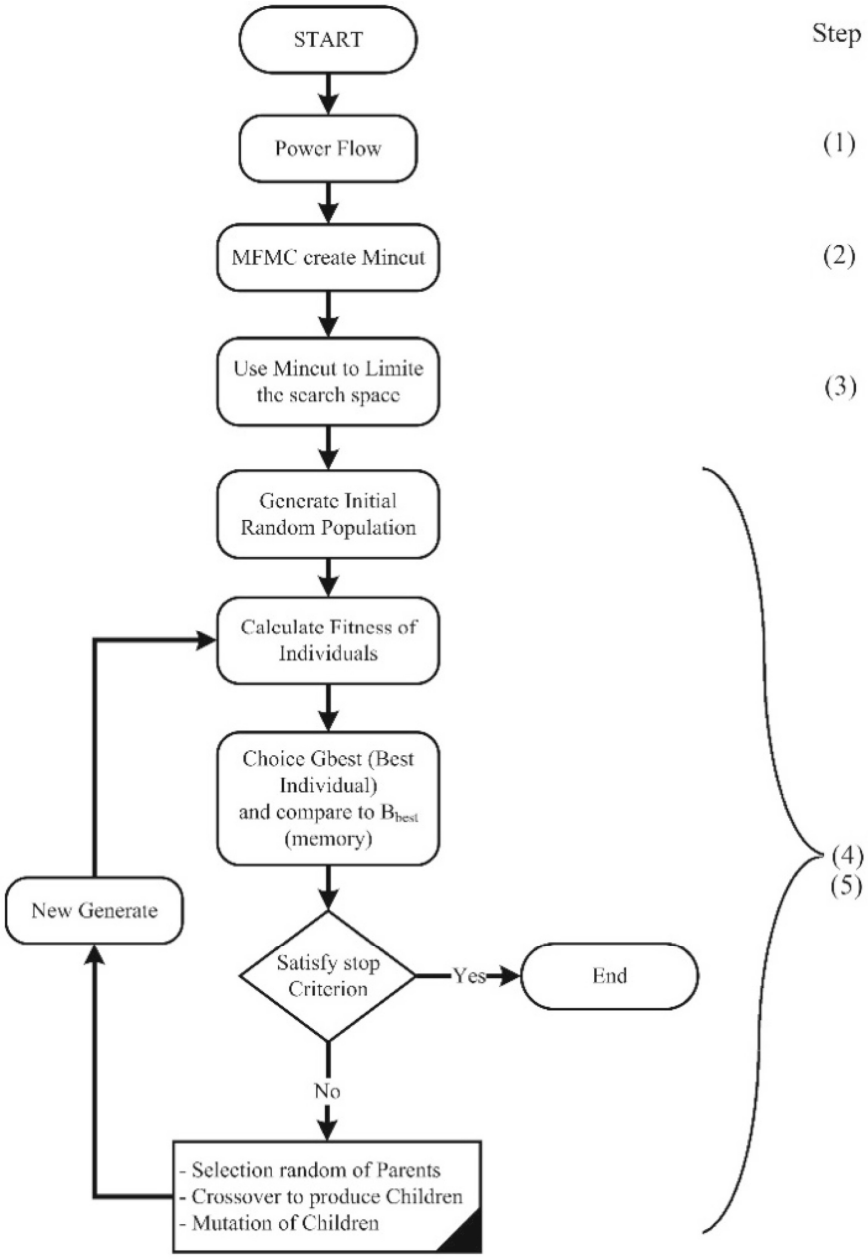

Fig. 3. Hybrid IMCA and GA algorithm flowchart

the minimum cross-section by step 2 (in 4.2). The results are shown in Tables 3 and 4 below.

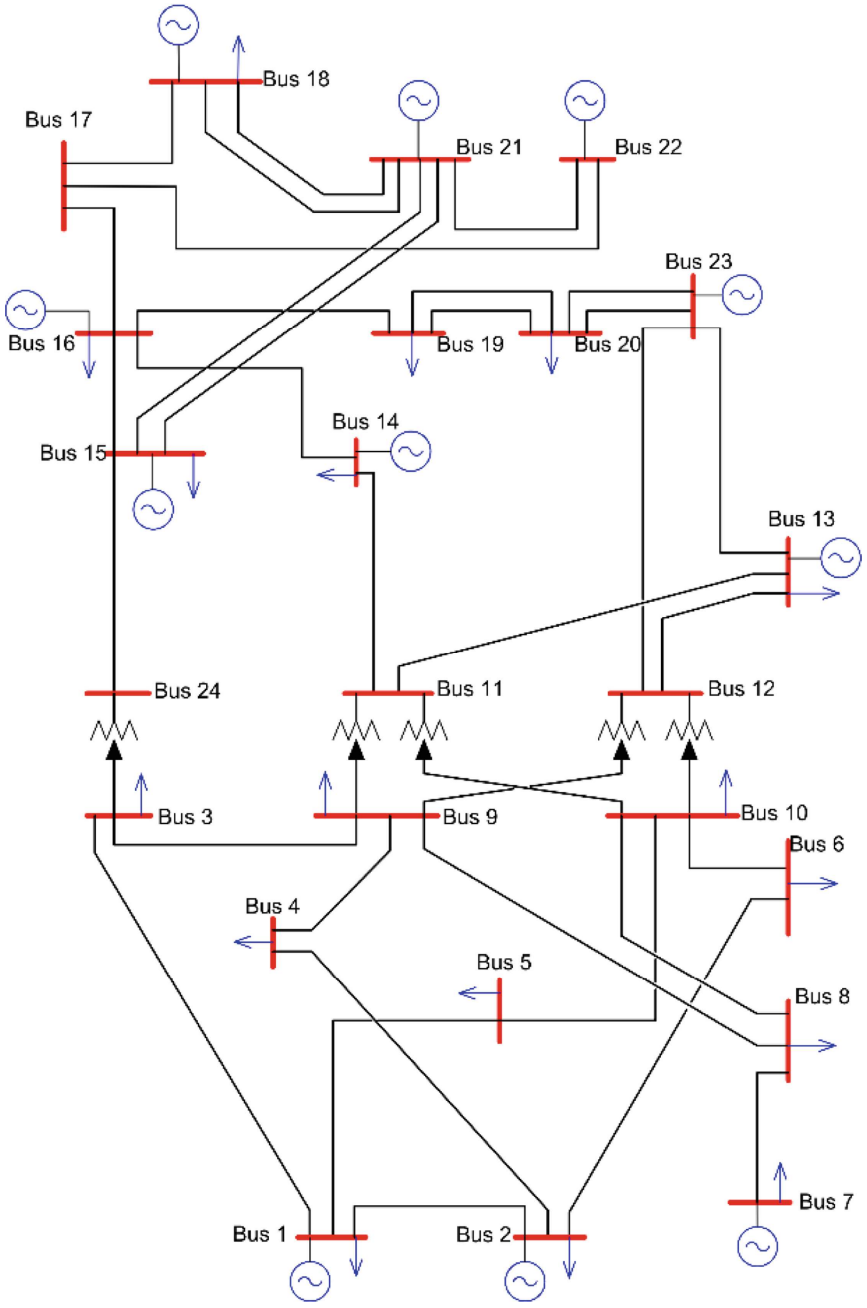

Fig. 4. 24-bus IEEE-RTS system

Compares the results of two algorithms, MCA and IMCA. Overloaded branches 8–7 and 10–6 (with overload coefficients of 104 and 133%) were excluded from the

Table 1. Power of generators (rate 160%)

Bus	1	2	7	13	15
P_g (MW)	307.2	307.2	480	945.6	344
Q_g (MVar)	99.84	99.84	120	331.2	106.08
Bus	16	18	21	22	23
P_g (MW)	248	640	640	480	1,056
Q_g (MVar)	86.88	160	160	96	397.76

Table 2. Power of loads (rate 160%)

Bus	1	2	3	4	5
P_d (MW)	172.8	155.2	288	118.4	113.6
Q_d (MVar)	35.2	32	59.2	24	22.4
Bus	10	13	14	15	16
P_d (MW)	312	424	310.4	507.2	160
Q_d (MVar)	64	86.4	62.4	102.4	32
Bus	6	7	8	9	
P_d (MW)	217.6	200	273.6	280	
Q_d (MVar)	44.8	40	56	57.6	
Bus	18	19	20		
P_d (MW)	532.8	289.6	204.8		
Q_d (MVar)	108.8	59.2	41.6		

Table 3. Min-cut result on 24-bus system

	Basic MC	New IMCA
Branches into min-cut	8–9	2–6
	8–10	6–10
		7–8
		8–9
		8–10

minimum cross-section in the MCA algorithm, while underloading branches (such as 9–8 and 10) −8 only 25 and 14% respectively) are included in the minimum cross-section. In contrast, with the IMCA algorithm, implemented with the coefficient $\gamma =$

Table 4. Power flow

Branch	10–8	8–7	9–8	10–6	6–2
Power flow (%)	14	133	25	104	51

175, the above-overloaded branches 6–10 and 7–8 are updated to the minimum cross-section set in Table 4, and this is the congestion area that needs to be expanded of the power system as stated [10].

According to the IMCA results, the set of nodes 10, 9, 8, 7, 6, and 2, which are related to the min-cut found, are six favourable locations for installing ESSs to solve the congestion of the power system at branch 9–8 and 10–8 as mentioned in [4]. This implementation is step 3 of the problem.

The GA algorithm to solve the optimization problem in programming (1) is implemented next in this step 4. The limit of the search space in the problem consists of six locations defined in step 3 above. The positions of the ESSs can be located at nodes 2, 6, 7, 8, 9, and 10, respectively. The capacity of the ESSs is assumed to allow a stepwise change of 10MW.

ESS capacity of 10MW at node 6 and 30MW at node 8 is the result of solving the problem. And this result is entirely consistent with the results calculated and checked by the corresponding AC mathematical method using Matpower 6.0 software.

6 Conclusion

Planning to expand the power system is indispensable in the process of socio-economic development of a country, and it is the task of scientists as well as strategic planners. In addition, in recent times, aiming at a strategic replacement for fossil fuels that pollute the environment, renewable energy sources are of great interest in the world. These sources and other canopies are widely used in TEP [8].

According to the research, the application of ESS source in power system planning is a flexible and feasible solution to prolong the investment period to expand the system and thus improve investment efficiency. This result brings economic benefits and has the effect of levelling power flow between peak and off-peak load times, helping to operate the power system more efficiently, making the most of renewable energy sources, like wind and solar.

In this paper, the research results have pointed out two outstanding issues:

(i) Improve the MCA algorithm suitable for the optimization problem and propose a hybrid method between IMCA and GA to reduce the search space of the optimization problem, thus reducing the computational load compared to the traditional GA method.

(ii) The combination of the improved IMCA and the GA algorithm used to improve the efficiency of the optimization problem and determine the result is a more powerful tool because it can find the plan results, and the ESS resources are more efficient.

Therefore, in the future, this method can be applied in practice and research and development more widely, specifically to continue testing other hybrid combinations, or it can also be developed for multi-stage planning.

Acknowledgments. This research is funded by Thai Nguyen University of Technology (TNUT).

References

1. Mahdavi, M., Monsef, H.: Review of static transmission expansion planning. J. Electr. Control. Eng. **1**(1), 11–17 (2011)
2. Lumbreras, S., Ramos, A.: The new challenges to transmission expansion planning. Survey of recent practice and literature review. Electr. Power Syst. Res. **134**, 19–29 (2016)
3. Lee, C., Ng, S.K., Zhong, J., Wu, F.F.: Transmission Expansion Planning From Past to Future. Proc Power Systems Conf. Expo. **PSCE 06**(03), 257–265 (2006)
4. Ilic, M., Galiana, F., Fink, L.: Power systems restructuring: engineering and economics. Springer Science and Business Media, LLC, New York (2013)
5. Duong, T.L., Yao, J., Truong, V.A.: A new method for secured optimal power flow under normal and network contingencies via optimal location of TCSC. Int. J. Electr. Power Energy Syst. **52**(8), 2013
6. Herbert, G.M.J., Iniyan, S., Sreevalsan, E., Rajapandiand, S.: A review of wind energy technologies. Renew. Sustain. Energy Rev. **11**(6), 1117–1145 (2007)
7. Solangi, K.H., Islam, M.R., Saidur, R., Rahim, N.A., Fayaz, H.: A review on global solar energy policy. Renew. Sustain. Energy Rev. **15**(4), 2149–2163 (2011)
8. Akinyele, D., Rayudu, R.: Review of energy storage technologies for sustainable power networks. Sustain. Energy Technol. Assess. **8**, 74–91 (2014)
9. Makansi, J., Abboud, J.: Energy Storage: the missing link in the electricity value chain-An ESC. White Paper, Energy Storage Counc 1–23 (2002)
10. Hemmati, R., Hooshmand, R.-A., Khodabakhshian, A.: Comprehensive review of generation and transmission expansion planning. Inst. Eng. Technol. **7**(9), 955–964 (2013)
11. Hadjipaschalis, L., Poullikkas, A., Efthimiou, V.: Overview of current and future energy storage technologies for electric power applications. Renew. Sustain. Energy Rev. **13**(6–7), 1513–1522 (2009)
12. Dunn, B., Kamath, H., Tarascon, J.-M.: Electrical energy storage for the grid: a battery of choices. Science **334**, 928–935 (2011)
13. Mendonça, I.M., Ivo, C.S., Marcato, A.L.M., Dias, B.H.: Transmission expansion optimization via constructive heuristic technique. IEEE Grenoble PowerTech. 1–5 (2013)
14. Garver, L.L.: Transmission network estimation using linear programming. IEEE Trans. Power Appar Syst. **PAS-89**(7), 1688–1697 (1970)
15. Sánchez, I.G., Romero, R., Mantovani, J.R.S., Rider, M.J.: Transmission—expansion planning using the dc model and nonlinear—programming technique. IEE Proc. Gener. Transm. Distrib. **152**(6), 763–769 (2005)
16. Duong, T.L., Yao, J., Truong , V.A.: Application of Min Cut Algorithm for Optimal Location of FACTS Devices Considering System Loadability and Cost of InstallationInt. J. Electr. Power Energy Syst. **63**(12) (2014)
17. Tran, T., Choi, J., Park, J.K., Moon, S.I., El-Keib, A.A.: A fuzzy branch and bound-based transmission system expansion planning considering ambiguities. IEEE Power Engineering Society General Meeting (2004)
18. Choi, J.S., Tran, T.T., Kang, S.R., Jeon, D.H., Lee, C.H., Billinton, R., Jaeseok, C.: A study on the optimal reliability criteria decision for a transmission system expansion planning. IEEE Power Engineering Society General Meeting (2004)
19. Rocha, M.C., Saraiva, J.T.: Multiyear Transmission Expansion Planning Using Discrete Evolutionary Particle Swarm Optimization. Energy Market (EEM), 2011—8th International Conference on the European, pp. 802–807 (2011)

Initiative for Integrating Wind and Thermal Power to Maximize Social Profit

Bui Xuan Luc[1,*], Dinh Ngoc Sang[2,3], Truong Viet Anh[3]

[1]*Student in Faculty of Electrical and Electronics Engineering, Ho Chi Minh City University of Technology and Education (HCMUTE), Ho Chi Minh City, Vietnam*
[2]*Department of Urban Engineering, University of Architecture Ho Chi Minh City (UAH), Ho Chi Minh City, Vietnam*
[3]*Faculty of Electrical and Electronics Engineering, Ho Chi Minh City University of Technology and Education (HCMUTE), Ho Chi Minh City, Vietnam*

[*]Email: 2230609@student.hcmute.edu.vn

Abstract

The issue of mitigating the consequences of uncertainty in the wind energy sector, especially when integrating into the electricity market, is becoming increasingly important in the context of renewable energy and modern grid systems. This uncertainty not only poses significant challenges to the profitability of wind farms but also threatens grid stability. An effective solution is to establish collaboration between wind farms and thermal power plants to balance electricity supply during critical periods. This collaboration helps increase profitability for wind farms and reduces fuel procurement costs for thermal power plants, while positively contributing to renewable energy development. Additionally, this paper emphasizes optimizing social benefits by maximizing profit for both energy models and minimizing fuel costs for thermal power plants, rather than solely focusing on the profit of each type of plant.

Keywords: *wind energy, electricity market, social profit*

1. INTRODUCTION

In recent years, renewable energy has become increasingly popular, especially wind energy, with a very rapid growth rate in the world [1]. Many studies have shown that the rate of construction of new wind power plants around the world is quite high [2].

The importance of wind energy has become clearer for economic and social development. Typically, after the energy restructuring in Europe in recent years, when policies to limit fossil energy supplies such as oil and gas from large countries were implemented. From there, countries must look for other energy sources, especially clean and abundant energy sources like wind energy [3].

Besides the significant advantages, there are still challenges that need to be overcome for renewable energy in general and wind energy in particular, one of which is the uncertainty of electricity production [4]. The unpredictable fluctuations of wind energy have a significant impact not only on the security and stability of the electricity system operation but also on the benefits of market participants [5]. The output capacity of wind power sources changes suddenly compared to the plan, leading to an imbalance in electricity supply and demand, which can cause fluctuations during operation. Furthermore, that sudden change makes power source owners have to evaluate the immediate benefits to react to the process of changing electricity output to balance the spot electricity market.

Therefore, scientists around the world have made many research efforts to improve this problem. A typical example is integrating wind energy into other energy sources that can meet other stability requirements such as thermal power plants [6], and Battery Energy Storage System (BESS) [7].

When integrating multiple power plants, the global optimization problem of all market participants is posed, whereby determining the optimal amount of power to offer to the electricity market is crucial for maximizing profit. Author of the article [8], has investigated the penalty coefficient factor to see the change in profit of wind power plants. In another article [9], the authors researched how to maximize wind power plant profits in a power source combination model.

Thus, researchers have researched and found ways to maximize profits for the factories under study. In reality, the inability of integrated power plants to maximize their own profits presents a significant challenge. This article introduces methods to evaluate the capacity of wind power plants in optimizing social welfare. The calculation method is based on maximizing the profits of wind power plants, along with the profits of thermal power plants.

The main contributions of the article are shown as follows:

(1) Propose capacity purchase cost coefficient when integrating wind power plants and thermal power plants.

(2) Maximize social profits when combining wind power plant and thermal power plant models together.

(3) Compare and evaluate the benefits of combining factories together.

2. MATHEMATICAL MODEL

2.1. Estimating power and wind probability

The actual power each wind blade puts out depends on the wind speed it is experiencing. Specifically, the power output of a wind turbine blade can be expressed as a function of wind speed [10]:

$$P_w(v) = \begin{cases} 0 & , v < v_{in} \text{ and } v > v_{out} \\ P_{wr}\left(\frac{v - v_{in}}{v_t - v_{in}}\right) & , v_{in} \le v \le v_r \\ P_{wr} & , v_r < v \le v_{out} \end{cases} \quad (1)$$

where v_{in}, v_r and v_{out} represent the starting wind speed, rated wind speed and cut−out wind speed of the blade. The rated output power of the 3 MW wind turbine is determined based on the Enercon E82−E4 product document, with specific values for the wind speed parameters being v_{in}= 3 m/s, v_r= 16 m/s and v_{out}= 25 m/s [10].

However, our load is taken according to the load of the whole country of Vietnam, so each wind power plant will be considered equivalent to an Enercon E82-E4 wind turbine.

The probability of wind speed according to the Weibull PDF has two important coefficients: the shape parameter (k) and the scale parameter (c):

$$f(v) = \left(\frac{k}{c}\right)\left(\frac{v}{c}\right)^{(k-1)} e^{-(v/c)^k}, \; 0 < v < \infty \quad (2)$$

2.2. Independent operation model of wind power plant

Normally, it is necessary to predict in advance the output that the plant can provide to sell to the electricity market, which is called a certain component. However, besides this certain component, wind speed will also fluctuate, increasing or decreasing compared to the initial prediction. This fluctuation is referred to as the uncertain profit of the wind power plant:

$$R_w(P_w) = \sum R_{w,i} = \sum\left[R_{ws,i}\left(P_{ws,i}\right) + R_{wu,i}\left(\Delta P_{w,i}\right)\right] \quad (3)$$

Where, P_w is the total amount of wind power sold in the electricity market; $R_{w,i}$, $R_{ws,i}$, $R_{wu,i}$ is the total revenue, direct and uncertain revenue of the ith wind farm; $P_{ws,i}$ and $\Delta P_{w,i} = P_{wav,i} - P_{ws,i}$ are the difference between planned capacity and actual capacity $P_{wav,i}$ compared to the plan of the ith wind power station.

2.3. Direct revenue

The direct revenue of the ith wind farm is determined corresponding to the proposed price and the wind capacity provided in the electricity market, determined by the formula (4).

$$R_{ws,i}(P_{ws,i}) = \lambda_{w,i} P_{ws,i} \quad (4)$$

In expression (4), revenue is proportional to two variables. The first variable is the wind energy output planned to be sold based on the production forecast at a particular time, P_{ws}. The higher this capacity, the higher the direct revenue and vice versa. However, setting a higher value carries increased risk for wind power owners due to the associated uncertainty.

Second proportional value, $\lambda_{w,i}$ represents the unit price directly related to the ith wind power producer. This coefficient is predicted and bid by the wind power plant owner. This may be a sufficient price to ensure enough income to compensate for the investment and operating costs of the wind power plant. However, in the market price mechanism, this number is calculated by some researchers to be influenced by the average price of energy from dominant energy sources in the electricity market, determined by the dynamics of supply and demand. Here, the article selects this coefficient so that this price is lower than the selling price of electricity from wind power plants to the electricity market, because an uncertain component cannot be priced the same as a high-certainty component.

2.4. Revenue from wind energy uncertainty

The second component of equation (3) represents the uncertainty of wind energy, and it is divided into two parts:

Component 1 represents the excess wind generation that occurs when the actual wind power output exceeds the power offered to the electricity market (known as reserve costs). If lucky, there may be one or a few wind farms with insufficient capacity that will buy this excess power. However, in most cases, this excess power will be curtailed because the output of each wind farm is fixed and offered in advance. Therefore, wind turbines are forced to turn their blades back to prevent the wind power from being fed into the grid, which would cause instability in the power system.

Component 2 represents the shortfall in wind power that occurs when the actual wind power output falls below the power offered to the electricity market (known as penalty costs). In this case, the investor has two options:

- Buy power from another power plant: This option is not feasible if there is no prior notice, as it is unlikely that another power plant will be able to supply the missing capacity in time.

- Pay a penalty fee: This option is often more expensive than the price at which the electricity was offered for sale.

Equation (5) represents the revenue from the stochastic component of wind farm i as follows [11]:

$$R_{wu,i}(\Delta P_{w,i}) = \begin{cases} R_{Rw,i}(\Delta P_{w,i}), & if\ P_{wav,i} \geq P_{ws,i} \\ C_{Pw,i}(\Delta P_{w,i}), & if\ P_{wav,i} \leq P_{ws,i} \end{cases} \quad (5)$$

Excess wind revenue:

$$R_{Rw,i}(\Delta P_{w,i}) = k_{R.i}(P_{wav,i} - P_{ws,i}) = k_{R,i}\int_{P_{ws,i}}^{P_{wr,i}}(p_{w,i} - P_{ws,i})f_w(p_{w,i})\,dp_{w,i} \quad (6)$$

Penalty from wind deficit:

$$C_{Pw,i}(\Delta P_{w,i}) = k_{P,i}(P_{wav,i} - P_{ws,i}) = k_{P,i}\int_{0}^{P_{ws,i}}(p_{w,i} - P_{ws,i})f_w(p_{w,i})\,dp_{w,i} \quad (7)$$

Where $P_{wav,i}$ and $P_{wr,i}$ is the actual capacity and rated capacity of the ith wind power plant. $f_w(p_{w,i})$ is the probability of this capacity appearing in the wind power plant i. $k_{R.i}$, $k_{P,i}$ is the reserve price coefficient when there is excess wind and the penalty price coefficient when there is a lack of wind capacity of the ith wind power plant.

2.5. Independent thermal power plant model

Thermal power plants need to use fossil fuels to produce electricity. The relationship between fuel costs (in units of $/hour) and generation capacity (in units of MW) can be more simply described by a quadratic model such as equation (8).

$$C_{T0}(P_{TG}) = \sum_{i=1}^{N_{TG}} a_i + b_i P_{TG,i} + c_i P_{TG,i}^2 \quad (8)$$

Where a_i, b_i, c_i is the cost coefficient of the ith thermal power plant to produce the amount of capacity P_{TGi}. N_{TG} is the total number of thermal power plants.

The profit R_{T0} of a thermal power plant is calculated as equation (9).

$$R_{T0}(P_{TG}) = \lambda_{TG,i} P_{TG,i} \quad (9)$$

$$\lambda_{TG,i} = b_i + 2c_i P_{TG,i} \quad (10)$$

Where $\lambda_{TG,i}$ denotes the unit price of the th thermal power plant i.

2.6. The combined operation of wind and thermal power plants model

When participating in the electricity market, factories will have to offer to sell a specific capacity of generation capacity to the electricity company so that the electricity company can have an operating strategy to stabilize the electricity system most. The problem of integrating wind power plants to improve stability and profitability for wind power plants is no longer unfamiliar in the research community [12]-[14]. The easiest integration in practice is between two wind power plants to reduce the probability of low power output. However, even with such integration, whether it is two, three, or four integrated plants, the power output level may still be unstable. Therefore, thermal power plants need to participate, as they are capable of providing stable power output to compensate for this shortfall.

If the capacity of the wind power plant offering electricity is P_{ws} then we will obtain the electricity offering capacity of the thermal power plant (P_{T0}) as:

$$P_{T0} = P_L - P_{ws} \quad (11)$$

Where P_L is the load capacity.

According to the article [15], variable thermal power plant capacity ranges from 1.26% to 6.31% of rated power per minute. In this study, the rate of change in the rated capacity of the thermal power plant is chosen as 1.26% per minute to extend its operational lifespan. Therefore, when

combining wind power plants and thermal power plants, there will be two more binding quantities for the thermal power plant's capacity besides the rated capacity P_{TGmax} which is:

$$P_{TGmax,new} = \begin{cases} P_{TGmax} & if\ P_{TGmax} < P_{T0} + P_{T0} * 1.26\% \\ P_{T0} + P_{T0} * 1.26\% & if\ P_{TGmax} > P_{T0} + P_{T0} * 1.26\% \end{cases} \quad (12)$$

$$P_{TGmin,new} = \begin{cases} P_{TGmin} & if\ P_{TGmin} > P_{T0} - P_{T0} * 1.26\% \\ P_{T0} - P_{T0} * 1.26\% & if\ P_{TGmin} < P_{T0} - P_{T0} * 1.26\% \end{cases} \quad (13)$$

Where P_{TGmin} is the smallest capacity of the thermal power plant (0MW), $P_{TGmax,new}$, $P_{TGmin,new}$ are the maximum capacity and minimum variable capacity of the thermal power plant, respectively. when integrated with wind power plants.

2.7. The case where the wind power plant generates sufficient capacity

The profit of the wind power plant will be calculated as formula (3)-(7) and the profit of the thermal power plant will be determined as formula (8)-(10).

2.8. The case where the wind power plant has excess generating capacity

At this point, the profit of the wind power plant will be calculated according to formula (3), and direct revenue according to formula (4), but at this time the coefficient k_R in formula (6) will be recalculated according to formula:

$$k_{R,new} = \frac{\lambda_{TG2}}{\lambda_{TG0}} \quad (14)$$

Where λ_{TG2} is the unit price of a thermal power plant when a wind power plant is involved, λ_{TG0} is the unit price of a thermal power plant when operating independently.

When excess wind capacity exceeds the available capacity of thermal power plants, the surplus wind energy cannot be utilized and is curtailed. But at this time there will be two cases: this excess wind capacity is larger than the capacity $P_{TGmin,new}$ and the case where the residual wind capacity is smaller than the capacity $P_{TGmin,new}$. When the excess wind capacity is greater than the amount of capacity the thermal power plant can meet, this excess wind component will be discarded. Thermal power plant profit ($R_{T0,new}(P_{TG})$) will be recalculated as follows:

$$R_{T0,new}(P_{TG}) = \begin{cases} \lambda_{TG} P_{TGmin,new} - R_{Rw,new} & if\ P_{T0} - P_{TGmin,new} < P_{wav} - P_{ws} \\ \lambda_{TG}(P_{T0} - P_{wav} + P_{ws}) - R_{Rw,new} & if\ P_{T0} - P_{TGmin,new} > P_{wav} - P_{ws} \end{cases} \quad (15)$$

2.9. The case where the wind power plant lacks generating capacity

At this point, the profit of the wind power plant will be calculated according to formula (3), and direct revenue according to formula (4), but at this time the coefficient k_P in formula (7) will be recalculated according to formula:

$$k_{P,new} = \frac{\lambda_{TG1}}{\lambda_{TG0}} \quad (16)$$

Where λ_{TG1} is the unit price of a thermal power plant when a wind power plant is involved.

When the wind power plant lacks generating capacity, the wind power plant will buy capacity from the thermal power plant. However, at this time there will be two cases: this lack of wind capacity is larger than the capacity $P_{TGmax,new}$ and the case where the excess wind capacity is smaller than the capacity $P_{TGmax,new}$. When the wind shortage capacity exceeds what the thermal power plant can supply, this shortfall will still incur penalties. The capacity of the wind shortage (P_{pw}) and the

maximum capacity of the thermal power plant that can be supplied (P_{pt}) will be calculated as follows:

$$P_{Pw} = P_{ws} - P_{wav} \quad (17)$$

$$P_{Pt} = P_{TGmax,new} - P_{T0} \quad (18)$$

The profit of the thermal power plant ($R_{T0,new}(P_{TG})$) will be recalculated as formula (19):

$$R_{T0,new}(P_{TG}) = \begin{cases} \lambda_{TG} P_{TGmax,new} + R_{Pw,new} & if\ P_{Pt} < P_{Pw} \\ \lambda_{TG}(P_{T0} + P_{pw}) + R_{Pw,new} & if\ P_{Pt} > P_{Pw} \end{cases} \quad (19)$$

The uncertain component wind power plant profit ($C_{Pw,new}(\Delta P_w)$) will be calculated as the formula (20):

$$C_{Pw,new}(\Delta P_w) = -\begin{cases} k_{P,new} P_{pt} + k_P(P_{pw} - P_{pt}) & if\ P_{Pt} < P_{Pw} \\ k_{P,new} P_{pw} & if\ P_{Pt} > P_{Pw} \end{cases} \quad (20)$$

In this case of insufficient generating capacity, there will be a scenario where if wind power plant capacity is much higher than the load demand, the actual output of the thermal power plant will be very low. Therefore, the coefficient $k_{P,new}$ will be very high because assuming the actual output of the thermal power plant is 300 MW, then the maximum power output the thermal power plant can achieve is 300 + 1.26%*Pdm*10 (because the wind power plant measures power changes every 10 minutes) will be much higher than 300. Therefore,$k_{P,new}$ will be much higher than k_P, meaning that the impact when combined with the wind power plant will be significant. So, if $k_{P,new} \geq k_p$ then the wind power plant will not purchase power from the thermal power plant but will incur penalties from the electricity company.

3. OBJECTIVE FUNCTION

The paper proposes a calculation method to select the generation capacity of each plant to achieve the maximum point of social profit. This social profit includes the profit of the thermal power plant, the profit of the wind power plant, and the fuel purchasing cost of the thermal power plant. All will be calculated according to formula (21):

$$\text{maximize}\{F = R_{w,new} + R_{T0,new} - C_{T0,new}\} \quad (21)$$

Where $R_{w,new}$, $R_{T0,new}$, $C_{T0,new}$ respectively represent the profit of the wind power plant, the profit of the thermal power plant, and the fuel purchasing cost of the thermal power plant after these two models are combined. The power system used in this paper is considered ideal, with no consideration given to transmission line overloads. The power plant capacity constraint function for the objective function is:

$$0 \leq P_{ws} \leq P_{wr} \quad (22)$$

$$0 \leq P_{T0} \leq P_{TGmax} \quad (23)$$

$$P_{TGmin,new} \leq \Delta P_{T0} \leq P_{TGmax,new} \quad (24)$$

With P_{ws} as the bid capacity of the wind power plant and P_{T0} as the bid capacity of the thermal power plant to the electricity market, ΔP_{T0} represents the variable capacity of the thermal power plant that can adjust to changes in the capacity of the wind power plant. $P_{TGmin,new}$, $P_{TGmax,new}$ denote the minimum and maximum adjusted capacities of the thermal power plant when linked with the wind power plant, calculated according to formulas (12) and (13).

After calculating and selecting the point of maximum social profit, the evaluation will be based on the increase in profit of the wind power plant and the thermal power plant, the reduction in fuel purchasing costs for the thermal power plant, as well as the rates of increase and decrease before and after integrating the two plants:

$$\%R_w = \frac{R_{w,new} - R_{w,old}}{R_{w,old}} * 100\% \quad (25)$$

$$\%R_{T0} = \frac{R_{T0,new} - R_{T0,old}}{R_{T0,old}} * 100\% \quad (26)$$

$$\%C_{T0} = \frac{C_{T0,new} - C_{T0,old}}{C_{T0,old}} * 100\% \quad (27)$$

Where $\%R_w, \%R_{T0}, \%C_{T0}$ respectively represent the percentage increase in profit of the wind power plant, the percentage increase in profit of the thermal power plant, and the percentage decrease in fuel purchasing cost of the thermal power plant. $R_{w,old}$, $R_{T0,old}, C_{T0,old}$ respectively represent the profit of the wind power plant, the profit of the thermal power plant, and the fuel purchasing cost of the thermal power plant before these two models are combined.

4. SIMULATION AND EVALUATION

The problem is calculated and processed on MATLAB software to program several solutions to OPF problems to calculate the profit of wind power plants, thermal power plants, and fuel purchase costs of thermal power plants.

4.1. Input data

4.1.1. Wind power plants

Actual wind speed data was collected at Binh Thuan province and recorded for analysis. The data collection period lasts from January 1, 2017, to December 31, 2021. Figure 1 shows wind speeds in 2017.

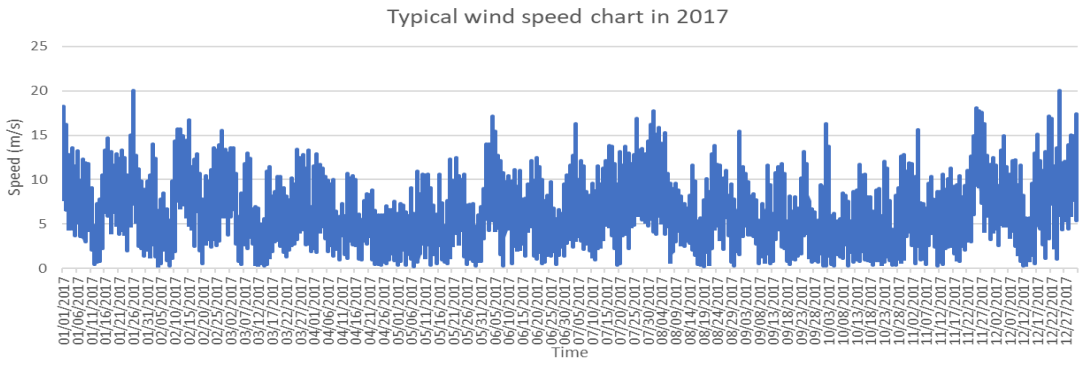

Figure 1. Typical wind speed chart in 2017

The wind data used covers January 2017 to December 2021, capturing historical changes in wind speed. This data helps estimate parameters for the Weibull distribution, which is crucial for accurately modeling wind conditions. This information is then applied to predict the auction capacity of the electricity market, with the goal of maximizing social profits. Additionally, load data from 2023 is used to simulate current electricity demand, ensuring our model reflects real-world operating scenarios.

However, to convert the data into Weibull coefficient form, it is necessary to estimate the parameters c and k of the Weibull distribution from real wind speed data. A common method to estimate these parameters is the Maximum Likelihood method [16]. This method optimizes the

Likelihood function based on the observed data, finding values of c and k that increase the likelihood of the observed data. This approach allows for accurate and reliable estimation of the parameters of the Weibull distribution from real wind speed data.

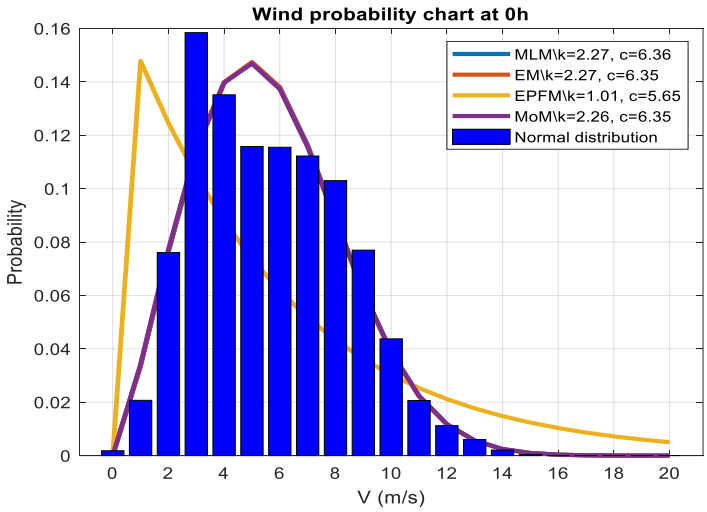

Figure 2. Wind speed probability chart using many Weibull coefficient estimation methods

Based on the calculation and simulation results, it is found that the error of MLM is the smallest compared to the other methods. Therefore, the parameters c and k calculated from this method will be used for further study.

Here, a wind power plant with a rated capacity of P_{wr}=42709.6 (MW) corresponds to the maximum load capacity for evaluating and demonstrating the uncertainty of wind power plant operation in the power system.

The electricity price will be divided into peak hours, off-peak hours, and normal hours according to the electricity selling price of Vietnam Electricity. The parameters in the problem are difficult to find online for security reasons. Therefore, here the author will take the coefficients during normal hours according to the parameters in the paper [10] then scale them to off-peak hours, peak hours with corresponding coefficients taken from the retail electricity prices for voltage levels from 110 kV and above to match the electricity selling prices of Vietnam Electricity.

Table 1. The selling price of wind power plants to the electricity market

Time frame	$\lambda_{w,i}$	Kp
Off-Peak Hour	1.01	1.9
Normal Hour	1.6	3
Peak Hour	2.88	5.41

4.1.2. Thermal power plants

The rated capacity of the thermal power plant is assumed to be 30,000 MW, which will correspond to about 70% of the rated capacity of the wind power plant.

Calculation parameters in the cost calculation formula of thermal power plants are taken according to the article [10].

Table 2. Cost of thermal power plant for the system under study [10]

a	b	c
0	2	0.00375

4.2. Load

Load data is collected from the Vietnam load graph in 2023 (https://www.nldc.evn.vn/). Below is a typical load graph for January 8, 2023.

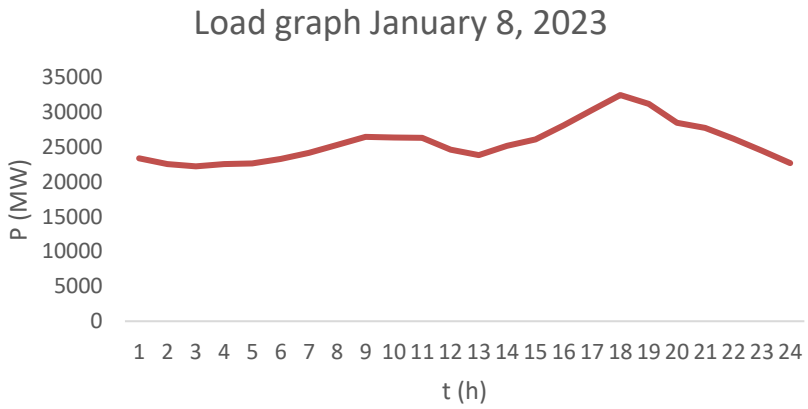

Figure 3. Symbolic graph on January 8, 2023

4.3. Simulation results for 0:00 January 8, 2023

Simulations will be run to find the maximum point of social profit for each hour. Then, calculations will be performed to determine the hourly capacity selection level of each factory to achieve the set goal of maximizing the social increase rate.

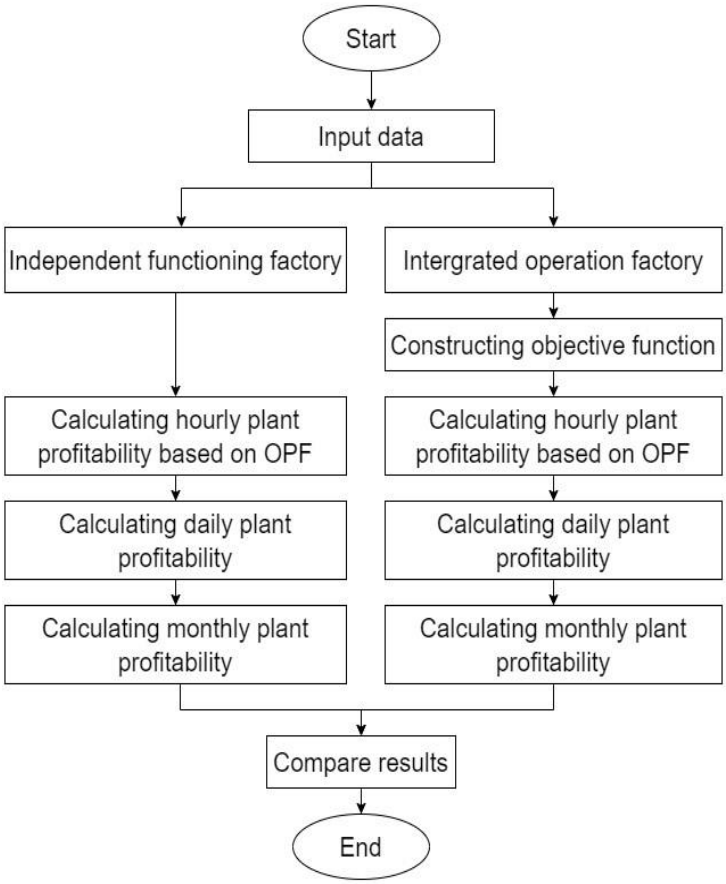

Figure 4. Implementation flow chart

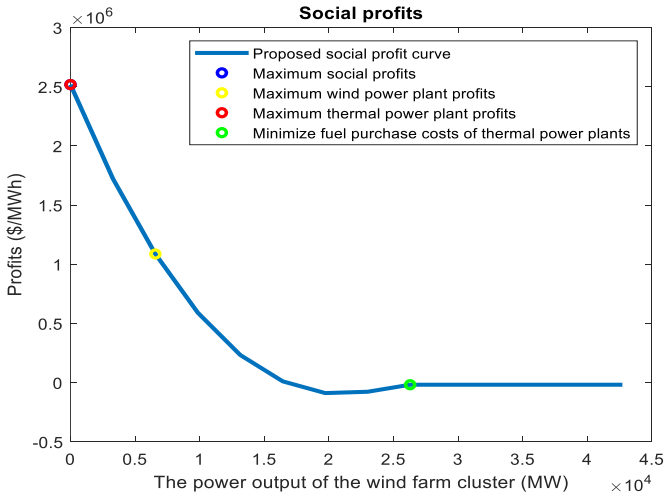

Figure 5. The maximum point of the social profits for a specific hour

Figure 5 illustrates the maximum point of social profit at 0h on January 08, 2023, when the wind power plant operates as a supporter for the thermal power plant by not bidding power to the grid. This result is because the rated capacity of the wind power plant is quite high compared to the load, so when bidding to the grid, there will be a surplus of power. Therefore, there is a scenario where only the surplus wind power is sold to the thermal power plant, and there is no need to worry about penalty costs from the grid when there is a shortage of wind.

4.4. Simulation results for 2023

Repeating the steps as for January 8, 2023 for the year 2023, the following result is obtained:

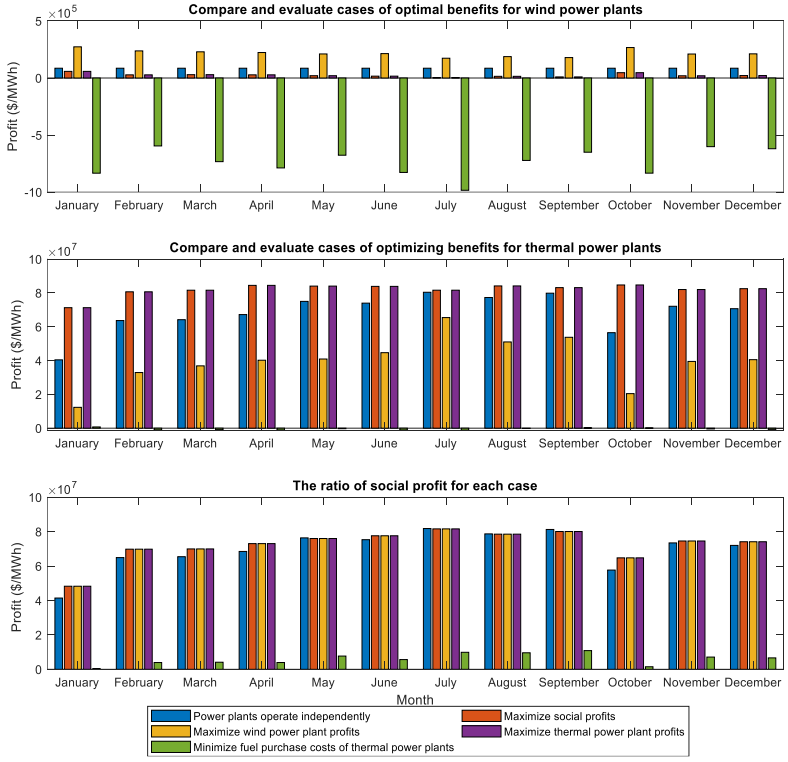

Figure 6. Evaluation results comparing profits in 2023 cases

Fig. 6 presents the results of optimizing social profit for loads and inputs of the power plants based on our initial assumptions. These results show that, when operating independently, the profit

of the wind power plant decreases compared to before, with the decrease from 1029389.3 to 21489.6 ($/MWh), reducing by 47.9 times. Meanwhile, the thermal power plant will benefit the most from the choice of objective functions and the purchase and sale coefficients when there is wind surplus or shortage, resulting in profit increasing from 821121294.8 ($/MWh) to 983955620.9 ($/MWh), an increase by 1.2 times. The fuel cost of the thermal power plant has increased slightly, from 836903159.4 ($/MWh) before integration to 868432315.5 ($/MWh) after integration, an increase of 1.04 times.

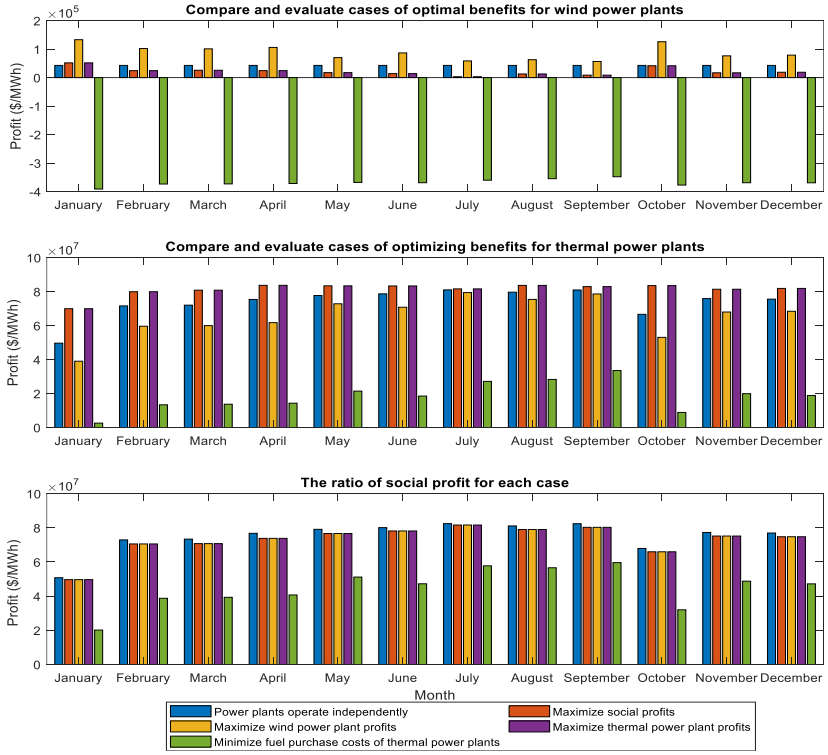

Figure 7. Evaluation results comparing profits in cases where the wind power plant's rated capacity being half of the original in 2023

As noted by the author in section 4.2, the simulation results for 0h on January 8, 2023, show significant changes when reducing the rated capacity of the wind power plant by half compared to the initial setting. The profit of the wind power plant has decreased from 514,685.8 ($/MWh) to 259,637.1 ($/MWh), a reduction of 1.98 times. However, this change has increased compared to the case using the rated capacity of the wind power plant, as in the previous scenario. Additionally, the wind power plant's profit will increase compared to operating independently during months with low load demand. The profit of the thermal power plant still increased from 901143789.5 ($/MWh) to 976007044.3 ($/MWh), a factor of 1.08.

In addition to maximizing social profit as proposed by the author, alternative scenarios include maximizing the wind power plant's profit, maximizing the thermal power plant's profit, or minimizing the thermal power plant's costs. Each of these cases with different primary objectives will result in distinct outcomes, as illustrated in Figures 6 and 7.

5. CONCLUSION

This paper addresses the challenge of forecasting and determining capacity for electricity market participation, focusing on renewable energy integration. A method combining forecasting models and capacity selection is proposed to optimize societal benefits. The research highlights the importance of renewable energy for economic and environmental sustainability, aiming to improve

the efficiency of power plants. Notably, the study excludes transmission line limitations, concentrating on power capacity limits to compare various objective functions and identify the most feasible and profitable combination of wind and thermal power plants. This approach aims to enhance renewable energy use in the electricity sector.

REFERENCES

[1] L. R. Amjith, and B. Bavanish, "A review on biomass and wind as renewable energy for sustainable environment," *Chemosphere*, vol. 293, 133579, 2022.

[2] D. Cao et al., "Bidding strategy for trading wind energy and purchasing reserve of wind power producer–a DRL based approach," *International Journal of Electrical Power & Energy Systems*, vol. 117, 105648, 2020.

[3] M. S. Nazir, N. Ali, M. Bilal, and H. M. N. Iqbal, "Potential environmental impacts of wind energy development: A global perspective," *Current Opinion in Environmental Science & Health*, vol. 13, pp. 85–90, 2020.

[4] K. N. Hasan, R. Preece, and J. V. Milanović, "Existing approaches and trends in uncertainty modelling and probabilistic stability analysis of power systems with renewable generation," *Renewable and Sustainable Energy Reviews*, vol. 101, pp. 168-180, 2019.

[5] A. M. Foley et al., "A critical evaluation of grid stability and codes, energy storage and smart loads in power systems with wind generation," *Energy*, vol. 205, 117671, 2020.

[6] J. Liu, Q. Yao, and Y. Hu, "Model predictive control for load frequency of hybrid power system with wind power and thermal power," *Energy*, vol. 172, pp. 555–565, 2019.

[7] E. Lobato et al., "Battery energy storage integration in wind farms: Economic Viability in the Spanish Market," *Sustainable Energy, Grids and Networks*, vol. 32, 100854, 2022.

[8] V. A. Truong, N. S. Dinh, and T. L. Duong, "Profit maximization of wind power plants in the electricity market based on linking models between energy sources," *Arabian Journal for Science and Engineering*, pp. 1–17, 2023.

[9] M. A. Lasemi, and A. Arabkoohsar, "Optimal operating strategy of high-temperature heat and power storage system coupled with a wind farm in energy market," *Energy*, vol. 210, 118545, 2020.

[10] P. P. Biswas, P. N. Suganthan, and G. A. J. Amaratunga, "Optimal power flow solutions incorporating stochastic wind and solar power," *Energy Conversion And Management*, vol. 148, pp. 1194-207, 2017

[11] A. Panda, and M Tripathy, "Security constrained optimal power flow solution of wind-thermal generation system using modified bacteria foraging algorithm," *Energy*, vol. 93, pp. 816-827, 2015

[12] M. A. Kamarposhti et al., "Optimal designing of fuzzy-PID controller in the load-frequency control loop of hydro-thermal power system connected to wind farm by HVDC lines," *IEEE Access*, vol. 10, pp. 63812–63822, 2022.

[13] A. Khouya, "Levelized costs of energy and hydrogen of wind farms and concentrated photovoltaic thermal systems: A case study in Morocco," *International Journal of Hydrogen Energy*, vol. 45, no. 56, pp. 31632–31650, 2020.

[14] J. Teh and C.-M. Lai, "Reliability impacts of the dynamic thermal rating and battery energy storage systems on wind-integrated power networks," *Sustainable Energy, Grids and Networks*, vol. 20, 100268, 2019.

[15] Y. Zhao et al., "Increasing Operational flexibility of supercritical coal-fired power plants by regulating thermal system configuration during transient processes," *Applied Energy*, vol. 228, pp. 2375–2386, 2018.

[16] D. Kang, K. Ko, and J. Huh, "Comparative Study of Different Methods for Estimating Weibull Parameters: A case study on Jeju Island, South Korea," *Energies*, vol. 11, no. 2, p. 356, 2018.

ENHANCING INVESTMENT EFFICIENCY IN WIND FARM EXPANSION UNDER MARKET COMPETITION WITH CONSIDERATION OF UNCERTAINTY

Dinh Ngoc Sang[1,2], Nguyen Tung Linh[3], Truong Viet Anh[1*]
[1]*Hochiminh City University of Technology and Education*
[2]*University of Architecture Hochiminh City*
[3]*Electric Power University*

ARTICLE INFO

Received: 18/9/2024
Revised: 26/11/2024
Published: 26/11/2024

KEYWORDS

Wind power
Electricity market
Energy storage systems
Generation expansion plan
Uncertainty

ABSTRACT

This paper examines the enhancement of investment efficiency in the expansion of existing wind power plants (WPP). The proposed approach addresses the challenges associated with diminishing incentive policies for renewable energy, while also aiming to mitigate the impact of wind speed variability and increase competitiveness as wind power penetrates the electricity market. To tackle these issues, the study optimizes key financial investment indicators and conducts a comparative analysis between wind farm expansion scenarios and conventional design approaches. In this optimization framework, a comprehensive design model is developed to enhance the efficiency of the transmission transformer system (TTS), accounting for the uncertainties in wind power generation. Furthermore, the integration of energy storage systems (ESS) is optimized to store surplus electricity with low utilization value, thereby maximizing the potential value of wind power output sold in the electricity market. Experimental results demonstrate the potential for a significant increase in the net present value, with the proposed scenario offering a 5.64-fold improvement, from 2.56 to 17.28 million euros. Additionally, the return on investment (ROI) is shown to increase 5.51 times, from 4.4% to 24.8%.

NÂNG CAO HIỆU QUẢ THIẾT KẾ ĐẦU TƯ MỞ RỘNG ĐIỆN GIÓ TRONG ĐIỀU KIỆN CẠNH TRANH THỊ TRƯỜNG ĐIỆN CÓ XÉT ĐẾN TÍNH BẤT ĐỊNH

Đinh Ngọc Sang[1,2], Nguyễn Tùng Linh[3], Trương Việt Anh[1*]
[1]*Trường Đại học Sư phạm Kỹ thuật Thành phố Hồ Chí Minh*
[2]*Trường Đại học Kiến trúc Thành phố Hồ Chí Minh*
[3]*Trường Đại học Điện lực*

THÔNG TIN BÀI BÁO

Ngày nhận bài: 18/9/2024
Ngày hoàn thiện: 26/11/2024
Ngày đăng: 26/11/2024

TỪ KHÓA

Nguồn điện gió
Thị trường điện
Nguồn trữ năng
Quy hoạch mở rộng nguồn
Bất định

TÓM TẮT

Bài báo này nghiên cứu nâng cao hiệu quả đầu tư mở rộng các trang trại điện gió (WPP) hiện hữu. Đề xuất này nhằm cải thiện các thách thức cố hữu trong thời đại ngày càng giảm chính sách ưu đãi cho loại hình năng lượng này. Hơn nữa còn chủ động giảm thiểu ảnh hưởng của tính bất định tốc độ gió kèm với tăng sức cạnh tranh khi nguồn điện gió tham gia vào thị trường điện. Để giải quyết các vấn đề đó, nghiên cứu tối ưu các chỉ tiêu đầu tư tài chính và đánh giá so sánh giữa các kịch bản mở rộng trang trại điện gió với kịch bản thiết kế truyền thống. Trong bài toán tối ưu đó, mô hình thiết kế chuyên sâu để nâng hiệu suất vận hành máy biến áp truyền tải (TTS) xét đến xác suất bất định công suất phát điện gió. Hơn thế nữa, công suất nguồn trữ năng (ESS) được xác định và xây dựng tích hợp để trữ điện dư có giá trị sử dụng thấp và nâng giá trị khai thác tối ưu sản lượng điện gió bán trên thị trường điện. Kết quả thử nghiệm đề xuất đã chỉ ra tiềm năng của hoàn vốn đầu tư tăng lên tới 5,64 lần cho kịch bản đề xuất, từ 2,56 lên 17,28 triệu Euro; và lợi tức đầu tư (ROI) cũng tăng 5,51 lần, từ 4,4% lên 24,8%.

DOI: https://doi.org/10.34238/tnu-jst.11135

* Corresponding author. *Email: anhtv@hcmute.edu.vn*

1. Giới thiệu

1.1. Tổng quan

Cam kết cắt giảm đến zero khí thải nhà kính vào năm 2050 của Chính phủ Việt Nam tại hội nghị Công ước khung của Liên hợp quốc về biến đổi khí hậu lần 26 (COP26), cũng như mục tiêu giảm 45% lượng khí thải của các bên tham gia COP27 là chính sách hành động mạnh mẽ theo xu hướng phát triển bền vững tất yếu trên toàn thế giới [1]. Trong đó, năng lượng gió nổi lên như một lĩnh vực chủ đạo, đang có sự tăng trưởng đáng kể và thu hút đầu tư đáng kể điện gió ở nhiều nước đã và đang phát triển [2]. Chính sách giá FIT ưu đãi cho loại nguồn điện này trong suốt hơn 20 năm kể từ những năm đầu thế kỷ 21 là một ví dụ điển hình tại Việt Nam [3]. Cụ thể hơn, những năm cuối thập niên 2010s và đầu thập niên 2020s đã chứng kiến các dự án điện gió đấu nối vào lưới điện quốc gia của Việt Nam. Trên 3.000 MW điện gió trên bờ đã được đóng điện vận hành tính đến năm 2022, chiếm khoảng 4% trong cơ cấu nguồn điện cả nước như Hình 1 [4], và dự kiến tăng lên đến 27.880 MW (chiếm khoảng 18,5% nguồn điện) vào năm 2030 theo quy hoạch [5].

Các nghiên cứu giảm thiểu ảnh hưởng bất định điện gió được đặt ra. Các mô hình tích hợp tối ưu kết hợp lợi ích của nhiều bên liên quan từ các lĩnh vực năng lượng khác nhau, nhằm mục đích tăng cường lợi ích thương mại của các nguồn năng lượng gió trong khuôn khổ thị trường điện trong tài liệu [6]. Bên cạnh đó, một hướng nghiên cứu nổi bật gần đây đã xuất hiện để nâng cao hiệu quả của các trang trại gió bằng cách đánh giá công suất máy biến áp, như kết hợp máy biến áp với biến tần để tối ưu hóa chuyển đổi năng lượng gió [7], [8]; mô hình vận hành của máy biến áp phân tán [9]. Chuyên sâu hơn trong nghiên cứu cải tiến máy biến áp truyền tải [10]; khảo sát động lực nhiệt của máy biến áp chi tiết trong tài liệu tham khảo [11].

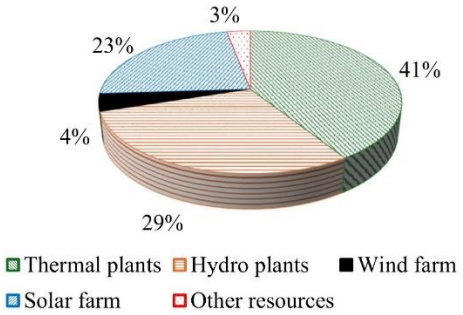

Hình 1. *Cơ cấu nguồn điện Việt Nam năm 2022* [4]

1.2. Định hướng nghiên cứu

Vấn đề thách thức lớn đối với phát triển điện gió là ngày càng giảm chính sách ưu đãi của chính phủ trong khi phải kiểm soát tính bất định cùng với tham gia vào thị trường điện cạnh tranh, điều này ảnh hưởng lớn đến chi phí và lợi nhuận của nhà đầu tư điện gió [12]. Vì vậy các nghiên cứu nâng hiệu quả đầu tư điện gió trong thị trường điện có xét đến xác suất bất định tốc độ gió. Nghiên cứu tích hợp rộng rãi năng lượng gió vào các hệ thống điện gây ra những trở ngại to lớn cho các nhà điều hành hệ thống và nhà sản xuất điện gió [13]. Nghiên cứu chênh lệch tốc độ gió dự báo sản lượng điện gió theo thời gian thực cho thị trường điện [14]. Nghiên cứu dự báo tốc độ gió chính xác hơn [15] và kết hợp ESS để tăng cường độ tin cậy của việc phát điện gió [16]; cũng như việc tái sử dụng sản lượng điện gió dư thừa và vận hành phối hợp thông minh trên thị trường điện [17], [18]; và hơn thế nữa là nghiên cứu phân bố công suất tối ưu trên hệ thống điện có đóng góp của nguồn điện gió như [19].

Một hướng nghiên cứu gần đây tập trung vào vai trò của máy biến áp trong các trang trại gió, do ảnh hưởng đến không chỉ chi phí mà còn cơ hội đầu tư, đặc biệt khi quá trình xây dựng hệ thống đấu nối điện gió gặp nhiều trở ngại ở các vùng sâu xa. Việc giải phóng mặt bằng và lắp đặt đường dây, trạm biến áp truyền tải thường phức tạp, nên tối ưu hóa máy biến áp trong thiết kế trang trại gió trở thành xu hướng nổi bật. Các tài liệu nghiên cứu [10], [20] khai thác máy biến áp động để nâng cao hiệu quả truyền tải điện gió nói chung và trang trại gió ngoài khơi nêu tại [21]. Tuy nhiên, các nghiên cứu trước đây chưa xem xét đầy đủ tác động của sự bất định trong tốc độ gió khi tích hợp vào thị trường điện, dẫn đến tình trạng vận hành máy biến áp quá tải hoặc non tải do biến động khó lường. Hơn nữa, sự không ổn định của điện gió cũng gây khó khăn trong thị trường cạnh tranh,

với nguy cơ bị phạt nếu thiếu hụt công suất hoặc bán với giá rẻ khi dư thừa. Giải pháp tích hợp hệ thống ESS với trang trại gió và máy biến áp giúp giảm thiểu thiệt hại, cân bằng lưu trữ điện dư thừa và bán khi giá cao hoặc khi thiếu hụt công suất.

1.3. Đóng góp

Đối với các trang trại điện gió trước đây thường thiết kế dựa trên dự đoán tốc độ gió như đã nêu trên, máy biến áp truyền tải đấu nối được chọn lựa theo các tiêu chuẩn có thể non tải trong phần lớn thời gian do sự bất định của vận tốc gió. Nghiên cứu này nhằm mở rộng trang trại điện gió mà không phải đầu tư thêm hệ thống truyền tải đấu nối, một bộ phận cản trở lớn đến quyết định đầu tư trang trại điện gió mới như đã nêu trên. Đạt được của nghiên cứu sẽ mang đến hiệu quả đầu tư mở rộng thuận lợi hàng loạt các trang trại điện gió đang vận hành, khai thác nâng khả năng vận hành các trạm biến áp truyền tải hiện hữu. Các đóng góp chính của bài báo gồm:

- Đề xuất hướng tiếp cận mới nâng hiệu quả đầu tư của các trang trại gió khi mở rộng chúng mà vẫn duy trì công suất trạm biến áp và đường dây truyền tải đấu nối điện gió.
- Kết hợp xác suất biến động tốc độ gió trong bài toán chọn lựa máy biến áp truyền tải để nâng tính khả thi và tối ưu vận hành máy biến áp.
- Tích hợp nguồn trữ năng trong mô hình thống nhất Điện gió – ESS – MBA. Theo đó, nâng hiệu quả đầu tư dựa vào tối ưu hóa sản lượng điện bán ra thị trường điện của mô hình.

2. Phương pháp luận

Để đánh giá bài toán nâng hiệu quả đầu tư mở rộng trang trại điện gió, ba kịch bản tương quan được xem xét như sau: kịch bản TS, đầu tư vào nhà máy điện gió thông thường; kịch bản OWS, mở rộng nhà máy điện gió; và kịch bản EWS mở rộng điện gió kết hợp ESS.

2.1. Hàm mục tiêu

Chỉ số hiệu quả đầu tư được xem xét gồm NPV theo biểu thức sau:

$$max\ NPV = \sum_{i=1}^{n} \frac{CF_i}{(1+IRR)^i} - C_{II} \quad (1)$$

Hiệu quả đầu tư được đánh giá bởi NPV. Trong nghiên cứu này, vòng đời dự án là 20 năm được trích dẫn [11]. Lãi suất được biểu thị bằng IRR và được thể hiện dưới dạng phần trăm.

$$C_{II} = C_{tw} + C_{tr} + C_{ESS} \quad (2)$$

$$CF_i = BF_i - Cost_i + Cer_i \quad (3)$$

$$Cost_i = C_{tur,i}^{O\&M} + C_{tr,i}^{O\&M} + C_{ESS,i}^{O\&M} \quad (4)$$

Dòng tiền theo năm i được ký hiệu CF_i; $Cost_i$ là chi phí; C_{tw}, C_{tr}, và C_{ESS} là vốn đầu tư điện gió, máy biến áp truyền tải, và ESS; $C_{tur}^{O\&M}$, $C_{tr}^{O\&M}$, và $C_{ESS}^{O\&M}$ là các chi phí vận hành và bảo trì thiết bị; P_t^{wav} là công suất vận hành điện gió. Đối với thu nhập chứng nhận khí thải, Cer, được xác định theo năm và tham khảo Thụy Điển là 0,305 [€/MWh] của năm 2019, tham khảo [8].

2.2. Mô hình hóa nguồn điện gió khi tham gia thị trường điện

Dòng thu nhập được xác định theo:

$$BF = \sum_{t=1}^{T} R_{ws}(P_t^{ws}) + \sum_{t=1}^{T} R_{wu}(\Delta P_t^w) \quad (5)$$

Thành phần đầu của biểu thức, R_{ws}, biểu diễn doanh thu trực tiếp thu được từ việc bán điện dựa trên các hợp đồng đấu thầu trong thị trường điện, tính theo giá chào và sản lượng sau khi khớp lệnh.

Thành phần thứ hai gọi là doanh thu bất định, R_{wu}, là thu nhập không chắc chắn so với công suất chào thầu, nó bao gồm doanh thu bán điện dư R_{Rw} và chi phí đền bù thiếu điện gió so với giá trị chào thầu C_{Pw}, các biểu thức tính toán theo [6],

$$R_{wu} = \begin{cases} \sum_{t=1}^{T} R_{Rw}(\Delta P_t^w),\ if\ \Delta P_t^w \geq 0 \\ \sum_{t=1}^{T} C_{Pw}(\Delta P_t^w),\ if\ \Delta P_t^w < 0 \end{cases} \quad (6)$$

Chênh lệch đơn giá bán điện dư và phạt thiếu điện thể hiện qua các hệ số tỷ lệ k_R, k_P. Dư điện là khi tốc độ gió tăng vượt so với dự đoán dẫn đến công suất phát điện gió cao hơn công suất

chào thầu. Khi đó, phần công suất dư được chào bán theo thời gian thực với giá thường thấp. Ngược lại, khi tốc độ gió thấp hơn dự đoán, công suất phát điện gió hiển nhiên thấp hơn công suất chào thầu. Chủ đầu tư buộc phải mua điện từ các nguồn chủ động khác để bù vào lượng công suất bị thiếu hụt với giá mua điện giao ngay cao hơn nhiều. Trong trường hợp không thể mua được điện, chủ đầu tư sẽ bị phạt hợp đồng với giá rất cao. Tham số xác suất bất định của tốc độ gió làm cơ sở xác định xác suất dư hoặc thiếu công suất điện gió, nghiên cứu này sử dụng hàm Weibull hai tham số [22], [23].

2.3. Mô hình hóa nguồn trữ năng

Trong nghiên cứu này giả sử sử dụng công nghệ pin lithium-ion để thử nghiệm [24], [25]. Mức hiệu suất tương đối ổn định lớn hơn 80%. Chi phí đầu tư ban đầu khoảng 100-200 €/kWh và chi phí O&M khoảng 1-3% [26], [27]. Doanh thu và chi phí được xác định như sau:

$$C_{ESS} = RI_{ESS}.E_{ESS} \quad (7)$$

$$Rev_{ESS} = \sum_{t=1}^{T}(\lambda_{D,t}.E_{D,t}) - \sum_{t=1}^{T}(\lambda_{R,t}.E_{R,t})$$

$$Cost_{ESS} = C_{ESS}^{O\&M} \quad (8)$$

$\lambda_{D,t}$ và $\lambda_{R,t}$ là giá bán và giá mua điện, sản lượng bán $E_{D,t}$ và mua $E_{R,t}$. Theo sự phối hợp vận hành ESS và TTS, việc thiết lập năng lượng sạc và xả của ESS cân bằng bởi hai quá trình: (i) Năng lượng trực tiếp: Tính toán mức năng lượng dư và thiếu hụt bằng cách khảo sát giới hạn công suất truyền tải của máy biến áp theo dự đoán công suất phát điện gió. Khi dư điện gió thì sạc, thiếu thì xả. (ii) Năng lượng không chắc chắn: Xác suất bất định điện gió là căn cứ xác định lượng công suất điện gió dư và thiếu so với chào thầu trên thị trường điện.

2.3.1. Tính toán năng lượng trực tiếp

Ví dụ trên Hình 2 cho thấy khi giới hạn công suất truyền tải máy biến áp tăng thì quá trình sạc năng lượng giảm (diện tích Recharge trên sơ đồ giảm), và năng lượng xả bán điện của ESS tăng lên. Trong khi đó, lượng năng lượng truyền tải vượt quá hay dưới giới hạn TTS phụ thuộc vào hai yếu tố, công suất phát điện gió và giới hạn truyền tải máy biến áp.

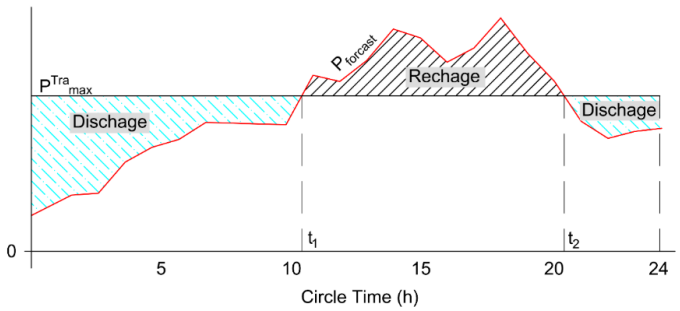

Hình 2. *Quá trình sạc và xả của ESS trong một ngày*

Trong trường hợp công suất định mức máy biến áp cố định, giới hạn công suất của nó phụ thuộc vào trạng thái và điều kiện vận hành máy biến áp. Hai thành phần năng lượng điện sạc E_R^D và xả E_D^D của ESS được xác định như sau:

$$E_R^D = \int_{t_1}^{t_2}\left(P_{forecast}(t) - P_{max}^{Tra}\right)dt \quad (9)$$

$$E_D^D = \int_0^{t_1}\left(P_{max}^{Tra} - P_{forecast}(t)\right)dt + \int_{t_2}^{24}\left(P_{max}^{Tra} - P_{forecast}(t)\right)dt \quad (10)$$

2.3.2. Năng lượng không chắc chắn

Phụ thuộc hai giá trị ngẫu nhiên: vận tốc gió bất định, khi thời tiết thay đổi đột ngột dẫn đến công suất gió đầu ra vượt quá giới hạn gây ra quá tải máy biến áp; và xác suất công suất phát điện gió vượt quá các giá trị chào thầu, dẫn đến thừa năng lượng trên thị trường điện.

$$E_R^U = \int_{t_1}^{t_2}\left(\int_{P_{max}^{Tra}}^{P^{wr}}(p_t^w - P_{max}^{Tra}).f_w(p_t^w).dp_t^w\right)dt + \int_{t_o}^{t_1}\left(\int_{P_{forecast}}^{P^{wr}}(p_t^w - P_{forecast}).f_w(p_t^w).dp_t^w\right)dt \quad (11)$$

$$E_D^U = \int_{t_o}^{t_1}\left(\int_{P_{forecast}}^{P^{wr}}(p_t^w - P_{forecast}).f_w(p_t^w).dp_t^w\right)dt \quad (12)$$

$(t_o - t_1)$ và $(t_1 - t_2)$ là thời gian công suất gió dưới hoặc vượt giới hạn của máy biến áp.

2.4. Mô hình hóa máy biến áp truyền tải (TTS)

Theo tài liệu [10], chi phí trạm biến áp truyền tải C_{tr} có thể xác định bằng biểu thức:

$$C_{tr} = RI_{tr}.P_{tr}^{r} \quad (13)$$

Trong đó, RI_{tr} là suất đầu tư và P_{tr}^{r} là công suất định mức máy biến áp, giá trị này được thiết kế theo tiêu chuẩn IEC [25].

2.4.1. Giới hạn truyền tải đối đa

$$I_t^2.S_{size} \geq P_t^{wav} \quad (14)$$

S_{size} là công suất biểu kiến TTS. Đây là điều kiện vận hành ổn định theo tiêu chuẩn IEC.

2.4.2. Giới hạn nhiệt độ vận hành

$$\theta_t^{hst} \leq \theta_t^{hst,max} \quad (15)$$

$$\theta_t^{top} \leq \theta_t^{top,max} \quad (16)$$

θ_t^{hst} là nhiệt độ điểm nóng nhất cuộn dây và θ_t^{top} là nhiệt độ bề mặt dầu cách điện. Các giá trị này được xác định theo phương trình phi tuyến theo tiêu chuẩn IEC [25].

2.4.3. Giới hạn tuổi thọ máy biến áp

$$LOL = \sum_t^T V_t \quad (17)$$

$$LOL \leq \frac{Transformer's\ Lifetime}{Wind\ Farm's\ Lifetime}.8760 \quad (18)$$

Tuổi thọ của máy biến áp *LOL*, và *V* là tốc độ già hóa hàng năm của máy biến áp phụ thuộc loại cách điện và được tham khảo theo tài liệu [25].

3. Thử nghiệm và Thảo luận

3.1. Dữ liệu ban đầu

3.1.1. Hệ thống điện chuẩn IEEE 30-Bus

Trong nghiên cứu này thử nghiệm trên hệ thống điện chuẩn IEEE 30-bus [28], có 41 nhánh và 6 nguồn điện, dữ liệu chi tiết tham khảo tại [23], [29]. Trong đó có hai nguồn điện được thay thế bởi trang trại điện gió tại bus 5 và 11. Thông số điện gió tham khảo tài liệu [23].

3.1.2. Nguồn điện gió

Đầu tư tài chính nguồn điện gió tham khảo [10], suất đầu tư 750.000 €/MW tương ứng với tuổi thọ 20 năm, chi phí O&M là 1,5%. Biểu đồ công suất phát điện gió ngày được dự đoán theo hai mùa cao điểm và thấp điểm được tham khảo trong tài liệu [30].

Phân bố xác suất bất định tốc độ gió tham khảo [22], sau khi tính toán năng lượng phát điện như đề cập tài liệu [6], sản lượng điện gió được chia ba thành phần: năng lượng dự đoán và được chào thầu cung cấp (OE hoặc OP), năng lượng xác suất vượt dự đoán (EE hoặc EP) và thấp hơn dự đoán (ES hoặc PS).

3.1.3. ESS

Có nhiều công nghệ lưu trữ đã và đang được sử dụng trong thương mại như các loại pin, siêu tụ điện, thủy điện tích năng, khí nén,…, trong đó pin vẫn là loại tiện lợi phổ biến trong kết hợp năng lượng tái tạo [24], nên chọn loại pin Lithium-ion để thí nghiệm, chi tiết như sau:

- Tuổi thọ tối thiểu 10 năm.
- Suất đầu tư là 200 €/kWh và chi phí vận hành 3% tham khảo [27].
- Công suất mỗi Block 1MW.
- Hiệu suất lưu trữ 90%.

3.1.4. TTS

- Suất đầu tư 30.000€/MVA và chi phí vận hành 3% tham khảo [10].

- Máy biến thế loại cách điện dầu OF, các tham số theo [25].
- Tỷ số tổn hao: R = 6
- Mức chênh lệch nhiệt độ cuộn dây và lớp dầu trên cùng: $\Delta\theta_{or}$= 49K
- Mức gia tăng nhiệt độ từ điểm nóng nhất cuộn dây đến điểm nóng nhất của dầu: $\Delta\theta_{hr}$= 29K
- Hằng số thời gian cuộn dây: τ_w= 7 phút
- Hằng số thời gian dầu: τ_o = 90 phút
- Nhiệt độ môi trường 25,6^{o}C

3.2 Kết quả thử nghiệm

3.2.1. Giá bán điện thị trường

Giả sử nguồn nhiệt điện chi phối nên giá bán điện trung bình nguồn nhiệt điện và có kết quả đã tính trong tài liệu [6]. Theo đó, giá chào bán điện trung bình thay đổi trong khoảng 26-31,7€/MW.

3.2.2. Kịch bản TS

Thiết kế chọn công suất máy biến áp truyền tải theo dữ liệu ban đầu nguồn điện gió tại bus 5 có công suất đỉnh 75MW. Quy trình thiết kế theo tiêu chuẩn IEC [25] với các điều kiện ràng buộc vận hành máy biến thế, trong đó biểu đồ biến thiên nhiệt máy biến thế có kết quả như Hình 3. Kết quả công suất vận hành tối ưu của máy biến áp được xác định là 57 MVA và được chọn 63 MVA. Dòng tiền quá trình đầu tư dự án tính được trong trường hợp này như Bảng 1.

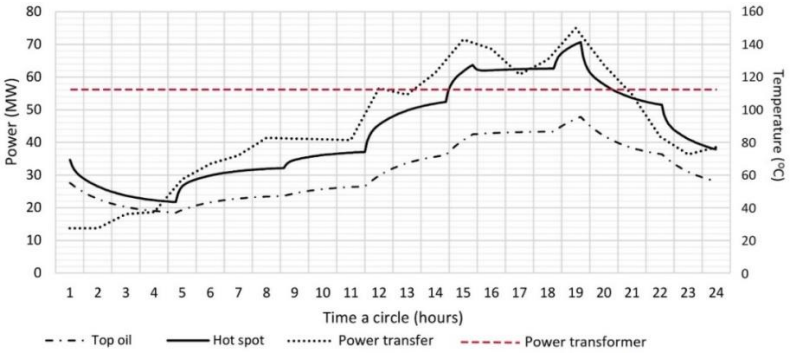

Hình 3. *Biến thiên nhiệt độ máy biến thế ngày cao điểm*

Bảng 1. *Dòng tiền dự án trong kịch bản TS*

Năm	0	1	2	…	20
Dòng tiền (k€)	-58,140	4,271	4,271	4,271	4,271
NPV (k€)	2,562				

Các kết quả này với giả sử giá điện không đổi qua các năm, và giảm một nửa với giá bán điện vượt đấu thầu, giá phạt thiếu điện sẽ tăng gấp đôi. Kết quả NPV dương cho thấy tính khả thi của dự án như một khoản đầu tư theo thiết kế truyền thống của kịch bản TS. Tuy nhiên khi giá phạt thay đổi thì NPV thay đổi theo.

3.2.3. Kịch bản OWS

Công suất trang trại điện gió tại bus 5 được mở rộng trong khi máy biến áp truyền tải và đường dây truyền tải không thay đổi. Mức tăng lên tối đa đạt đến khả năng giới hạn truyền tải của máy biến thế. Hai bước thiết kế được thực hiện. *Bước 1:* Sử dụng phương pháp tối ưu toán học trình bày tại [25] để xác định công suất đỉnh mới của điện gió dựa vào biến đổi nhiệt độ và điều kiện vận hành máy biến áp theo tiêu chuẩn IEC. Kết quả đạt được thể hiện trong Hình 4 tương ứng với công suất đỉnh điện gió mới là 90 MW, tăng 20% so với kịch bản TS trước đây. Sự gia tăng này dẫn đến tăng công suất đấu thầu cực đại, từ khoảng 57 MW lên 74 MW, tức tăng gần 30%. Tuy nhiên, hai khoảng thời gian trong ngày mà công suất gió vượt quá công suất định mức của máy biến áp cần đánh giá. *Bước 2:* NPV được xác định tương tự kịch bản TS nhưng dựa trên dữ liệu mở rộng trang trại gió.

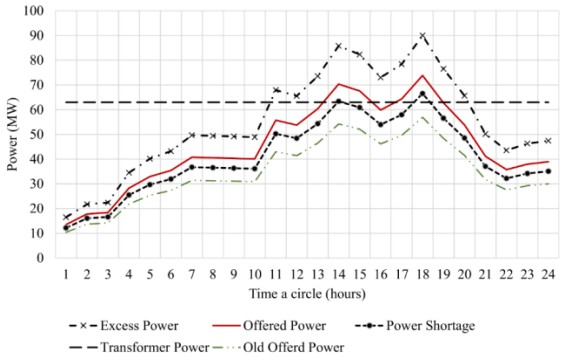

Hình 4. *Biến đổi công suất điện gió ngày cao điểm với kịch bản OWS*

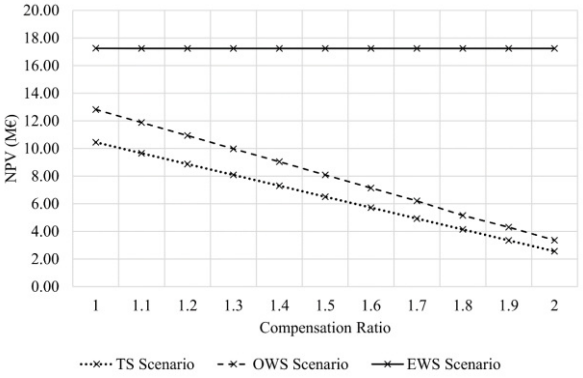

Hình 5. *So sánh biến đổi NPV các kịch bản*

3.2.4. Kịch bản EWS

Tích hợp ESS trong kịch bản OWS để khai thác năng lượng gió dư thừa khi cần thiết. Với công suất gió đỉnh 90MW và máy biến áp 63MVA, năng lượng sạc và xả tối ưu cho chế độ trực tiếp và bất định. Có thể chia thành hai khoảng thời gian chính. Khoảng thời gian từ 11 giờ sáng đến 9 giờ tối ưu tiên sạc do năng lượng gió dư thừa. Trong khoảng thời gian còn lại ưu tiên phát cung cấp điện cho thị trường điện khi cần thiết. Kết quả được tổng hợp theo các tham số tính toán như sau:

- E_R^D=24 MWh; E_R^U=214+7=221 MWh; E_D^D=319 MWh; E_D^U=97 MWh.
- Khả năng sạc E_R=245 MWh; Công suất sạc P_{ERmin}=10,2 MW.
- Khả năng xả E_D=416 MWh; Công suất phát cực đại P_{EDmax}=46,5 MW và trung bình P_{EDmean}=17,3 MW.
- ESS có công suất 10 MW và năng lượng lưu trữ 140 MWh, với loại xả sâu đến 20%.

3.3. Thảo luận

Hình 5 mô tả kết quả NPV biến đổi theo tỷ lệ phạt thiếu hụt công suất điện gió cả ba kịch bản. Nổi bật nhất là cả ba kịch bản đều mang lại giá trị NPV dương chứng tỏ tính khả thi về mặt tài chính của các dự án đầu tư. Trong khi đó, kịch bản mở rộng điện gió kèm ESS thể hiện tiềm năng doanh thu cao nhất cho các nhà đầu tư điện gió, và đặc biệt hơn, NPV của kịch bản này ít bị ảnh hưởng bởi hệ số đền bù. Ngược lại, NPV kịch bản TS giảm đột ngột đến hơn 75% khi tỷ lệ phạt tăng cho thấy bất kỳ thay đổi nào trong chính sách giá điện ảnh hưởng lớn hiệu quả đầu tư.

Xét về trình tự các kịch bản, NPV tăng dần từ TS, OWS và đến EWS. Như vậy, các kịch bản mở rộng trang trại điện gió mang lại hiệu quả đầu tư cao hơn đầu tư xây dựng mới. Cụ thể hơn, trong kịch bản EWS, NPV tăng đột biến 65,1% khi hệ số bồi thường bằng 0 và lên đến 573% khi hệ số đó bằng 2. Ba lợi ích có thể được lý giải cho nguyên nhân này: thứ nhất, sản lượng điện gió dư khi vượt chào thầu được giữ lại để bán với giá cao hơn; thứ hai, giảm thiểu bồi thường do xác suất thiếu hụt công suất điện gió trên thị trường điện; và cuối cùng, chênh lệch giá giữa mua sạc và bán điện của ESS mang lại lợi ích thiết thực.

Để đánh giá khách quan hơn, một so sánh với kịch bản đã được nghiên cứu và công bố trong tài liệu [10], thể hiện một trường hợp tương tự mà trong đó các nhà nghiên cứu tối ưu trạm biến áp 63 MVA cải tiến chế độ làm mát được trang bị để nâng cao hiệu quả truyền tải điện gió. Kết quả các chỉ tiêu được đối chiếu trong Bảng 2.

Bảng 2. *So sánh các chỉ tiêu của kịch bản tham khảo tài liệu* [10]

Kịch bản	**EWS**	[10]
Công suất đỉnh trang trại gió (MW)	90	75
Bao gồm bất định vận tốc gió	Có	Không
NPV (M€)	17,28	11,2
NPV/P (k€/MW)	192	149,3

Các chỉ số của kịch bản EWS đề xuất trong nghiên cứu này cải thiện đáng kể so kịch bản [10]. Đặc biệt là cả NPV và ROI trong kịch bản EWS đều tăng vượt mức 54% và 29% tương ứng. Điều đó chứng tỏ kết quả đề xuất mở rộng trang trại điện gió kết hợp xây dựng nguồn ESS đạt hiệu quả đầu tư đáng được xem xét. Tuy nhiên rủi ro biến động thị trường điện có thể tác động đến các chỉ số nhưng ảnh hưởng đến tất cả các kịch bản là như nhau, ngoài ra các chỉ số gần như ít bị thay đổi theo mức phạt (như thể hiện trên Hình 5) cho thấy kịch bản EWS là hiệu quả hơn như đã đánh giá.

4. Kết luận

Nghiên cứu đã chỉ ra một chọn lựa đáng được quan tâm trong lĩnh vực đầu tư trang trại gió, theo đó cần khám phá khả năng mở rộng của các trang trại hiện có được chứng minh mang lại lợi nhuận đầu tư cao hơn đáng kể, trước khi quyết định đầu tư một trang trại gió mới. Điều này đặc biệt hữu ích trong thời đại cắt giảm ưu đãi và cạnh tranh trên thị trường điện. Khẳng định này được thực nghiệm minh chứng với kết quả phương án đầu tư mở rộng trang trại điện gió kết hợp xây dựng nguồn trữ năng bằng bài toán tối ưu các chỉ số đầu tư tài chính NPV và ROI. Cụ thể số liệu cho thấy sự gia tăng đáng kể về lợi tức đầu tư từ 4,4% trong kịch bản thiết kế truyền thống lên 24,8% trong kịch bản mở rộng trang trại điện gió kết hợp ESS. Tuy có thể những rủi ro vận hành ESS do chưa hoàn thiện công nghệ trữ năng như hiện nay, nhưng xu hướng phát triển công nghệ trong tương lai có thể cải thiện khiếm khuyết, rõ ràng giảm giá thành và tăng hiệu suất trữ năng so với loại pin trong thử nghiệm như đề cập trong bài [24], điều đó có thể mang đến hiệu suất cao hơn nữa.

Cuối cùng, kết quả cho thấy vấn đề đặc biệt trong nghiên cứu này lợi ích độc đáo là minh chứng cho phương án thiết kế mở rộng trang trại gió mà không cần tăng thêm trạm biến áp và đường dây truyền tải điện để đấu nối. Và từ đó giảm đáng kể chi phí tài chính và nhân công để đánh giá môi trường nơi xây dựng trạm và đường dây truyền tải. Loại bỏ sự cần thiết phải giải phóng mặt bằng và bồi thường cho các trạm biến áp và đường dây truyền tải mới không được khuyến khích. Hơn thế nữa, nghiên cứu cho thấy chỉ tiêu lợi ích đầu tư kịch bản đề xuất mang đến hiệu quả mà gần như ít bị ảnh hưởng bởi các thay đổi chính sách ưu đãi về giá bán điện trong các điều kiện thị trường điện.

TÀI LIỆU THAM KHẢO/ REFERENCES

[1] J. Em-Udom and N. Jaisumroum, "SDT Smart Hybrid Streetlight Pole Design Utilizing Renewable Energy for a Smart City in Thailand," *Smart Grids and Sustainable Energy*, vol. 16, no. 8, pp. 1-11, 2023.

[2] B. A. B. Mohamed, "Principle Parameters and Environmental Impacts that Affect the Performance of Wind Turbine: An Overview," *Arabian Journal for Science and Engineering*, vol. 47, pp. 7891-7909, 2022.

[3] Vietnam Energy Institute, "Vietnam's National Electricity Development Plan for the Period 2021-2030, Vision to 2050," Hanoi, Vietnam, 2023.

[4] Vietnam Prime Minister, *Plan 262/QD-TTg: Implementing Vietnam's National Electricity Development Plan for the period 2021-2030, vision to 2050*, Hanoi, 2024.

[5] Vietnam Prime Minister, *Decision 500/QD-TTg: Approving the Vietnam's National Electricity Development Plan for the Period 2021-2030, Vision to 2050*, Hanoi, 2023.

[6] V. A. Truong, N. S. Dinh, and T. L. Duong, "Profit Maximization of Wind Power Plants in the Electricity Market Based on Linking Models Between Energy Sources," *Arabian Journal for Science and Engineering*, vol. 48, no. 8, pp. 6275-6291, 2023.

[7] C. Dhanamjayulu, P. Sanjeevikumar, and S. Muyeen, "A structural overview on transformer and transformer-less multi level inverters for renewable energy applications," *Energy Reports*, vol. 8, pp. 10299-10333, 2022.

[8] A. V. Truong, L. T. Nguyen, and S. N. Dinh, "Controlling Output Power to Enhance the Investment Efficiency of Wind Farms by Maximizing the Capacity of Transmission Transformers and Integrating Energy Storage Systems," *Engineering, Technology & Applied Science Research*, vol. 14, no. 4, pp. 15751-15756, 2024.

[9] O. D. A. Rocha, K. Morozovska, T. Laneryd, O. Ivarsson, C. Ahlrot, and P. Hilber, "Dynamic rating assists cost-effective expansion of wind farms by utilizing the hidden capacity of transformers," *International Journal of Electrical Power & Energy Systems*, vol. 123, 2020, Art. no. 106188.

[10] A. M. Gomez, K. Morozovska, T. Laneryd, and P. Hilber, "Optimal sizing of the wind farm and wind farm transformer using MILP and dynamic transformer rating," *International Journal of Electrical Power and Energy Systems*, vol. 107645, no. 136, 2022, Art. no. 107645.
[11] M. Fantauzzi, D. Lauria, F. Mottola, and D. Proto, "Estimating Wind Farm Transformers Rating through Lifetime Characterization Based on Stochastic Modeling of Wind Power," *Energies*, vol. 14, no. 1498, pp. 1-16, 2021.
[12] T. Cai, M. D. K. Chen, and T. Gong, "Methods of participating power spot market bidding and settlement for renewable energy systems," *Energy Reports*, vol. 8, pp. 7764-7772, 2022.
[13] K. Sharma, A. Gupta, and R. Bhakar, "Wind Power Scenario Generation Considering Spatiotemporal Correlations: A Distribution Free Hybrid VARMA-Copula Approach," *Smart Grids and Sustainable Energy*, vol. 8, no. 17, pp. 1-18, 2023.
[14] P. Spodniak, K. Ollikka, and S. Honkapuro, "The impact of wind power and electricity demand on the relevance of different short-term electricity markets: The Nordic case," *Applied Energy*, vol. 283, 2021, Art. no. 116063.
[15] H. Wang, N. Zhang, E. Du, J. Yan, S. Han, and Y. Liu, "A comprehensive review for wind, solar, and electrical load forecasting methods," *Global Energy Interconnection*, vol. 5, no. 1, pp. 9-30, 2022.
[16] T. Zuo, Y. Zhang, X. Xie, K. Meng, Z. Tong, Z. Y. Dong, and Y. Jia, "A Review of Optimization Technologies for Large-scale Wind Farm Planning with Practical and Prospective Concerns," *IEEE Transactions on Industrial Informatics*, vol. 19, no. 7, pp. 1-14, 2022.
[17] L. Al-Ghussain, A. D. Ahmad, A. M. Abubaker, and M. A. Mohamed, "An integrated photovoltaic/wind/biomass and hybrid energy storage systems towards 100% renewable energy microgrids in university campuses," *Sustainable Energy Technologies and Assessments*, vol. 46, 2021, Art. no. 101273.
[18] M. A. Mohamed, T. Jin, and W. Su, "An effective stochastic framework for smart coordinated operation of wind park and energy storage unit," *Applied Energy*, vol. 272, 2020, Art. no. 115228.
[19] T. T. Nguyen, H. D. Nguyen, and M. Q. Duong, "Optimal Power Flow Solutions for Power System Considering Electric Market and Renewable Energy," *Applied Sciences*, vol. 13, no. 5, 2023, Art. no. 3330.
[20] L. Dawson and A. M. Knight, "Investigating the impact of a dynamic thermal rating on wind farm integration," *IET Generation, Transmission & Distribution*, vol. 17, pp. 2449-2457, 2023.
[21] S. H. H. Kazmi, T. Laneryd, K. Giannikas, S. F. Ahrenfeldt, T. S. Sørensen, and J. Holbøll, "Cost optimized dynamic design of offshore windfarm transformers with reliability and contingency considerations," *International Journal of Electrical Power & Energy Systems*, vol. 128, 2021, Art. no. 106684.
[22] P. Wais, "A review of Weibull functions in wind sector," *Renewable and Sustainable Energy Reviews*, vol. 70, pp. 1099-1107, 2017.
[23] P. P. Biswas, P. N. Suganthan, and G. A. J. Amaratunga, "Optimal power flow solutions incorporating stochastic wind and solar power," *Energy Conversion and Management*, vol. 148, pp. 1194-1207, 2017.
[24] M. Hannan, S. Wali, P. Ker, M. A. Rahman, M. Mansor, V. K. Ramachandaramurthy, K. Muttaqi, T. Mahlia, and Z. Dong, "Battery energy-storage system: A review of technologies, optimization objectives, constraints, approaches, and outstanding issues," *Journal of Energy Storage*, vol. 42, 2021, Art. no. 103023.
[25] The International Electrotechnical Commission (IEC), *International Standards: Power transformers – Part 7: Loading guide for mineral-oil-immersed power transformers*, IEC 60076-7, The International Electrotechnical Commission (IEC), 2018.
[26] M. M. Rahman, A. O. Oni, E. Gemechu, and A. Kumar, "Assessment of energy storage technologies: A review," *Energy Conversion and Management*, vol. 223, 2020, Art. no. 113295.
[27] K. Mongird, V. V. Viswanathan, P. J. Balducci, M. J. E. Alam, V. Fotedar, V S. Koritarov, and B. Hadjerioua, "Energy Storage Technology and Cost Characterization Report," U.S. Department of Energy Office of Scientific and Technical Information, 2019.
[28] L. T. Seguro, J. V. Seguro, and T. W. Lambert, "Modern estimation of the parameters of the Weibull wind speed distribution for wind energy analysis," *Journal of Wind Engineering and Industrial Aerodynamics*, vol. 85, pp. 75-84, 2000.
[29] D. Z. Ray and E. M.-S. Carlos, "MATPOWER Test Cases," 24 January 2018. [Online]. Available: https://matpower.org/docs/ref/matpower5.0/case_ieee30.html. [Accessed July 25, 2023].
[30] D. Cao, W. Hu, X. Xu, T. Dragičević, Q. Huang, Z. Liu, Z. Chen, and F. Blabjerg, "Bidding strategy for trading wind energy and purchasing reserve of wind power producer – A DRL based approach," *Electrical Power & Energy Systems*, vol. 117, 2020, Art. no. 105648.

A robust hybrid algorithm AI and GA for optimizing wind power in electricity market

Dinh Ngoc Sang[1, 2], Truong Viet Anh[1], Nguyen Tung Linh[3*]

[1]Ho Chi Minh City University of Technology and Education, 01 Vo Van Ngan, Thu Duc, Ho Chi Minh City, Vietnam;
[2]University of Architecture Ho Chi Minh City, 196 Pasteur, District 3, Ho Chi Minh City, Vietnam;
[3]Electric Power University, 235 Hoang Quoc Viet, Bac Tu Liem, Hanoi, Vietnam.
[*]Corresponding author: linhnt@epu.edu.vn
Received: 30 Mar. 2024; Revised 13 Jul. 2024; Accepted 12 Nov. 2024; Published 25 Nov. 2024.
DOI: https://doi.org/10.54939/1859-1043.j.mst.99.2024.24-34

ABSTRACT

This paper proposes a robust hybrid method to optimize benefits under adverse conditions due to the uncertainty of wind power when integrated into competitive electricity markets. The hybrid algorithm synergizes an artificial intelligence technique to enhance the optimization efficiency of evolutionary algorithms. Results from the novel hybrid algorithm significantly enhance optimization speed and surpass local optima to achieve more favorable global optimum results. Experimental validation on the IEEE 30-bus power system, compared with previous studies and the original evolutionary algorithm, demonstrates notably higher profitability with the proposed algorithm. Based on experimental findings, the hybrid wind power-thermal power plant model also proves to mitigate compensation risks stemming from wind speed uncertainty, thereby stabilizing the electricity market and enhancing energy security. Encouraging optimal wind power capacity bidding on the electricity market in this context should entail a reduction of 15% to 18% compared to predictive expectations to attain optimal benefits.

Keywords: Optimal algorithm; Artificial intelligence; Long short term memory; Genetic algorithm; Wind farm; Electricity market.

1. INTRODUCTION

The rapid development of renewable energy, particularly wind energy in Vietnam, presents challenges to energy security due to the inherent uncertainty, leading to financial risks and market operations [1]. Accurate wind speed prediction methods using artificial intelligence and advanced forecasting techniques have emerged to address these issues [2, 3]. Implementing energy storage systems alongside wind sources is a practical approach to mitigate uncertainty impacts [4]. Technological research focuses on improving supercapacitors and batteries, as well as optimizing their placement and capacity [5]. Optimization methods are crucial for enhancing energy security, especially in dynamic electricity markets. Recent studies highlight strategic trading decisions, optimal planning of lithium battery locations in distribution grids, and experimental optimization of hydro energy storage systems, underscoring the necessity of optimization for energy security in competitive electricity markets [6, 7].

The rapid development of artificial intelligence (AI) has become inevitable, with numerous fields using AI techniques for decision-making [8]. Energy security is also benefiting from AI, with applications predicting factors like electricity prices, wind speeds, and solar radiation [9]. The integration of meta-heuristic (MH) in neural networks for prediction has advanced. However, most studies focus on using MH techniques to optimize AI network architecture and prediction processes [10]. For

example, particle swarm optimization (PSO) has been used to optimize neural network weights [11] and predict traffic flow distribution [12]. This leaves a notable gap in research towards the opposite trend, harnessing the predictive advantages of DL to enhance the optimization efficiency of MH algorithms. First, future individuals typically possess better attributes, and bringing these qualities back to the present can aid the community in developing and evolving more rapidly. Second, the advanced individuals of the future can serve as a driving force, motivating the community to overcome local barriers and achieve global optimization.

On the other hand, one effective method for promoting sustainable renewable energy, as proposed in [6], involves integrating wind power with existing thermal power sources (WTM) to enhance energy security during wind power instability [13]. In the electricity market, changes by any participant trigger reactions to restore stability [14]. Sudden changes due to wind energy uncertainty often harm the wind power sector; wind power prices drop with increased capacity, but sudden decreases lead to severe consequences, such as higher immediate electricity purchase costs or contract penalties [6, 15]. Therefore, optimizing wind power output bidding in the electricity market is a necessary endeavor to enhance efficiency for both wind power owners and sustainable renewable energy development in the new era, characterized by reduced reliance on government subsidies and the random effects of competitive electricity markets.

The Genetic Algorithm (GA) remains one of the recently improved meta-heuristic methods for solving multi-variable optimization problems due to its diversity and flexibility [16]. Meanwhile, Long Short-Term Memory (LSTM) is a rapidly developed artificial neural network suitable for short-term prediction tasks, making it an ideal candidate for hybridization with meta-heuristics, especially in cases with limited learning data and complex variability. Therefore, this paper proposes a hybrid LSTM-GA method as a representative case, suggesting that this approach can be extended to other hybrid algorithms, such as LSTM-PSO, or other combinations of meta-heuristic and deep learning algorithms. The main contributions and limitations of the article are summarized as follows:

Contributions	Limitations
1) Introduction of a novel hybrid method for solving optimization problems. The fusion of the LSTM algorithm with GA aims to leverage the superior advantages of AI algorithms to enhance the optimization quality in each iteration, facilitating the rapid achievement of global optimization objectives. 2) The new hybrid algorithm optimizes wind power bidding strategies by determining bid capacities that maximize benefit efficiency in the WTM model. The computational results highlight the highest benefits achieved with the proposed wind auctioning output power.	1) Although the experiment on the IEEE 30-bus system provides acceptable evaluation results, it is not representative of a large power system. Therefore, further research on larger power systems is warranted. 2) The original algorithms selected for hybridization are GA and LSTM. The development of hybrid meta-heuristics with deep learning can be extended to other algorithms not considered in this paper. This presents an idea for future extension studies.

2. PROBLEM

The mathematical model of the optimization problem and proposed solution are detailed in this section.

2.1. Theoretical foundations

2.1.1. Assumption

The optimization problem considered here pertains to the proposed optimal bidding power output for wind farms in the day-ahead electricity market, taking into account the uncertainty of predicted wind speeds. Optimizing the bidding power deviation for wind power, denoted as WPD, to maximize profit for wind power owners is necessary to promote renewable energy development as outlined in the [6] document. WPD represents the deviation between the bidding wind power output in the electricity market and the forecast wind power output with the highest probability. Additionally, the Weibull probability distribution is used to simulate the probability of wind power output.

2.1.2. Objective Function

$$Maximize\,\{F = R_{\Sigma} = R_w + IC_W\} \tag{1}$$

The revenue of electricity plants in the linking of wind farms, R_{Σ}, as [17, 6], comprises two main components: direct electricity sales revenue, R_w, and uncertain income, IC_W.

$$R_w = R_w^d(P_{ws}) + R_T^d(P_{Ts}) \tag{2}$$

Here, R_w^d and R_T^d denote the direct revenue of wind farms and thermal plants, respectively, corresponding to the bid output power P_{ws} and P_{Ts}, proportional to the bid prices λ_w and λ_T, as referenced in [18] as follows:

$$R_w^d = \lambda_w x P_{ws} \tag{3}$$

$$R_T^d = \lambda_T x P_{Ts} \tag{4}$$

The uncertain income component R_w^u comprises revenue from selling wind energy if there is a surplus; conversely, in the event of wind power shortage, the owners incur expenses to purchase electricity energy from the thermal plants C_T, from the ESS C_E, or pay penalty costs C_P.

$$IC_w = R_w^u(\Delta P_w) - (C_E + C_T + C_P) \tag{5}$$

The cost for ESS reference [19], the cost for thermal power reference [17]. The penalty cost, however, depends on the penalty electricity price, λ_P. Regarding the wind power probability distribution function f_w, parameters c and k of the Weibull distribution according to documents [6, 20], uncertain income components are allocated following expressions presented in document [21], specifically as follows:

$$R_w^u = k_R \lambda_w \sum_{(P_{ws}+\tau_{in})}^{P_{wr}} (p_w - P_{ws}) f_w(p_w) \Delta p_w \tag{6}$$

$$C_T = k_{P1} \lambda_w \sum_{(P_{ws}-\tau_{in}-\Delta P_T)}^{(P_{ws}-\tau_{in})} (P_{ws} - p_w) f_w(p_w) \Delta p_w \tag{7}$$

$$C_E = k_{P2}\lambda_w \sum_{(P_{ws}-\tau_{in}-\Delta P_T-P_E)}^{(P_{ws}-\tau_{in}-\Delta P_T)} (P_{ws} - p_w) f_w(p_w) \Delta p_w \quad (8)$$

$$C_P = k_{P0}\lambda_w \sum_{0}^{(P_{ws}-\tau_{in}-\Delta P_T-P_E)} (P_{ws} - p_w) f_w(p_w) \Delta p_w \quad (9)$$

Here, the power deviation within the permissible range of the electricity market is denoted as τ_{in}. Meanwhile, Δp_w represents the discrete step of wind power output. The scaling coefficients, k_R and k_{Pi}, signify the reduction rate of surplus electricity price and the increase rate of compensation electricity price, respectively. These coefficients are stochastic and contingent upon the supply and demand of the electricity market at the spot trading time. The value of k_R ranges from 0 to 1, while k_{Pi} is greater than 1.

2.1.3. Constraints

The operational constraints of the transmission system refer to documented conditions, including optimal operation for societal benefits, stable power transmission conditions, node voltage operation limits, and transmission line limits [22]. Operational conditions of wind turbines are constrained by wind speed requirements for turbine functionality, with low wind speeds rendering insufficient energy for turbine blades to operate and high wind speeds, such as in storm conditions, necessitating blade closure and turbine shutdown for protection. The existence of an ESS is contingent upon the emergence of system-building benefits, with constraints outlined in [19]. Market operation references [23], wherein the day-ahead electricity market model operates based on matching supply and demand quantities and prices.

2.2. Optimization Approach

Building on the original GA and LSTM algorithms, a new hybrid algorithm is proposed that uses LSTM embeddings in each evolutionary cycle of GA. The LSTM embeddings are used to predict the genetic set of future individuals. Detailed explanations are provided in the sections below.

2.2.1. Evolution Algorithm

The evolutionary algorithm, exemplified by GA [10], is a versatile method for solving complex optimization problems involving multiple variables. Evolution unfolds over generations, with each generation containing populations that undergo selection, crossover, and mutation [24]. Each individual in the population is defined by a chromosome comprising genes representing problem variables, initially initialized randomly to form the starting population, which then evolves iteratively. The process involves five main steps: (1) Initializing a random population and setting objectives. (2) Initiating an evolutionary loop by selecting individuals to survive, employing methods like Tournament selection or Rank selection. (3) Generating offspring through genetic recombination techniques such as single-point and double-point crossover, Uniform crossover, or others. (4) Introducing genetic diversity via population-based mutation rates, utilizing methods like Power mutation or Uniform mutation. (5) Evaluating the population and its objectives to determine whether to continue the evolutionary process or conclude the optimization procedure.

2.2.2. LSTM Algorithm

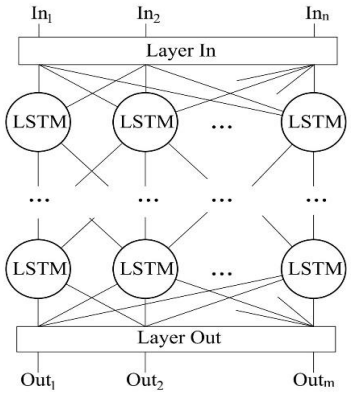

Figure 1. *Architecture LSTM.*

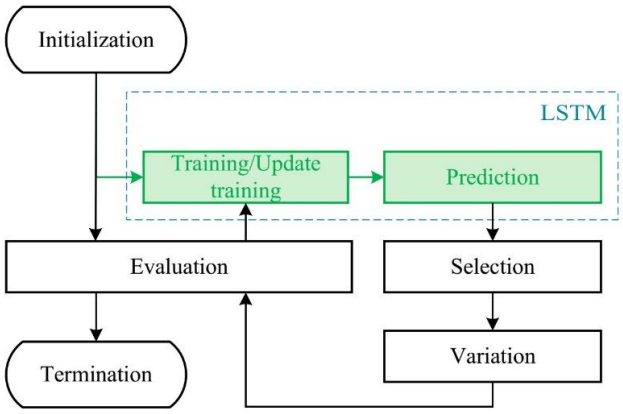

Figure 2. *Flowchart LSTM-GA Algorithm.*

Hochreiter and Schmidhuber [25] devised the LSTM algorithm based on the deep learning theory of the neural network architecture. The network architecture comprises interconnected and recurrent network units, the Cells, aimed at preserving weight values over both short and long-time intervals, as depicted in figure 1. The LSTM architecture minimally consists of three network layers: an input layer, an output layer, and a set of LSTM layers situated between the input and output layers. The LSTM layers consist of multiple hidden layers connected by Cells. The mathematical model representing the input-output relationships of each Cell is referenced [26] and is depicted in the equations below.

$$f_t = \sigma\left(W_f X_t + W_{Hf} h_{t-1} + b_f\right) \quad (10)$$

$$i_t = \sigma(W_i X_t + W_{Hi} h_{t-1} + b_i) \quad (11)$$

$$O_t = \sigma(W_o X_t + W_{Ho} h_{t-1} + b_o) \quad (12)$$

$$C_t = C_{t-1} \otimes f_t + i_t \otimes tanh(W_c X_t + W_{Hc} h_{t-1} + b_c) \quad (13)$$

$$h_t = O_t \otimes tanh(C_{t-1}) \quad (14)$$

The weight matrix, along with the bias terms, is represented as $W(f, i, O, C)$ for the weight matrix and $b(f, i, O, C)$ as the bias coefficient. h_t denotes the hidden unit at step *t* and C_t represents the current Cell coefficient after processing. ⊗ signifies multiplication; tanh and σ denote transformation functions. Equations (10) - (12) respectively express the forget, input, and output values. Equations (13) and (14) depict the current memory cell and hidden unit at time step *t*.

2.2.3. Hybrid LSTM-GA Algorithm

Figure 2 illustrates the cycle and hybrid structure of the LSTM-GA algorithms. The deep learning algorithm is embedded within the evolutionary algorithm, introducing a transformative step in the evolutionary cycle of each generation. This added transformation is the result of predicting chromosomes evolved through a more advanced LSTM algorithm with a time-series regression prediction architecture. Individuals with these improved chromosomes are integrated into the population community to grow alongside it, fostering better evolutionary outcomes. This process is delineated into five detailed steps: Step 1 involves initializing system parameters for the power grid, including source parameters, load

parameters, nodes, and branches. It initializes wind speed probability distribution data using the Weibull model, constructs the wind power probability distribution, and initializes GA parameters. It selects methods and rates for selection, crossover, mutation processes, and future prediction. The chromosome of each individual is defined by two gene segments: the first gene segment represents the power deviation level of a wind power source between bidding and prediction, and the second gene segment represents the compensatory ESS power for the corresponding wind power source. In cases with multiple wind farms, each gene pair represents one source. LSTM parameters are initialized, including input and output layer structures, the number of intermediate LSTM hidden layers, and related parameters. Step 2 involves initializing the initial random population according to a predetermined selection size. Step 3 entails running OPF on the system and constraints, determining wind power selling prices and electricity price adjustment factors, and calculating the objective function for individuals within the population. Step 4 trains LSTM for the initial loop iteration or updating training for subsequent iterations and subsequently predicting future chromosomes. The GA processes are executed, encompassing selection, recombination, and mutation. Step 5 constructs a population for the new generation and evaluates objectives.

2.3. Experiment Preparation

Three experimental scenarios proposed for comparison are as follows: Scenario 1, the mixed-integer linear programming approach (AC): The electricity source linkage model has been established and computed using this mathematical method in the paper [6]. Scenario 2, original genetic algorithm (GA): Employing the GA algorithm to determine optimal profits. Scenario 3 (LSTM-GA): Utilizing the novel hybrid algorithm LSTM-GA to ascertain optimal profits.

3. RESULTS AND DISCUSSION

This section presents data and experiments conducted on an IEEE 30-bus power system. The test results are then presented, commented on, and evaluated.

3.1. Input data

An IEEE 30-bus power system was utilized for testing [27], with specified parameters cited in [28]. Data were extracted from four thermoelectric sources located at nodes 1, 2, 8, and 13, while wind power data from nodes 5 and 11 are detailed in [17]. The wind speed based on data from [2], were categorized into peak and off-peak seasons. Probability values for exceeding and falling below capacity predictions were calculated using the Weibull distribution. The GA algorithm parameters included an initial population size of 50 individuals, a crossover rate of 0.8, and a mutation rate of 0.1. The LSTM architecture comprised a single input layer with five features (four variables from the chromosome and fitness of the corresponding individual), 120 LSTM hidden layers, one fully connected layer for output, and a final regression layer.

3.2. Simulation results

3.2.1 AC Scenario

Document [6] constructed and evaluated the WTM model with the aim of optimizing wind farm profits under fluctuating wind speeds that impact electricity market benefits. The optimization approach employed was mixed-integer linear programming. Experimental outcomes on the IEEE 30-Bus power system were subject to varying penalty electricity price

ratios ranging from 1.0 to 2.5. For detailed information, please refer to document [6].

3.2.2. GA Scenario

Executing the problem 15 times with a maximum of 20 generations per execution, the profitability results of the problem are presented in figure 3 (a). The GA typically converges to a local optimum after approximately 10 to 15 generations, as illustrated in the figures. Some instances result in local optima, leading to suboptimal outcomes. Hence, the solutions from the GA executions exhibit considerable dispersion.

3.2.3. LSTM-GA Scenario

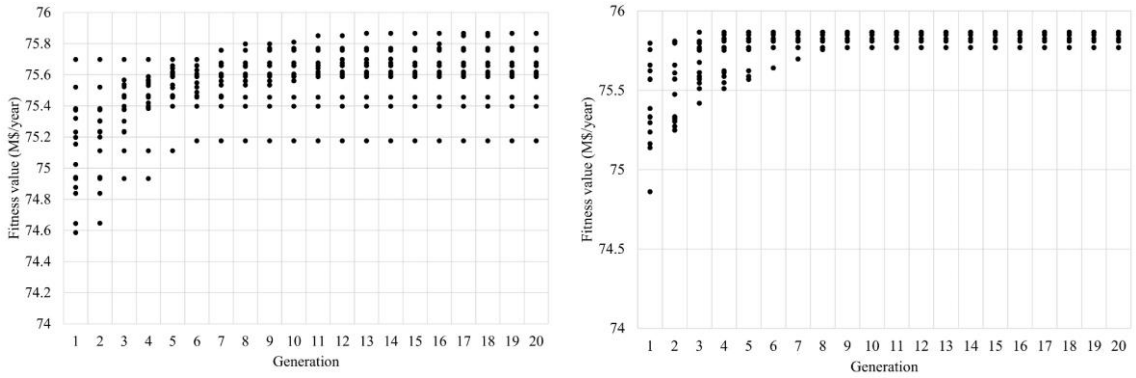

(a) GA *(b) LSTM-GA*

Figure 3. *Revenue at 15 times.*

Figure 3 (b) illustrates the outcomes of 15 executions of the LSTM-GA algorithm. The results indicate that WPD_{bus5} decreased by 16.7%, WPD_{bus11} decreased by 16.4%, P_{ESS5} is 9MW, and P_{ESS11} is 10MW.

3.3. Discussion

3.3.1. Evaluating the Optimization of Wind Farms

The optimal profit target is highest in the two GA scenarios, reaching M$75.9/year, surpassing M$71/year in the AC scenario. The LSTM-GS hybrid algorithm converges wind power capacity within 111-114MW, while other scenarios vary from 95MW to 114MW. Thus, adopting wind power output from the LSTM-GA scenario enhances efficiency in the electricity market, with bidding capacities around 64MW for bus five and 51MW for bus 11. This approach minimizes risks, maximizes efficiency, and harnesses the highest wind power potential, offering societal benefits.

Table 1. *Compare the results of the scenarios.*

Scenarios		AC [6][1]	GA	LSTM-GA
WPD (%)	Bus 5	-30%	(-15%) ÷ (-28%)	(-15%) ÷ (-18%)
	Bus 11	-30%	(-16%) ÷ (-28%)	(-16%) ÷ (-17%)
Wind power output bidding (MW)		95	97 ÷ 114	111 ÷ 114
ESS power (MW)		10	18	19
Benefit (M$/year)		71	75.9	75.9
Speed of convergence (generations)			10 ÷ 15	5 ÷ 9

[1] The compensation coefficient corresponds at 1.6

3.3.2. Evaluating the hybrid algorithm LSTM-GA

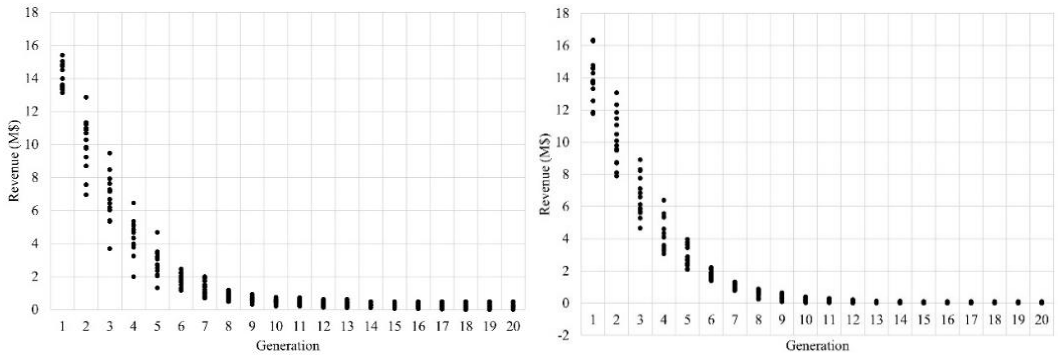

(a) GA *(b) LSTM-GA*

Figure 4. *Compare GA and LSTM-GA mean deviation.*

The LSTM-GA algorithm demonstrated accelerated convergence, as depicted in figure 4 (b). Initially, both algorithms exhibited similar trends in population development, with gradual improvement in population quality and relatively unchanged profits. This suggests that integrating LSTM into the optimization algorithm had minimal impact on performance during this phase, likely due to low yields in the initial iterations of artificial intelligence network training. However, from the sixth generation onwards, the hybrid algorithm showed increased convergence towards the objective, stabilizing at local optima within approximately two to three generations after that, resulting in faster achievement of the aim by two to five generations compared to the base GA algorithm, as illustrated in figure 4 (a). Analyzing the fitness function deviation at each iteration step, figure 5 indicates a more apparent distinction in the slope of the mean error fitness representation curve in the LSTM-GA algorithm compared to the GA algorithm. While the GA algorithm's curve maintains a steeper and stable slope with an error close to 0.2%, the LSTM-GA algorithm demonstrates not only a steeper slope but also a much more significant reduction in error, approaching a substantially lower stable value of approximately 0.04%. Ultimately, the results indicate that the proposed LSTM-GA hybrid algorithm holds a clear advantage in convergence speed and outcome. Convergence speed, denoting the number of iterations required to reach a minimum, is notably shorter, approximately 5-8 iterations, compared to over ten iterations in the GA algorithm. Moreover, convergence outcomes are more concentrated and achieve higher optimality compared to mathematical scenarios, specifically M$75.9/year higher than AC scenarios.

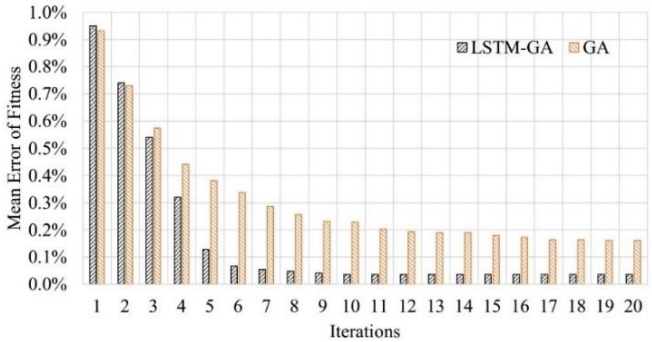

Figure 5. *Comparison of GA and LSTM-GA implementations.*

4. CONCLUSIONS

The novel hybrid algorithm proposed, which integrates LSTM with GA, showcases improved energy security through the stabilization of renewable energy sources by integrating wind farms with thermal power plants. This outcome is derived from the evaluation of three test scenarios conducted on the IEEE 30-bus power system. Notably, the hybrid algorithm, when applied to the integrated model of power plants supported by energy storage systems, yielded the most optimal results across this third scenario. In comparison to the conventional GA algorithm, the proposed hybrid algorithm demonstrated a more focused convergence, attributed to its capability to evade local optima. Moreover, its accelerated convergence rate may facilitate more efficient optimization resolution for large-scale or super-large-scale problems. This development suggests avenues for further exploration, such as integrating other meta-heuristic algorithms with deep learning techniques and conducting experiments on larger and more intricate power systems.

Societal benefits are also evident in the experimental findings. The maximizes bidding wind power output on the electricity market, alleviating concerns about risks that could otherwise deter investment in renewable energy. The risk reduction of penalties for wind power output shortage in the wind-thermal power integration model is a significant factor in ensuring financial stakeholders' confidence in investing in future wind energy development.

REFERENCES

[1]. IRENA, *"FUTURE OF WIND Deployment, investment, technology, grid integration and socio-economic aspects"* (A Global Energy Transformation paper), International Renewable Energy Agency, Abu Dhabi, (2019).

[2]. D. Cao, W. Hu, X. Xu, T. Dragičević, Q. Huang, Z. Liu, Z. Chen e F. Blabjerg, *"Bidding strategy for trading wind energy and purchasing reserve of wind power producer – A DRL based approach"*, Electrical Power & Energy Systems, vol. 117, p. 105648, (2020).

[3]. K. Abaci e V. Yamacli, *"Differential search algorithm for solving multi-objective optimal power flow problem"*, International Journal of Electrical Power & Energy Systems, vol. 79, pp. 1-10, (2016).

[4]. T. B. Nkwanyana, M. W. Siti, Z. Wang, I. Toudjeu, N. T. Mbungu e W. Mulumb, *"An assessment of hybrid-energy storage systems in the renewable environments"*, Journal of Energy Storage, vol. 72, p. 108307, (2023).

[5]. Z. Sun, Z. Wang, Y. Tian, G. Wang, W. Wang, M. Yang, X. Wang, F. Zhang e Y. Pu, *"Progress, Outlook, and Challenges in Lead-Free Energy-Storage Ferroelectrics"*, Advanced Electronic Materials Excellence in Electronics, vol. 6, n. 1, p. 1900698, (2020).

[6]. V. A. Truong, N. S. Dinh e T. L. Duong, *"Profit Maximization of Wind Power Plants in the Electricity Market Based on Linking Models Between Energy Sources"*, Arabian Journal for Science and Engineering, vol. 48, n. 8, (2023).

[7]. R. Fallahifar e M. Kalantar, *"Optimal planning of lithium ion battery energy storage for microgrid applications: Considering capacity degradation"*, Journal of Energy Storage, vol. 57, p. 106103, (2023).

[8]. M. Kaveh e M. S. Mesgari, *"Application of Meta-Heuristic Algorithms for Training Neural Networks and Deep Learning Architectures: A Comprehensive Review"*, Neural Processing Letters, vol. 55, p. 4519–4622, (2022).

[9]. K. Rajwar, K. Deep e S. Das, *"An exhaustive review of the metaheuristic algorithms for search and optimization: taxonomy, applications, and open challenges"*, Artificial Intelligence Review, vol. 56, p. 13187–13257, (2023).

[10]. M. A. Elaziz, A. Dahou, L. Abualigah, L. Yu, M. Alshinwan, A. M. Khasawneh e S. Lu, *"Advanced metaheuristic optimization techniques in applications of deep neural networks: a review"*, Neural Computing and Applications, vol. 33, p. 14079–14099, (2021).

[11]. B. A. S. Emambocus, M. B. Jasser e A. Amphawan, *"A Survey on the Optimization of Artificial Neural Networks Using Swarm Intelligence Algorithms"*, IEEE Access, vol. 11, pp. 1280 - 1294, (2023).

[12]. Bharti, P. Redhu e K. Kumar, *"Short-term traffic flow prediction based on optimized deep learning neural network: PSO-Bi-LSTM"*, Physica A: Statistical Mechanics and its Applications, vol. 625, p. 129001, (2023).

[13]. S. N. Dinh, A. V. Truong e L. T. Nguyen, *"Enhancing Wind Energy Investment Efficiency in The Electricity Market through The Integration of Power Uncertainty with Thermal Power Plant Operation"*, Tạp chí Khoa học va Công nghệ - Đại học Đà Nẵng, vol. 22, n. 2, pp. 81-87, (2024).

[14]. X. Lu, K. Li, H. Xu, F. Wang, Z. Zhou e Y. Zhang, *"Fundamentals and business model for resource aggregator of demand response in electricity markets"*, Energy, vol. 204, (2020).

[15]. S. N. Dinh, L. T. Nguyen e A. V. Truong, *"Enhancing Wind Power Profitability Through Integrated Clusters in the Electricity Market"*, in Conference: 2023 Asia Meeting on Environment and Electrical Engineering (EEE-AM), Hanoi, Vietnam, (2023).

[16]. M. A. Elaziz, A. Dahou, L. Abualigah, L. Yu, M. Alshinwan, A. M. Khasawneh e S. Lu, *"Advanced metaheuristic optimization techniques in applications of deep neural networks: a review"*, Neural Computing and Applications, vol. 33, p. 14079–14099, (2021).

[17]. P. P. Biswas, P. N. Suganthan e G. A. J. Amaratunga, *"Optimal power flow solutions incorporating stochastic wind and solar power"*, Energy Conversion and Management, vol. 148, pp. 1194-1207, (2017).

[18]. *"Energy Prices and Costs in Europe: Report from the commission to the european parliament, the council*", the european economic and social committee and the committee of the regions, European Commssion, Brussels, (2020).

[19]. M. Cao, Q. Xu, X. Qin e J. Cai, *"Battery energy storage sizing based on a model predictive control strategy with operational constraints to smooth the wind power"*, International Journal of Electrical Power & Energy Systems, vol. 115, pp. 1-10, (2020).

[20]. P. Wais, *"A review of Weibull functions in wind sector"*, Renewable and Sustainable Energy Reviews, vol. 70, pp. 1099-1107, (2017).

[21]. Z. Wang, W. Wang, C. Liu, Z. Wang e Y. Hou, *"Probabilistic Forecast for Multiple Wind Farms Based on Regular Vine Copulas"*, IEEE Transactions on Power Systems, vol. 33, n. 1, pp. 578 - 589, (2018).

[22]. A. Abedi, M. R. Hesamzadeh e F. Romerio, *"Adaptive robust vulnerability analysis of power systems under uncertainty: A multilevel OPF-based optimization approach"*, International Journal of Electrical Power & Energy Systems, vol. 134, p. 107432, (2022).

[23]. G. Bertrand e A. Papavasiliou, *"An Analysis of Threshold Policies for Trading in Continuous Intraday Electricity Markets"*, 15th International Conference on the European Energy Market (EEM), p. 18130454, (2018).

[24]. S. Mirjalili, Genetic Algorithm, *"Evolutionary Algorithms and Neural Networks"*. Studies in Computational Intelligence, vol. 780, p. 43–55, (2019).

[25]. S. Hochreiter e J. Schmidhuber, *"Long Short-Term Memory"*, Neural Computation, vol. 9, n. 8, pp. 1735 - 1780, (1997).

[26]. F. Shahid, A. Zameer e M. Muneeb, *"A novel genetic LSTM model for wind power forecast"*, Energy, vol. 223, p. 120069, (2021).

[27]. O. Alsac e B. Stott, *"Optimal Load Flow with Steady-State Security"*, IEEE Transactions on Power Apparatus and Systems, Vol. PAS-93, n. 3, pp. 745-751, (1974).

[28]. MATPOWER Test Cases, (2018). [Online]. Available: https://matpower.org/docs/ref/matpower5.0/case_ieee30.html.

TÓM TẮT

Đề xuất thuật toán lai trí thông minh nhân tạo với biến đổi gen để tối ưu nguồn điện gió trong thị trường điện

Bài báo này đề xuất một phương pháp lai mạnh mẽ để tối ưu hóa lợi ích trong điều kiện bất lợi do sự bất định của nguồn điện gió khi chúng tham gia vào thị trường điện cạnh tranh. Thuật toán lai cộng sinh bởi một thuật toán thông minh nhân tạo để nâng hiệu quả tối ưu hóa của thuật toán tiến hóa. Kết quả thuật toán lai mới đã cải thiện đáng kể tốc độ tối ưu hóa và vượt qua được các cực trị địa phương để mang lại kết quả tối ưu toàn cục thuận lợi hơn. Thực nghiệm trên hệ thống điện chuẩn IEEE 30-bus và so sánh với nghiên cứu trước đây cũng như thuật toán tiến hóa gốc cho thấy lợi nhuận điện gió cao hơn rõ ràng ở thuật toán đề xuất. Dựa vào kết quả thử nghiệm, mô hình liên kết nguồn điện gió với nguồn nhiệt điện cũng được minh chứng mang lại ít rủi ro bồi thường do sự không chắc chắn bởi tốc độ gió nên ổn định thị trường điện và nâng tầm an ninh năng lượng. Khuyến khích công suất điện gió tối ưu chào đấu thầu trên thị trường điện trong trường hợp này nên giảm 15% đến 18% so với kỳ vọng của dự đoán để đạt được lợi ích tốt nhất.

Từ khóa: Thuật toán tối ưu; Trí thông minh nhân tạo; Long Short Term Memory; Thuật toán biến đổi gen; Trang trại điện gió; Thị trường điện.

TĂNG CƯỜNG HIỆU QUẢ ĐẦU TƯ ĐIỆN GIÓ TRONG THỊ TRƯỜNG ĐIỆN THÔNG QUA KẾT HỢP SỰ BẤT ĐỊNH CỦA ĐIỆN GIÓ VỚI VẬN HÀNH NHÀ MÁY NHIỆT ĐIỆN

ENHANCING WIND ENERGY INVESTMENT EFFICIENCY IN THE ELECTRICITY MARKET THROUGH THE INTEGRATION OF POWER UNCERTAINTY WITH THERMAL POWER PLANT OPERATION

Đinh Ngọc Sang[1], Trương Việt Anh[1], Nguyễn Tùng Linh[2]*

[1]Trường Đại học Sư phạm Kỹ thuật Tp. Hồ Chí Minh, Hồ Chí Minh, Việt Nam
[3]Trường Đại học Điện lực, Hà Nội, Việt Nam

*Tác giả liên hệ / Corresponding author: linhnt@epu.edu.vn

(Nhận bài / Received: 08/11/2023; Sửa bài / Revised: 24/01/2024; Chấp nhận đăng / Accepted: 26/01/2024)

Tóm tắt - Bài báo giới thiệu giải pháp giảm thiểu ảnh hưởng từ sự bất ổn của điện gió, đặc biệt khi điện gió ngày càng phải tham gia vào thị trường điện. Sự không chính xác trong dự báo và biến đổi thời tiết đột ngột khiến cho công suất phát điện thực tế của các trang trại gió có thể chênh lệch lớn so với dự kiến, dẫn đến giảm doanh thu cho nhà đầu tư và tổn thất cho xã hội. Nhà đầu tư có thể phải chịu phạt do không cung cấp đủ điện theo cam kết hoặc bán điện dư ra với giá thấp. Nghiên cứu đề xuất kết hợp các nguồn điện, đặc biệt là sự tích hợp giữa điện gió và nhiệt điện, nhằm cân bằng công suất và giảm thiểu rủi ro phạt hoặc đền bù. Thực nghiệm trên mô hình hệ thống IEEE 30-nút cho thấy, việc liên kết này mang lại lợi nhuận cao hơn so với khi các nhà máy điện hoạt động độc lập.

Từ khóa - Năng lượng điện gió; Thị trường điện; Không chắc chắn; Chiến lược đầu tư; Kế hoạch mở rộng nguồn điện

Abstract - The paper presents a solution to mitigate the impact of the inherent uncertainty of wind power, especially as it increasingly participates in the electricity market. Inaccuracies in forecasting and sudden weather changes can lead to significant discrepancies between actual and predicted wind power output, resulting in revenue losses for investors and societal damage. Investors may face penalties for not delivering the promised power or must sell excess electricity at low prices. The study proposes the integration of power sources, particularly the coordination between wind and thermal power, to balance capacity and minimize the risk of penalties or compensations. Experiments on the IEEE 30-nút system model demonstrate that this integration yields higher profits than independent power plant operations.

Key words - Wind Power; Electricity Market; Uncertain; Investment Strategy; Generation Expansion Plan

1. Giới thiệu

Trên toàn cầu, sự gia tăng của năng lượng tái tạo đang chứng kiến một sự tăng trưởng mạnh mẽ, đặc biệt qua sự mở rộng của các trang trại gió có quy mô từ trung bình đến lớn [2]. Trong khoảng thời gian 2017-2018, ngành này đã ghi nhận mức tăng trưởng ấn tượng, khoảng 10% hàng năm, một mức độ tăng trưởng chưa từng thấy và khó dự đoán trước [3]. Sau cuộc khủng hoảng năng lượng 2022 tại Châu Âu, sự phát triển của năng lượng tái tạo đã được đẩy mạnh hơn bao giờ hết, nhằm thay thế cho nguồn cung năng lượng khí đốt bị hạn chế. Các quốc gia toàn cầu đã quyết định đầu tư và tăng cường phát triển năng lượng tái tạo, trong đó năng lượng gió nắm giữ một vai trò trung tâm, để giảm thiểu sự phụ thuộc vào nhiên liệu hóa thạch [4]. Sự gia tăng của tỷ lệ năng lượng từ gió cũng mang lại những lợi ích môi trường không thể phủ nhận [5, 6], và tham gia vào thị trường điện cạnh tranh nay đã trở thành một xu hướng ở châu Âu [7].

Ở Việt Nam, sự chấp thuận của quy hoạch phát triển điện lực quốc gia từ 2021 đến 2030 với tầm nhìn xa đến 2050 đã đặt nền móng vững chắc cho việc mở rộng cả nguồn điện và mạng lưới truyền tải, cũng như việc phát triển cấu trúc vận hành cho thị trường điện trong tương lai [8]. Với một chính sách phát triển năng lượng tái tạo được định hình rõ ràng, Việt Nam đã thiết lập mục tiêu phát triển năng lượng gió và năng lượng mặt trời như những ưu tiên chiến lược để tiến tới mục tiêu phát thải ròng bằng không vào năm 2050. Quy hoạch cũng kỳ vọng vào sự mở rộng không hạn chế của năng lượng gió cả ngoài khơi lẫn trong đất liền, với mục tiêu cụ thể là đến năm 2030, công suất năng lượng gió của Việt Nam sẽ vượt quá 28 GW và phấn đấu để đạt mức trên 100 GW vào năm 2050.

Một trong những hạn chế của năng lượng gió khi được kết hợp vào hệ thống thị trường điện theo thời gian thực là đặc tính không thể dự đoán trước của nó. Tính không ổn định này gây ra trở ngại không nhỏ cho việc hội nhập của năng lượng gió vào thị trường điện một cách công bằng và không giới hạn. Do đó, việc áp dụng chiến lược đấu thầu cẩn trọng và có kế hoạch được xem xét kỹ lưỡng là cần thiết để năng lượng gió có thể cạnh tranh ngang hàng với các loại năng lượng truyền thống trong thị trường điện cạnh tranh. Một số nghiên cứu đã được thực hiện để khám phá những tác động của năng lượng gió đối với hệ thống điện và các vấn đề phát sinh từ tính không ổn định của nó [9]. Đã có những giải pháp được đề xuất để giảm thiểu chi phí do sự mất cân đối năng lượng gây ra bằng cách tham gia vào thị trường [10], trong khi một số ý kiến khác lại cho rằng thị trường điện có thể hưởng lợi từ việc giảm giá và cân bằng lượng cung cấp nhờ

[1] Hochiminh City University of Technology and Education, Hochiminh, Vietnam (Dinh Ngoc Sang, Truong Viet Anh)
[2] Electric Power University, Hanoi, Vietnam (Nguyen Tung Linh)

vào sự linh hoạt của hệ thống [11].

Để giải quyết những thách thức này, việc phát triển chiến lược đấu giá hiệu quả cho nguồn năng lượng gió dựa trên các mô hình xác suất có liên kết giữa năng lượng gió và năng lượng nhiệt điện được đề xuất trong bài báo này, làm tăng khả năng thực thi cho các nhà đầu tư năng lượng gió. Phương pháp này nhằm tăng cường độ tin cậy cho những nhà đầu tư và thị trường bằng cách cung cấp cái nhìn sâu sắc hơn về rủi ro doanh thu liên quan đến năng lượng gió. Các chủ sở hữu nhà máy gió có thể cải thiện hiệu suất tài chính và tối đa hóa lợi ích xã hội bằng cách áp dụng các chiến lược quản lý tiên tiến và tối ưu hóa quyết định đấu thầu.

Điều này được chứng minh qua việc sử dụng mô hình mạng IEEE 30-BUS để mô phỏng kịch bản năng lượng gió, cho thấy rằng sự không ổn định có thể được giảm thiểu đáng kể khi kết hợp năng lượng gió với nguồn năng lượng nhiệt điện. Kết quả này khuyến khích các chủ nhà máy điện gió mở rộng đầu tư, cải thiện hiệu quả kinh tế, và đóng góp vào sự phát triển bền vững của hành tinh.

2. Mô hình bài toán

Đầu tư một trang trại gió bao gồm các thành phần : (i) Turbine gió; (ii) Hệ thống lưới điện nội bộ kết nối các tua-bin; (iii) Đường dây và trạm biến áp để kết nối điện gió với lưới điện địa phương. Trong tài liệu này chỉ xét đến sự ảnh hưởng của kênh đầu tư turbine gió bởi giá trị đầu tư của nó là lớn nhất và sự biến động tốc độ gió tác động lên turbine gió

2.1. Doanh thu điện gió trong thị trường điện

Không giống như các loại nguồn chủ động khác, các nhà máy điện gió nhận được hai thành phần doanh thu là doanh thu trực tiếp và doanh thu bất định, biểu diễn theo [11] như sau:

$$R_w(P_w) = \sum R_{w,i} = \sum \left[R_{ws,i}(P_{ws,i}) + R_{wu,i}(\Delta P_{w,i})\right] \quad (1)$$

Doanh thu trực tiếp R_{ws} được tạo ra từ việc bán điện theo lịch đấu thầu trực tiếp trên thị trường điện, sản lượng điện gió dự kiến trước. Đối với doanh thu bất định R_{wu} gồm hai thành phần: doanh thu bán năng lượng dư thừa ngoài dự đoán ban đầu và chi phí bồi thường (hoặc phạt) phát sinh do thiếu hụt năng lượng so với dự báo ban đầu.

P_w là sản lượng điện bán ra theo thời gian thực; $P_{ws,i}$ và $\Delta P_{w,i} = P_{wav,i} - P_{ws,i}$ là công suất chào đấu thầu và mức chênh lệch giữa thực tế và chào thầu.

i) Doanh thu trực tiếp, theo [1] được tính,

$$R_{ws,i}(P_{ws,i}) = g_i P_{ws,i} \quad (2)$$

g_i giá bán điện chào thầu của nguồn điện gió thứ i tương ứng với sản lượng $P_{ws,i}$.

Đối với các thị trường điện có nguồn nhiệt điện chi phối, điển hình như thị trường điện Châu Âu, giá điện gió chào thầu trước đó thường được dự đoán dựa trên giá bán điện trung bình của các nguồn nhiệt điện khí [6]. Trong nghiên cứu này giả sử giá bán điện gió xác lập theo giá điện trung bình của nhiệt điện trên thị trường điện,

$$C_{T0}(P_{TG}) = \sum_{i=1}^{N_{TG}} \left(a_i + b_i P_{TG,i} + c_i P_{TG,i}^2\right) \quad (3)$$

$$\lambda_{TG,i} = b_i + c_i P_{TG,i} \quad (4)$$

$$g = \overline{\lambda_{TG}} = \frac{\sum_{i=1}^{N_{TG}} \lambda_{TG,i}}{P_{TG}} \quad (5)$$

a_i, b_i, và c_i là các hệ số tính thành phần chi phí phát điện của các nguồng nhiệt điện tương ứng với sản lượng nghiệt điện phát ra $P_{TG,i}$. $\lambda_{TG,i}$ và $\overline{\lambda_{TG}}$ là đơn giá giả sử của các nguồn nhiệt điện và trung bình giá của các nguồng nhiệt điện.

ii) Doanh thu bất định của điện gió

$$R_{wu,i}(\Delta P_{w,i}) = \begin{cases} R_{Rw,i}(\Delta P_{w,i}), & nếu\ P_{wav,i} \geq P_{ws,i} \\ C_{Pw,i}(\Delta P_{w,i}), & nếu\ P_{wav,i} \leq P_{ws,i} \end{cases} \quad (6)$$

R_{Rw} là doanh thu bán điện dư thừa và C_{Pw} là chi phí bồi thường (hoặc phạt) của điện gió khi bị thiếu hụt sản lượng điện. Thành phần doanh thu và chi phí phí, theo [1]:

$$R_{Rw,i}(\Delta P_{w,i}) = k_{R,i} g_i (P_{wav,i} - P_{ws,i}) = k_{R,i} g_i \int_{P_{ws,i}}^{P_{wr,i}} (p_{w,i} - P_{ws,i}) f_w(p_{w,i}) dp_{w,i} \quad (7)$$

$$C_{Pw,i}(\Delta P_{w,i}) = k_{P,i} g_i (P_{wav,i} - P_{ws,i}) = k_{P,i} g_i \int_{0}^{P_{ws,i}} (p_{w,i} - P_{ws,i}) f_w(p_{w,i}) dp_{w,i} \quad (8)$$

$k_{R,i}$ và $k_{P,i}$ là các hệ số chênh lệch giá bán điện dư thừa và hệ số phạt đối với sản lượng điện thiếu hụt, so với giá chào bán điện gió theo kế hoạch trên thị trường điện. Hệ số phạt (hay bồi thường) là tỷ lệ giữa đơn giá điện gió bị bồi thường hoặc bị phạt so với đơn giá chào thầu điện gió trước đó. Chỉ xảy ra khi công suất gió thực tế không đạt được so với công suất chào thầu. Khi đó, chủ đầu tư điện gió phải mua điện giao ngay để bù cho khoản thiếu hụt, hoặc chấp nhận phạt hợp đồng nếu không mua điện đền bù.

2.2. Mô hình xác suất không ổn định của điện gió

Một số nghiên cứu gần đây sử dụng phân bố xác suất Weibull hai tham số để đánh giá năng lượng gió [2]. Mô hình tần suất của tốc độ gió được viết như sau,

$$f(v) = \left(\frac{k}{c}\right)\left(\frac{v}{c}\right)^{k-1} e^{-\left(\frac{v}{c}\right)^k} \quad (9)$$

Các hệ số k và c gọi là hệ số hình dạng và hệ số tỷ lệ. Hình 1 dưới đây biểu diễn mô phỏng kết quả tần suất gió của một mô hình gió tương ứng *c=9; k=2* và *c=10; k=2*, Kết quả từ [3, 4, 5, 6]. Theo [1], Công suất điện gió theo tốc độ gió được mô tả như sau,

$$P_w(v) = \begin{cases} 0, & v < v_{in}\ và\ v > v_{out} \\ P_{wr}\left(\dfrac{v - v_{in}}{v_r - v_{in}}\right), & v_{in} \leq v \leq v_r \\ P_{wr}, & v_r < v \leq v_{out} \end{cases} \quad (10)$$

v_{in}, v_r và v_{out} là tốc độ gió bắt đầu, trung bình và khép cánh của turbine gió; P_{wr} là công suất định mức tương ứng. Trên Hình 2 thể hiện phân bố xác suất công suất điện gió của turbine ở hai vị trí khác nhau: Gen 1 có c = 9m/s; k = 2 và Gen 2 có c = 10m/s; k = 2. Thông số kỹ thuật cơ bản của turbine gió: P_{wr}=3MW; v_{in}=3m/s; v_r=16m/s và v_{out}=25m/s.

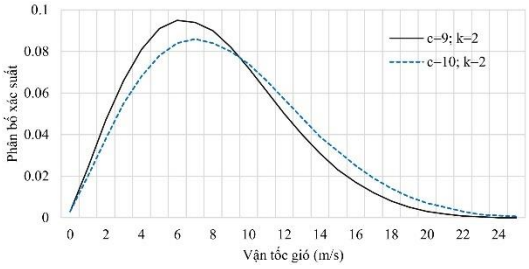

Hình 1. *Phân bố xác suất Weibull tốc độ gió với cá mô hình c=9; k=2 và c=10; k=2*

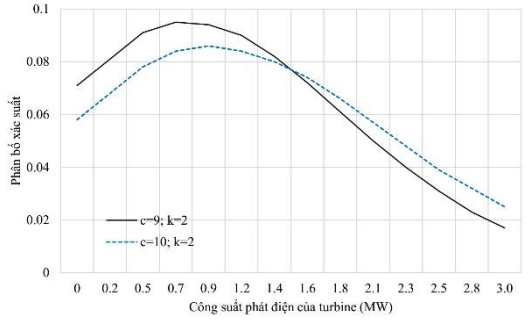

Hình 2. *Phân bố xác suất công suất điện gió theo Weibull tại hai vị trí khác nhau*

2.3. Hàm mục tiêu của bài toán

Mục tiêu chính được nêu ngay từ đầu của nghiên cứu này là tập trung vào hiệu quả tài chính của việc đầu tư vào năng lượng gió trong thị trường điện. Để một trang trại gió phát triển mạnh trên thị trường điện, việc tham gia vào quá trình đấu thầu giá bán điện và sản lượng điện là bắt buộc nhằm mục đích tối đa hóa doanh thu. Cũng đã trình bày, doanh thu được tạo ra từ điện gió gồm có doanh thu trực tiếp và doanh thu bất định. Hàm mục tiêu toán học cho các yêu cầu này thể hiện như sau:

$$Cực\ đại\ \{F = R_w(P_w)\} \quad (11)$$

2.4. Các kịch bản nghiên cứu

(i) Kịch bản trang trại gió độc lập (GĐK): Kịch bản truyền thống này liên quan đến nhiều turbine gió trong một trang trại được đầu tư.

(ii) Kịch bản tích hợp nhiều trang trại gió (GLK): Trong kịch bản này, các trang trại gió khác nhau có thể cùng một chủ đầu tư hoặc các chủ khác nhau nhưng trong đó vận hành phối hợp để bù đắp cho nhau khi cần thiết.

(iii) Tích hợp trang trại điện gió và nguồn nhiệt điện (GNK): Có thể chủ một nguồn nhiệt điện đầu tư thêm trang trại điện gió, hoặc chủ các nguồn nhiệt điện và điện gió kết hợp điều hành bù đắp sản lượng khi cần thiết.

(i) Kịch bản GĐK

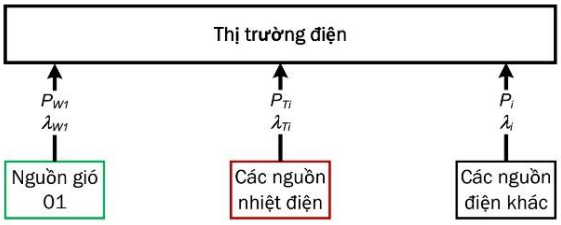

Hình 3. *Kịch bản điện gió độc lập trong thị trường điện (*GĐK*)*

Xác suất công suất điện một turbine gió được thể hiện như trên Hình 2, theo quy luật xác suất thì một trang trại điện gió gồm nhiều turbine thì phân bố xác suất sẽ là tổ hợp của tất cả các turbine gió đơn lẻ. Và hai trang trại gió thi phân bố xác suất được tổ hợp của từng trang trại. Biểu thức tổ hợp như sau,

$$PDF_{\mathrm{F}}(P_t) = \prod_{i=1}^{N_T} PDF_{T,i}(P_{t,i}) \quad (12)$$

$$P_F = \sum_{i=1}^{N_T} P_{t,i} \quad (13)$$

Trong đó, PDF_{F} và P_F lần lượt là phân bố xác suất và công suất điện của turbine gió (nếu tổ hợp các turbine) hoặc của trang trại gió (nếu tổ hợp các trang trại gió).

Khi đó doanh thi của điện gió được xác định bởi giá trị doanh thu trực tiếp khi chào đấu thầu và thành phần phạt (nếu có) khi sản lượng điện không đạt theo kế hoạch dấu thầu. Kết quả xác định theo các biểu thức (2), (6), và mục tiêu được xác lập theo biểu thức (11).

(ii) Kịch bản GLK

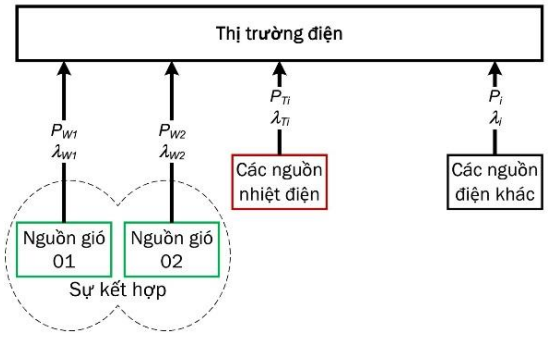

Hình 4. *Kịch bản liên kết các điện gió trong thị trường (GLK)*

Trong trường hợp các nguồn điện gió có tác động tương hỗ lẫn nhau trong quá trình vận hành, theo xác suất nguồn gió này có thể thiếu sẽ được bù đắp bởi nguồn gió khác dư thừa công suất. Điều này có thể dẫn đến một tổng thể giảm đi xác suất bồi thường hoặc phạt do thiếu hụt sản lượng điện khi đấu thầu trên thị trường điện.

(iii) Kịch bản GNK

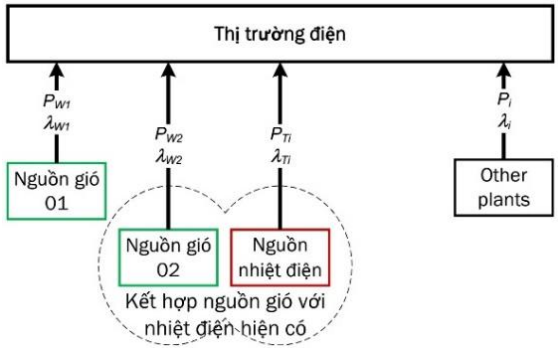

Hình 5. *Kịch bản liên kết điện gió với nhiệt điện trên thị trường (GNK)*

$$R_{wu}(P_{\mathrm{p}}) = \begin{cases} R_w(P_{\mathrm{p}}), & nếu\ P_p \geq 0 \\ C_p(P_{\mathrm{p}}), & nếu\ P_{TR} \geq -P_p > 0 \\ C_{Pw}(P_{\mathrm{p}}), & nếu\ -P_p > P_{TR} \end{cases} \quad (14)$$

$P_p = P_{Tav} - P_{Ts}$ Khi $-P_p > P_{TR}$,

$C_{Pw}(P_{\mathrm{p}}) = C_{Pw}(\Delta P_{\mathrm{p}}) + C_p(P_{\mathrm{TR}})$

$\Delta P_p = P_p - P_{TR}$

Sự đóng góp của nguồn nhiệt điện trong tổ hợp gió và nhiệt điện tỏ ra hiệu quả nhiều hơn. Doanh thu theo biểu thức (6) được viết lại khi có sự tham gia của nguồn nhiệt điện như sau,

P_p là lượng công suất chênh lệch giữa lượng điện bán ra thực tế so với kế hoạch đấu thầu đã chào cho thị trường điện trước đó; R_w, C_p và C_{Pw} là doanh thu bàn điện dư thừa, chi phí trả cho nguồn nhiệt điện lượng công suất được nguồn nhiệt điện đó bù cho thiếu hụt của điện gió, và chi phí phạt còn lại nếu vẫn còn xảy ra thiếu sản lượng điện sau khi nhiệt điện đã bù; P_{Tqv} và P_{Ts} là để xác định lượng công suất dự phòng của nguồn nhiệt điện, lượng điện tối đa có thể bù đắp cho nguồn điện gió.

2.5. Lưu đồ thuật toán đề xuất

Tất cả các bước trong biểu đồ quy trình được hiển thị trong sơ đồ Hình 6,

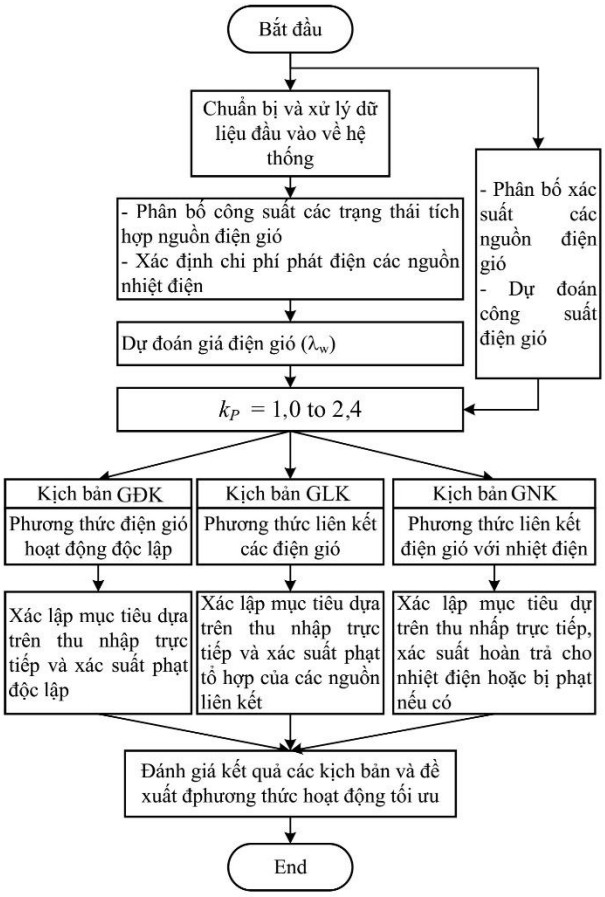

Hình 6. *Lưu đồ đánh giá các kịch bản đề xuất*

Quá trình thực thi mô hình để đánh giá và đề xuất được tính toán và phân tích kết quả theo 4 bước như sau:

i) Xây dựng cơ sở dữ liệu xác suất cho các turbine, tổ hợp cho các trang trại điện gió.

ii) Xây dựng dữ liệu vận hành hệ thống điện. Mô phỏng xác suất nguồn điện gió trong hệ thống điện và phân bốp công suất tối ưu của hệ thống để dự đoán công suất các nguồn điện và giá bán điện của họ.

iii) Mô hình doanh thu của các nguồn điện gió theo từng kịch bản, từ đó xác định vùng công suất điện gió tối ưu theo từng kịch bản.

iv) Đánh giá, lựa chọn mô hình và kết quả đấu thầu giá điện gió và lịch trình phát điện trên thị trường điện.

3. Mô phỏng và đánh giá

3.1. Dữ liệu và thông số mô hình

3.1.1. Hệ thống điện IEEE 30 nút

Hệ thống IEEE 30 nút được chọn lựa để thử nghiệm các kịch bản theo mô hình đề xuất của bài báo này. Cấu hình hệ thống điện có 30 nút, 41 nhánh và 6 nguồn và các thông số lưới điện của nó được lấy từ tài liệu tham khảo [7, 8]. Hình lưới điện và các chi tiết khác của lưới điện chuẩn tham khảo tại [9]. Bốn nhà máy nhiệt điện được đặt tại các nút 1, 2, 8 và 13 có thông số như Bảng 1, và hai trang trại gió đã tại các nút 5 và 11 thông số theo Bảng 2. 25 turbine gió 3MW định mức tại nút 5 với tổng công suất là 75MW; và 20 turbine ở nút 11 tổng công suất là 60MW. Phân xác suất tốc độ gió tại hai địa điểm này dùng hai tham số Weibull và PDF tương ứng cho mỗi trang trại được trình bày trong Hình 1.

Bảng 1. *Thông số nhà máy nhiệt điện*

Nguồn	Nút	a	b	c
TG1	1	0	2	0,00375
TG2	2	0	1,75	0,0175
TG3	8	0	3,25	0,00834
TG4	13	0	3	0,025

Bảng 2. *Thông số nhà máy điện gió*

Các nguồn điện gió				
Nút	Số turbine	Công suất định mức, P_{wr}(MW)	Hệ số Weibull	Vận tốc trung bình, M_{wbl}
5	25	75	c=9, k=2	v=7,976m/s
11	20	60	c=10, k=2	v=8,862m/s

3.1.2. Sản lượng điện của nguồn điện gió tại Nút 5

Về dự đoán sản lượng điện gió ngày giả sử tại hai địa điểm nguồn điện gió là như nhau, được chia thành hai mùa: mùa cao điểm (giả sử kéo dài sáu tháng) và mùa thấp điểm (giả sử sáu tháng còn lại), tham khảo từ [10] cho ở Hình 7.

Một thị trường điện giả sử cho phép điện gió chào thầu với sai số 10%, Vùng suất công suất các thành phần được thể hiện trong biểu đồ Hình 8. Trong hình có thể hiện hai đường biên xác định xác suất công suất dư thừa (nét đứt hai chấm) và xác suất công suất thiếu hụt (nét đứt một chấm). Trên cơ sở này, sản lượng điện ngày cao điểm được cho ở Hình 9.

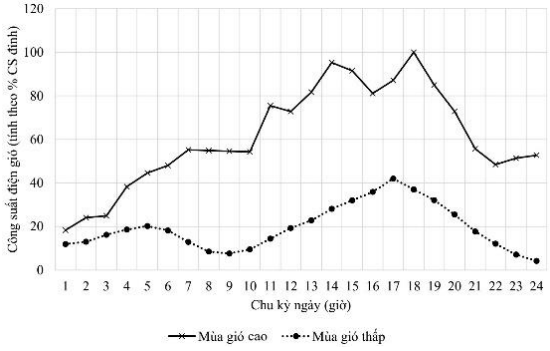

Hình 7. *Biểu đồ công suất điện gió dự đoán ngày*

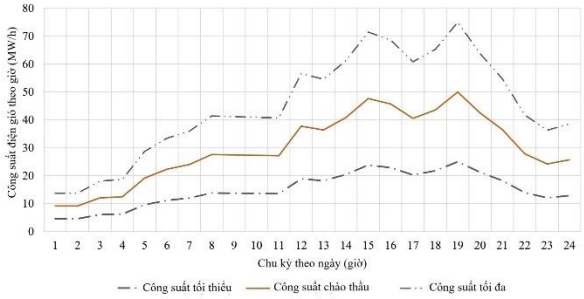

Hình 8. *Biểu đồ xác suất công suất điện gió ngày cao điểm tại Nút 5*

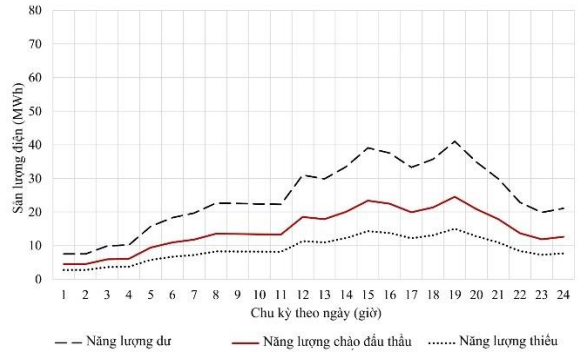

Hình 9. *Biểu đồ xác suất sản lượng điện gió ngày cao điểm tại Nút 5*

3.2. Kịch bản GĐK

Doanh thu của một nguồn điện gió tại nút 5 được chọn khảo sát trong kịch bản này. Phân bố xác suất tổ hợp của 25 turbine gió trong trang trại tại nút 5 và doanh thu biến đổi theo mức phạt được cho tại Hình 10 và Hình 11.

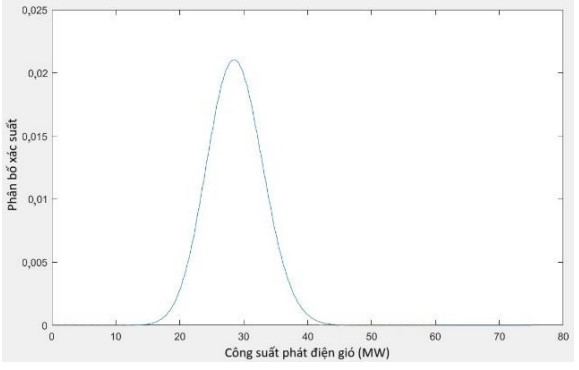

Hình 10. *PDF trang trại gió nút 5*

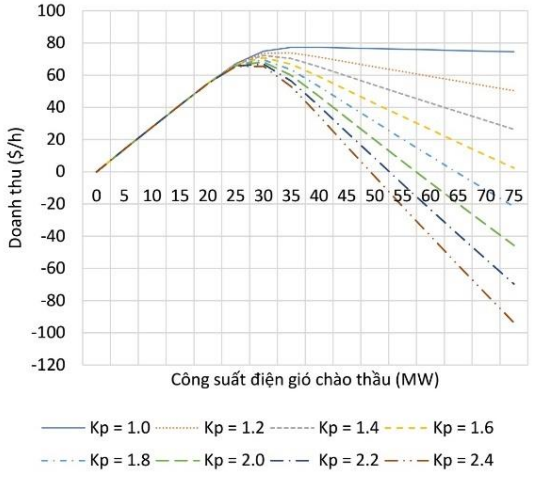

Hình 11. *Doanh thu độc lập trang trại gió nút 5*

Doanh thu được tạo ra bởi nguồn điện gió tại Nút 5 xác lập đỉnh trong khoảng từ 30MW đến 40MW đối với gần như tất cả mức phạt khác nhau.

3.3. Kịch bản GLK

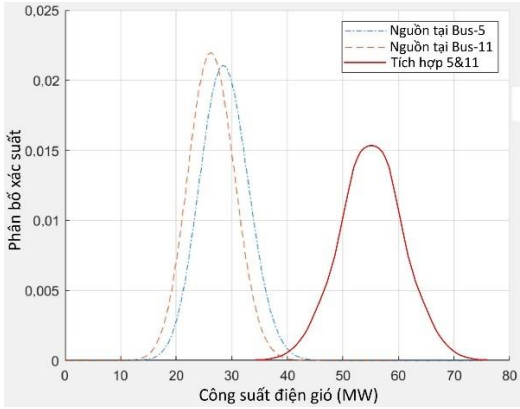

Hình 12. *PDF từng trang trại gió nút 5, nút 11 và PDF tổ hợp*

Khi các nguồn điện gió liên kết với nhau, trong kịch bản này xét hai nguồn điện gió tại nút 5 và 11, PDF của tổ hợp hai nguồn điện gió được xác định trên Hình 12. Hình dạng của đường cong là tương tự từng trang trại gió, nhưng có đỉnh thấp hơn một chút và độ dốc thoải hơn về hai phía so với xác xuất gốc.

Đánh giá doanh thu của việc liên kết này, xét phân tích kết quả doanh thu của trang trại gió nằm ở nút 5 so với kịch bản trước đó, kịch bản gió độc lập, cho kết quả như mô tả trong Hình 13. Đúng như dự đoán, khi tỷ lệ bồi thường trong thị trường điện tăng, doanh thu ở tất cả các kịch bản đều giảm. Tuy nhiên, việc liên kết hai trang trại gió cho thấy doanh thu giảm vừa phải hơn do hiệu ứng bù trừ lẫn nhau giữa các trang trại.

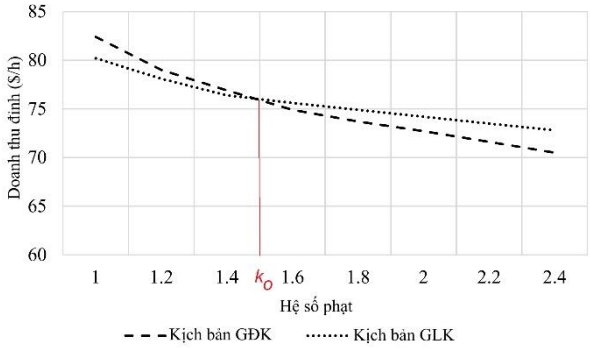

Hình 13. *So sánh doanh thu hai kịch bản* GĐK *và* GLK *theo tỷ số bồi thường*

3.4. Kịch bản GNK

Giả sử nguồn nhiệt điện tại nút 1 liên kết với nguồn điện gió tại nút 5. Lượng công suất dự phòng của nguồn nút 1 xác định dựa vào phân bố công suất tối ưu trên hệ thống khi tất cả các nguồn tham gia. Kết quả doanh thu điện gió nút 5 được mô tả trên Hình 14.

Có một giá trị tỷ lệ phạt mà đường cong doanh thu không thay đổi so với kịch bản trước đó, đó là khi k=1,0. Còn lại, rõ ràng là hình dạng của đa số các đường cong thể hiện một sự gợn sóng về phía tăng trưởng doanh thu tại vị trí gần đỉnh. Khi giá trị đền bù vượt quá chi phí sản xuất của các nhà máy nhiệt điện, khi đó thay vì để phạt thì sử

dụng nguồn nhiệt điện để bù cho khoản công suất thiếu hụt, dẫn đến đỉnh dòng tiền tăng lên đáng kể. Ví dụ: khi k>1,1, doanh thu tối đa sẽ tăng từ dưới 150 USD/h lên trên 180 USD/h. Tuy nhiên, có một điểm giống như các kịch bản trước đây, đó là tỷ lệ bồi thường cao hơn tương ứng sẽ dẫn đến việc giảm đỉnh doanh thu.

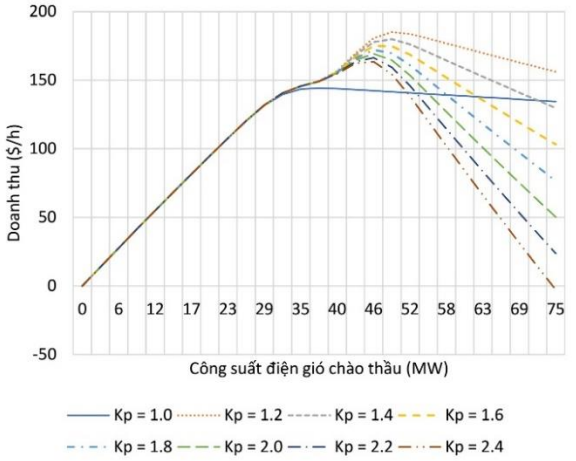

Hình 14. *Doanh thu nguồn điện gió nút 5 khi có liên kết với nhiệt điện*

Ngoài ra, tương ứng với đỉnh doanh thu tăng lên thì công suất đỉnh cũng tăng lên so với các kịch bản trước đây. Cụ thể, công suất đỉnh tăng từ khoảng 60 MW trong kịch bản GĐK lên gần 90 MW trong kịch bản này. Đó là sự chắc chắn ngày càng cao bởi sự hỗ trợ của nguồn nhiệt điện, mà tác động của nó càng cao khi mức phạt càng lớn. Do đó, việc chào sản lượng điện gió cao hơn trên thị trường điện trong trường hợp này là lý do dẫn đến sự gia tăng doanh thu cực đại này.

3.5. Nhận xét

Một sự so sánh lợi ích của nhà đầu tư điện gió nút 5 từ ba kịch bản theo ba phương thức hoạt động giao dịch thương mại (GĐK – hoạt động độc lập; GLK – liên kết giữa hai nguồn điện gió; và GNK – liên kết giữa điện gió và nguồn nhiệt điện). Kết quả doanh thu đỉnh của từng kịch bản biến đổi theo mức độ phạt (hay bồi thường khi thiếu hụt công suất phát điện) cho ở biểu đồ trên Hình 15.

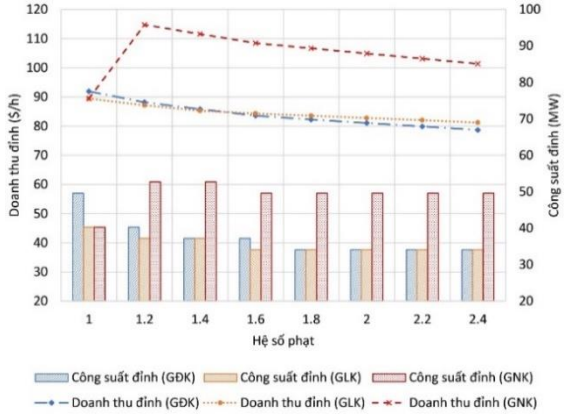

Hình 15. *So sánh tối ưu của các kịch bản theo tỷ số bồi thường*

Với doanh thu đỉnh thể hiện bằng các đường, trên hình cho thấy cả ba kịch bản đều có doanh thu giảm đi khi mức độ phạt thiếu hụt công suất phát điện theo thơi gian thực so với kế hoạch chào thầu tăng lên. Mức giảm dường như có tỷ lệ giảm gần tương đồng nhau, nhưng trong đó có kịch bản liên kết giữa các nhà máy điện gió dường như tốc độ giảm thấp hơn. Điều này giúp cho kịch bản liên kết các điện gió này mang lại lợi nhuận cao hơn khi mức phạt tăng lên.

Trong khi đó, kịch bản liên kết điện gió với nguồn nhiệt điện cho doanh thu tăng cao hơn hẳn so với các kịch bản còn lại khi thị trường điện tồn tại hình thức phạt thiếu hụt công suất khi phát điện so với kế hoạch chào thầu. Như vậy, hiệu quả liên kết sử dụng lượng công suất dự phòng của nhà máy nhiệt điện để bù đắp cho công suất thiếu hụt của điện gió khi cần thiết là đáng khích lệ và nên khai thác triệt để.

Về công suất chào thầu tối ưu của nguồn điện gió được khuyến khích làm sao để mang lại lợi ích lớn nhất cho chủ sở hữu điện gió đó. Trên hiểu đồ Hình 15 là biểu đồ thanh đứng, cho thấy trong trường hợp tồn tại phạt, kịch bản liên kết gió với nguồn nhiệt điện có xu hướng khuyến khích chào công suất đỉnh cao hơn so với các kịch bản còn lại. Mức công suất cao hơn lên đến trên 10MW (tức trên 20% công suất định mức của nguồn điện gió). Điều này được lý giải là do chủ điện gió tin tưởng vào việc bù đắp của nguồn nhiệt điện trong liên doanh để chào công suất chắc chắn cao hơn, và như vậy lợi nhuận trực tiếp cho nguồn điện gió tăng lên đáng kể.

4. Kết luận

Dự báo chính xác công suất sản xuất của các trang trại gió là một thách thức quan trọng khi tham gia đấu thầu cung cấp điện trong thị trường điện. Việc cắt giảm gần đây các chính sách thúc đẩy phát triển điện gió đã làm tăng thêm những khó khăn mà các chủ trang trại gió phải đối mặt, dẫn đến đầu tư vào các dự án điện gió bị chậm lại, đặc biệt các quốc gia đang phát triển như Việt Nam.

Nghiên cứu này giới thiệu một phương pháp đánh giá và các kịch bản mô hình vận hành liên kết các nhà máy điện, trong đó chủ yếu kết hợp các trang trại gió với nhà máy nhiệt điện nhằm mang lại hiệu quả đầu tư cho cả chủ sở hữu điện gió và phúc lợi xã hội toàn diện hơn trong thị trường điện.

Kết quả khảo sát và thử nghiệm đã cung cấp cái nhìn sâu sắc hơn, tính ưu việt hơn đối với kịch bản thứ ba, kịch bản liên kết giữa điện gió với nhà máy nhiệt điện hiện có. Trong liên kết này, lợi nhuận đỉnh cho các trang trại gió đạt được khi mức phạt của thị trường điện càng tăng cao, đặc biệt khi hệ số bồi thường vượt quá 1,5 thì doanh thu cao hơn kịch bản kế cần ít nhất 10% và lên đến hơn 25% so với kịch bản truyền thống, nguồn gió hoạt động độc lập. Những phát hiện này nhấn mạnh trong mọi hình thức sở hữu hoặc liên kết nguồn điện gió với nguồn nhiệt điện sẽ nâng cao tính chắc chắn của năng lượng gió và mang lại nhiều lợi ích đáng kể hơn trong thị trường điện cạnh tranh, mà các nhà hoạch định chiến lược, các nhà tài phiệt, và cả các nhà quản lý cũng cần quan tâm khai thác.

Ngoài ra, việc chào công suất điện gió cao hơn hẳn so với các kịch bản còn lại, sự liên kết giữa điện gió và nguồn nhiệt điện đã mang lại hiệu quả sử dụng năng lượng tái tạo cao lên đáng kể, giúp khai thác tối đa nguồn năng lượng tái tạo và giúp phát triển bền vững hơn cho lĩnh vực năng lượng tái tạo theo đúng mục tiêu và xu hướng của toàn thế giới.

TÀI LIỆU THAM KHẢO

[1] REN21 Secretariat, *"Renewables 2021 - Global status report"*, International Energy Agency (IEA), Paris, France, 2021.

[2] D. Cao *et al.*, "Bidding strategy for trading wind energy and purchasing reserve of wind power producer – A DRL based approach", *Electrical Power & Energy Systems*, vol. 117, pp. 105648, 2020. https://doi.org/10.1016/j.ijepes.2019.105648

[3] T. J. Hammons, "Integrating renewable energy sources into European grids", *Electrical Power & Energy Systems*, vol. 30, no. 8, pp. 462-475, 2008. https://doi.org/10.1016/j.ijepes.2008.04.010

[4] N. Wang, J. Li, W. Hu, B. Zhang, Q. Huang and Z. Chen, "Optimal reactive power dispatch of a full-scale converter based wind farm considering loss minimization", *Renewable Energy*, vol. 139, pp. 292-301, 2019. https://doi.org/10.1016/j.renene.2019.02.037

[5] J. Li, N. Wang, D. Zhou, W. Hu, Q. Huang, Z. Chen and F. Blaabjerg, "Optimal reactive power dispatch of permanent magnet synchronous generator-based wind farm considering levelised production cost minimisation", *Renewable Energy*, vol. 145, pp. 1-12, 2020. https://doi.org/10.1016/j.renene.2019.06.014

[6] European Commssion, *"Energy Prices and Costs in Europe: Report from the commission to the european parliament, the council, the european economic and social committee and the committee of the regions"*, Brussels, 2020.

[7] Energy Institute, *"The Planning for Vietnam's Power Development for the Period 2021-2030, with a Vision to 2050 (Power Development Plan VIII)"*, Hanoi, 2023.

[8] P. Shinde and M. Amelin, "A Literature Review of Intraday Electricity Markets and Prices", *IEEE Milan PowerTech*, 2019, pp. 18938508. doi: 10.1109/PTC.2019.8810752

[9] H. Holttinen, "Handling of wind power forecast errors in the Nordic power market", *International Conference on Probabilistic Methods Applied to Power Systems*, 2006, pp 9475028. doi: 10.1109/PMAPS.2006.360288

[10] J. Dobschinski *et al.*, "The potential of advanced shortest-term forecasts and dynamic prediction intervals for reducing the wind power induced reserve requirements", *Scientific Proceedings of the European Wind Power Conference*, 2010, p. 177–182.

[11] P. P. Biswas, P. N. Suganthan, and G. A. J. Amaratunga, "Optimal power flow solutions incorporating stochastic wind and solar power", *Energy Conversion and Management*, vol. 148, pp. 1194-1207, 2017. https://doi.org/10.1016/j.enconman.2017.06.071

[12] P. Wais, "A review of Weibull functions in wind sector", *Renewable and Sustainable Energy Reviews*, vol. 70, pp. 1099-1107, 2017. https://doi.org/10.1016/j.rser.2016.12.014

[13] R. Roy and H. T. Jadhav, "Optimal power flow solution of power system incorporating stochastic wind power using Gbest guided artificial bee colony algorithm", *Electrical Power and Energy Systems*, vol. 64, pp. 562-578, 2015. https://doi.org/10.1016/j.ijepes.2014.07.010

[14] A. Panda and M. Tripathy, "Optimal power flow solution of wind integrated power system using modified bacteria foraging algorithm", *Electrical Power and Energy Systems*, vol. 54, pp. 306-314, 2014. https://doi.org/10.1016/j.ijepes.2013.07.018

[15] A. Panda and M. Tripathy, "Security constrained optimal power flow solution of wind-thermal generation system using modified bacteria foraging algorithm", *Energy*, vol. 93, no. 1, pp. 816-827, 2015. https://doi.org/10.1016/j.energy.2015.09.083

[16] L. Shi, C. Wang, L. Yao, Y. Ni and M. Bazargan, "Optimal Power Flow Solution Incorporating Wind Power", *IEEE Systems Journal*, vol. 6, no. 2, pp. 233-241, 2012. doi:10.1109/JSYST.2011.2162896

[17] O. Alsac and B. Stott, "Optimal Load Flow with Steady-State Security", *IEEE Transactions on Power Apparatus and Systems*, Vol: PAS-93, no. 3, pp. 745-751, 1974. doi: 10.1109/TPAS.1974.293972

[18] R. Ferrero, S. Shahidehpour and V. Ramesh, "Transaction analysis in deregulated power systems using game theory", *IEEE Transactions on Power Systems*, vol. 12, no. 3, pp. 1340-1347, 1997. doi:10.1109/59.630479

[19] R. Christie, "Power Systems Test Case Archive", August 1993. [Online]. Available: https://labs.ece.uw.edu/pstca/pf30/pg_tca30bus.htm. [Accessed 10 September 2023].

NGHIÊN CỨU ỨNG DỤNG PHƯƠNG PHÁP LAI TRONG BÀI TOÁN LỰA CHỌN HỢP LÝ VỊ TRÍ VÀ DUNG LƯỢNG HỆ THỐNG LƯU TRỮ NĂNG LƯỢNG TRONG HỆ THỐNG ĐIỆN

EXPLORING THE APPLICATION OF HYBRID METHODS FOR OPTIMAL LOCATION AND POWER SELECTION OF ENERGY STORAGE SYSTEMS IN POWER SYSTEMS

Trương Việt Anh[1], Nguyễn Tùng Linh[2,*], Đinh Ngọc Sang[3]

DOI: https://doi.org/10.57001/huih5804.2023.100

TÓM TẮT

Hệ thống lưu trữ năng lượng trong lưới điện truyền tải đang trở thành một lĩnh vực nghiên cứu và ứng dụng ngày càng quan trọng. Bài báo này đề xuất một phương pháp lai mới, nó đưa ra một định hướng xác định vị trí lắp đặt hệ thống lưu trữ năng lượng (ESS) phù hợp. Điều đó giúp cải thiện khả năng ổn định của lưới điện, giảm thiểu sự gián đoạn và sự cố, tăng cường tính linh hoạt và đáp ứng tốt hơn với nhu cầu sử dụng năng lượng của các khách hàng trước khi cần quy hoạch mở rộng truyền tải điện (TEP). Phương pháp này kết hợp lai giải thuật Min Cut (MC) với thuật toán di truyền (GA). Trước tiên, MC được cải tiến bằng một hình thức phạt để giảm thiểu không gian tìm kiếm cho bài toán tối ưu mà không làm mất đi nghiệm toàn cục. Tiếp theo, thuật toán GA được áp dụng để giải bài toán tối ưu trong không gian đã được giới hạn để tìm ra vị trí và công suất ESS phù hợp nhất có thể. Nghiên cứu được thử nghiệm và cho ra kết quả khả thi trên hệ thống điện IEEE 24-bus. Kết quả nghiên cứu cho thấy phương pháp đề xuất giảm đáng kể khối lượng tính toán so với các bài toán trước đây và từ đó rút ngắn thời gian tính toán giúp các nhà đầu tư đưa ra quyết định đầu tư hệ thống ESS kịp thời và cạnh tranh.

Từ khóa: *Thuật toán Mincut, thuật toán di truyền, bộ lưu trữ năng lượng, quy hoạch lưới truyền tải, thị trường điện.*

ABSTRACT

Energy storage systems (ESS) within the transmission system have emerged as a critical area of research and application. This paper presents a novel hybrid approach that offers a framework for determining optimal locations and power for deploying ESS. The primary objective is to enhance grid stability, minimize disruptions and failures, bolster flexibility, and effectively meet the energy demands of consumers prior to the need for transmission expansion planning (TEP). The proposed methodology combines the Min Cut (MC) algorithm with the genetic algorithm (GA). Initially, the MC algorithm is improved through the incorporation of a penalty mechanism, aimed at reducing the search space for the optimization problem while preserving global optimality. Subsequently, the GA algorithm is employed to solve the optimization problem within the constrained search space, thereby identifying the most suitable local and power for the ESS. The research findings are evaluated on the IEEE 24-bus power system and demonstrate promising feasibility. Notably, the proposed approach significantly reduces computational complexity when compared to previous separate methodologies, consequently diminishing computation time and facilitating timely and competitive investment decisions pertaining to ESS systems.

Keywords: *Min cut algorithm, gene algorithm, energy storage systems, transmission expansion plan, electricity market.*

[1]Trường Đại học Sư phạm kỹ thuật Thành phố Hồ Chí Minh
[2]Trường Đại học Điện lực
[3]Trường Đại học Kiến trúc Thành phố Hồ Chí Minh
[*]Email: linhnt@epu.edu.vn
Ngày nhận bài: 15/4/2023
Ngày nhận bài sửa sau phản biện: 05/6/2023
Ngày chấp nhận đăng: 15/6/2023

1. GIỚI THIỆU

Quy hoạch TEP và GEP đã được trình bày trong nghiên cứu [1, 2], theo đó TEP vẫn là giải pháp chính về lâu dài để phát triển mạng lưới năng lượng, đáp ứng nhu cầu thiết yếu cho công cuộc phát triển kinh tế và xã hội. Tuy nhiên, không phải lúc nào giải pháp xử lý quá tải hoặc tắc nghẽn, là các biện pháp chính trong quy hoạch TEP, cũng hoàn hảo để đạt được độ ổn định và độ tin cậy [3]. Vì vậy, các

biện pháp quy hoạch tối ưu và kinh tế hơn thường được sử dụng để cải thiện hệ thống điện, chẳng hạn như tái cấu trúc lưới điện có xét đến nguồn điện [4], điều khiển dòng công suất điện bằng thiết bị chuyển tải dòng điện linh hoạt (FACTS) [5], hoặc giải pháp xây dựng các nguồn năng lượng tái tạo mới [6, 7]. Kết quả, những phương pháp này cũng có nhiều ưu điểm nhưng cũng phát sinh các nhược điểm ở các mức độ khác nhau và chúng không thể thay thế cho nhau một cách hoàn hảo.

Trong giai đoạn phát triển mạnh mẽ của nguồn năng lượng tái tạo thời gian vừa qua, đặc biệt sau sự khủng hoảng năng lượng năm 2022 do giới hạn nguồn cung khí đốt từ một số quốc gia, thì năng lượng từ mặt trời và gió đã phát triển nhanh chóng ở nhiều nước trên thế giới [6, 7]. Toàn cầu đã bổ sung hơn 50 GW công suất hàng năm kể từ năm 2014. Riêng năm 2018 điện gió đạt 591GW, tăng 9,6% so với năm 2017 [8]. Nhưng hậu quả của nguồn năng lượng tái tạo để lại theo một khía cạnh vận hành hệ thống điện trong thị trường điện cạnh tranh là không hề nhỏ, như sự không chắc chắn, sự mất ổn định, sự mất an ninh, ….

Trong khi nhu cầu phụ tải điện ngày càng tăng để phục vụ cho phát triển kinh tế xã hội, kết hợp với sự phát triển của nguồn năng lượng tái tạo như vừa nêu có thể đẩy lưới điện đi đến quá tải cục bộ, hay còn gọi là tắc nghẽn truyền tải tại một thời điểm nào đó. Có nhiều cách để giải quyết các tắc nghẽn hệ thống điện [9-12], mở rộng lưới điện là cách kinh điển nhất chủ yếu dành cho quy hoạch dài hạn, điều chuyển phân bố công suất bằng các thiết bị FACTS và trong bài báo này hướng đến phương pháp quy hoạch nguồn ESS [5, 13]. Phương pháp mở rộng lưới điện truyền tải thường có kinh phí khá lớn và cần các điều kiện khá khó khăn khác như: đền bù giải tỏa, thay đổi điều kiện sống người dân nơi đường dây điện đi qua. Trong khí đó, mặc dù vốn đầu tư hiện nay không thấp nhưng ESS khá linh động vị trí lắp đặt và mang lại hiệu quả kép: giải quyết tắc nghẽn (như bài báo đề xuất) và cải thiện sự không chắc chắn mà nguồn năng lượng tái tạo gây ra.

Vấn đề xác định vị trí và công suất ESS thích hợp để giải quyết tắc nghẽn cục bộ cho hệ thống điện hiện có nhiều phương pháp, trong số đó có thể kể đến như mô hình toán AC và DC, thuật toán meta-heuristic như: bầy đàn (PSO), GA [2, 14]. Theo các nghiên cứu thời gian gần đây, một bài toán tối ưu có thể đề xuất phát triển theo chiều hướng hiệu quả hơn như sau:

Thuật toán tối ưu hóa cổ điển được sử dụng nhiều trước đây: là một kỹ thuật phân tích thường được sử dụng và kết quả thường là các giải pháp tối ưu toàn cục cho phiên bản phổ quát của bài toán số nguyên ban đầu, trong đó dữ liệu ban đầu là các số nguyên, được thay thế bằng các biến liên tục. Khối lượng tính toán trong các thuật toán này thường rất lớn và phương pháp này có thể can thiệp vào vấn đề hội tụ trong một số trường hợp, như trong [15, 16];

Giải thuật MC: khác với các thuật toán khác, nó luôn cho kết quả khá chính xác, khối lượng tính toán tương đối thấp, nhưng đôi khi rơi vào cực trị địa phương do chưa xét đến phân bố công suất. Vì vậy, một số nghiên cứu sử dụng nó để tìm vị trí tối ưu lắp đặt FACTS [5, 17], giải quyết nút cổ chai trong hệ thống điện [17], cũng như các nghiên cứu về độ ổn định và độ tin cậy trong quy hoạch mở rộng truyền tải [18, 19].

Các thuật toán meta-heuristic: là các thuật toán lấy cảm hứng từ sự tối ưu hóa trong các quy luật tự nhiên. Chúng được mở rộng cho các thủ tục tìm kiếm cụ thể và có thể được sử dụng trong hầu hết mọi trường hợp, và đây là một giải pháp đặc biệt thích hợp cho các bài toán phức tạp với nhiều ràng buộc không chắc chắn. Các thuật toán thường được sử dụng để xác định kết quả tối ưu hoặc không tối ưu của các vấn đề chung, ngay cả đối với các hệ thống lớn tương ứng liên quan đến nỗ lực tính toán lớn [20].

Mặc dù có các ưu điểm nhất định nhưng xác suất hội tụ và khối lượng tính toán lớn của thuật toán meta-heuristic là mối quan tâm của các nhà nghiên cứu và đây là cơ hội để đề xuất áp dụng một phương pháp lai ghép trong bài báo này. Sự lai tạo này dẫn đến một thuật toán kết hợp hai giai đoạn. Đầu tiên, cải tiến thuật toán MC để phù hợp với mục tiêu của vấn đề tối ưu hóa, được gọi là "giới hạn không gian tìm kiếm". Giai đoạn tiếp theo, được gọi là "Tối ưu hóa giải pháp", sử dụng thuật toán GA để tìm ra kết quả tối ưu toàn cục trong không gian thu hẹp của giai đoạn trước. Quá trình này được thiết kế hoàn hảo để khắc phục nhược điểm của thuật toán meta-heuristic như vừa đề cập.

Kết quả mô phỏng trên hệ thống IEEE 24 bus cho quy trình 5 bước chứng minh tính hiệu quả của biện pháp đề xuất trong việc tìm ra vị trí và công suất tối ưu để lắp đặt ESS. Những đóng góp chính của bài báo là:

i) Đề xuất thay đổi nguyên lý giải thuật MC và lai tạo với thuật toán GA để tạo ra một phương pháp tối ưu mới trong quy hoạch mở rộng lưới điện truyền tải;

ii) Đề xuất mô hình đầu tư ESS để giải quyết tắc nghẽn ngắn hạn và ứng dụng phương pháp tối ưu mới để tìm vị trí và công suất ESS;

iii) Sử dụng hệ thống điện mẫu của IEEE 24-bus tích hợp ESS để thử nghiệm trong nghiên cứu này.

2. MÔ HÌNH TOÁN

2.1. Mô hình ESS trong hệ thống điện

Một trong các loại hình nguồn điện chủ động như ESS có thể cung cấp điện khi hệ thống điện bị tắc nghẽn ở phụ tải cao điểm và đảm bảo hệ thống điện vận hành ổn định mà không cần mở rộng hệ thống điện truyền tải. Mặt khác, ESS còn nâng cao khả năng truyền tải của hệ thống bằng cách đưa thêm công suất lên lưới nhằm giảm ùn tắc và áp lực lên các nguồn điện hiện có, đảm bảo an ninh hệ thống điện [13, 21]. Trong thị trường thương mại gần đây với các công nghệ lưu trữ năng lượng khác nhau, pin vẫn là thiết bị lưu trữ phổ biến nhất hiện nay [21]. Ngoài ra, để giải quyết vấn đề thiếu hụt công suất trong thời gian ngắn còn có các loại công nghệ khác như bánh đà, siêu tụ điện. Lưu trữ năng lượng bằng Hydrogen, khí nén là những công nghệ có công suất lớn hơn, khả năng lưu trữ năng lượng cao hơn

nên linh hoạt hơn trong hệ thống điện. Các điều kiện ứng dụng cụ thể tương ứng với từng loại công nghệ được phân loại như hình 1.

Cho đến nay, vốn đầu tư ESS về cơ bản dường như vẫn quá cao không thể mang lại lợi nhuận cho nhà đầu tư độc lập. Vì vậy, thường ESS chỉ được xây dựng để phục vụ các mục đích cần thiết cụ thể nào đó mà không có giải pháp thay thế khác [22-24]. Một trong số đó là ổn định hệ thống điện bởi nhiễu từ các loại nguồn năng lượng tái tạo. Đó là kết quả ESS thường được xây dựng đồng bộ với các dự án năng lượng tái tạo. Một trong những tác dụng chính của chúng được sử dụng như một nguồn năng lượng để bù đắp cho sự thiếu hụt. ESS là loại năng lượng có thể cung cấp điện khi cần thiết và lưu trữ năng lượng khi quá nhu cầu [13, 21]. Chi phí đầu tư ESS trong thị trường có thể được tính gần đúng như biểu thức (1).

$$C_j^{ESS} = \sum_{i \in G_{ess}} P_i^{ess}.c_{ess} + C_0 \quad (1)$$

Trong đó:

P_i^{ess} - Công suất định mức của ESS (MW).

c_{ess} - Vốn đầu tư nguồn ESS (USD).

C_0 - Chi phí cố định nguồn ESS (USD).

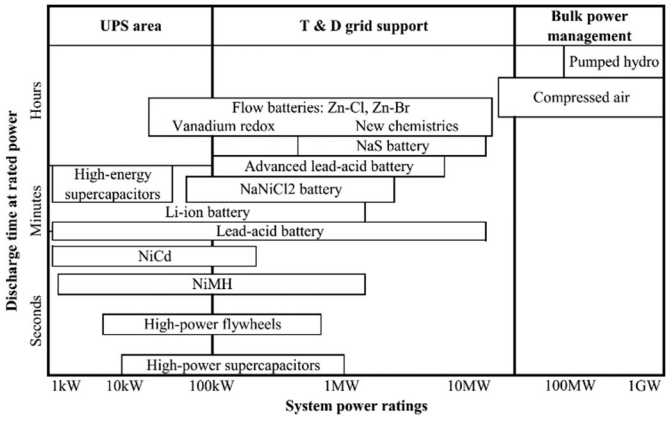

Hình 1. Phân loại các loại nguồn ESSs [6]

2.2. Mô hình cải tiến thuật toán MC

(i) Giải thuật mặt cắt tối thiểu gốc (Basic MC Algorithm - BMC)

Vào những năm 1950, bài toán tìm tắc nghẽn của đồ thị vô hướng được Ford và Fulkerson đề xuất bằng cách xác định lát cắt nhỏ nhất của đồ thị vô hướng đó. Giải pháp này là tiền đề cho giải thuật MC. Mechtild Stoer và Frank Wagner đã phát triển thuật toán này để áp dụng cho các chương trình máy tính vào năm 1997 và gọi nó là thuật toán Min-Cut [25]. Mô hình này cũng được sử dụng để xác định vị trí tối ưu của TCSC nhằm giải quyết vấn đề tắc nghẽn trong HTĐ [5]. Sơ đồ thuật toán MC cơ bản được hiển thị trong hình 2.

Diễn giải:

Một ma trận (n x n) trọng lượng [A] (trọng lượng trong trường hợp này là công suất định mức các đường dây truyền tải điện).

n là số đỉnh.

$\sum sj = \sum a_{sj}$, $\sum jt = \sum a_{jt}$ - tổng trọng lượng bên phía nguồn điện, bên phía phụ tải, của mặt cắt thứ i tương ứng nhánh thứ j.

S(i), T(i) - i mặt cắt hướng nguồn, hướng tải tương ứng.

u, v - các nút tương ứng.

{s}, {t} - tập hợp đỉnh hướng nguồn, tải.

MC(i) - mặt cắt tối thiểu của bước thứ i.

MF - cực đại phân bố công suất.

(ii) Giải thuật cải tiến min cut bằng kết hợp yếu tố phạt (Penalty MC Algorithm - PMC)

Giải thuật BMC như nêu trên bị hạn chế do không xét đến phân bố công suất truyền tải trên đường dây điện trong quá trình tìm ra vùng tắc nghẽn trên hệ thống điện. Do đó nhánh điện được chọn thay thế hay xây dựng mới để giải quyết tắc nghẽn có thể là nhánh điện còn non tải với khả năng dẫn điện vẫn có thể tăng cao hơn. Kết quả này dẫn đến có thể chưa tối ưu theo mục tiêu của bài toán. Cụ thể là mục tiêu của việc giải quyết tắc nghẽn khi phụ tải tăng lên phải được ưu tiên các tuyến đường dây điện có tỷ lệ công suất truyền tải cao trong quá trình vận hành. Trong khi đó, BMC vì không xét đến khả năng mang tải của các đường dây điện nên có thể bỏ qua các đường dây truyền tải có phân bố công suất lớn, trong khi đây là những vị trí xung yếu cần khắc phục hơn các đường dây có công suất mang tải thấp hơn. Vì lý do đó, cải tiến BMC để giải thuật có thể quan tâm hơn đến các nhánh mang công suất tải lớn hơn vào mặt cắt tối thiểu cuối cùng để nâng cao hiệu quả bài toán giải quyết tắc nghẽn.

Giải thuật PMC về cơ bản vẫn là phương pháp GRAPH như BMC để tìm ra một mặt cắt trong đó tổng trọng lượng các nhánh là nhỏ nhất giữa nguồn điện và phụ tải điện. Tuy nhiên, điểm khác biệt lớn đó là yếu tố phạt truyền tải. Giá trị trọng lượng của một nhánh sẽ được bổ sung thêm một lượng gọi là phạt truyền tải điện. Nghĩa là khi đường dây mang tải càng cao thì phạt càng lớn và trọng lượng của nhánh đó càng cao, và ngược lại. Phạt truyền tải điện (p), được tính trong mỗi vòng lặp phân bố công suất dựa theo tỷ lệ giữa công suất điện truyền tải P_i^f trên nhánh thứ i so với công suất định mức P_i^r của cùng nhánh đó, như biểu thức (2).

$$p_j = \frac{P_{i,j}^f}{P_i^r} \quad (2)$$

Tỷ trọng trọng lượng của mặt cắt trong bước 2 và 5 của lưu đồ BMC trên sẽ thay đổi trong mỗi bước lặp một lượng như (3).

$$G_j = A(1 - p_j) \quad (3)$$

Các trọng lượng của mặt cắt được thay thế bằng các biểu thức (4) và (5).

$$s_j(new) = s_j + G_j \quad (4)$$

$$t_j(new) = t_j + G_j \quad (5)$$

A trong biểu thức (3) là hệ số tỷ lệ xét đến mức độ đóng góp của phân bố công suất trên các đường dây điện đến kết quả hội tụ của giải thuật PMC. Khi hệ số A được chọn quá lớn, các đường dây điện quá tải sẽ càng được ưu tiên nhưng vai trò mặt cắt tối thiểu bị giảm đi, điều đó dẫn đến kết quả có thể loại vùng tắc nghẽn ra khỏi nghiệm. Trong khi đó nếu hệ số đó quá nhỏ, vai trò của các đường dây điện phân bố công suất cao không còn tác dụng dẫn đến kết quả không khác gì với giải thuật BMC. Thông thường, hệ số này được chọn tương ứng gần với công suất truyền tải định mức của các đường dây truyền tải điện.

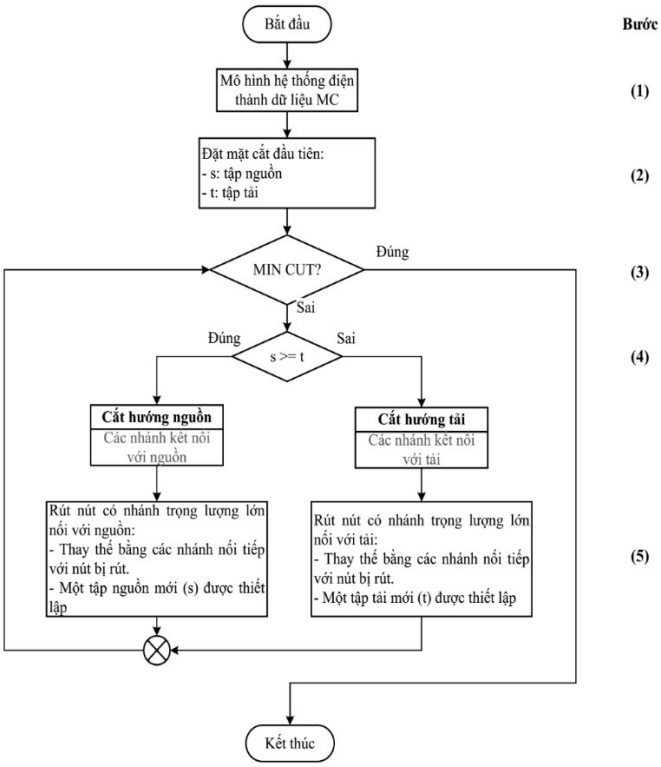

Hình 2. Lưu đồ giải thuật BMC [5]

Với cải tiến bổ sung hình phạt truyền tải điện trong giải thuật PMC như vừa nêu, sự đóng góp của dòng công suất điện trên mỗi đường dây điện vào tỷ trọng trọng lượng của mỗi mặt cắt, như trong biểu thức (4) và (5). Theo đó cho thấy khi công suất truyền tải càng lớn, theo biểu thức (6), thì trọng lượng càng nhỏ nên thông thường đường dây truyền tải điện có phân bố công suất lớn đó sẽ được ưu tiên chọn trong mặt cắt tối thiểu. Kết quả là mục tiêu xác định vùng tắc nghẽn sẽ càng chính xác hơn so với phương pháp trước đây.

$$[P_f] = \text{runopf(sys)} \quad (6)$$

2.3. Hàm mục tiêu

(i) Hàm mục tiêu

Một số nghiên cứu gần đây về quy hoạch TEP đã xem xét việc lắp đặt ESS. Tuy nhiên, nó vẫn chưa phổ biến trên thị trường thương mại vì vốn đầu tư của ESS vẫn còn tương đối cao [26]. Vì vậy, bài toán tối ưu hóa vị trí và công suất của các ESS trong quy hoạch TEP để đạt được chi phí hợp lý khi đầu tư nguồn ESS mới và chi phí đầu tư đường dây điện phải xây dựng mới hoặc cải tạo nâng cấp năng lực truyền tải điện được thể hiện bởi hàm mục tiêu sau:

$$\min C^T = \sum_{i\in L} C_i^L + \sum_{j\in ESS} C_j^{ESS} + \sum_{l\in B} C_l^{\Delta A} \quad (7)$$

ở đây, C_i^L là chi phí đầu tư nâng cấp đường dây truyền tải thứ i, US$, và $C_l^{\Delta A}$ là chi phí do tổn hao điện năng trên đường dây truyền tải thứ l, US$, thuộc tập hợp B, là tập hợp đường dây truyền tải của hệ thống điện, chi phí này trong một chu kỳ xem xét T được tính theo công thức:

$$C_l^{\Delta A} = \lambda . \Delta P_l^{max} . LLF . T \quad (8)$$

Với λ là giá điện bình quân, US$/kWh; ΔP_l^{max} là tổn hao công suất cự đại trên nhánh l, W; và LLF là tỷ số tổn hao.

Các ràng buộc về vận hành và giới hạn truyền tải của hệ thống điện thể trên các biểu thức (9) – (12) gồm:

$$P_{Gi} - P_{Di} - \sum_{j\in bus} V_i V_j (G_{ij} \cos\delta_{ij} + B_{ij} \sin\delta_{ij}) = 0 \quad (9)$$

$$Q_{Gi} - Q_{Di} - \sum_{j\in bus} V_i V_j (G_{ij} \sin\delta_{ij} + B_{ij} \cos\delta_{ij}) = 0 \quad (10)$$

$$V_{i\in bus}^{min} \le V_{i\in bus} \le V_{i\in bus}^{max} \quad (11)$$

$$S_{i\in branch} \le S_{i\in branch}^{max} \quad (12)$$

ở đây,

t - một chu kỳ đánh giá (năm).

$c_i(t)$ - chi phí nguồn điện thứ i ở chu kỳ t, US$.

$P_{Gi}, Q_{Gi}, P_{Di}, Q_{Di}$ - công suất nguồn điện và phụ tải, MW và MVAr.

$S_{i\in branch}^{max}$ - công suất định mức của nhánh thứ i, MVA.

δ_{ij} - góc lệch điện áp nút.

$V_{i\in bus}^{min}, V_{i\in bus}^{max}$ - điện áp tối thiểu và cực đại của nút, kV.

(ii) Phương pháp lai hai bước (MCGA)

Bài toán tối ưu (7) với nhiều phương pháp giải đã được nghiên cứu trước đây bằng nhiều phương pháp trong đó có thuật toán heuristic, meta-heuristic hay toán học [14]. Các lợi thế và bất lợi của từng phương pháp không giống nhau, nhưng tất cả những vấn đề mà các nhà khoa học và quy hoạch quan tâm nhất đều liên quan đến việc tìm cực trị toàn cục của bài toán nhanh nhất, đặc biệt đối với các hệ thống điện lớn.

Trong số các thuật toán được sử dụng gần đây, GA là một trong các phương pháp tiêu chuẩn được sử dụng trong lập trình quy hoạch TEP để giải bài toán tối vì nó đơn giản. Tuy nhiên, đặc điểm của nó là khối lượng tính toán quá lớn trong một số trường hợp tương tự như hầu hết các phương pháp meta-heuristic khác và đôi khi kết quả của bài toán có thể bị mắc kẹt ở các cực trị cục bộ.

Vì vậy, phương pháp lai được đề xuất trong bài báo này nhằm giải quyết vấn đề cực trị toàn cục của bài toán quy hoạch TEP. Sự kết hợp hai giai đoạn đó là, thứ nhất dùng giải thuật PMC để giới hạn không tìm kiếm nhằm giảm số

lượng thao tác, và thứ hai là sử dụng thuật toán GA để tìm cực trị cho bài toán tối ưu trong không gian đã được thu nhỏ ở bước đầu.

Sơ đồ trong hình 3 mô tả vấn đề lai như đã đề cập ở trên theo trình tự năm bước:

1) Mô hình dữ liệu hệ thống điện.

2) Phân bố công suất tối ưu của hệ thống điện đang vận hành.

3) Tìm tập mặt cắt nhỏ nhất bằng giải thuật PMC.

4) Giới hạn không gian tìm kiếm căn cứ vào mặt cắt nhỏ nhất được xác định trong bước 2.

5) Giải bài toán tối ưu (7) bằng thuật toán GA trong không gian không gian thu nhỏ ở bước 3.

6) Cuối cùng là đánh giá vị trí và công suất của các nguồn ESS.

3. MÔ PHỎNG TRÊN LƯỚI ĐIỆN MẪU 24 NÚT (IEEE)

(i) Dữ liệu thử nghiệm

Hệ thống điện IEEE RTS 24-bus tiêu chuẩn được sử dụng để kiểm tra tính khả thi của phương pháp được đề xuất trong bài báo này. Thông số kỹ thuật thông lệ hệ thống này có 36 nhánh và 10 nguồn điện, dữ liệu của hệ thống điện này có thể được tìm thấy trong các tài liệu [27, 28], được thể hiện bảng 1, 2 và trong hình 4.

Bảng 1. Công suất nguồn điện

Generator	Bus	P_g (MW)	Q_g (MVar)
G1	1	192	62.375
G2	2	192	62.375
G3	7	300	75
G4	13	591	207
G5	15	215	66.313
G6	16	155	54.313
G7	18	400	100
G8	21	400	100
G9	22	300	60
G10	23	660	248.563

Bảng 2. Công suất phụ tải cực đại

Load	Bus	P_d (MW)	Q_d (MVar)
L1	1	108	22
L2	2	97	20
L3	3	180	37
L4	6	136	28
L5	7	125	25
L6	8	171	35
L7	10	195	40
L8	13	265	54
L9	14	194	39
L10	18	333	68
L11	19	181	37
L12	20	128	26

Để tạo vị trí tắc nghẽn trong hệ thống để thử nghiệm, bài báo giả thiết các kịch bản công suất phụ tải và nguồn phát cùng tăng như nhau tại tất cả các nút. Sau khi phân bố công suất tối ưu bằng công cụ Matpower được xây dựng sẵn trên nền tảng Matlab, kết quả các điểm mang tải cao trong hệ thống 24 bus được thể hiện ở bảng 3. Theo đó, với tỷ lệ này tăng lên từ 1,1 đến 1,5 thì phân bố công suất cũng tăng dần lên và nơi có công suất cao tập trung vào vị trí các nhánh 6-10, 7-8, và 14-16. Và tỷ lệ tăng tải lên đến 1,6 (tương ứng 160%) thì hệ thống bắt đầu xảy ra nghẽn mạch tại các nhánh 6-10 và 7-8.

Bảng 3. Tắc nghẽn hệ thống theo tỷ lệ phụ tải và nguồn điện

Kịch bản tăng tỷ lệ nguồn và tải	**1.1**	Nhánh mang tải cao nhất hoặc quá tải	6-10			
		Tỷ lệ mang tải (%)	97%			
	1.2	Nhánh mang tải cao nhất hoặc quá tải	6-10			
		Tỷ lệ mang tải (%)	99%			
	1.3	Nhánh mang tải cao nhất hoặc quá tải	6-10			
		Tỷ lệ mang tải (%)	100%			
	1.4	Nhánh mang tải cao nhất hoặc quá tải	6-10	14-16		
		Tỷ lệ mang tải (%)	100%	100%		
	1.5	Nhánh mang tải cao nhất hoặc quá tải	6-10	7-8	14-16	
		Tỷ lệ mang tải (%)	100%	100%	100%	
	1.6	Nhánh mang tải cao nhất hoặc quá tải	6-10	7-8		
		Tỷ lệ mang tải (%)	133%	104%		
	1.7	Nhánh mang tải cao nhất hoặc quá tải	6-10	7-8	8-9	8-10
		Tỷ lệ mang tải (%)	120%	116%	111%	108%

Về nguồn ESS, chọn loại trữ năng bằng công nghệ Compressed Air thuận lợi để xây dựng cho mọi khu vực, vị trí, cũng như công suất yêu cầu lớn đáp ứng được nhu cầu cần thiết, đặc biệt có thể lắp ghép từ các modul để nâng công suất theo từng thời kỳ với kinh phí đầu tư tương đối hợp lý [9, 26]. Một trong những đặc điểm đáng chú ý của công nghệ trữ năng là có thể san bằng phụ tải giữa thời gian thấp điểm và cao điểm trong hệ thống điện như thể hiện trong [9, 10].

Phương pháp quy hoạch ở đây, thay vì phải có các biện pháp TEP để đảm bảo cung cấp điện cho nhu cầu tất cả các phụ tải trong thời gian đỉnh tải, nguồn trữ năng có thể cung cấp năng lượng trong thời gian quá tải do đỉnh tải gây ra để đảm bảo hệ thống điện hoạt động ổn định mà không cần TEP.

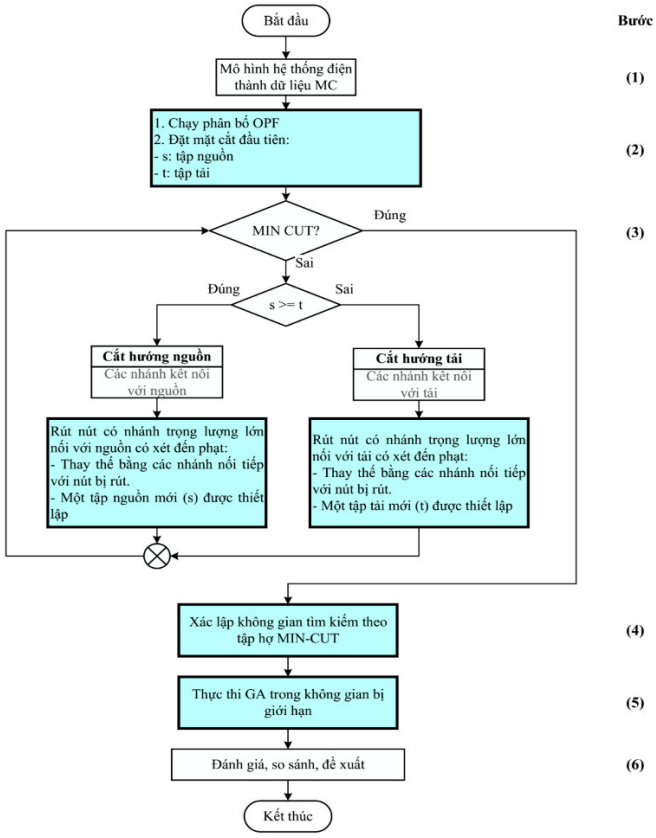

Hình 3. Lưu đổ giải thuật lai PMC và GA

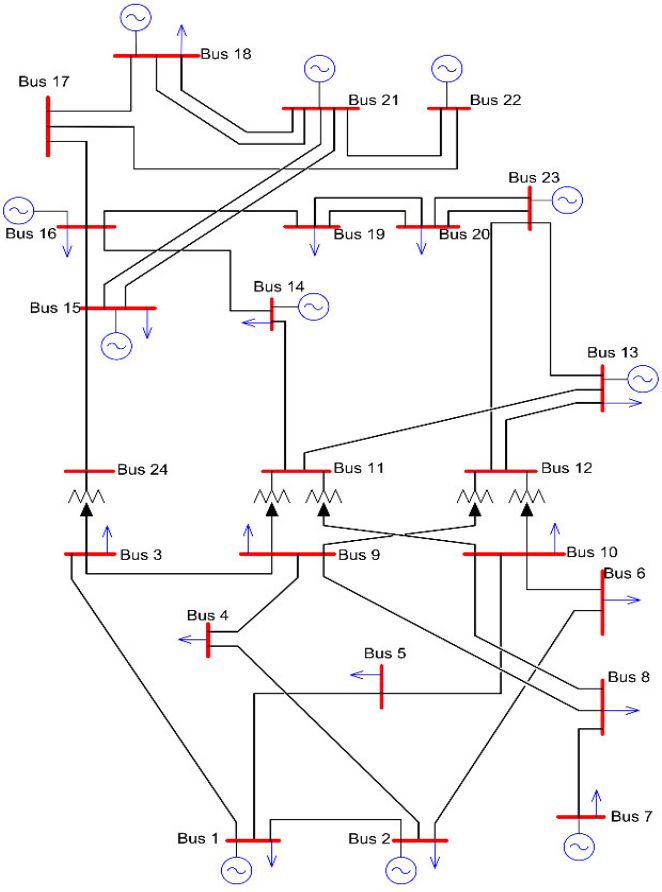

Hình 4. Sơ đồ lưới điện chuẩn 24-bus IEEE

(ii) Thực thi

Ba kịch bản sẽ được xem xét để so sánh và đánh giá. Kịch bản thứ nhất sử dụng giải thuật BMC kết hợp với GA (BMC-GA), nó là kịch bản đơn giản để giải quyết một số bài toán tắc nghẽ trong hệ thống điện. Kịch bản thứ hai là lai PMC với GA như đề xuất trong bài báo này (PMC-GA). Kịch bản này sẽ được xem xét đánh giá hiệu quả sau khi thử nghiệm. Kịch bản thứ ba dùng phương pháp phân tích đánh giá số nguyên sau khi phân bố công suất tối ưu AC để tìm ra vị trí lắp đặt ESS (AC+). Kịch bản này đã được thể hiện tại [11].

Hai kịch bản đầu tiên tương ứng sáu bước theo quy trình cải tiến và đề xuất tại hình 3, được thực thi trên ngôn ngữ matlab trong đó có ứng dụng một số công cụ trong Matpower 6.0 được biên soạn sẵn. Phần lớn các nội dung giải thuật PMC và GA được lập trình để thực thi theo nội dung đã được trình bày trong phần 2.

Đối với thuật toán GA, phương pháp giải bài toán tối ưu tham khảo theo [29] và dữ liệu áp dụng trong trường hợp lưới điện IEEE 24 bus tham khảo [29, 30]. Tóm tắt một số thông số đầu vào cho ví dụ này gồm: khởi tạo với 20 biến số ngẫu nhiên ban đầu; tối đa 50 biến số trong quần thể; tỷ lệ lai tạo là 0,8; phương pháp lựa chọn lai tạo là "Roulette Wheel"; tỷ lệ đột biến 0,2.

Kết quả được thể hiện trong các bảng 4, 5.

Bảng 4. Kết quả Mincut thực thi trên hệ thống IEEE 24-bus

Trường hợp	MIN-CUT
	Branchs
BMC	8-9; 8-10
PMC	6-2; 6-10; 8-7; 8-9; 8-10

Bảng 5. Phân bố công suất trên các nhánh thuộc min-cut

Nhánh	Tỷ lệ (%)
6-2	51
6-10	104
8-7	133
8-9	25
8-10	14

Bảng 6. Kết quả nguồn ESSs theo các kịch bản

Senario		Bus	Power (MW)
1	BMC-GA	Nul	Nul
2	PMC-GA	6	10
		8	30
3	AC+	6	40

(iii) Thảo luận

Bảng 4 cho thấy sự khác biệt của các mặt cắt tối thiểu khi có sự tham gia của giá trị phạt công suất điện mang tải trên đường dây điện. Số lượng nhánh được chọn lựa trong mắt cắt tối thiểu nhiều hơn khi xét đến yếu tố phạt trong trường hợp PMC, 5 nhánh so với chỉ 2 nhánh trong trường hợp BMC. Điều đó dẫn đến giải thuật BMC có giới hạn

không gian tìm kiếm thu hẹp hơn, nhưng việc quá rút gọn này dẫn đến đôi khi loại bỏ các kết quả có thể là nghiệm của bài toán cần giải.

Thật vậy, bảng 5 cho thấy phân bố công suất của các nhánh trong các mặt cắt tối thiểu đã tìm được. Theo đó, các nhánh quá tải 8-7 và 10-6 (với hệ số quá tải là 104% và 133%) đã bị loại khỏi mặt cắt tối thiểu trong giải thuật BMC, trong khi các nhánh có phân bố công suất trên đó rất thấp, chẳng hạn như các nhánh 9-8 hoặc 10-8 chỉ hoạt động ở khoảng 25% và 14% khả năng tải tương ứng, lại được bao gồm trong mặt cắt tối thiểu của giải thuật BMC. Kết quả là các cơ hội khả thi có thể dẫn đến là nghiệm của bài toán đã bị loại ra khỏi không gian tìm kiếm, điều đó dẫn đến trong kịch bản BMC-GA không tìm ra nghiệm như đã thể hiện trên bảng 6.

Ngược lại, với giải thuật cải tiến PMC nhờ có xem xét đến hệ số phạt mang tải công suất điện nên các nhánh mang tải cao, đặc biệt các nhánh quá tải 8-7 và 10-6 đã bị loại trong giải thật BMC nói trên, lại được giữ lại trong không gian tìm kiếm như trong bảng 4. Để từ đó kết quả giải bài toán GA trong không gian giới hạn này đã tìm được vị trí và công suất tối ưu của các nguồn ESSs như trong bảng 6, đó là công suất 10MW tại nút 6 và 30MW tại nút 8.

So sánh với kịch bản AC+ trên bảng 6 nhận thấy có một sự trùng hợp về vị trí lắp đặt nguồn ESS tại bus 6. Với kịch bản PMC-GA chỉ cần công suất 10MW trong khi AC+ là 40MW, lớn hơn 30MW so với kịch bản PMC-GA. Tuy nhiên, thay vì phải đầu tư thêm 30MW tại bus 6 thì PMC-GA lại chọn đầu tư lượng công suất này tại bus 8. Việc đầu tư hai vị trí có thể dẫn đến gia tăng vốn đầu tư ban đầu nguồn ESS, nhưng xét góc độ vận hành hệ thống điện thì phân tán nguồn ESS có thể mang lại lợi ích nhiều hơn nhờ xác suất cung cấp năng lượng nhiều hơn. Hơn nữa, khi phần tán nguồn ESS cũng giảm công suất tổn hao cực đại trên các đường dây truyền tải của hệ thống điện xuống còn 109MW so với tổn hao cao hơn 114MW của phương án AC+. Cuối cùng, mặc dù kịch bản PMC-GA có nhiều vị trí đặt ESS hơn nhưng tổng dung lượng công suất của các nguồn ESSs là không đổi so với kịch bản AC+ nên hoàn toàn phù hợp.

Trong khi đó, khi lai hai thuật toán PMC với GA, khối lượng tính toán giảm đi rất lớn nhờ PMC lược bỏ đi phần lớn các nhánh chắc chắn không phải là nghiệm của bài toán GA. Cụ thể trong ví dụ trên hệ thống 24 bus nêu trên, nhờ PMC mà số nhánh được xem xét tính toán chỉ còn lại 5 nhánh, như trên bảng 4, trong khi phải khảo sát cả 36 nhánh đối với kịch bản không giới hạn không gian tìm kiếm trước đó. Trong khi đó, khối lượng phép toán được tính theo hàm mũ của số nhánh khảo sát, nên với 7 lần số nhánh nhỏ hơn làm giảm đi đáng kể lượng lớn phép tính trong quá trình tính toán bài toán GA, đặc biệt là với các hệ thống điện có số lượng nhánh cao.

4. KẾT LUẬN

Xây dựng nguồn ESS đang là vấn đề được quan tâm của toàn xã hội, đặc biệt là các nhà quản lý vận hành hệ thống điện và các nhà đầu tư tài chính, để giải quyết sự không chắc chắn cũng như các hậu quả trong vận hành hệ thống điện của sự phát triển tăng cao nguồn năng lượng tái tạo. Vì vậy, quy hoạch TEP và GEP ngày nay luôn đặt vấn đề tìm kiếm vị trí và công suất tối ưu cho nguồn ESS để đảm bảo các điều kiện hoạt động và lợi ích nhất cho tất cả các bên, kể cả lợi ích xã hội.

Kết quả nghiên cứu và đề xuất phương pháp lai trình bày cụ thể trong bài báo này mang lại hiệu quả là khá cao. Việc kết hợp giữa thuật MC và thuật toán GA đã cải thiện kết quả tính toán trong bài toán quy hoạch TEP và GEP, ngoài ra việc đề xuất đưa thêm yếu tố phạt truyền tải vào tỷ trọng mặt cắt tối thiểu vào hàm mục tiêu cũng làm giảm thiểu đáng kể không gian tìm kiếm cho các giai đoạn sau mà không làm thay đổi kết quả nghiệm của bài toán tối ưu trong bài toán quy hoạch TEP và GEP.

Phương pháp đề xuất đã thử nghiệm trên hệ thống điện chuẩn IEEE 24-bus, một trong các hệ thống điện mà dữ liệu thường dùng để mô phỏng kiểm tra trong các nghiên cứu về hệ thống điện. Kết quả chứng minh được phương pháp lai được đề xuất có kết quả tương đồng hoặc tốt hơn so với nghiên cứu trước đây, nhưng hiệu quả hơn nhiều về quá trình và số lượng phải thực thi bài toán.

Với hiệu quả của phương pháp đề xuất như đã nêu, việc tìm vị trí lắp đặt cho các nguồn ESSs với công suất tối ưu có thể giúp cho các nhà quản lý xây dựng quy hoạch TEP và GEP hiệu quả hơn, khai thác tốt nhất nguồn năng lượng tái tạo. Mặt khác, phương pháp đề xuất có thể giúp hoạch định thị trường điện hiệu quả hơn khi định hướng được những nguồn ESSs và nguồn năng lượng tái tạo khi tham gia vào thị trường. Xa hơn nữa, nó còn có thể giúp nhà đầu tư tài chính yên tâm hoạch định và đầu tư các nguồn ESSs.

LỜI CẢM ƠN

Bài báo này được hỗ trợ bởi Trường Đại học Sư phạm Kỹ thuật Thành phố Hồ Chí Minh, Việt Nam, theo đề tài T2022-69.

TÀI LIỆU THAM KHẢO

[1]. M. Mahdavi, H. Monsef, 2011. *Review of Static Transmission Expansion Planning*. Journal of Electrical and Control Engineering, vol. 1, no. 1, pp. 11-17.

[2]. S. Lumbreras, A. Ramos, 2016. *The new challenges to transmission expansion planning. Survey of recent practice and literature review*. Electric Power Systems Research, vol. 134, pp. 19-29.

[3]. C. Lee, S. K. Ng, J. Zhong, F. F. Wu, 2006. *Transmission Expansion Planning From Past to Future*. Proc Power Systems Conf. Expo., vol. PSCE 06, no. 03, pp. 257-265.

[4]. M. Ilic, F. Galiana, L. Fink, 2013. *Power Systems Restructuring: Engineering and Economics*. New York: Springer Science & Business Media, LLC.

[5]. T. L. Duong, J. Yao, V. A. Truong, 2013. *A new method for secured optimal power flow under normal and network contingencies via optimal location of TCSC*. International Journal of Electrical Power & Energy Systems, vol. 52, no. 8.

[6]. G. M. J. Herbert, S. Iniyan, E. Sreevalsan, S. Rajapandiand, 2007. *A review of wind energy technologies*. Renewable and Sustainable Energy Reviews, vol. 11, no. 6, pp. 1117-1145.

[7]. K. H. Solangi, M. R. Islam, R. Saidur, N. A. Rahim, H. Fayaz, 2011. *A review on global solar energy policy*. Renewable and Sustainable Energy Reviews, vol. 15, no. 4, pp. 2149-2163.

[8]. D. Cao, W. Hu, X. Xu, T. Dragičević, Q. Huang, Z. Liu, Z. Chen, F. Blabjerg, 2020. *Bidding strategy for trading wind energy and purchasing reserve of wind power producer - A DRL based approach*. Electrical Power & Energy Systems, vol. 117, p. 105648.

[9]. D. Akinyele, R. Rayudu, 2014. *Review of energy storage technologies for sustainable power networks*. Sustainable Energy Technologies and Assessments, vol. 8, pp. 74-91.

[10]. J. Makansi, J. Abboud, 2002. *Energy Storage: the missing link in the electricity value chain-An ESC*. White Paper, Energy Storage Counc, pp. 1-23.

[11]. S. N. Dinh, L. T. Duong, A. V. Truong, T. T. Nguyen, 2020. *Determine the location and capacity of energy storage in the power system using the improved Min-Cut algorithm*. Science & Technology Development Journal – Engineering and Technology, vol. 3, no. 1, pp. 339-351.

[12]. S. N. Dinh, V. H. Q. Nguyen, L. T. Duong, A. V. Truong, 2019. *Determining location for power system expansion planning using Min Cut algorithm*. Journal of Science and Technology, Hanoi University of Industry, vol. 50, pp. 15-20.

[13]. L. Hadjipaschalis, A. Poullikkas, V. Efthimiou, 2009. *Overview of current and future energy storage technologies for electric power applications.* Renewable and Sustainable Energy Reviews, vol. 13, no. 6-7, pp. 1513-1522.

[14]. R. Hemmati, R.A. Hooshmand, A. Khodabakhshian, 2013. *Comprehensive review of generation and transmission expansion planning*. The Institution of Engineering and Technology, vol. 7, no. 9, p. 955 - 964.

[15]. L. L. Garver, 1970. *Transmission Network Estimation Using Linear Programming.* IEEE Trans. Power Apparatus and Systems, Vols. PAS-89, no. 7, pp. 1688-1697.

[16]. I. G. Sánchez, R. Romero, J. R. S. Mantovani, M. J. Rider, 2005. *Transmission - Expansion Planning Using the DC Model and Nonlinear - Programming Technique*. IEEE Proceedings of Generation, Transmission and Distribution, vol. 152, no. 6, pp. 763-769.

[17]. T. L. Duong, J. Yao, V. A. Truong, 2014. *Application of Min Cut Algorithm for Optimal Location of FACTS Devices Considering System Loadability and Cost of Installation*. International Journal of Electrical Power & Energy Systems, vol. 63, no. 12.

[18]. T. Tran, J. Choi, J. K. Park, S. I. Moon, A. A. El-Keib, 2004. *A fuzzy branch and bound-based transmission system expansion planning considering ambiguities*. IEEE Power Engineering Society General Meeting.

[19]. J. S. Choi, T. T. Tran, S. R. Kang, D. H. Jeon, C. H. Lee, R. Billinton, Jaeseok, 2004. *A study on the optimal reliability criteria decision for a transmission system expansion planning*. IEEE Power Engineering Society General Meeting.

[20]. M. C. Rocha, J. T. Saraiva, 2011. *Multiyear Transmission Expansion Planning Using Discrete Evolutionary Particle Swarm Optimization*. Energy Market (EEM), 2011 - 8th International Conference on the European, pp. 802-807.

[21]. B. Dunn, H. Kamath, J. M. Tarascon, 2011. *Electrical Energy Storage for the Grid: A Battery of Choices*. Science, vol. 334, pp. 928-935.

[22]. H. Ding, P. Pinson, Z. Hu, Y. Song, 2016. *Integrated Bidding and Operating Strategies for Wind-Storage Systems*. IEEE Transactions on Sustainable Energy, vol. 7, no. 1, pp. 163-172.

[23]. A. A. Thatte, L. Xie, D. E. Viassolo, S. Singh, 2013. *Risk Measure Based Robust Bidding Strategy for Arbitrage Using a Wind Farm and Energy Storage*. IEEE Transactions on Smart Grid, vol. 4, no. 4, pp. 2191-2199.

[24]. L. M. Costa, F. Bourry, J. Juban, G. Kariniotakis, 2008. *Management of Energy Storage Coordinated with Wind Power under Electricity Market Conditions*. Conference on Probablistic Methods Applied to Power Systems, p. 10646172.

[25]. M. Stoer, F. Wagner, 1997. *A Simple Min-Cut Algorithm*. Journal of the ACM, vol. 44, no. 4, pp. 585-591.

[26]. S. Teleke, 2011. *Energy Storage Overview: Applications, Technologies and Economical Evaluation*. White Paper, Quanta Technology, pp. 1-11.

[27]. IEEE Commmitte Report, 1979. *IEEE Reliability Test System*. IEEE Transactions on Power Apparatus and Systems, Vols. PAS-98, no. 6, pp. 2047-2054.

[28]. IEEE Commmitte Report, 1999. *The IEEE Reliability Test System - 1996*. IEEE Transactions on Power Systems, vol. 14, no. 3, pp. 1010-1020.

[29]. D. E. Goldberg, 1989. *Genetic Algorithms in Search, Optimization and Machine Learning - Third Edition*. Addison - Wesley.

[30]. H. Abdi, M. Moradi, S. Lumbreras, 2021. *Metaheuristics and Transmission Expansion Planning: A Comparative Case Study*. Energies, vol. 14, no. 12, p. 3618, 2021.

AUTHORS INFORMATION

Truong Viet Anh[1], Nguyen Tung Linh[2], Dinh Ngoc Sang[3]

[1]Hochiminh City University of Technology and Education, Vietnam

[2]Electric Power University, Vietnam

[3]University of Architecture Hochiminh City, Vietnam